Laboratory of Earth's Environment Physics

Effects of relative climate variability on malaria incidence with a regional-scale dynamical malaria model over Cameroon.

A thesis submitted for the degree of Doctor of Philosophy in Physics.

Option: Atmospheric Sciences

By

MBOUNA DJOUDA Amelie

Registration number : 08Y642

Master degree in Physics

Under the supervision of

LENOUO Andre

Professor

University of Douala

TCHAWOUA Clement

Professor

University of Yaoundé I

Year 2023

DEPARTEMENT DE PHYSIQUE
DEPARTMENT OF PHYSICS

ATTESTATION DE CORRECTION DE LA THESE DE DOCTORAT/Ph.D

Nous, Professeur, **ENYEGUE A NYAM Françoise,** et Professeur **NOUAYOU Robert** respectivement Examinateur et Président du Jury de la thèse de Doctorat/Ph.D de Madame **MBOUNA DJOUDA Amelie** Matricule **08Y642**, préparée sous la direction des Professeurs **LENOUO André** et **TCHAWOUA Clément,** intitulée : « **Effects of relative climate variability on malaria incidence with a regional-scale dynamical malaria model over Cameroon** », soutenue le **Mercredi 03 Mai 2023**, en vue de l'obtention du grade de Docteur/PhD en Physique, Spécialité **Physique de l'Environnement Terrestre**, option **Sciences de l'atmosphère** attestons que toutes les corrections demandées par le Jury de soutenance ont été effectuées.

En foi de quoi, la présente attestation lui est délivrée pour servir et valoir ce que de droit.

Fait à Yaoundé le ... **2 6 JUIN 2023** ...

Examinateur

Le Président du Jury

Pr NOUAYOU Robert

Pr **ENYEGUE A NYAM Françoise**

Le Chef de Département de Physique

Dedication

Dedicated to my Family

Acknowledgements

I first thank the Almighty God for his unending mercies and grace towards me throughout the duration of this work.

I would like to express my sincere gratitude to my supervisors:

- Pr **LENOUO** Andre for having accepted to conduct this work. I benefited a lot of his cordial way of advising, guiding, and encouraging me during this work.

- Pr **TCHAWOUA** Clement for his support, encouragements and critical comments for the fulfilment of the present work.

- Pr **TOMPKINS** Adrian Mark. I am grateful for having had the chance to work with him. I learnt from his works and experiences as scientist, benefited of guidance and expertise that made this work possible.

I am deeply grateful:

- To my parents Mr **DJOUDA Daniel** and Mrs **DJOUDA Véronique**.

- To my children **Daniel**, **Francesco**, **Kylian** and **Chloé**.

- To my husband **Dr MESSANGA ETOUNDI Honoré**.

Special thanks to the entire staff of The University of Yaounde I as well as all my University Lecturers, and especially the coordinators of the Laboratory for Environmental Modelling and Atmospheric Physics (LEMAP), and the Earth Atmosphere Physics Laboratory (LAPHATE) in the Physics Department.

I warmly thank the Abdus Salam International Centre of Theoretical Physics (ICTP) through its Sandwich Training and Educational Programme (STEP) for funding our researches visits in Trieste and provides good computational skills for our experimentations.

Contents

List of Figures

List of Tables

Abbreviations

CORDEX : **CO**ordinated **R**egional climate **D**ownscaling **EX**periment

ECMWF : **E**uropean **C**entre for **M**edium-range **W**eather **F**orecasts

EIR : **E**ntomological **I**noculation **R**ate

FEWS : **F**amine **E**arly **W**arning **S**ystems

HBR : **H**uman **B**iting **R**ate

HYDREMATS: **HYD**rology **E**ntomology and **MA**laria **T**ransmission **S**imulator

ibp^{-1}n^{-1}: **i**nfective **b**ites per **p**erson, per **n**ight

ICTP: **I**nternational **C**entre for **T**heoretical **P**hysics

IRS : **I**ndoor **R**esidual **S**prays

ITN : **I**nsecticide **T**reated Mosquito **N**ets

LMM: **L**iverpool **M**alaria **M**odel

MAP: **M**alaria **A**tlas **P**roject

MARA : **M**apping **M**alaria **R**isk in **A**frica

NMCP : **N**ational **M**alaria **C**ontrol **P**rogramme

PR: **P**arasite **R**atio

RBM: **R**oll **B**ack **M**alaria

RCP : **R**epresentative **C**oncentration **P**athways

GCM : **G**lobal **C**limate **M**odel

RCA : **R**ossby **C**entre **A**tmospheric model

SEIR : **S**uceptible **E**xposed **I**nfectious **R**ecovered

SSA : **S**ub-**S**ahara **A**frica

VECTRI: **VECT**or borne disease community model of ICTP, **TRI**este

WHO : **W**orld **H**ealth **O**rganisation

Symbols

E + I : **Total evaporation and infiltration losses**

K$_{gono}$: **Gonotrophic cycle degree days**

K_{sporo} : **Sporogonic cycle degree days**

$K_{flush,\infty}$: **Larvae flushing factor for infinite rain rate**

$K_{mar1,0}$: **Constant of Martens I vector survival scheme**

$K_{mar1,1}$: **Constant of Martens I vector survival scheme**

$K_{mar1,2}$: **Constant of Martens I vector survival scheme**

$K_{mar2,0}$: **Constant of Martens II vector survival scheme**

$K_{mar2,1}$: **Constant of Martens II vector survival scheme**

$K_{mar2,2}$: **Constant of Martens II vector survival scheme**

km : **kilometer**

km^2 : **kilometer square**

K$_w$: **Pond growth factor**

$M_{L,max}$: **Carrying capacity of water bodies**

$P_{L,surv}$: **Lavae base daily survival rate**

P_{hv} : **Probability of transmission from infective host to vector during single bloodmeal**

$T_{L,min}$: **Minimum T_{wat} for larvae development**

$T_{gono,min}$: **Minimum T_{2m} for egg development**

$T_{sporo,min}$: **Minimum T_{2m} for sporogonic cycle**

W_{max} : **Maximum temporary pond fraction in cell**

τzoo : **Population density zoophilic factor**

Abstract

Malaria is sensitive to climate, environment and socio-economic conditions; but how these drivers interact to control malaria transmission is complex and difficult to predict. Understanding these relationships is important to develop effective control strategies to reduce malaria burden. In this work, climate driven dynamical malaria model was used to examine the impact of climate and population density on malaria incidence in Cameroon using field observed malaria Parasite Ratio (PR) and Entomological Inoculation Rate (EIR) data. The evaluation of the ability of a malaria model is made, to simulate the spread of malaria in Cameroon using rainfall and temperature data from FEWS-ARC2 and ERA-interim respectively. In addition, simulations coupling the model with five results of the dynamical downscaling of the regional climate model RCA4 are made within two-time frames named near future (2035-2065) and far future (2071-2100); aiming to explore the potential effects of global warming on the malaria propagation over Cameroon

Geo-referenced, climate and population data is compared to the results of 103 surveys points of PR. A limited set of campaigns with a year-long field-survey data of EIR are examined to determine the seasonality of malaria transmission. Climate-driven simulations of the VECTRI malaria model are evaluated with this analysis. The model then couples RCA4 models under RCP4.5 and RCP8.5 scenarios, to predict PR and EIR pattern, and examines the link with temperature and rainfall.

The model results show that PR peaks at temperatures ranging between 22°C to 26°C, which agrees with recent findings that suggest a lower malaria peak temperature relative to what has been established in the literature. On the contrary the model estimated daily minimum amount of rainfall (7 mm day^{-1}) that sustains malaria transmission was higher than values found in literature. The VECTRI model was able to reproduce the observed PR patterns, however the peak occurs at slightly higher temperatures than observed, while the PR peaks at a much lower rainfall rate of 2 mm day^{-1}. Transmission tends to be high in rural and peri-urban relative to urban centres in both model and observations.

The EIR follows the seasonal rainfall with a lag of one to two months, and is well reproduced by the model for most of the study sites. However, for locations near permanent water sources, where EIR peaks were out of phase with rainfall, VECTRI failed to accurately predict EIR peak months. The analysis of the malaria projection using PR and EIR, confirm the impact of temperature and rainfall on malaria incidence. PR and EIR peaks between 26 and 28°C which agrees with previous studies. The seasonality of transmission is also observed with EIR pattern.

For each of the scenario under the future climate, the impact of temperature and rainfall on the evolution of malaria indicators is confirmed. During the historical period (1985-2005), the model satisfactorily reproduces the observed PR and EIR. Results of projections reveal that under global warming, heterogeneous changes feature the study area, with localized increases or decreases in PR and EIR. As the level of radiative forcing increases (from 2.6 to 8.5 W.m-2), the magnitude of change in PR and EIR also gradually intensifies. The occurrence of transmission peaks is projected in the temperature range of 26-28°C. Moreover, PR and EIR vary depending on the three agro-climatic regions of the study area. VECTRI still needs to integrate other aspects of disease transmission, such as population mobility and intervention strategies, in order to be more relevant to support actions of decision and policy makers.

keywords : Malaria, Climate, Cameroon, Parasite Ratio, Entomological Inoculation Rate, Global warming, RCA4, VECTRI.

Résumé

Le paludisme est sensible au climat, à l'environnement et aux conditions socio-économiques, mais la relation avec ces moteurs est encore incertaine et difficile à prédire. Une meilleure compréhension de cette relation est importante pour développer les stratégies de contrôle visant a attenuer l'évolution de la maladie. Ce travail utilise un modèle de paludisme, pour examiner l'impact du climat, de la densité de la population sur l'évolution de la maladie au Cameroun en utilisant un recueil de données d'enquêtes sur la prévalence (PR) de la maladie ainsi que du taux d'inoculation entomologique (EIR). L'évaluation de la capacité d'un modèle dynamique à simuler la propagation du paludisme au Cameroun a été conduite en utilisant les données de précipitations et de température de FEWS-ARC2 et ERA-Interim respectivement. De plus des simulations couplées avec cinq modèles de climats RCA4 sont realisées dans deux horizons de temps: un futur proche (2035-2065) et un futur lointain (2071-2100); visant à explorer les éffets potentiels du réchauffement climatique sur la propagation du paludisme au Cameroun.

Les données de climat et de population sont comparées aux résultats de 103 enquètes obtenues sur la prévalence (PR) au Cameroun. Des données similaires donnant les valeurs du taux d'inoculation entomologique (EIR) sont examinées pour évaluer le caractère saisonnier de la transmission de la maladie. En utilisant les données climatiques, les simulations réalisées avec le modèle VECTRI sont evaluées. Par la suite, le modèle est couplé aux RCA4 suivant les scénarios RCP4.5 et RCP8.5, pour prédire l'évolution des paramètres PR et EIR et examiner le lien avec la température.

L'analyse des résultats du modèle présente le pic de PR à des témpératures d'environ 22°C à 26°C, en accord avec de récents travaux qui ont suggéré une témperature de pointe plus froide par rapport à la littérature, et à des taux de précipitations de 7 mm jour^{-1}, quelque peu supérieur aux estimations précédentes. Ce modèle est capable de reproduire de façon générale l'allure attendue, bien que le pic de transmission se produise à des témperatures légèrement supérieures à celles observées, tandis que PR culmine à des taux de précipitations

de 2 mm jour^{-1} inférieure à la valeur observée. La transmission a tendance à être élevée en zone rurale et péri-urbaine comparativement aux centres urbains aussi bien pour le modèle que pour les données d'observations; bien que le modèle soit trop sensible à la population. L'évolution de l'EIR est en accord avec l'évolution saisonnière des précipitations avec un décalage d'un à deux mois. Cette évolution a été bien reproduite par le modèle, tandis que dans les zones proches des rivières permanentes, le cycle annuel de transmission du paludisme est en déphasage avec des précipitations. L'analyse des projections de PR et de EIR confirme l'impact spécifique de la température sur l'incidence du paludisme. Le PR et l'EIR culminent entre 26 et 28 °C, résultats en accord avec d'autres travaux menés au Cameroun. De plus, les zones montagneuses sont moins affectées et la transmission saisonnière est bien observée avec le paramètre EIR.

Pour chacun des scénarios utilisés relatif au changement climatique, l'impact de la température sur l'évolution des indicateurs de paludisme est confirmé. Pendant la période historique (1985-2005), le modèle reproduit de façon satisfaisante les paramètres PR et EIR. Les projections futures revèlent des changements hétérogènes caractérisant la zone d'étude, avec des augmentations et/ou des diminutions localisées de PR et EIR. A mesure que le degré de forçage radiatif augmente (de 2.6 à 8.5 W.m^{-2}), l'amplitude du changement de PR et EIR s'intensifie également. L'apparition des pics de transmission est projetée dans la plage de temperature 26-28°C. Par ailleurs, PR et EIR varient selon les trois régions agro-climatiques de la zone d'étude. Le modele VECTRI devrait encore prendre en compte d'autres aspects de la transmission de la maladie. Aspects tels que la mobilité de la population, les stratégies d'interventions etc. lesquelles sont susceptibles d'améliorer le modèle VECTRI en le rendant plus pertinent face aux décideurs politiques.

Mots clés : Paludisme, Climat, Cameroun, Prévalence, Taux d'inoculation entomologique, Changement Climatique, RCA4, VECTRI.

General Introduction

Malaria is a common and life-threatening disease that affects many countries in the world [1]. It remains a major cause of death and sickness in most tropical and subtropical regions. In 2006, there were an estimated 247 million malaria cases among 3.3 billion people at risk in the world [1]. Of these cases, 86% were in Africa. Among the estimated 881,000 malaria deaths, 91% took place in Africa. More importantly, the report indicated that a child dies every two minutes due to malaria in Sub-saharan Africa (SSA). This highlight the fact that SSA is most affected by the disease in the world and continues to carry an extremely high portion of the global malaria burden [2].

Malaria transmission varies in space and time with high endemicity in the tropical and sub-tropical regions of Africa. Consequently, malaria incidence has been linked to climatic environmental, and socioeconomic factors [3]. In Cameroon, situated in SSA, the disease is a major health burden and its climate is suitable for mosquito development and malaria transmission [4]. Malaria is endemic in Cameroon with children under five (< 5) and pregnant women being the most vulnerable population [5]. The 2020 world malaria report recorded an estimatimation of 20 000 number of malaria deaths in Cameroon between 2018 and 2019 [6].

The disease is caused by a parasites which is a protozoan from the genus *plasmodium* and transmitted to people through the bites of infected females *anopheles* mosquitoes [7]. A single bite by a malaria-carrying mosquito can lead to extreme sickness or death. Malaria starts with an extreme cold, followed by high fever and severe sweating. These can be accompanied by joint pain, abdominal pain, headaches, vomiting, and extreme fatigue.

As malaria is climate dependent, drivers like rainfall, temperature, wind speed and relative humidity are some of the key parameters that influence its transmission [8, 9]. The extent of vulnerability due to malaria also depends on determinants other than the climate such as

environmental factors, population density or migration [10]. Rainfall and temperature influence the life cycles of the anopheles mosquito vector and the malarial *plasmodium* parasite [2]. The impact of fluctuations in rainfall, temperature or population density, on malaria incidence, between the different epidemiological pattern observed in Cameroon is still under study. Improvement in the understanding of how these factors interact to influence malaria transmission in Cameroon is required to develop and implement effective control strategies.

Some scattered field studies have already been carried out to understand spatio-temporal variation in malaria transmission over towns and villages in Cameroon. For example, In Nkoteng village located in the centre region, all year-round intense malaria transmission were found with peak of transmission during the rainy season [11]. A similar situation was observed in Ebolakounou and Koundou with seasonal variations in malaria infection among children under fifteen (< 15) years old [12]. Moreover, a 12-month survey conducted in the southwest region found malaria transmission to be perennial and rainfall dependent [13].

Although studies have been limited to specific towns and villages in Cameroon regarding malaria, there are no studies that attempt to use model to predict local or national scale disease variability. Consequently, there is limited understanding of the impact changes in parameters such as rainfall, temperature and population density have on malaria incidence across different epidemiological zones.

An improved understanding of the relationship between the disease and its climate drivers can contribute to health mitigation and adaptation planning. For this, an appreciation of the observed relationships between climate and malaria indicators is required. If dynamical models can account for these relationships then they could be eventually used for targeted intervention planning. Dynamical models that account for climate parameters are available [14, 15, 16, 10]. One of the recent, named VECTRI, which can simullate malaria transmission at both local and regional scales was used to examine impact of climate on malaria transmission in Cameroon. Specifics goals of the present work are:

- Understanding the links between climate parameters (rainfall, temperature) and population density on malaria incidence in Cameroon.

- Use the VECTRI dynamical malaria model, to check if it is able to reproduce the links between rainfall, temperature, population density and malaria transmission in Cameroon.

- Use VECTRI model coupled to the atmospheric regional climate model RCA4 to explore the impact of global warming under the Representative Concentration Pathway (RCP 2.6 and 8.5) on malaria distribution.

One impediment to these goals relates to the availability and reliability of malaria indices such as lab-confirmed cases, which are also often subject to restricted access for research purposes. We therefore make use of alternative databases of two malaria indicators, the parasite ratio (PR) and the entomological inoculation rate (EIR), which are metrics of the prevalence and the transmission intensity of the disease. For the EIR, a recent released database is used which contains year-long records of monthly EIR in order to examine the seasonality of disease transmission. First the relationship between these two malaria indicators, gridded climate and population density datasets are examined. Finally, VECTRI driven with temperature and rainfall data from five (5) RCA4 models to investigate future PR and EIR distribution over Cameroon.

The present dissertation has been subdivided in three chapters. The chapter one literature review, talks about generalities on malaria with emphasis on Cameroon, the mosquito and parasite life cycles, and generality on malaria modeling. Chapter two entitled, Study domain, Data and Methodology presents the VECTRI model, the used data and explains the methodology applied. Chapter three named Results and Discussions, presents the results, and discuss them. A conclusion that summarizes the results and gives outlooks for forthcoming researches, closes the document.

LITERATURE REVIEW

1.1 General overview of malaria in Africa

Malaria is transmitted through bites of infected females *Anopheles* mosquitoes. Both male and female feeds on various sources of sugar such as nectar, but female also requires blood meal which contains the necessary amount of proteins needed to produce eggs for reproduction [17]. This explain why only females *Anopheles* pick-up plasmodium parasite that transmit the disease. There are almost 465 recognised *Anopheles* species, but only 70 among them have the capacity to transmit human malaria [18]. In Africa, *Anopheles gambiae*, *arabiensis* and *funestus* are the most important. Figure 1.1 below presents the global distribution of dominant anopheles species in Africa. Anopheles mosquitoes are common in the West, Central, East and South African countries; even in South-Africa, Namibia and Botswana, anopheles are found in some locations. Countries in the Magreb zone like Algeria, Libya, Egypt, are anopheles mosquitoes free.
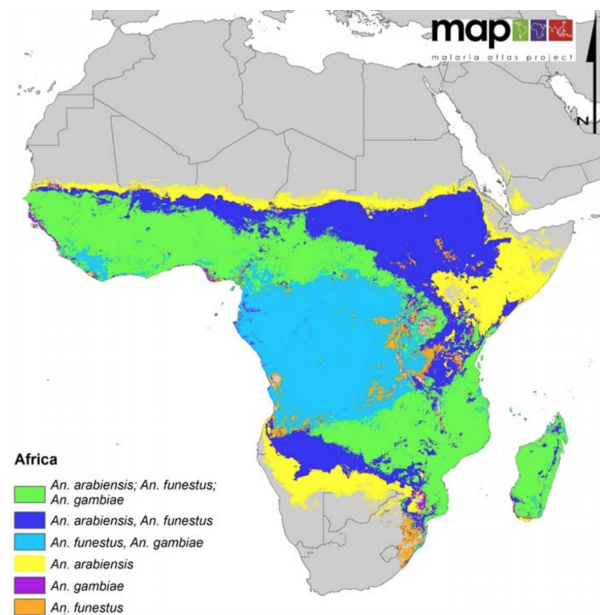
Figure 1.1: Distribution of the three most dominant malaria vectors in Africa [19].

1.2 Malaria parasite

Malaria is caused by a parasite called *Plasmodium*. There are more than 120 species of *Plasmodium* that infect various groups of vertebrates but only five of them can cause malaria to Human beings [7]:

- *Plasmodium falciparum* that predominates in Africa can causes serious form of malaria infections. Symptoms are usually high temperature, intense nausea, vomiting and diarrhoea [20]. The different blood stages in human are characterized by the presence of slightly smaller and numerous ring stages than the other species.

- *Plasmodium vivax,* is found mostly in Asia, Latin America, and in some parts of Africa. It causes benign tertiary malaria which can be identify by headache, nausea, anorexia and vomiting. Other symptoms include perspiration, shivers and very high temperature. The parasite has dormant liver stages that can activate and invade the blood several months after the infecting mosquito bite [21].

- *Plasmodium ovale* is found predominately in West Africa and in the islands of the western Pacific. It is biologically and morphologically very similar to *Plasmodium vivax.* In humans, these forms rapidly invade the liver and symptoms generally appear 9 days after the parasite has entered the blood system. The parasite's replication cycle lasts approximately 49 hours, causing tertian fever [22].

- *Plasmodium malariae* found worldwide, it has three-day life cycle. In the human, following introduction into the bloodstream, the liver is rapidly invade and If untreated, it causes a long-lasting, chronic infection that in some cases can last a lifetime [23].

- *Plasmodium knowlesi* is found throughout Southeast Asia. The parasite has a 24-hour replication cycle. Malaria causes by this parasite can rapidly progress from an uncomplicated to a severe infection in humans, with rapid development of anemia or renal failure [24].

1.3 *Plasmodium* life cycle

Plasmodium parasite requires both female *Anophele* and human as hosts to proceed and complete its life cycle. The different steps of the cycle are presented on figure 1.2 below.
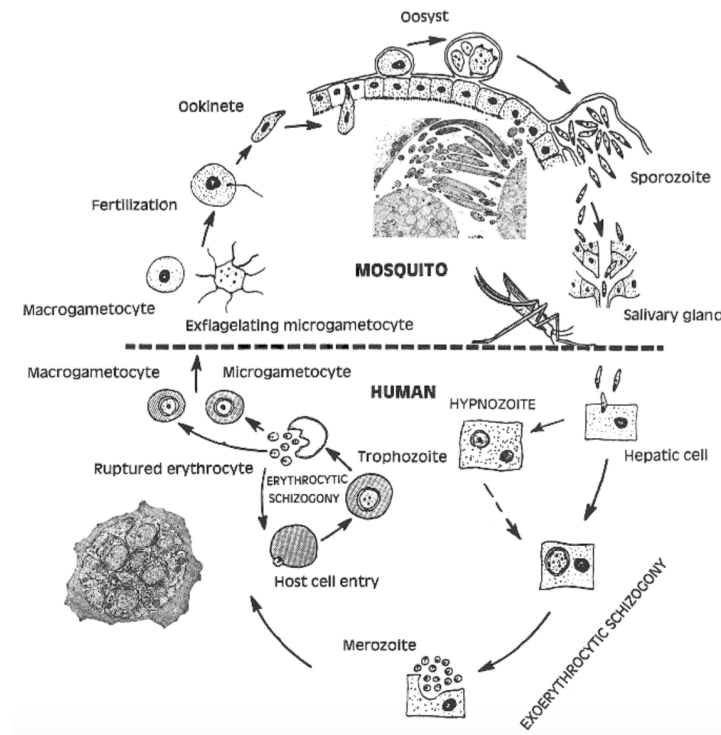
Figure 1.2: Life cycle of the malaria parasite. The cycle goes from an infected mosquito to human host, and from human to the mosquito [25].

During blood meal, an infected female *Anophele* inoculates sporozoites into the human bloodstream. The sporozoites take few minutes to an hour to migrate into the liver and invade their cells [26]. Within the period of 5-15 days depending on the plasmodium specie (5-9 days in *Plasmodium falciparum*, 11-13 days in *Plasmodium vivax*, 10-14 days in *Plasmodium ovale*, 15 days in *Plasmodium malariae* and 9-12 days in *Plasmodium knowlesi*), the parasite goes through an asexual multiplication process called schizogony, within the liver cells (hepatocytes) [27]. The infected hepatocytes are developed into schizonts, which when mature release the merozoites that will invade the red blood cells (erythrocytes). This step is known as the exo-erythrocytic stage of the parasite [28]. However, some sporozoites from *Plasmodium vivax* and *Plasmodium ovale* can either result in release of merozoites or establishment of hypnozoites which cause a latent phase of infection in the liver and can remain so for years [29].

Within the erythrocytes, merozoites are developed successively to rings, trophozoites and schizonts that mark the end of the erythrocytic schizogony stage [25]. This continuous replication process releases other merozoites ready to invade fresh red blood cells. The repeated

cycle is responsible for the disease, and length for about 48 hours for *Plasmodium falciparum*, *Plasmodium vivax* and *Plasmodium ovale*, 72 hours for *Plasmodium malariae* while *Plasmodium knowlesi* takes 24 hours [28] .

As the infection process goes on, some of the young merozoites develop into male and female gametocytes that circulate in the peripheral blood, and are taken up by uninfected females *Anopheles* during blood meal [30]. It marks the onset of the parasite sexual cycle within the mosquito: the sporogonic cycle. Further the gametocytes mature to female (macrogametocyte) and male (microgametocyte). After fertilization the fusion between them form zygotes which can takes around 24 hours to be transformed into motile ookinetes, which invade the midgut wall of the mosquito where they develop into oocysts [7]. From 7 to 30 days depending on the ambient temperature, the oocysts grow, mature and release thousands of sporozoites which migrate to the mosquito salivary glands. After about a day of residence, they became highly infective and ready for inoculation into a new human host to perpetuate the life cycle [27] .

1.4   Anophele mosquito life cycle

To understand malaria transmission, once has to know the different steps of mosquito life cycle. *Anopheles* mosquitoes go through four separate and distinct development stages: egg, larva, pupa, and adult which are presented on figure 1.3.
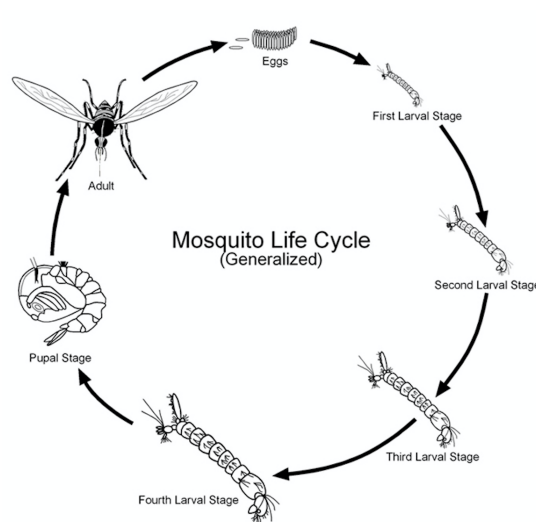
Figure 1.3: *Anophele* mosquito life cycle. (Source: Purdue University, Scott Charlesworth)

1.4.1 Egg stage

Mosquito eggs are laid in slow-moving or stagnant pools of water. Different species of mosquito prefer different water conditions; some prefer sunlight water bodies, whereas some prefer more direct sunlight. For instance, *Anopheles gambiae* the major vector in Africa known to breed in temporary clean and clear water [31]. Eggs are laid one at a time or attached together; they are almost transparent when first laid, but gradually darken to brown or black as they mature. Adult females can lay from 50-200 eggs per oviposition which takes between 2 and 4 days [7].

1.4.2 Larva stage

Larvae usually hatch from the eggs after a couple of days. They feed on algae, bacteria, and other aquatic insects and organisms, but themselves can also be eaten by fish, copepods and other creatures [32]. They live in the water and comes to the surface to breath because they lack the siphon. Each larva must shed its skin four times, before reaching the stage where it forms a pupa. This can take between 7 to 14 days, depending on the water temperature [33].

1.4.3 Pupae stage

The pupa stage is a resting, non-feeding but highly mobile stage. This is the time the mosquito turns into adult it takes about two days before the adult is fully developed. When development is complete, the pupa skin splits and the mosquito emerges as an adult [7].

1.4.4 Adult stage

The newly emerged adult rests on the surface of the water for a short time to allow itself to dry. The wings have to spread out and dry properly before they can fly, and males are usually first to emerge from the larval habitat. The duration of each stage depends on both temperature and species characteristics [34]. Male adult mosquitoes usually live for about a week, feeding on nectar. They also possess very bushy antennae for seeking females to mate with. Female mosquitoes have specialised mouth parts that allow them to feed on blood; they require the extra nutrients that blood meal provides in order to lay their eggs. The lifespan of a female adult depends on a number of environmental factors, but also her ability

to get sufficient blood meals; in nature, they usually live 1-2 weeks [7]. These growth stages are strongly influenced by rainfall, temperature, relative humidity, and other environmental factors.

1.5 Climate impact on malaria transmission

1.5.1 Rainfall

Regarding the transmission process of malaria, rainfall is a crucial parameter for the mosquito life cycle and for the life span of adult mosquito [35, 36]. The seasonality and amounts of precipitation may alter the abundance of aquatic habitats, the longevity and the productivity of the oviposition sites [37, 38]. Rainy seasons thus lead to high disease incidence than the dry seasons; figure 1.4 presents hotspot of malaria transmission during dry and wet seasons. Malaria risk surface is more important in figure 1.4 B during wet period than figure 1.4 A in dry period.
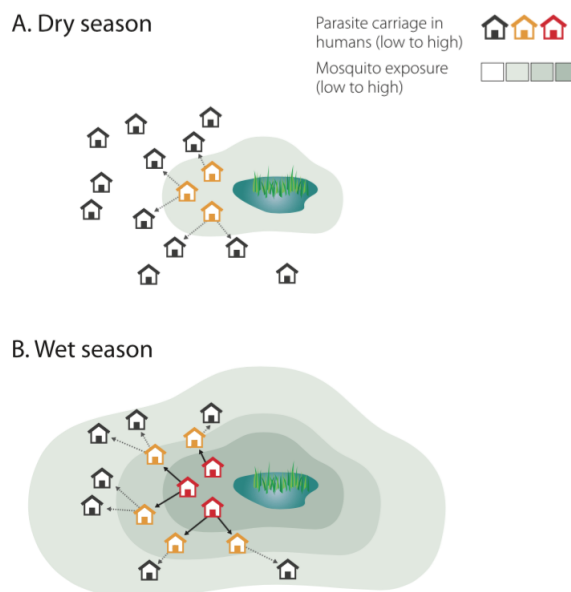
Figure 1.4: Malaria hotspot during dry(A) and wet(B) seasons [39].

A study conducted in Kintampo district in Ghana, found the abundance of *Anopheles* vectors to be strongly correlated with rainfall patterns [40]. In Mbita in western Kenya, high numbers of adults *Anopheles* were observed from November 2000 to February 2001 following extended rainfall events [41]. A study conducted in coastal south-western Cameroon

reveals that the density of anopheline species followed trends in rainfall patterns, with peaks during periods of heavy rainfall between July and September [13]. In Uganda, a study on epidemic of malaria associated with El Niño event in 1997 reveals that rainfall was positively correlated with vector density with one month gap [42]. Heavy and exceed rainfall was also one determinant cause of malaria epidemic that occurred in Ethiopia highlands between June and December of 1958 [43].

Inversely excessive rain may result in higher water levels, high flow velocities and flooding of water impoundments which are unfavourable to mosquitoes survival [44]. For instance, long-term reductions in rainfall in Senegal and Niger were associated with reductions in breeding sites for *Anopheles* [37]. In addition, in western Kenya the effect of natural rainfall on flushing, ejection and mortality of *Anopheles gambiae* larvae were explored. The results reveals that immature populations of malaria mosquitoes suffer high losses during rainfall events [45].

1.5.2 Temperature

Occurrence of malaria vectors is strongly influenced by temperature, although the overall relationship between development rate of *Anopheles* and temperature is non-linear [33]. The aquatic stages of mosquitoes develop faster as temperature increases [46], leading to an increase in adult turnover, vector density and disease transmission [47].

Laboratory experiments made between 10 and 40°C, to assess egg to adult anopheles development rate found the suitable growing temperature range between 16 and 34°C. Larval survival is shortest less than 7 days at 10-12°C and 38-40°C; and longest for more than 30 days at 14-20°C [48]. Similar laboratory study also found that the optimum temperature that leads to high larval survival was 27°C. At 30°C survival decreased as density increased [49]. Precisely for *Anopheles gambiae* and *arabiensis* survival to adult was highest at 25°C and start to decreased with increasing temperature [50]. Moreover experiments showed that if *Anopheles gambiae* pupae is maintained in constant light, the duration of the pupal stage is a direct function of temperature: It lasts about 2 days at 22°C but only 1 day at 32°C [51]. A more recent work found the rate of development from one immature stage *Anopheles* to the next one, increases at higher temperatures to a peak around 28°C; while high adult emerge was between 22 and 26°C [33].

The minimum temperature required for the development of *Plasmodium falciparum* and *vivax* is approximatley to 18°C and 15°C, respectively [38, 52]. Within the mosquito, a temperature-development model shows that diurnal temperature fluctuation around mean temperature < 21°C could speed up parasite development, whereas fluctuation around mean > 21°C lead to a slower development [53].

Study conducted in Usambara Mountains of Tanzania, on the sporozoite rate (the proportion of mosquitoes with sporozoites in their salivary glands) during 1997-1998, found the warmest month mean temperature of 20.6°C in the Mlalo basin was linked to the malaria outbreak [54]; indicating that temperature is important for sporozoite development. For Zimbabwe from 1988-1999, a model-study reported that annual mean values of temperature (20-22°C) was a strong positive predictors of increased annual incidence malaria rate whereas maximum and minimum temperature had the opposite effects [55].

1.5.3   Relative humidity

Relative humidity usually refers to the amount of moisture in the air. Mosquitoes survive better under conditions of high humidity than low. A study conducted in the Sahel region of Africa on mosquito desiccation, showed that extremely low levels of relative humidity were fatal to *Anopheles* mosquitoes [56]. More importantly, the mosquito life span is greatly enhanced at relative humidity over 60% thus increasing the chance that the mosquito will survive sporogony and became infectious to humans [57, 35].

In Senegal for example, during the month of October at the end of rainy season, relative humidity was found favourable for the development of mosquito vectors [58]. Also in Gambia, the number of adults *Anopheles gambiae* that increases towards the end of the dry season, was found to be linked to the increases of humidity [59]. In India, from 1970 to 2000 it was noticed that the average relative humidity range from 55 to 80% within the period of May to October, coincides with the maximum number of positive reported malaria cases [9]. Furthermore in southern China, an average relative humidity of 70-80%, represented one of the optimum conditions for malaria transmission [60]. Others studies conducted in Kenya found that, average maximum relative humidity of about 80% (for Ternan and Lunyerere) and 93% (for Nyalenda) provide favourable conditions for malaria transmission [61].

1.6 Population density and malaria transmission

Population density is a metric that helps distinguish malaria transmission intensity from rural, peri-urban and urban settings [62], due to land use patterns, density of households, access to basics social and health services and the dilution effect [63]. Low population densities in rural areas and high population densities in urban areas can influence malaria transmission substantially [64]. A survey in sub-Saharan Africa found a negative relationship between mean annual Entomological Inoculation Rates (EIR) and the level of urbanicity; with mean annual EIR values of 7.1 in the city centres, 45.8 in periurban areas, and 167.7 in rural locations [63]. Similar study found that urban areas are characterized by low malaria transmission, with the estimated annual EIR in city centres near to zero(0) and high as 54 have in peri-urban areas [65]. Another study carries out in sub-saharan Africa found the highest number of annual *plasmodium falciparum* EIR were in rural zones, precisely in locations with population less than 100 inhabitants per km^2 [62].

Field survey in southern Ghana found high malaria risk (almost 100%) in rural zones per year than urban areas (15%) [66]. In Tanzania between 2006 and 2014, a study found that the risk of malaria infection increased away from the city centre: lower parasite prevalence in administrative units in the city and higher in peri-urban suburbs [67]. A school parasitaemia survey for children in Ouagadougou in Burkina Faso found that the prevalence malaria rate were 24.1%, 38.6% and 68.7% in the centre, intermediate and periphery areas, respectively [68]. A more classification made in Chimoio in Mozambique found that sites with over 9000 people per km^2 were classified to be at the highest risk of malaria, those between 6001 to 9000 people per km^2 were classified to be at moderate risk, and those with less than 6000 person km^2 were classified to be at low risk [69].

Authough urbanisation is generally expected to reduce malaria transmission, the disease still persists in some African cities, in some cases at higher levels than in nearby rural areas [70]. For instance in Libreville town in Gabon, malaria transmission level was high and heterogeneous. The highest EIR was recorded in the most central and urbanized quarter, while the lowest were noticed in a peripheral area. This decrease of transmission from peri-urban to urban settings is probably socio-economic dependent [71]. School surveys conducted in Cotonou found that the prevalence rates of parasitaemia were 2.6% in the centre, 9.0% in the intermediate and 2.5% in the periphery zones. The reasons of this, might be associated

with urban transformation and/or a high bed-net usage [72].

1.7 Environmental impact on malaria transmission

1.7.1 Surface elevation

The effect of surface elevation on malaria incidence is important. Increasing in altitude was related with decreasing mosquito abundance [73]. Breeding *Anopheles* mosquitoes sites are more common in lowland than highland [74]. This lower incidence is most likely due to the decreased temperatures at these altitudes [75, 76]. With every 1000 meters of elevation, temperature decreases by an average of 6°C, highland areas are then often inadequate to support sustained malaria transmission [77]. Temperature in highland zones, low temperature prevents parasite development in mosquitoes during rains periods; malaria vector abundance is thus limited [78].

Field study in Tanzania revealed that, EIR were about seven times greater in the lowland than the highland areas, malaria morbidity was also less prevalent in the highlands than the lowlands [79]. In Usambara village in North-east Tanzania altitude was negatively associated with malaria risk with evidence of a malaria infection at a lower elevation [74]. Furthermore, in Kenya, the overall prevalences of *Plasmodium falciparum* parasite were significantly higher in the lowland villages (24%), than in the highland villages (2%) [80]. A study conducted in Northern Ethiopia, reveals an appreciably greater amount of malaria in villages at altitudes below 1900 m than above [81].

1.7.2 Permanent water bodies

Water bodies areas are characterised by predominance of water which determines the nature of soils [82], that can be completely partially or temporarily inundated. Such areas are likely to serve as potential habitat for water-bound stages of malaria vectors [83]. Malaria burden may indeed rise after impoundment of large bodies especially at the vicinity of humans habitations. Field studies have established the relationship between malaria transmission and water bodies. For example a study conducted in Ethiopia showed that, the proximity to water reservoirs was associated with greater disease rates in periods of intense transmission. The number of positive malaria cases decreases when moving away far from the reservoirs [84]. More, assessing the impact of construction of micro-dams on the disease

occurrence, further works proved that the overall incidence of malaria for the villages close to dams was higher for children under 10 years living in villages within 3 km, than those living within 8-10 km [85].

In Shri Lanka a field study found that, people living within 750 m of the local stream, were at much higher risk for malaria than people living further away [86]. Similar study conducted in Mozambique classified areas with less than 500 m from a water source as high-risk areas of malaria [69]. Another study conducted in western Kenya demonstrated that the proximity to terrain with high predicted water accumulation was associated with increased household-level malaria incidence; most of the reported malaria households were located 280 m closer to regions with very high wetness indices [87]. More higher abundances of adults *Anopheles gambiae* and *funestus* were found along the Yala river valley and more than 80% of anopheline-positive habitats identified were located within 100 m of the nearest streams [88]. Furthermore, in an endemic malaria region of Shri Lanka, the imposition of a buffer zone of 200 m around water bodies from houses, was estimated to lead to a 21% reduction of the malaria incidence in the overall population and a 43% reduction in the relocated community [89].

Each water body can be easily identify by its particularities, but the most common one is the groundwater level that can be near the surface or not [90]. The water in such areas is also controlled by hydrological processes. Some namely main water bodies are lakes, streams, rivers, but also swamps: situated within forests and dominated by trees; marshes: frequently inundated and dominated by emergent herbaceous vegetation; bogs: characterised by wet spongy, water provided directly from rain; fens: dominated by grasslike plants, water provided from surfaces and groundwater sources; mangrove: a tidal swamp is sensitive to the cold, most found in tropics and subtropics regions [88, 90, 91].

1.7.3   Land use change

Some land use changes process are likely to modify the hydrology of an area and create new favourable breeding conditions for malaria vectors. For instance, irrigation projects in endemic areas were noticed to increase the number of breeding habitats, thus malaria transmission [92]. In India in the 1990s, malaria became endemic and widespread in a population of about 200 million, after a poorly constructed irrigation projects improved breeding

conditions of malaria vectors (*Anopheles culcifacies*) [93].

Agricultural pratices that combine deforestation and irrigation can increase malaria risk. In Thailand for example, cassava and sugarcane cultivation led to creation of widespread breeding grounds for *Anopheles minimus* [94]. Similar work was conducted in highland area in Uganda from December 1997 to July 1998 for villages located along papyrus swamps. The study found that all the measured malaria indices, were on average high near cultivated swamps [95]. In Ghana, Swampy areas and banana/plantain production at the vicinity of villages were strong predictors of a high malaria incidence. Precisely, an increase of 10% of swampy area coverage in the 2 km radius around a village led to a 43% higher malaria incidence; further each 10% increase of area with banana/plantain production around a village tripled the risk for malaria [96].

Malaria endemicity was also noticed to follow deforestation process [97]. A study conducted in the Peruvian Amazon found that biting rates of *Anopheles darlingi* in deforested areas were 278 times higher than bitting in the forested areas [98]. Distance from human habitations to high wetness zones were found to account for differences in malaria risk. In Kenya for instance, 423 malaria case households were located 280 m closer to regions with very high wetness indices [87]. Further, in Dar es Salaam, a study found a dependance relationship between the wetness idex and the *Plasmodium* parasite prevalence [67].

1.8 Malaria in Cameroon

Malaria is a major public health problem in Cameroon. It is an endemic illness and the leading cause of morbidity and mortality in the country [99]. Its transmission is aggravated by changes in climate, poverty, and lack of efficient mechanism of control, but also new parasites strains. Children under five and pregnant women are the most vulnerable population categories accounting 22% of morbidity and mortality risk [99, 5]. The 2000-2010 national health report noticed that malaria was responsible for medical consultation (40 - 45%), morbidity (50%), deaths in children under five (40%), deaths, (30 to 40%), days spent in hospital (57%) and sick leave (26%) in the country [100, 101]. Moreover, the 2008 World Health Organisation report, mentioned that Cameroon had an estimated 5 million malaria cases in 2006, with an average of 100 cases noticed per 1000 inhabitants [99]. Figure 1.5 shows malaria distribution map for Cameroon in 2005 produced by the MARA (Mapping

Malaria Risk in Africa) project. The map presents the whole country as malaria endemic but also some marginal endemic zones like Yaounde, and the highland ares (West, South-west and Adamaoua).
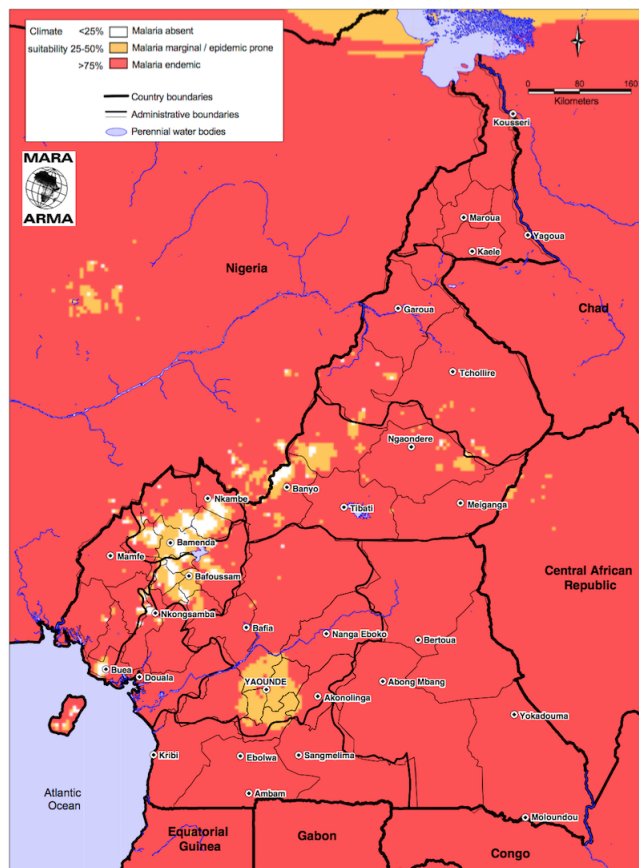
Figure 1.5: Malaria endemicity in Cameroon (Source: MARA project).

1.8.1 Economic costs of malaria in Cameroon

There is an evidence that malaria burden is greatest among the poorest countries in sub-saharan Africa. It contributes towards national poverty through its impact on foreign direct investment as tourism, labour productivity and trade [102]. Studies conducted across severals countries between 1965-1990 period confirm the relationship between malaria and economic growth [103]. In Cameroon malaria has a noticed socio-economical impact, and can easily drive affected population to poverty. Indeed It was found to be one major reason of 40% of household expenses [101]. A study focussed on the direct malaria costs for households in some African countries, found the highest cost being in urban Cameroon settings comparatively to others countries [104]. For this purpose, Cameroon government have recently instructed

the free treatment of uncomplicated malaria cases, for children under five years of age and pregnant women [100].

1.8.2 Ecological niche profile of malaria vectors in Cameroon

The high incidence of malaria in Cameroon is not surprising, this because Cameroon's anopheline fauna is one of the richest in Africa with almost 48 species [105]. But only 13 of them hold sporozoites that makes infectious; with *Anopheles gambiae*, *Anopheles funestus* and *Anopheles arabiensis* being the most common across the country [106, 107]. Figure 1.6 that follows represents the global distribution of anopheles species present in Cameroon. In terms of species distribution, Hamadou et al [108] found *Anopheles gambiae* alone accounts for 90% with the remaining 10% made up of *Anopheles funestus, arabiensis* and others [108].

Figure 1.6: Mapping of malaria vectors distribution in Cameroon. *Anophele gambiae* is the most present in the country [109].

Similar to other Sub-Saharan African countries [8, 110, 58, 111, 112], there is a spatio-temporal variation in malaria transmission across ecological zones in Cameroon. Specifically there is:

- The Soudano-Sahelian zone, where *Anopheles arabiensis, funestus* and *gambiae* are the most present;

- The Adamaoua plateau that hold *Anopheles gambiae and funestus* as majors vectors;

- The South equatorial forest with *Anopheles gambiae* as major but also *Anopheles moucheti* and *Anopheles nili* along the Sanaga river;

- The Western plateau and in Atlantic coast where *Anopheles gambiae* is predominant.[113, 108, 109, 114].

1.8.3 *Plasmodium* parasites in Cameroon

Among the five *Plasmodium* species known to infect human, four are prevalent in Cameroon. Namely *Plasmodium falciparum*, *Plasmodium vivax*, *Plasmodium malariae* and *Plasmodium ovale* [115]. These species are distributed along the major hydro-ecological zones of the country but *Plasmodium falciparum* is the most common one [116]. Table 1.1 presents proportion of human malaria parasites distribution in Cameroon, across the different ecological facies.

Table 1.1: Distribution of the major human malaria parasite species in Cameroon [117].

Ecological facies	*P. falciparum (%)*	*P. malariae (%)*	*P. ovale (%)*
Adamaoua facies	100	0	0
Savanah-forest facies	93.6-98.7	0-6.4	0-1.3
Transition facies	89.8-100	4.3-8.4	0-1.8
Forest facies	62.0-96.3	0.6-3.0	1.1-35.0
Altitude facies	91.5-96.0	1.7-7.0	0-6.8
Coastal facies	97.7-100	0-0.7	0-2.3

1.8.4   Climate and malaria incidence in Cameroon

Seasonal variations in malaria is highly sensitive to climate variables. The disease is controlled by rainfall, as temperatures are usually within the range that support both mosquito survival and parasite development [118, 119]. During the onset of monsoon season, temporary transient ponds and puddles become abundant, and can serves as potential breeding habitats for malaria vectors [58].

Studies have been carried out to understand this spatio-temporal variation over some towns and villages in the country. For example, from June 1997 to May 1998, in Koundou and Ebolakounoua located in the South Cameroon, a rapid increase in the anopheline population at the beginning of the rainy season was immediately followed by a parallel increase in the entomological inoculation rate in both villages [120]. The annual EIR value of 31 infective bites per person, were obtained with peak in the month of May during the rainy period [121]. In the southwest region of Cameroon, a 12-month survey from August 2001-July 2002 found *Anopheles gambiae, funestus* and *nili* to be the human malaria vectors in the areas. Anopheline density and EIR, were correlated to the rainfall variability during the study period. Annual EIR values for Tiko, Limbe and Idenau were 287, 160 and 149 infective bites/person respectively, within July to September, period of intensive rainfall in the areas [13]. Further, in Nkoteng village located in the Centre region where both *Anopheles funestus* and *gambiae* are present, a survey from February 1999-October 2000 found all year-round malaria transmission with peaks value of 15.4ib/p/m in June 1999 and 15.7ib/p/m in April 2000, both within periods of higher rainfalls events [11].

Heavy rainfall can also negatively impact malaria occurrence. For instance in Buea municipality in the Southwest region of Cameroon, within 2010-2014, a negative correlation was found between malaria incidence and rainfall in July and August during the rainy season. Meanwhile a positive correlation was found with temperature within the same months. This is because very high rainfall causes overland flow which then sweeps away mosquito eggs from the breeding habitats [122].

1.8.5   Human activities and malaria incidence in Cameroon

Human activities like agriculture, water drainage or deforestation are likely to increase or decrease malaria endemicity in the country. For example an entomological study from

May 1997-May 1998 were conducted in Ebolakounou (forest area), and Koundou (degraded forest area) all located within the Mengang district in the South region. The result present malaria intensity in the degraded forest habitat in Koundou (EIR: 176.1 ib/p/y), 10 times higher than in the forest habitat in Ebolakounou (EIR: 17.7 ib/p/y). Peaks of transmission occurred with one month lag time following heavy rainfall events [12]. Another series of surveys conducted in 386 villages across the ecological zones in the country, reveals that the distribution of major malaria vectors were strongly affected by the impact of human activities on the environment [113]; productive ecological niches of mosquitoes were sunlight exposure, rainfall, evapotranspiration, relative humidity or wind speed dependent.

Agriculture activities may also increase human malaria incidence in Cameroon. For instance Ngom et al, [123] found that rainfall and proximity to urban agricultural activities are the most important ecological factors accounting for variability in malaria transmission in Yaounde, with *Anopheles gambiae* playing a key role in the transmission process. Furthermore a study in Gounougou within a rice cultivated area in the North region, characterised by a long dry season (from April to November), found high density of *Anopheles gambiae, rufipes, coustani* and *welcomei* species in July, August and second half of September, during the dry season [124]. A similar study was conducted in the rubber cultivated area of Niete in south Cameroon. From a total of 1187 *Anopheles* collected, 35.3% were caught during the rainy season and 64.7% within the dry season [125]. Malaria in Niete is noticed both in the dry and rainy season, but with the peak during the dry season, surely because of farming activities in the zone that increase the *Anopheles* number at that period.

1.8.6   Inland water bodies and malaria in Cameroon

Local hydrology of an endemic malaria area may impact on *Anopheles* vectors density. Permanent water bodies like rivers, lakes, streams etc. or stagnant water around residences are likely to provide appropriate larval breeding sites in dry periods. For instance, in 1959 the considerably abundance in intensity of *Anopheles gambiae* noticed during dry season, in the villages situated along the Sanaga river, were attributed to new breeding sites situated at the edges of the river [126]. Additional study found that the, mean densities of *Anopheles gambiae* were 5 times higher in houses located at 200 m than those at 1.5km from the Sanaga river [127]. A study conducted in Mbalmayo in the South Cameroon, demonstrated that the river Nyong and its banks were the most important permanent breeding source for all malaria

vector a very high vector densities were found very high in the vicinity of the river Nyong, and rapidly decreased with distance from the river [128].

A similar entomological study were conducted in two communities, Simbock and Etoa, irrigated by water from the Mefou and Biyeme rivers. The results demonstrated the endemicity of malaria during both wet and dry seasons. Individuals in Simbok receive about 1.9 and 1.2 infectious bites per night in the wet and dry season, respectively, whereas those in Etoa receive 2.4 and 0.4 infectious bites per night, respectively [129]. In Molyko, located in Southwest Cameroon, a study were conducted among pupil aged 4-15years on environmental factors accounting in malaria occurrence. The results demonstrated that, stagnant water around residences was associated with significantly higher malaria parasite prevalence, when compared to those who did not have stagnant water around their home [130].

1.8.7 Urbanisation and malaria in Cameroon

The process of urbanisation is likely to influence malaria transmission in Cameroon. The 2010 national census report estimated that over 52% of the population live in urban areas and the total urban population has almost doubled in the last 25 years [131]. A study in rural and semi-urban communities in the Southwest found a high malaria parasitaemia prevalence in the rural than semi-urban settings. This due to specifics characteristics of rural settings (predominance of plank houses, absence of health facilities, proximity of animals sheds to sleeping areas) that may facilitate human-mosquito contacts [132].

In Cameroon, malaria incidences vary across different social groups. For instance, a study in Molyko among pupils belonging to poor middle and rich classes in 2000 and 2004 showed that the presence of malaria was significantly associated with the social class of the pupil [133]. Another comparative study were conducted for pupils in rural Bomaka and Urban Molyko, both in the Southwest region of Cameroon. Among the overall 33% of malaria prevalence, children from Bomaka had higher value (38.51%) than those from Molyko (25.58%) [130]. Then urbanisation process may influence by reducing malaria endemicity in Cameroon.

1.8.8 Malaria control in Cameroon

Interventions strategies against malaria in Cameroon usually take place at the level of vectors, with the use of indoor residual sprays and Insecticide Treated Mosquito Nets (ITNs).

A study in Yaounde and Douala, the two most populated cities in Cameroon investigated the coverage of various malaria control methods. Their results showed that, environmental sanitation (76.1%), use of bed nets (69%), insecticide spray/coils (12.3%) and netting of doors or windows (1.9%) were the methods used for malaria prevention in these cities [134]. But protection by the use of ITNs is the major government strategies for controlling malaria. For instance, the National Malaria Control Programme (NMCP) distributed about two millions of ITNs within the period 2004-2009 in Cameroon, with emphasise on children under 5 years old and pregnant women [100].

Between 1997 and 1998 in Mbadjock, located in the South, a study were conducted on the malaria incidence, after about 4,000 impregnated bed nets were distributed to the population. The results found a significant decrease of mosquito parity rate; 52% before and 46.5% after bed nets distribution. EIR was also reduced by 74% varying from 124.1 ib/p/y before, to 32.5 ib/p/y after two (2) bed nets distributions sessions [135]. Another study conducted in the South, in Mbebe village after two bed-nets impregnations sessions in January 1991 and March 2000. The obtained results demonstrated that the use of ITNs significantly decreases malaria incidence in the village; Human Biting Rate (HBR) decreases by 60% and EIR by 78% [136].

Nevertheless, the 2006 World Health Organisation survey found that 32% of households owned a simple mosquito net, 20% an Insecticide Treated Nets (ITN), but only 13% of children slept under [1]. The government then came on a scaling-up process of ITN coverage in 2011, in line with the Roll Back Malaria (RBM) program recommendation of universal coverage [137, 138]. The direct impact was then assess in a community in South west Cameroon between August and December 2013 after the free distribution campaign of ITNs in 2011. Results showed that, use of ITNs by participants was associated with reduced asexual *parasitemia* prevalence, a measure of malaria endemicity [132].

1.9 Malaria modelling

1.9.1 Overview

Roland Ross was the first to develop a mathematical model of malaria transmission in 1911 [139]. The model was formulated using deferential equations describing the rate of

transmission between the host-compartments; how the disease is transmitted from vectors to human hosts and vice versa. In the 1950s further developments were made by Macdonald, in order to improve Ross' model. For instance the proportion of infective anopheline (*Anopheles* with sporozoites in their glands) bites were added in the equations [140]. Therefore several modelling works have been conducted based on the Ross-Macdonald model. One of the most famous, regarding malaria dynamics and immunity is the Garki model [141] and its improvements [142, 143, 144]. Others studies expanded these first models by using different approaches like accounting for population density [145, 146] or environmental conditions [147].

Malaria transmission have been also investigate using severals dynamical models. Many of these model are driven by climate parameters like rainfall, temperature, humidity and etc. They may also serve as a predictors for future disease outbreaks [148, 149, 150]. Such climate-driven malaria models are able to assess each step of the transmission process using daily data [36] at local or regional scale. For instance, the Liverpool Malaria Model (LMM), relate the oviposition rate to a 10 day rainfall rate [14].The HYDrology Entomology and MAlaria Transmission Simulator (HYDREMATS) model developed for Sahelian zones [16] runs at very high resolution (10 metres) and incorporates land cover and topography data in simulating breeding pool formation and persistence, and the inter-annual variability in malaria vector mosquito population. When the model was applied in the Banizoumbou village in Southwest Niger between 2005 and 2006 wet seasons showed a good agreement with observations, and was able to predict seasonal mosquito abundance [16]. Another model, the VECtor-borne disease community model of the International Centre for Theoretical Physics, TRIeste (VECTRI) [10] accounts for the impact of both climate and human populations.

1.9.2   Malaria modelling in Cameroon

Some modelling works have been conducted for Cameroon at the level of vectors environmental niches. For instance, a survey was conducted in 386 villages covering the full range of ecological settings of the country in order to model the ecological niche of mosquito vectors. The distribution of major malaria vectors were found to be strongly influenced by the impact of humans on the environment. In addition, the productivity of the ecological mosquitoes niche was link to sunlight exposure, rainfall, evapotranspiration, relative humidity and wind speed [113]. A malaria-climate and socioeconomic approach discover that, rainfall and prox-

imity to urban agricultural activities are the most ecological factors associated to malaria transmission in Yaounde, with *Anopheles gambiae* playing a key role in the transmission process. The disease occurrence was also noticed to be higher all along the small rainy season and dropped down during the two dry seasons [123]. Another model approach was developed to define the limits of contemporary malaria transmission. The model uses a basic reproduction number metric, and the result demonstrated that projections at scale related to population can potentially deliver adequate highlight on the number of individuals at risk of malaria infection [151].

STUDY DOMAIN, DATA AND METHODOLOGY

2.1 Study domain

2.1.1 Geographical description

The study domain covers central Africa between 1-13°N and 7-17°E as presented on figure 2.1. Cameroon territory is our specific point of interest.
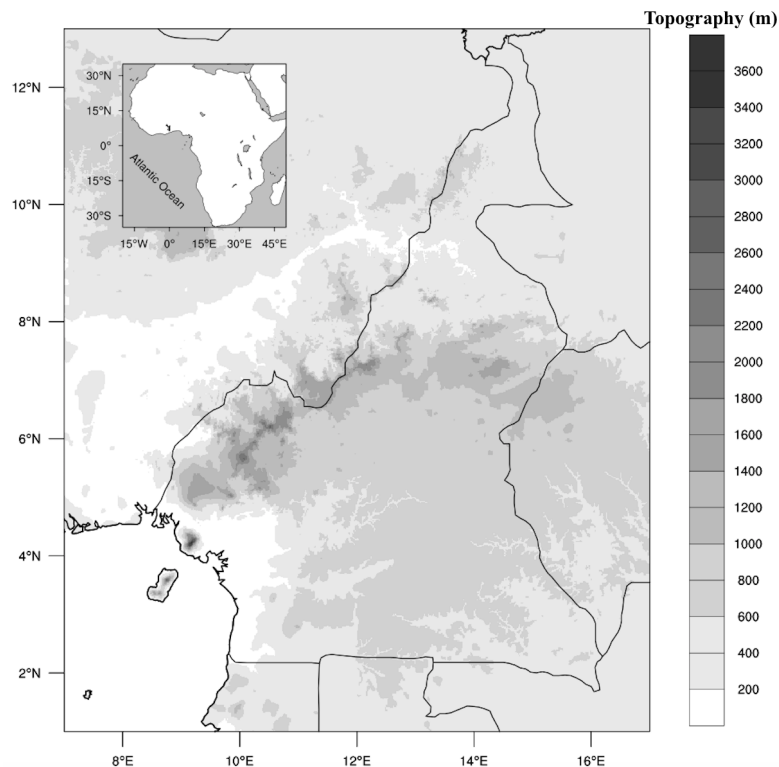
Figure 2.1: Study domain, map of Cameroon and boundaries countries. On top, the map of Africa and position of Cameroon.

2.1.2 Climate

The area climate varies from humid in the south to arid and hot in the north. Cameroon's climate is particularly influenced by the Harmattan and the Atlantic Monsoon winds, and characterised by two climatic domains. The tropical climatic domain that stretches from the north and extending to the Sahel zone ($\sim 8°$ to 13°N) [152, 153] and the humid equatorial domain covers the rest of the country ($\sim 1.5°$ to 8°N).

The equatorial domain is characterised by heavy rainfall events, with increasing temperatures and a degrading vegetation as one moves far from the equator [154]. It presents four distinct seasons: a major rainy season (March to June), a dry season (July and August), a minor rainy season (September to November) and a dry season (December to February) [109, 155]. This domain is also divided in three sub-types. First the guinean type that extends from the coast and covers the southern plateau with abundant rainfall up to 2200 mm/year with average temperature of 25°C [156]. Second, the Cameroonian type which is dominant in the southern part of the south Cameroon plateau, extending into the east of the country (with mean temperature of 23°C and total rainfall below 1500 mm/year). The third one is the Guinean-sudanese type with longer dry seasons and minimum rainfall [154].

The tropical area that is associated with high temperatures and low rainfall, has one rainy season (May to October), and one dry season (November to March). The length of these seasons is likely to change depending on the topographical profile of the area [109, 155].The domain is also subdivided into three zones. The tropical humid zone in the Adamaoua plateau (rainfall up to 1500 mm/year and average temperature of 20°C), the Sudanian zone around the Benoue basin (rainfall 1200 mm/year and average temperature up to 28°C), and the Sahelian zone in the north, identified with its accentuated drought (rainfall less than 900 mm/year and temperature that can reach 33°C during the long dry season) [152, 156].

2.2 Materials

2.2.1 Climate Data

The mean rainfall and temperature of Cameroon and neighbours countries from 1985 to 2006 (study period) is presented on Fig 2.2. It shows higher rainfall intensity in the western and coastal part of the country and increasing mean temperature moving to the

north towards the Soudano-Sahelian zone. These precipitation data are obtained from Famine Early Warning Systems Network ARC vesion 2 (FEWS-ARC2) [157], while temperature data is taken from the ECMWF ERA-Interim reanalysis data [158].

(a) Rainfall (mm/day)
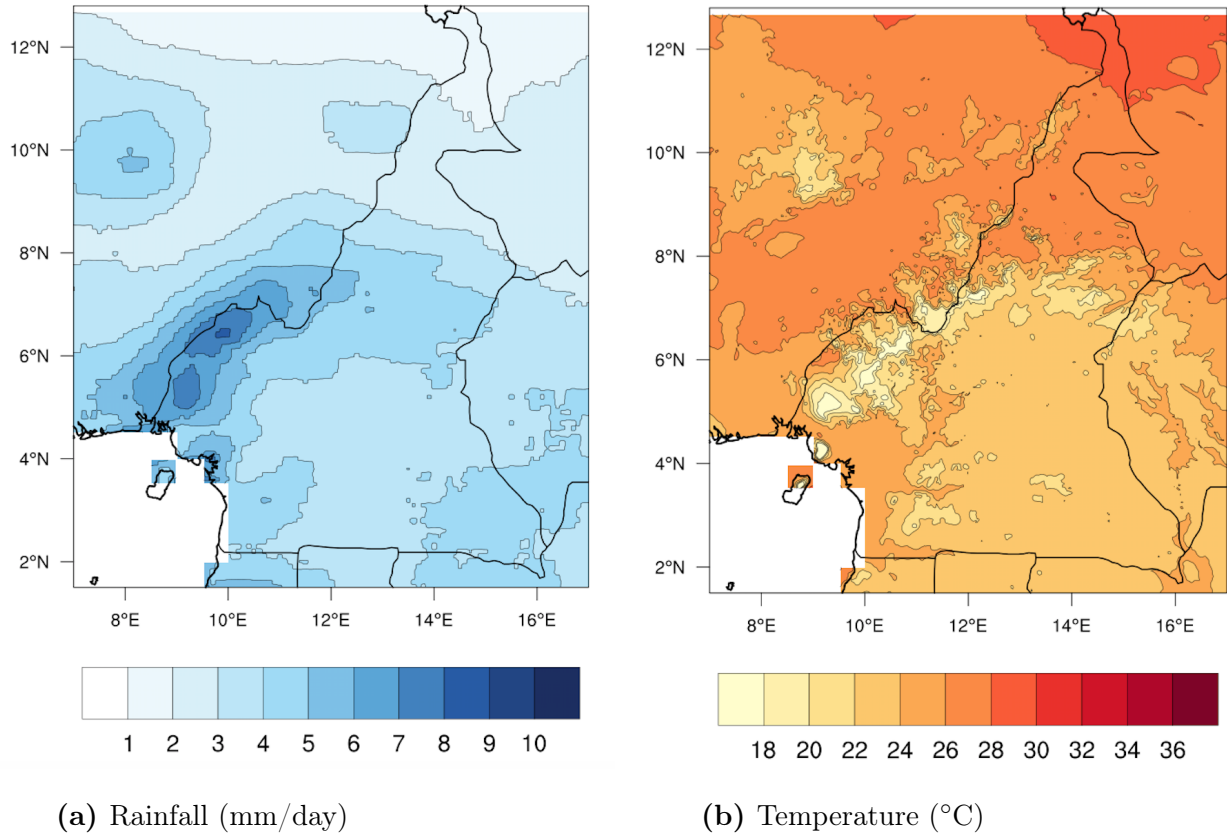
(b) Temperature (°C)

Figure 2.2: Map of Cameroon and neighbouring countries showing mean daily rainfall and temperature from 1985 to 2006.

2.2.2 Malaria Data

Two malaria indicators are used in this study. The parasite ratio (PR) that expresses the proportion of individuals infected at a given point in time [159]. A publicly available database of parasite ratio is obtained from the Malaria Atlas Project (MAP) program [140]. The public PR database consists of data collected by individuals researchers or organisations and published in the literature, which were collected within the MAP program. Table 2.1 presents all the data points used for this work in Cameroon; Consisting of 103 surveys, with a total of 18011 people tested, with the survey dates ranging from 1985 to 2006.

Table 2.1: Sites of PR data points used in Cameroon ranged from 1 to 103.

Site	Longitude	Latitude	Reference	Site	Longitude	Latitude	Reference
1	11.507	3.872	[160]	53	11.0833	4	[161]
2	13.507	9.398	[162]	54	14.364	4.978	[161]
3	11.899	4.449	[163]	55	13.584	7.324	[161]
4	14.932	10.902	[164]	56	9.3833	4.6666	[161]
5	10.412	5.486	[161]	57	11.116	4.201	[165]
6	10.126	3.797	[161]	58	11.523	3.876	[160]
7	9.238	4.153	[166]	59	9.364	4.07	[13]
8	11.149	4.216	[165]	60	11.033	4.131	[161]
9	11.432	3.717	[167]	61	11.415	3.682	[161]
10	11.526	3.886	[168]	62	12.668	2.664	[169]
11	10.126	3.797	[170]	63	11.483	3.816	[129]
12	10.126	3.797	[170]	64	10.178	5.164	[161]
13	11.502	3.875	[170]	65	9.282	4.167	[133]
14	11.05	4.2	[165]	66	11.449	3.8833	[161]
15	10.15	5.2	[161]	67	8.983	4.234	[13]
16	9.193	4.015	[171]	68	9.509	4.666	[172]
17	13.66667	9.08333	[173]	69	11.615	3.767	[174]
18	8.999	5.184	[161]	70	11.149	4.216	[165]
19	13.584	7.324	[175]	71	13.53333	7.32222	[161]
20	11.483	3.767	[129]	72	11.017	4.134	[165]
21	11.525	3.852	[176]	73	11.05	4.2	[165]
22	14.4333	4.9833	[161]	74	12.63	2.73	[177]
23	9.932	2.351	[178]	75	9.2463	4.4549	[172]
24	10.517	3.85	[161]	76	13.34	2.72	[177]
25	10.118	2.81	[161]	77	11.016	4.2	[165]
26	11.033	4.131	[165]	78	9.441	4.625	[172]
27	9.298	4.166	[179]	79	9.461	4.637	[172]

Table 2.2: Table 2.1 continued.

Site	Longitude	Latitude	Reference	Site	Longitude	Latitude	Reference
28	15.087	10.638	[164]	80	13.52	8.78	[177]
29	9.435	4.634	[180]	81	10.517	5.149	[161]
30	11.483	3.816	[129]	82	11.033	4.131	[161]
31	12.37	4.663	[170]	83	14.26	8.45	[177]
32	9.364	4.07	[171]	84	11.6	3.768	[174]
33	14.2	10.4	[178]	85	9.45	4.501	[172]
34	11.07	4.134	[165]	86	9.455	4.605	[172]
35	14.327	10.594	[181]	87	14.327	10.594	[175]
36	9.45	4	[182]	88	9.299	4.2	[183]
37	15.043	10.878	[164]	89	12.64	2.69	[177]
38	9.705	4.047	[171]	90	9.3833	4.6666	[161]
39	9.238	4.153	[184]	91	9.3305	4.5447	[172]
40	9.238	4.153	[184]	92	9.436	4.639	[172]
41	9.282	4.167	[133]	93	9.451	4.534	[172]
42	9.435	4.634	[185]	94	9.2	4.483	[172]
43	11.016	4.2	[165]	95	12.67	2.43	[177]
44	14.692	6.8333	[186]	96	9.467	4.833	[172]
45	10.05	5.452	[163]	97	12.52	2.77	[177]
46	9.193	4.015	[13]	98	13.53	8.75	[177]
47	11.623	4.444	[187]	99	9.463	4.63	[172]
48	9.932	2.351	[178]	100	9.249	4.466	[172]
49	11.523	3.876	[160]	101	11.116	4.201	[165]
50	9.936	4.956	[188]	102	13.65	8.27	[177]
51	9.193	4.015	[189]	103	14.09	8.29	[177]
52	11.483	3.816	[129]				

The second malaria indicator is the entomological inoculation rate (EIR), which measures the number of infected bites received per person for a given period of time [140], and as such is an indicator of the malaria transmission intensity. It is often calculated as the product of the human biting rate (HBR) and the sporozoite rate. HBR represents the number of bites per person per day, while the sporozoite rate is the fraction of vector mosquitoes that are infectious [190]. A new database of monthly EIR values has been constructed from various sources for all Africa by Yamba et al [191], with the emphasis on long term field studies lasting at least a year, in order to be able to study the seasonality of malaria transmission. For Cameroon, the database has recorded 16 sites with validated data presented in table 2.3. The rarity of long-term, continuous monthly EIR records that allow the analysis of seasonality, necessitates the use of data from 30 years ago, but we reiterate that this has the advantage that recent upscaling of (sometimes seasonal) interventions does not obfuscate the analysis. The availability of data for only two years in time precludes any analysis of longer terms changes in seasonality that may be associated with climate warming which could potentially be significant [192].

Table 2.3: Sites of EIR data points for Cameroon. Indicated are sites names, study period and their geo-referenced locations

Site	Location	Longitude	Latitude	Period	Reference
1	Sanaga village	11.52	4.92	April 1989-March 1990	[193]
2	Mbebe	10.12	3.38	April 1989-March 1990	[194]
3	Nkol-bikok	11.52	3.87	March 1989-February 1990	[118]
4	Nkol-bisson	11.44	3.86	April 1989-March 1990	[118]
5	Limbe	9.19	4.02	August 2001-June 2002	[13]
6	Tiko	9.35	4.07	August 2001-June 2002	[13]
7	Likoko	9.3	4.39	October 2002-September 2003	[195]
8	Essuke-camp	9.31	4.1	October 2004-September 2005	[196]
9	Ebogo	11.47	3.4	April 1991-March 1992	[197]
10	Simbock	11.3	3.5	January 1999-December 1999	[198]
11	Koundou	12.12	3.9	June 1997-May 1998	[199]
12	Ekombite	11.83	3.12	January 2007-December 2007	[200]
13	Nsimalen-Ekoko	12.12	3.82	April 1991-March1992	[201]
14	Nsimalen-Nkol-mefou	11.58	3.62	April 1991-March1992	[201]
15	Nsimalen-3	11.55	3.72	April 1991-March1992	[201]
16	Ndogpassi	10.08	3.48	January 2011-December 2011	[121]

All database entries have been quality controlled in terms of data collection methodology and geographical location to ensure continuity across the collection period.

In addition to climate, others factors such as population density, vicinity to permanent water, socioeconomic conditions, conflict, breakdown in health services, population movements and interventions can influence malaria transmission. However most of the factors are difficult to account in models due to lack of reliable data to quantify their effect. As long as these factors are not correlated with spatial or temporal variability of climate, they will act as a form of noise in the analysis, increasing scatter in the climate-malaria relationships, but not obscuring them completely if climate is a significant driver of malaria variability. This is also the case for data inaccuracies and uncertainties in both the climate due to instrument error and sampling uncertainty [202] and health records. One complication might be if these

factors influence the trends over the period, but this would most likely be associated with ramping up of interventions (climate trends are captured in the analysis) and this period predates the large-scale up of interventions that occurred in Cameroon that could confound the climate-malaria relationship. In addition, there is no evidence for major changes in vector distributions during this period, therefore this study assumes that such changes would not have affected the mean climate-malaria relationships.

PR and EIR data sites are highlighted on Fig 2.3. The majority of surveys points are located in the west, the far north and east of the country.
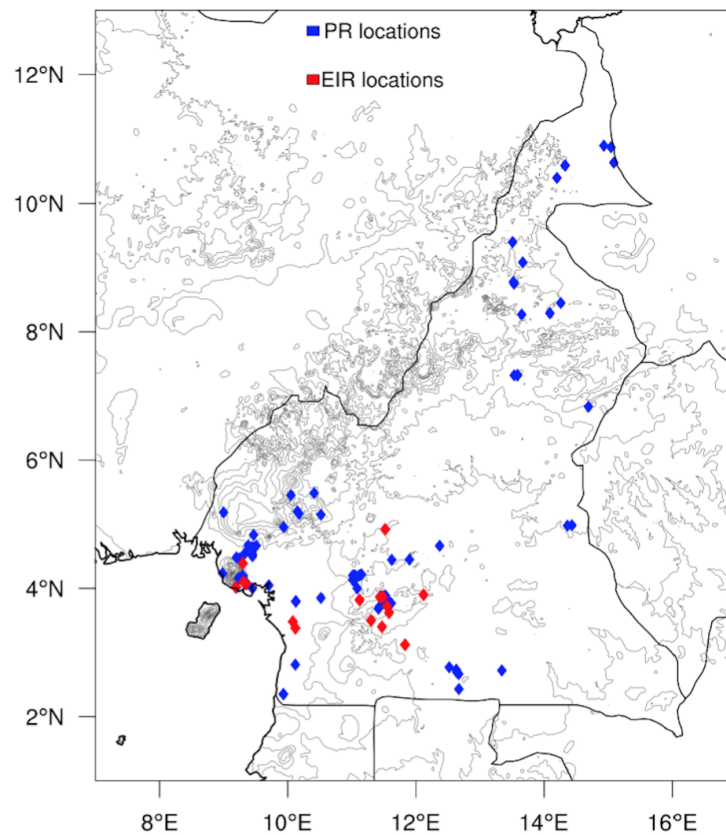
Figure 2.3: Map highlighting PR and EIR studies locations.

2.3 Methodology

2.3.1 VECTRI malaria model

VECTRI is a dynamical model, made to use daily time step data and can be flexibly integrated using several resolutions [10]. Its structure is made of links compartments representing

each step of the transmission process from Anopheles breeding site to human host. The global scheme account for temperature and rainfall to assess each growth step of mosquitoes, especially the egg-larvae-pupa development, the gonotrophic and the sporogonic cycles [10]. VECTRI also specify the interaction between host and vector by integrating human population density, in order to estimate daily biting rates. The figure 2.4 shows a schematic description of the schemes used in VECTRI model.
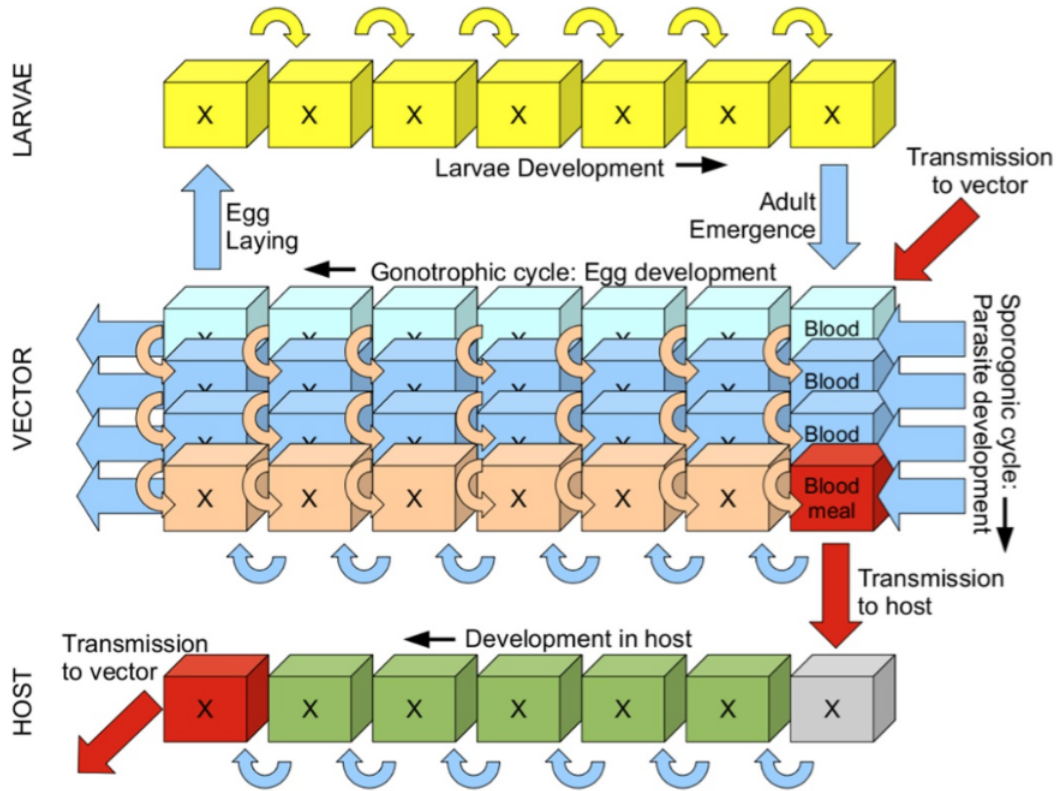
Figure 2.4: Schematic representation of VECTRI model. The following schemes are highlighted: egg-larvae-adult development, sporogonic, gonotrophic cycles and parasite development into host [10].

Larvae development scheme

The VECTRI larvae growth rate scheme is based on the pond water temperature (T_{wat}) and expressed by the following equation:

$$R_L = \frac{T_{wat} - T_{L,min}}{K_L}. \tag{2.1}$$

$T_{L,min}$ is the temperature below which larvae grow stops and K_L is the coefficient indicating the degree days required for adult emergence. But there are uncertainty related to the calculation of R_L. For instance, K_L from laboratory studies was estimated at 90.9 degree days [203], while linear approximations of the equation, predict a much slower rate of 200 degrees day [33]. In addition, water temperature relies on the shading, as well as on the geometry of the pond. In order to avoid these uncertainties VECTRI set the larvae growth rate to have a cycle of 12 days, independently of T_{wat} [15].

The larvae mortality rate and the vector daily survival are strongly temperature dependent. VECTRI sets the daily survival rate for larvae $(P_{L,surv0})$ equals to 0.0825 [15]. But over population in ponds is able to negatively affect larvae, because of competition for living resources. The larvae survival rate is then given by equation 2.2:

$$P_{L,surv} = \left(1 - \frac{M_L}{wM_{L,max}}\right) K_{flush} P_{L,surv0}. \tag{2.2}$$

M_L is the total larvae biomass per unit surface area of a water body, $M_{L,max}$ is the maximum carrying capacity set to 300 mg m^{-2} [204, 16] and above a water temperature of $T_{L,max}$ all larvae die. The flushing effect rate expressed by K_{flush} usually happen during heavy rainfall and leads to high larvae losses [205, 45]. The K_{flush} depends on the larvae fractional growth state L_f and exponential of rainfall rate R_d.

$$K_f lush = L_f + (1 - L_f)\left((1 - K_{flush,\infty})e^{\frac{-R_d}{\tau flush}} + K_{flush,\infty}\right). \tag{2.3}$$

In this equation, $K_{flush,\infty}$ is the maximum value of K_{flush} for newly hatched, R_d is the rainfall rate in mm day^{-1} and τ_{flush} set to 50 mm day^{-1} describes how quickly flushing increases as a function of R_d.

Gonotrophic cycle

VECTRI assumes all females vectors are able to find a blood meal in the first night of searching; but this is set as a tuned parameter since many parameters like use of insecticide treated nets can slow down the mosquitoes host-seeking process [206]. The egg development

process begin after the blood meal is taken. The rate is controlled by the local 2 metre temperature (T_{2m}) following the degree day concept, and is presented on the following equation 2.4.

$$R_{gono} = \frac{T_{2m} - T_{gono,min}}{K_{gono}}. \tag{2.4}$$

Where $K_{gono} = 31.1$ K day [207], and $T_{gono,min} = 16$ °C which is the minimum temperature that support the gonotrophic cycle [15].

Sporogonic cycle

During blood feeding, malaria parasite can be transfer from the host to vector or vice versa. The probability of malaria transmission from an infected host to the vector during blood meal is assume to be constant: $P_{hv} = 0.2$ relying on [15], and the overall probability $P_{h \to v}$ is given by:

$$P_{h \to v} = \frac{H_{inf}}{H} P_{hv}. \tag{2.5}$$

H_{inf} and H are respectively infected and total host population densities. Using this equation assumes that bites are randomly taken. Furthermore the heterogeneity of feeding habits, related to perennial breeding sites or interventions strategies for example, is also ignored [208, 209].

At each time step, a proportion of vectors $P_{h \to v}$ get infected and the parasite development that starts in the midgut, relies on temperature and follows the degree day concept (equation 2.6). Once the sporozoites has invaded the salivary glands, the mosquito becomes infective to humans and remains so until death.

$$R_{sporo} = \frac{T_{2m} - T_{sporo,min}}{K_{sporo}}. \tag{2.6}$$

In this equation for temperatures above 18°C, K_{sporo} is equal to 111 K day for *Plasmodium falciparum* [207]. $T_{sporo,min}$ equals to 16°C is the minimum threshold temperature below which sporogony ceases [15]

Vector survival

Vector survival relies on air temperature. Higher values tends to increase vector mortality. The survival rate scheme is given as quadratic function of temperature and presented by these two schemes: Scheme 1 represented by equation 2.7 [210, 211] and scheme 2 by equation 2.8 [212, 38].

$$P_{V,surv1} = K_{mar1,0} + K_{mar1,1}T_{2m} + K_{mar1,2}T_{2m}^2 \tag{2.7}$$

Constant values: $K_{mar1,0} = 0.45$, $K_{mar1,1} = 0.054$ and $K_{mar1,2}$ = -0.0016

$$P_{V,surv2} = exp\left(\frac{-1.0}{K_{mar2,0} + K_{mar2,1}T_{2m} + K_{mar2,2}T_{2m}^2}\right) \tag{2.8}$$

Constant values: $K_{mar2,0}$ = -4.4, $K_{mar2,1}$ = 1.31 and $K_{mar2,2}$ = -0.03

$P_{V,surv1}$ and $P_{V,surv2}$ are daily vector survival probability, respectively for scheme 1 and scheme 2, and T_{2m} is the 2 metre air temperature. VECTRI uses equation 1.8 as its vector survival based scheme following [213].

Host-vector interaction

VECTRI uniquely incorporates interactions between human host (H) and vectors using the human biting rate expressed as follows:

$$hbr = \left(1 - e^{\frac{-H}{\tau zoo}}\right)\frac{\sum_{j=1}^{N_{sporo}}V(1,j)}{H}. \tag{2.9}$$

The term $(1 - e^{\frac{-H}{\tau zoo}})$ express the level of vector zoophily and $\sum_{j=1}^{N_{sporo}}$ V(1,j) /H indicate the ratio of biting vectors to the host population. The factor τ_{zoo} equals to 50 km^{-2} has an important impact for rural populations below its. This helps the model avoid to produce high biting rates and EIR for sparsely populated areas.

The probability of transmission for an infectious vector to the host after a single bite is given by P_{vh}. The value is assumed constant and the probability of transmission for an individual receiving n infections bites is given by $\left(1 - (1 - P_{vh})^n\right)$. The daily overall transmission probability per person is then express by equation 2.10.

$$P_{v \to h} = \sum \,^{\infty}_{n=1} G_{\overline{EIR_d}}(n)\big(1 - (1 - P_{vh})^n\big) \qquad (2.10)$$

$G_{\overline{EIR_d}}$ is the Poisson distribution for mean $\overline{EIR_d}$. EIR_d is the daily number of infectious bites by infectious vectors, and calculated as the product of human bitting rate (hbr) and the circumsporozoite protein rate ($CSPR$). Equation 2.10 is likely to be modify if one has to take into account factors as bed nets usage that makes the biting rate to fluctuate. Generally population host has about 20 days after infection to assume the infective status [214, 215].

Surface hydrology

VECTRI surface hydrology scheme estimates at each time step the fractional coverage in each grid cell. This fraction is the sum of two parameters:

$$W = W_{pond} + W_{perm} \qquad (2.11)$$

W_{pond} represents the fractional pond water coverage due to rainfall events and W_{perm} is associated to permanent water bodies such as lakes, rivers, streams, that mosquitoes also exploit on their edges as breeding sites [41]. In this hydrology scheme, breeding sites are assume to be filled by water after rainfalls events and W_{perm} is incorporate as tuned parameter depending on hydrological conditions of the area, this is because its spatial parameterization is not yet available in the model. The fractional pond coverage in a grid cell is then express by the following.

$$\frac{dW_{pond}}{dt} = K_w \big[P(W_{max} - W_{pond}) - W_{pond}(E + I)\big] \qquad (2.12)$$

Where W_{max} is the maximum temporary fractional water coverage in a grid cell, K_w is the pond factor constant that links rainfall to the growth of the pond; P, E and I are respectively: precipitation rate, constant evaporation and infiltration. Default values of these parameters as used by VECTRI are presented on table 2.4 that follows.

Table 2.4: Default constants related to equation 2.12 [10].

Symbol	Value	Units
Kw	0.001	mm^{-1}
E + I	250	mm day^{-1}

VECTRI hydrology scheme as presented in equation 2.12, ignored some important aspects such as soil texture, topographical slope, or variation in infiltration and evaporation rate. Fluctuations in these factors are likely to influenced the stability of the pond [216, 217], and make VECTRI over or underestimate the pond water fraction.

2.3.2 VECTRI model Setup for the Study

The model used for this work is an open source, the Abdus Salam International Centre for theoretical physics (ICTP) vector borne disease model (VECTRI), a grid distributed dynamical model that couples a biological model for the vector and parasite life cycles, to a simple compartmental Suceptible-Exposed-Infectious-Recovered (SEIR) representation of the disease progression in the human host. The calculation of PR and EIR is based on equations 2.9 and 2.10.

The model runs using daily time step temperature and rainfall data, but also accounts for the population density which is important for the calculation of daily biting rates [10]. The model incorporates several parameterizations schemes for larvae, adult vector and parasite development rates, which are both temperature sensitive, as are the larvae and adult vector daily survival. Larvae survival, especially in the early development stages, is also impacted negatively by intense precipitation through the inclusion of a flushing effect [45]. The model also allows for over-dispersive biting rates and incorporates a simple treatment of host immunity [218]. Another feature of the model is that it also includes a simple treatment of rain-driven pond formation and loss through evaporation and infiltration [219, 220, 221]. VECTRI simulates several parameters that help in assessing malaria incidence. Among them are the parasite ratio and entomological inoculation rate that we are interested in.

In this study, the model is integrated for 22 years (1985-2006) with a 3 years spin-up period at 0.03° x 0.03° resolution. Mean daily precipitation data are obtained from Famine

Early Warning Systems Network ARC vesion 2 (FEWS-ARC2) [157], available at a spatial resolution of 0.1° x 0.1°. The daily gridded 2-metre temperature data is taken from the ECMWF ERA-Interim reanalysis data at 0.75° x 0.75° spatial resolution [158], which are then statistically downscaled to the model resolution assuming a lapse rate of 6.5 K km^{-1} to adjust to the high resolution topography. For each grid cell point, population density is obtained from AFRIPOP [222], again interpolated to the model resolution using conservative remapping. AFRIPOP database links informations on contemporary census data across Africa using geographical longitude and latitude position points.

VECTRI simulated EIR and PR results from, the nearest grid cell to each field survey location were extracted for comparison. For each field survey of PR, the comparison to climate variables is made this way. We take the average rainfall and temperature of:

- The second month preceding the study, M(-2);

- The month preceding the study, M(-1);

- The average of the preceding month and the study month, M(-1)+M(0);

- The average of the preceding two months, M(-2)+M(-1).

With this methodology we are accounting the fact that, there is an observed lag from 1 to 2 months between malaria and rainfall peaks and also because PR is a time-integrated; thus smoothed quantity that reflects climatic conditions over the preceding period [16].

For the time series analysis of EIR, we instead compare directly to the time series of climate variables for the observed period. As the precise days of surveys were not usually available (only the month), there is then an uncertainty in the lag of 2 weeks.

2.3.3   Futures projections with VECTRI

Performances of VECTRI with observed temperature and rainfall to simulate malaria metrics (PR and EIR) are demonstrated but, studies conducted under global warming are still needed. Yet, such analyses might contribute to a long-term plan for disease prevention, adaptation and to mitigate the parasite transmission. In this part, we couple VECTRI with the atmospheric regional climate model RCA4 (VECTRI-RCA4) to address the issue. The goal here is twofold: first, assess the ability of the combination VECTRI-RCA4 to model

malaria metrics over Cameroon. Second, explore the impact of global warming under the Representative Concentration Pathway (RCP) 2.6 and 8.5 on malaria distribution. Through examination of projections, we hope to portray preliminary aspects of malaria propagation in a warmer world over Cameroon, as well as to alert decision-makers about the challenges and opportunities of mitigation. The study area is subdivide for the purpose in three agro-climatic sub-regions as presented on figure 2.5.
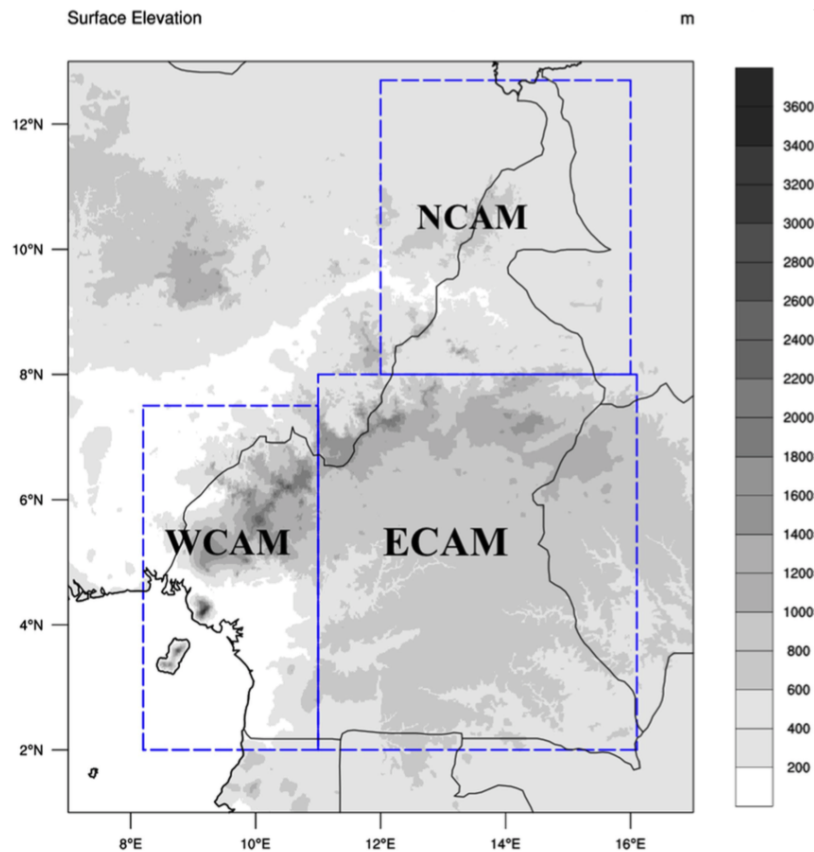
Figure 2.5: Study domain, Highlighted in blue are the three agro-climatic sub-regions: North Cameroon (NCAM), West Cameroon (WCAM) and East Cameroon (ECAM).

Climate inputs for VECTRI, specifically rainfall and temperature data at 0.44° grid spacing are taken from the results of dynamical downscaling of the fourth version of the Rossby Centre Atmospheric (RCA4) model, participating in the Coordinated Regional Climate Downscaling Experiment (CORDEX) project. RCA4 was forced with five global climate models (GCMs) involved in the Coupled Model Intercomparison Project phase 5 (CMIP5; Taylor et al., 2012). Details of downscaled global climate models (GCMs) are provided in Table 2.5.

Table 2.5: Details of GCMs used to force RCA4

Model name	Institution	Native resolution	References
EC-EARTH-ES	European community Earth-System Model Consortium	1.125° x 1.125°	[223]
MPI-ESM-LR	Max Planck Institute for Meteorology	1.9° x 1.9°	[224]
MIROC-5	Atmosphere and Ocean Research Institute	1.40° x 1.40°	[225]
NorESM1-M	Norwegian Climate Centre	2.5° x 1.9°	[226]
HadGEM2-ES	Met Office Hadley Centre	1.875° x 1.25°	[227]

Observed malaria PR data are obtained from the Malaria Atlas Project programme (MAP) that collects results of individuals researchers or organizers already published in the literature while EIR is obtained from a recent database for Africa [191].

VECTRI was first integrated from January 1985 through December 2005 using historical data from the downscaled GCMs which is compared against simulations when VECTRI is forced by the observation FEWS-ARC2, Famine Early Warning Systems Network ARC version 2 ([157]) for rainfall and the reanalysis ECMWF ERA-Interim ([158]) for temperature. Secondly, the model is integrated under global warming using two Representative Concentration pathway scenarios: the high-mitigated, low-emission RCP2.6, and the low-mitigated, high-emission RCP8.5 scenarios [228]. Using these two contrasted scenarios enables us to get an insight into the way each warming level might impact the malaria metrics' distribution. Therefore, this offers the possibility to stimulate discussion about the opportunity or not to mitigate the changing climate.

Population density is taken from AFRIPOP [222] for each grid cell point and to account for the growth of the population in the malaria simulations. We fixed the population growth parameter in VECTRI to be equal to the annual population growth rate in Cameroon, which is 2.6 according to the results of the third National Population Census [131] taking advantage of the fact that the model is dynamic. VECTRI simulations are performed with a 0.1° x 0.1° horizontal resolution. Driving data are statistically downscaled to the land model resolution assuming a lapse rate of 6.5 K.km^{-1} to adjust to the high-resolution topography.

Results and Discussions

3.1 Results

3.1.1 Parasite Ratio evaluation

The spatial maps of PR obtained are presented on figure 3.1. The PR value highlighted here then represent the average of all the points located within the same coordinates.

The maps reveals a very heterogeneous landscape of malaria prevalence, particularly in the observed surveys, but also in the model. It should be recalled that the surveys are taken during different years and periods of the year, thus some of the variations are simply due to changes in the climate at the survey time. Other factors such as interventions and population movements will also impact prevalence, but will not be reflected in the model simulations. Concerning the model, some regional biases stand out clearly. For example, the model produces PR values around 0.5 in the drier and warmer north east of the country, indicating conditions that are borderline between meso and hyperendemic, while the prevalence in the observations is far lower, indicating that the model is too sensitive to low rain rates.

To examine the relationship between PR and climate indicators in more details, the survey data and model results are divided into bins according to the two key climatic drivers of the disease: mean daily rainfall and temperature as mentioned in the methodology. Figure 3.2 presents the observed and simulated PR function of rainfall and temperature from the second-month preceding the survey-month. Blue bars are field data while red ones are results of simulations with VECTRI.
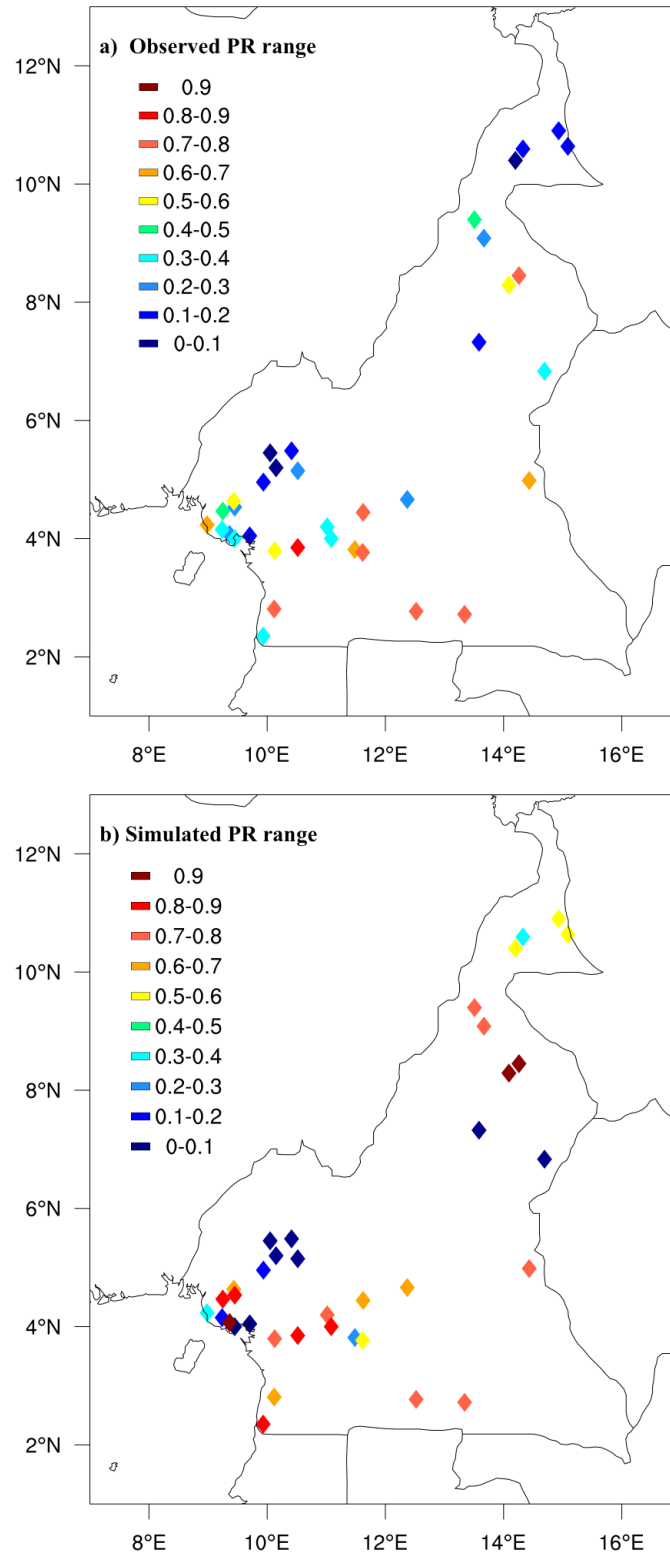
Figure 3.1: Observed **(a)** and simulated **(b)** parasite ratio ranges for Cameroon data points. The present maps highlight 36 points, which PR values represent the average of all the points located within the same coordinates
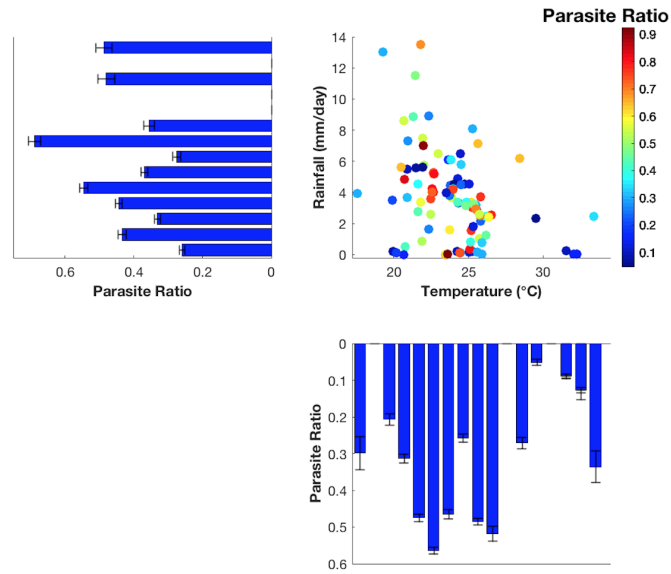
(a) Observed data
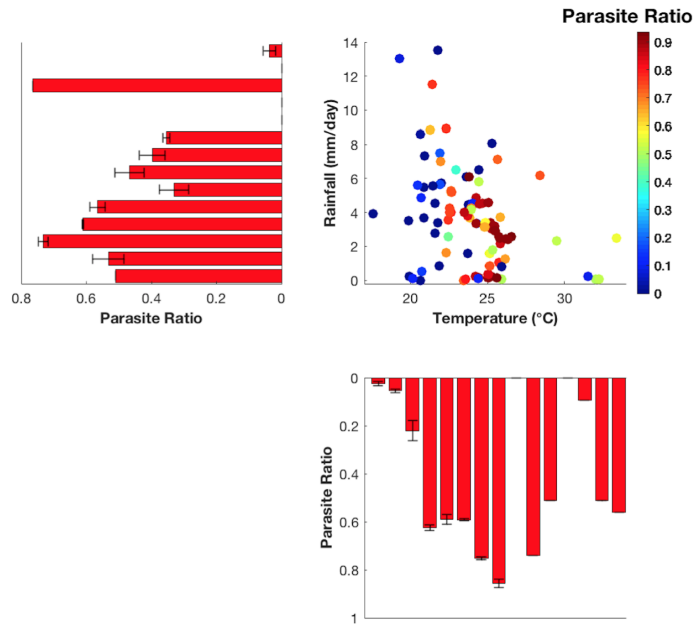
(b) VECTRI model

Figure 3.2: Observed and simulated parasite ratio, function of mean rainfall (mm/day), temperature (°C) from the second-month before the survey-month over Cameroon. Panels plots present how parasite ratio fluctuates with ranges of rainfall and temperature for observations and simulations. The little bars indicate uncertainty, which for the observations is based on a statistical test on the proportion given the total number of people surveys in each bin. For the model the uncertainty measure is the standard deviation of the survey locations in each bin.

The field data shows the prevalence as measured by PR, it increases to a values between 22 to 26ºC. It then falls off but in still non-zero in the locations with mean temperatures above 30ºC. The relationship with temperature is not smooth, as expected due to the fact that climate is only one of many external factors that impact the prevalence from location to location. The model produces a much sharper response to temperature, with low prevalence in the 18-21ºC range, and the peak transmission occurring around 26ºC with prevalence far higher than reported in the survey exceeding 80%. The response in PR to precipitation is more distinct in the model than observations. The observations reveal an increase in PR with increasing rainfall to a local maximum at 7 mm day^{-1}. After the peak, PR decreases with increasing rainfall with the exception of the final bins of 10-13 mm day^{-1}. The model instead peaks at a lower rainfall rate of 2 mm day^{-1}, reducing thereafter, again with the exception of the second last, high rainfall bin.

Figure 3.3 presents the observed and simulated PR function of rainfall and temperature from the month preceding the survey-month. Again blue bars are field data while red ones are results of simulations with VECTRI.
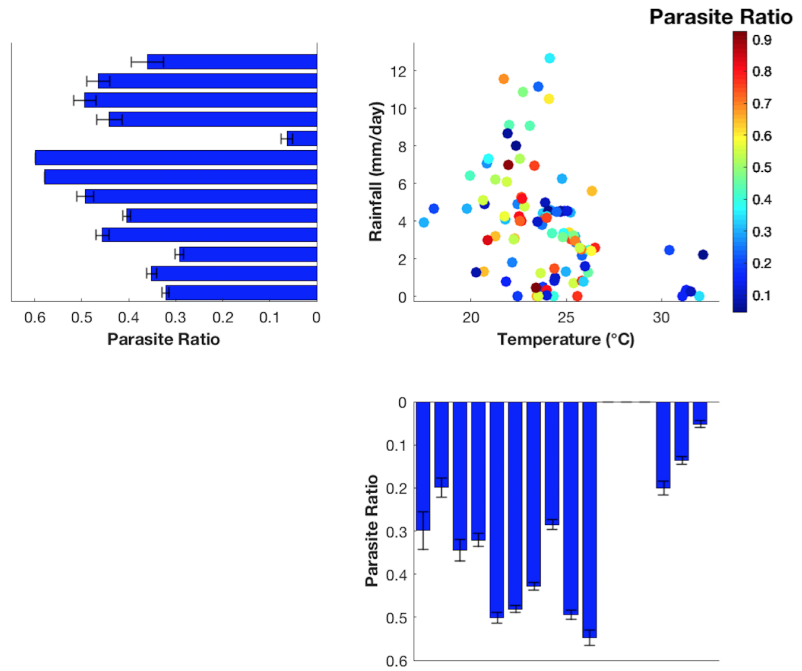
(a) Observed data
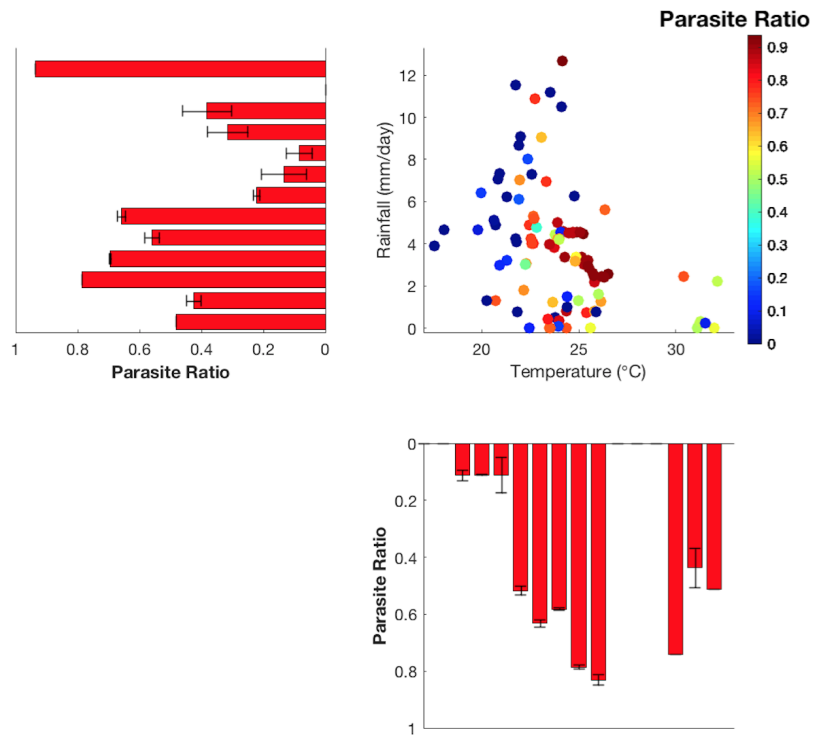
(b) VECTRI model

Figure 3.3: Same as figure 3.2 but rainfall and temperature data are mean value for the month preceding the survey-month.

Field data shows the prevalence increasing to value between from 22 to 26°C and falls again in the locations with mean temperatures above 30°C. The model response with the temperature indicates peak of prevalence within 24-26°C but with a prevalence of more than 70% above 30°C. The response to precipitation is less distinct in the model than observations. The observations reveal an increase in PR with increasing rainfall to a local maximum at 7 mm day^{-1} and decreases progressively till the finals bins. With the model the peak is obtained at 2 mm day^{-1} the prevalence decreases progressively but there is an important peak at 12 mm day^{-1}.

Figure 3.4 that follow, presents the observed and simulated PR function of rainfall and temperature, obtained by doing the mean of the survey-month and the preceding month. Blue bars are field data while red ones are results of simulations with VECTRI.
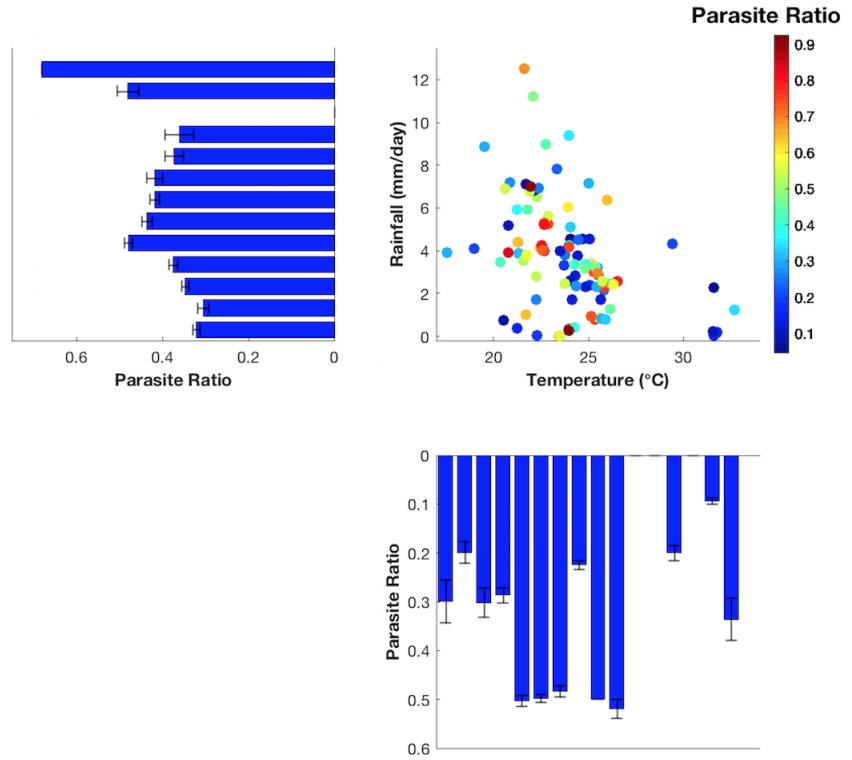
(a) Observed data
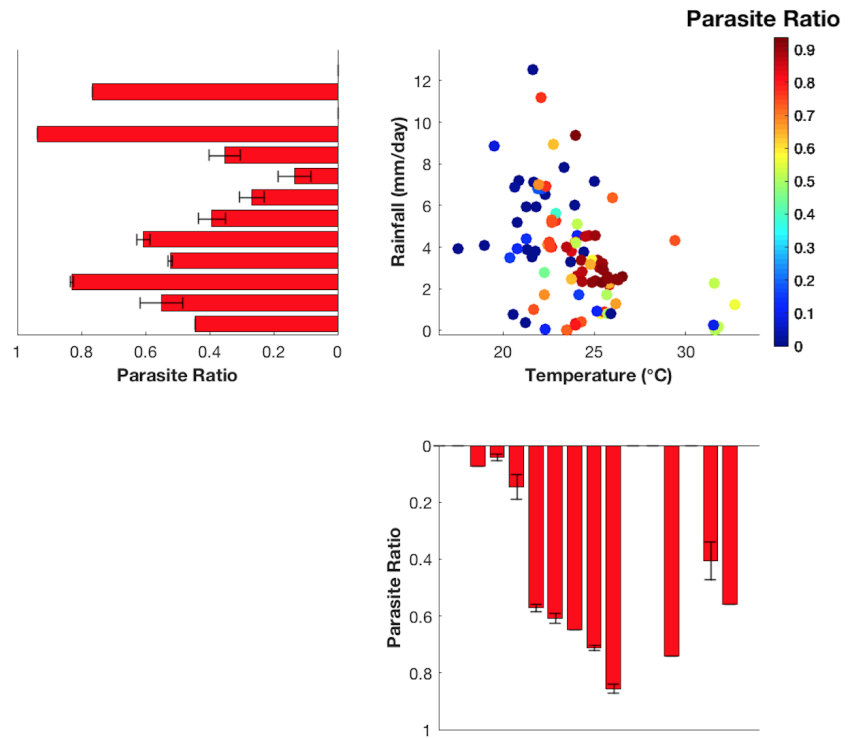
(b) VECTRI model

Figure 3.4: Same as figure 3.2 but rainfall and temperature data are mean value of the survey-month and the preceding month.

With the field data, PR maximises between 20 to 26°C. The model response to the temperature is more smooth with the peak at 26°C. Rainfall response is more distinct with the observed data than the model. For field data PR first shows a maximum at 4 mm day^{-1} with a prevalence value around 50% and decreases progressively till the finals bin where its presents more important value above 60%, around 12 mm day^{-1}.

Figure 3.5 below, shows the observed and simulated PR function of rainfall and temperature, obtained by doing the mean value of the preceding two months before the survey-month. As before blue bars are observed data and red ones are results of VECTRI simulations.
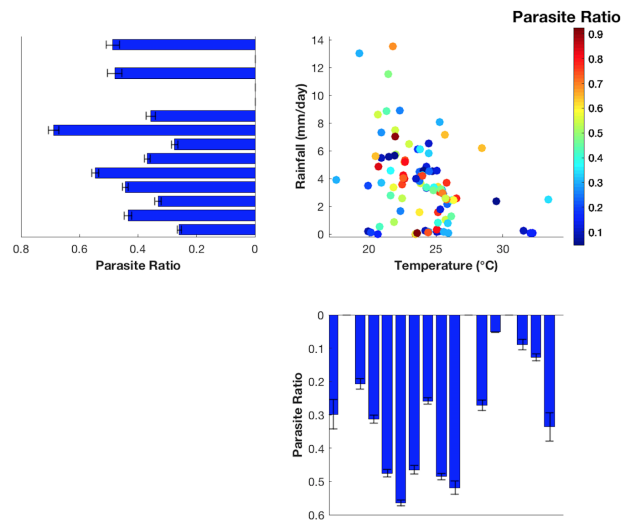
(a) **Observed data**
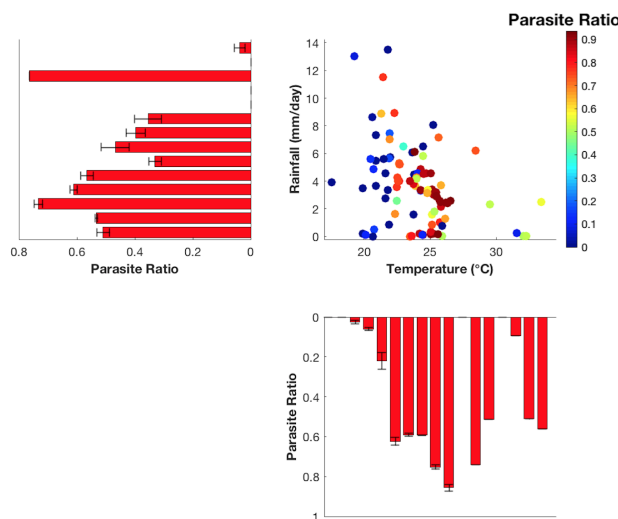
(b) **VECTRI model**

Figure 3.5: Same as figure 3.2 but rainfall and temperature data are mean value of the preceding two months before the survey-month.

 The observed data presents a maximum prevalence at 22ºC while the model peaks at 26ºC. Peak obtained with rainfall is at 7 mm day^{-1} for the field data and at 3 mm day^{-1} for the model, with a second peak within 11-12 mm day^{-1}.

 The PR is compared to population density assigned to three classes of rural (0 to 250 inhabitants per km^2); peri-urban (250 to 1000 inhabitants per km^2); and urban (>1000 inhabitants per km^2) according to Hay et al [229] (Fig. 3.6). PR reduces with increasing population, but with the relationship much stronger in the model relative to observations, a trait that was also observed by Tompkins et al [10] when comparing EIR as a function of population to the survey data compiled by Kelly-Hope et al [62]. Thus the model appear to overestimate malaria prevalence in rural locations and underestimate it in urban centres.
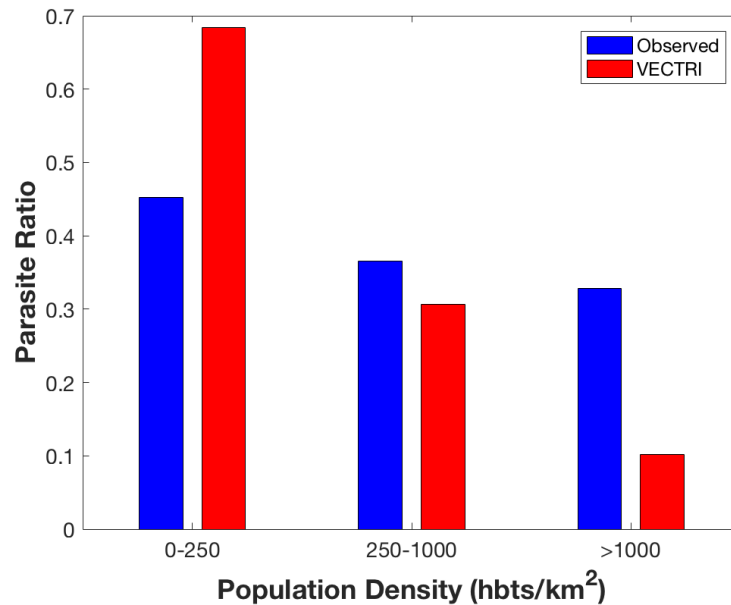
Figure 3.6: VECTRI and observed parasite ratio as a function of population density.

3.1.2 Seasonal EIR evaluation

 The seasonal changes in monthly EIR for both model and observations for the sixteen (16) sites are presented on the following figures 3.7, 3.8, 3.9 and 3.10.
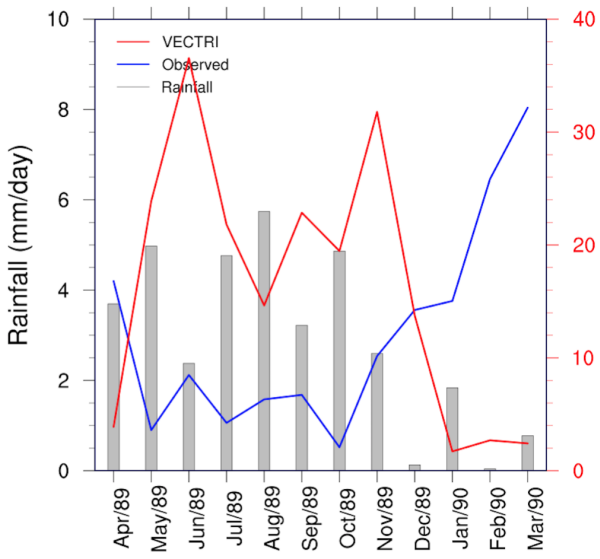
(a) Sanaga villages 4°92'N, 11°52'E
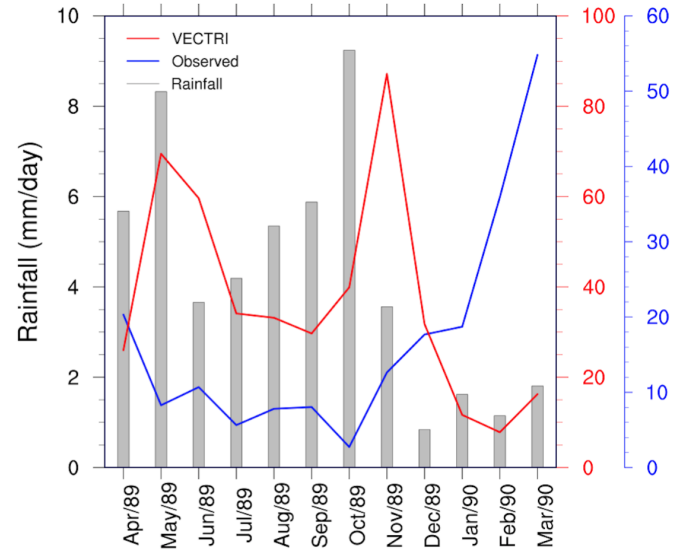
(b) Mbebe 3°38' N, 10°12' E
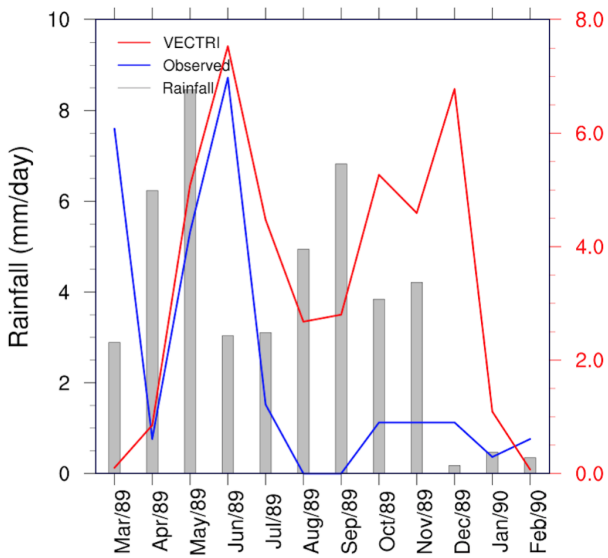
(c) Nkol-bikok 3°87'N, 11°52'E
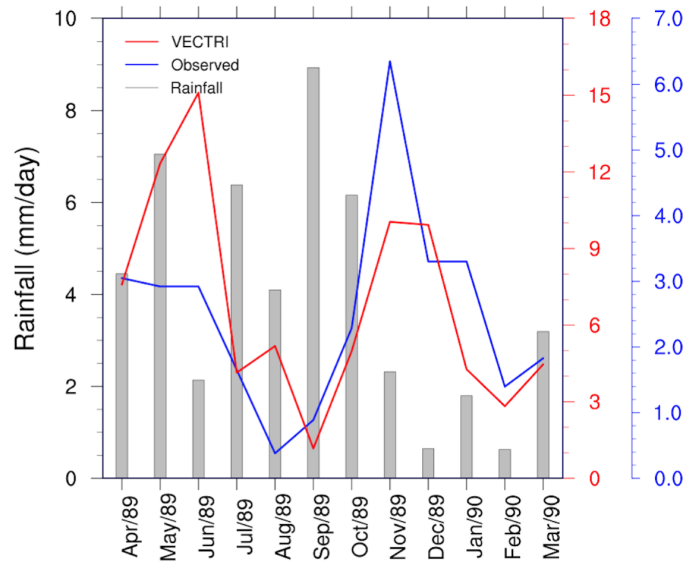
(d) Nkol-bisson 3°86'N, 11°44'E

Figure 3.7: Observed and simulated Entomological Inoculation Rate. The value are given in infective bites per person per month (ib/p/m).
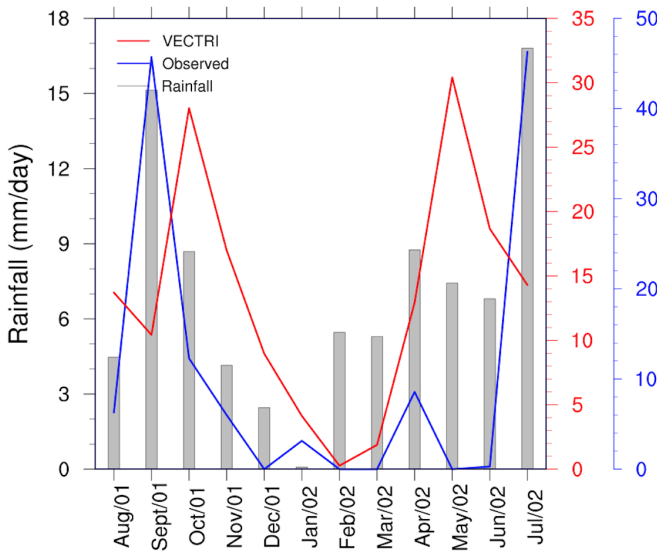
(a) Limbe 4°02'N, 9°19'E
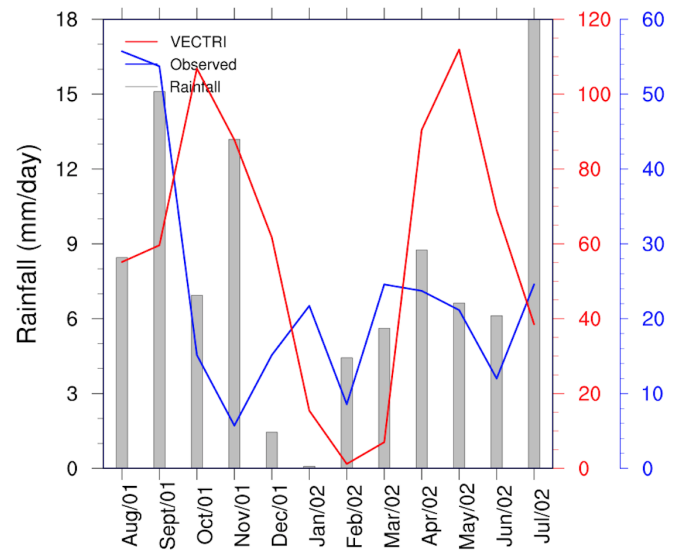
(b) Tiko 4°07' N, 9°35'E
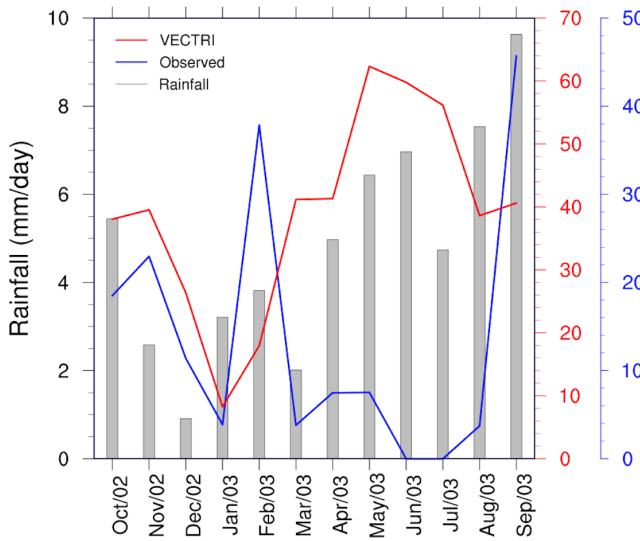
(c) Likoko 4°39'N, 9°3'E
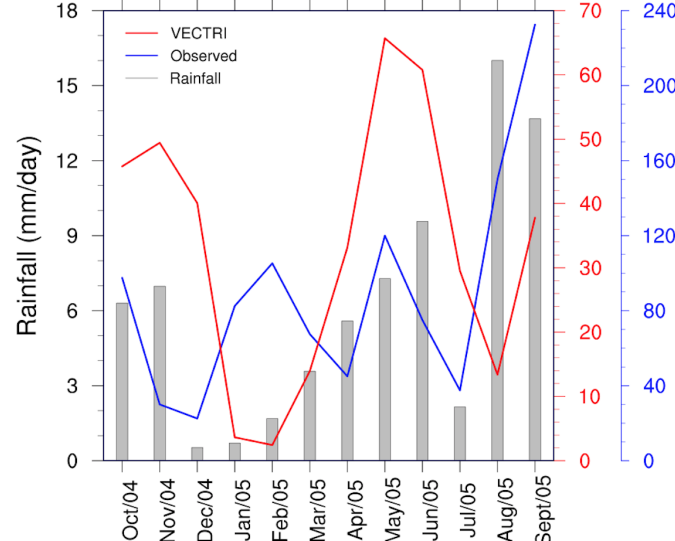
(d) Essuke-camp 4°1'N, 9°31'E

Figure 3.8: Observed and simulated Entomological Inoculation Rate. The value are given in infective bites per person per month (ib/p/m).
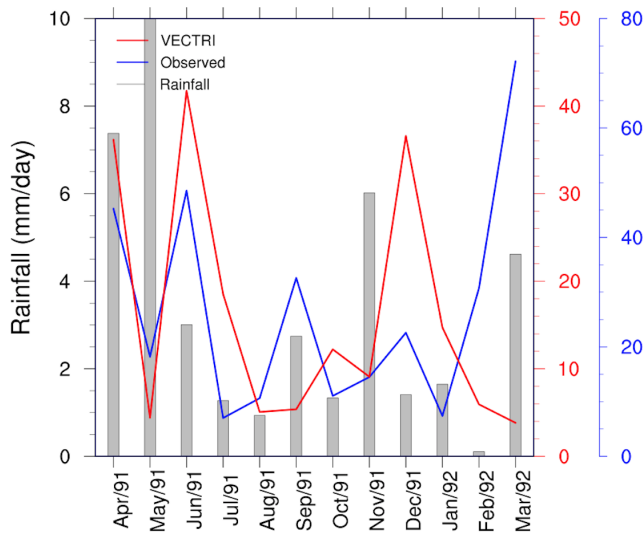
(a) Ebogo 3°4'N, 11°47'E
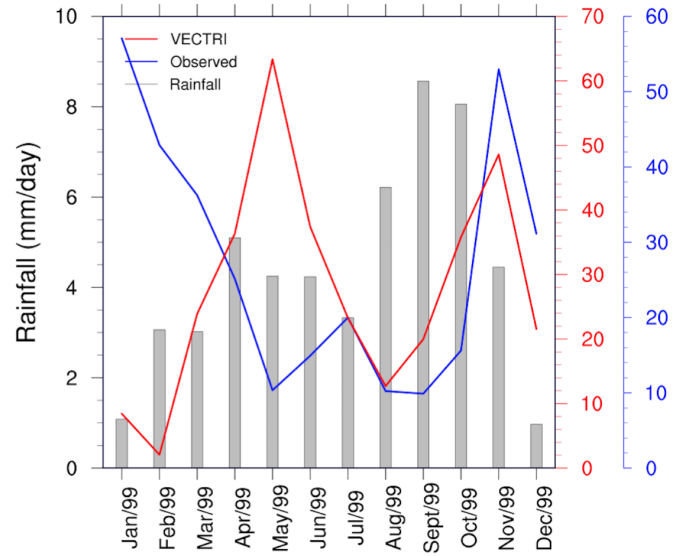
(b) Simbock 3°5' N, 11°3'E
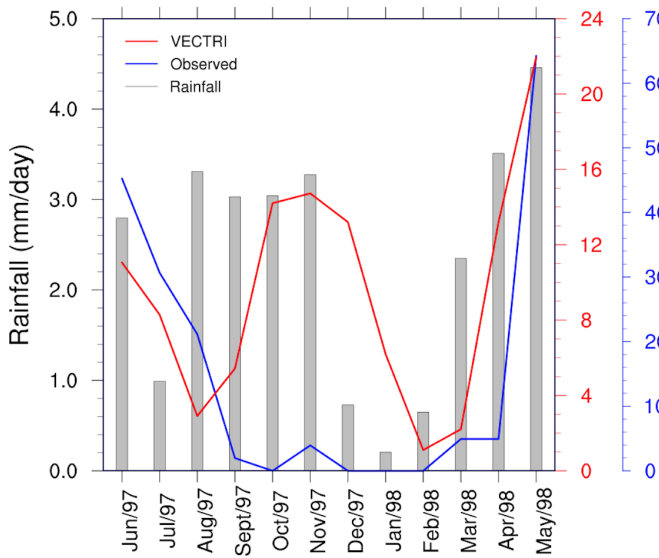
(c) Koundou 3°9'N, 12°12'E
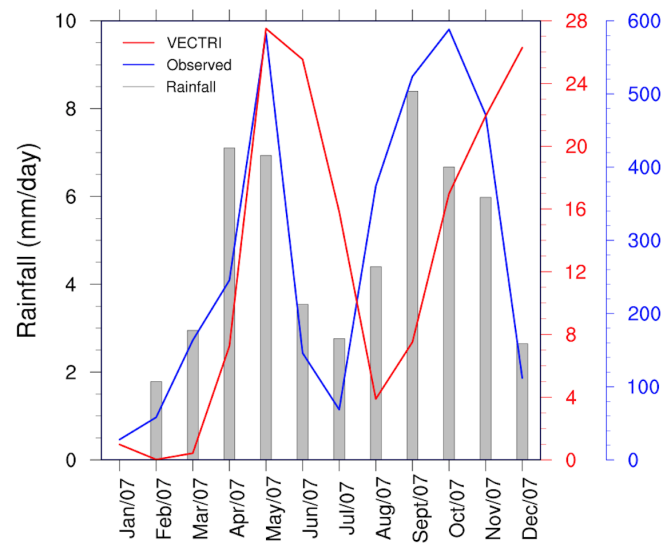
(d) Ekombite 3°12'N, 11°83'E

Figure 3.9: Observed and simulated Entomological Inoculation Rate. The value are given in infective bites per person per month (ib/p/m).
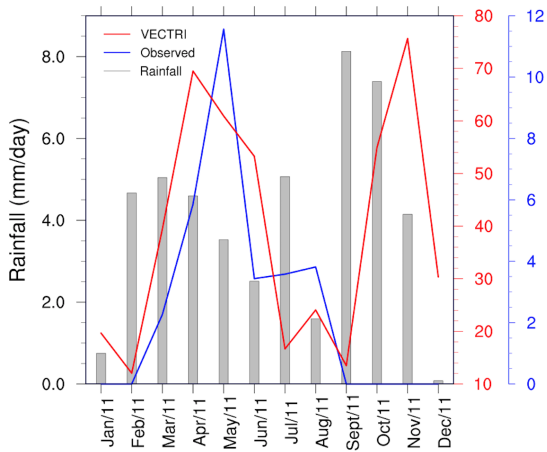
(a)   Ndogpassi

3°48'N, 10°08'E
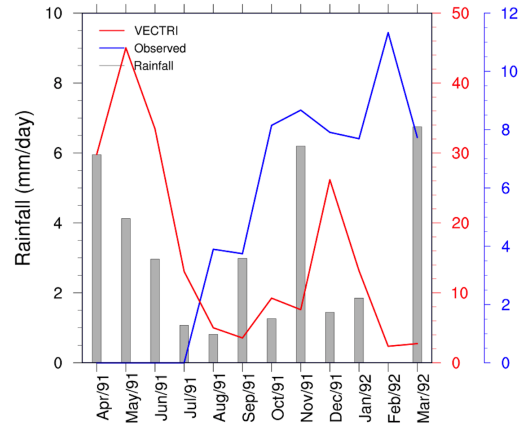
(b)   Nsimalen-

Nkol-mefou 3°7' N,

11°58'E
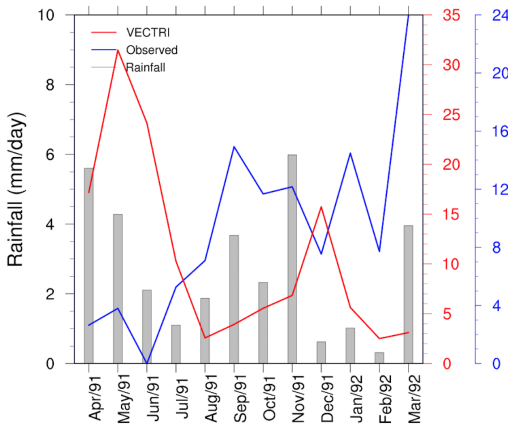
(c)   Nsimalen-

ekoko   3°82'N,

12°12'E
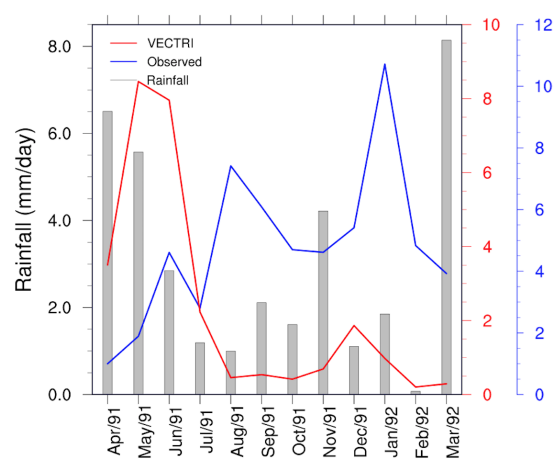
(d)   Nsimalen-3

3°72'N, 11°55'E

Figure 3.10: Observed and simulated Entomological Inoculation Rate. The value are given in infective bites per person per month (ib/p/m).

The EIR from the model and survey data clearly follows the rainfall patterns in the study locations. The 2-months time lag period, after peak of rainfall is identified in Simbock, Koundou, Ekombite and Ndogpassi. For the others sites, it is the 1-month lag time that is noticed. In certain locations like Sanaga village, Mbebe, Simbock, or Nsimalen-Nkol-mefou, the seasonality of EIR is reversed, with second peaks values of EIR occurring during the relatively dry periods.

The preceeding figures 3.7, 3.8, 3.9 and 3.10, can be can be resume on figure 3.11 below, where the observed EIR have been scaled in order to ease the comparison.
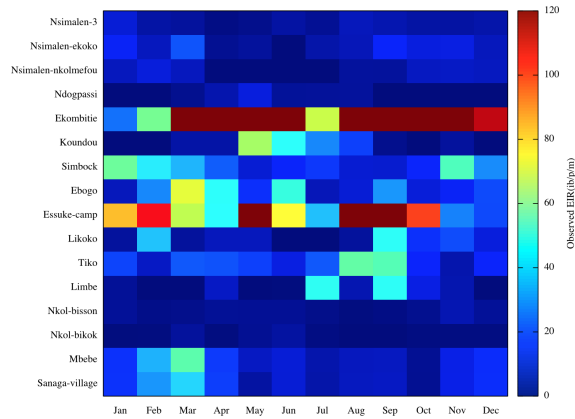
(a) Observed EIR (ib/p/m)
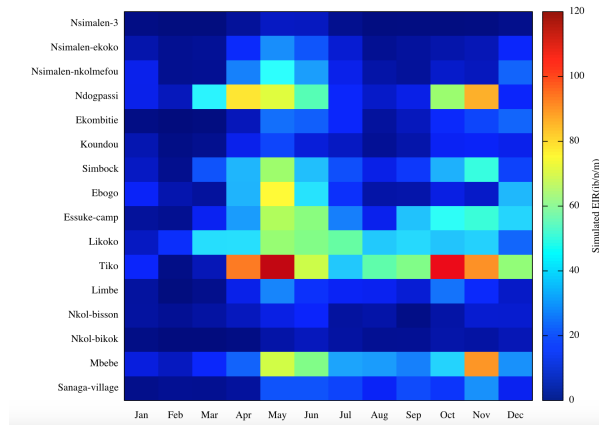
(b) Simulated EIR (ib/p/m)
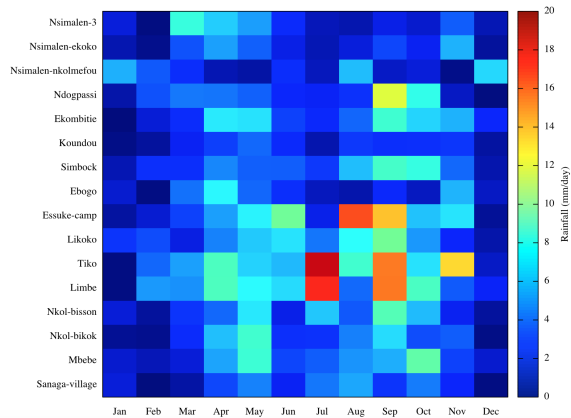
(c) Rainfall (mm/day)

Figure 3.11: Observed **(a)**, simulated **(b)** monthly mean entomological inoculation rate and **(c)** rainfall maps for the 16 EIR sites in Cameroon.

On figure 3.11 each boxes on the rainfall grill presented at (**c**), has a correspondent one on the maps of the observed (**a**) and simulated (**b**) EIR.

3.1.3 Forecasting malaria indicators

1. **Model evaluation**

   This section aims at evaluating the ability of the RCA4 model to reproduce the climatology of the study area as well as the VECTRI model to simulate malaria (malaria metrics) observed data.

   - RCA4 model evaluation

     We started by investigating whether the atmospheric regional climate model RCA4 satisfactorily reproduces the climatological mean of the Cameroon rainfall and temperature. We investigated the three agro-climatic sub-regions termed North Cameroon (NCAM), West Cameroon (WCAM) and East Cameroon (ECAM) (see figure 2.5). We present results based on the ensemble mean of RCM experiments (RCA-EnsMean thereafter).
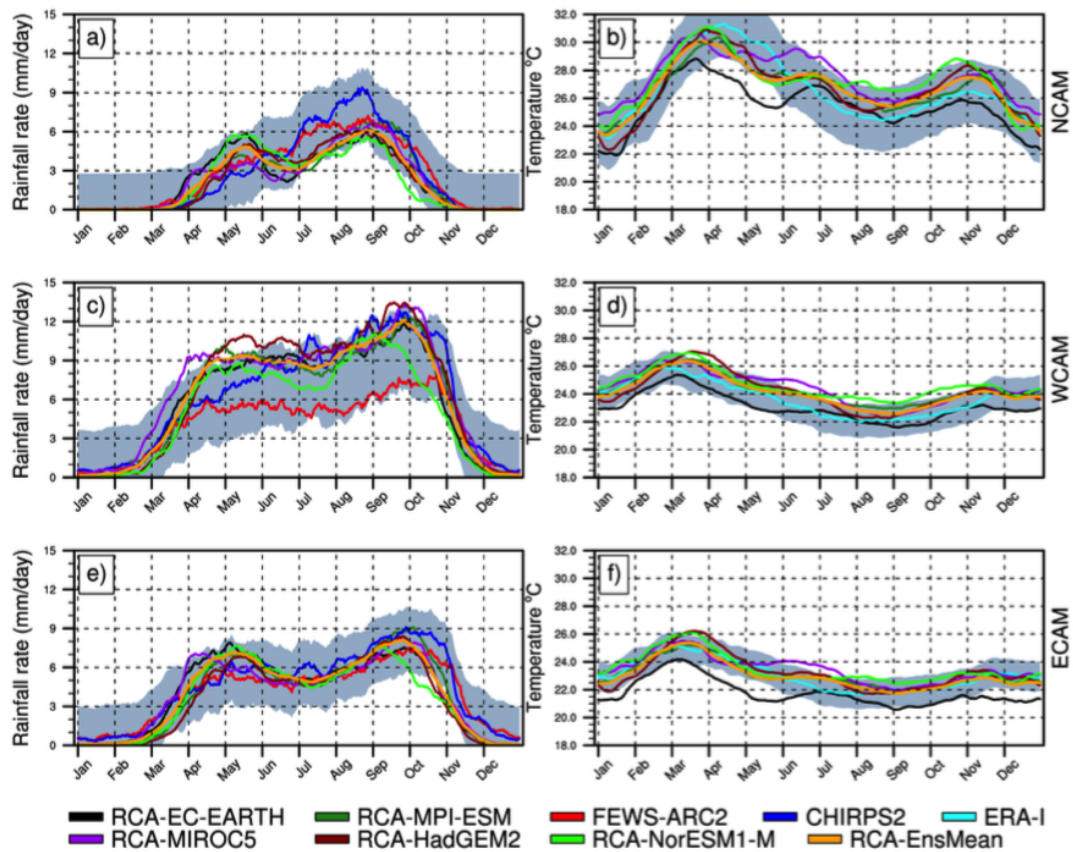
Figure 3.12: Seasonality of mean (1985-2005) rainfall (in mm/day, left panels) and temperature (°C, right panels). The study area is subdivided into three agro-climatic regions: (a,b) North Cameroon (NCAM, row 1), (c,d) West Cameroon (WCAM, row 2) and (e,f) East Cameroon (ECAM, row 3). Data used are from RCA4 simulations and the ensemble mean of RCM runs (RCA-EnsMean), and from observed rainfall FEWS-ARC2 (red), CHIRPS2 (blue). The temperature reference is extracted from the ERA-Interim (cyan) reanalysis dataset.

Figure 3.12 shows the seasonality of rainfall (left panels) and temperature (right panels) over the three agro-climatic regions. The grey shade band is the standard deviation obtained from the FEWS-ARC2 for precipitation, and from the reanalysis ERA-Interim for the temperature. For a given month, a mean rainfall value greater than the corresponding standard deviation is considered as a clear failing of the considered experiment. Two peaks are observed for rainfall in WCAM (3.12**a**) and ECAM (3.12**e**) in May and October (highest peak at ∼ 12 mm/day

and ~ 9 mm/day respectively), while NCAM experiences a unimodal rainfall regime, with the peak (~ 9 mm/day) occurring during August-September months (3.12**c**). Although some divergences in terms of rainfall magnitude are noticed between datasets (more pronounced in NCAM), they all nevertheless vary within the range of the observed standard deviation. The seasonality of temperature is also well captured with the highest values in March and the ones in December for WCAM (Figure 3.12**b**) and ECAM (Figure 3.12**f**). Two obvious peaks are observed within April-May (upto 30°C) and within November-December (upto 28°C) for NCAM (Figure 3.12**d**). RCA-EC-EARTH failed to simulate the temperature for NCAM from April to June (Figure 3.12**d**); from April to June and from November to December over ECAM (Figure 3.12**f**). Overall, the climatological annual cycle of both rainfall and temperature are realistically captured over all subregions. The RCA-EnsMean is quite similar to individual RCM runs and is well contained in the natural variability of observations. This suggests that the ensemble mean of experiments is representative of individual simulations and can be used without changing the conclusion.

Statistical performance measures are summarized in Figure 3.13, through the Taylor diagram. Three statistical metrics are used, including the root-mean-square difference (RMSD), the pattern correlation (r) and the standard deviation (STD), computed between downscaled results and FEWS-ARC2 for precipitation, and ERA-Interim for temperature used as a point of reference.
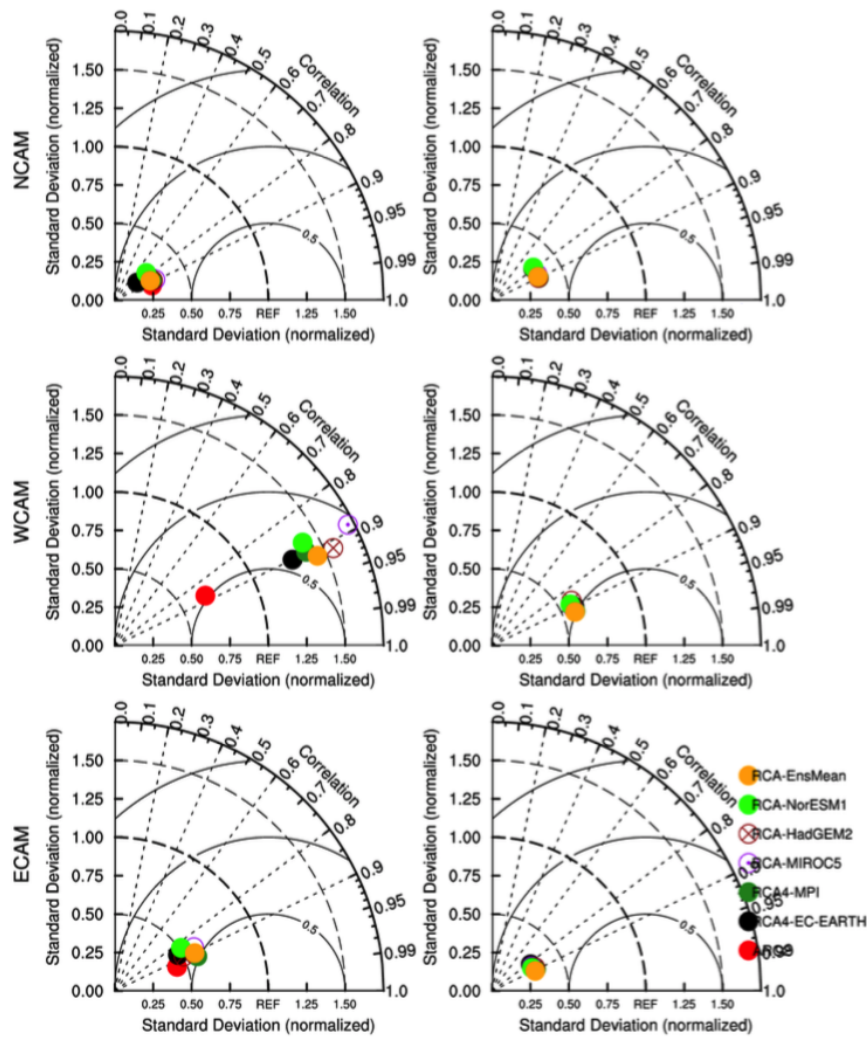
Figure 3.13: Taylor diagrams displaying the statistics of daily precipitation and comparing RCA4's experiments and the ensemble mean (RCA-EnsMean) with observations FEWS-ARC2 (reference field for precipitation). For temperature, the reanalysis ERA-Interim is used as a point of reference. The first row shows statistical parameters over NCAM, the second over WCAM and the third over ECAM. The first column displays statistical parameters for precipitation while the second does so for temperature.

Regarding precipitation statistics, for NCAM and ECAM, RCA4's experiments and FEWS-ARC2 clustered but not so close to the reference field with average performances (RMSD < 1; r ~ 0.90, and STD <0.75). There are fewer performances of RCA4's model for WCAM compared to the reference field with 1<RMSD<1.5, r ~ 0.90 and 1<STD<1.5. For temperature, RCA4's runs clustered and out-

performed (compared to what was observed with precipitation) over the three agro-climatic regions, with r ~ 0.90, 0.5<RMSD<1 and STD<0.75.

- VECTRI model evaluation

Figure 3.14 presents how observed PR and EIR (blue lines) fit with simulated values (red lines) over the different measurement stations. Here, simulated values are results of the combination VECTRI-RCA-EnsMean, i.e. VECTRI driven by RCA-EnsMean.
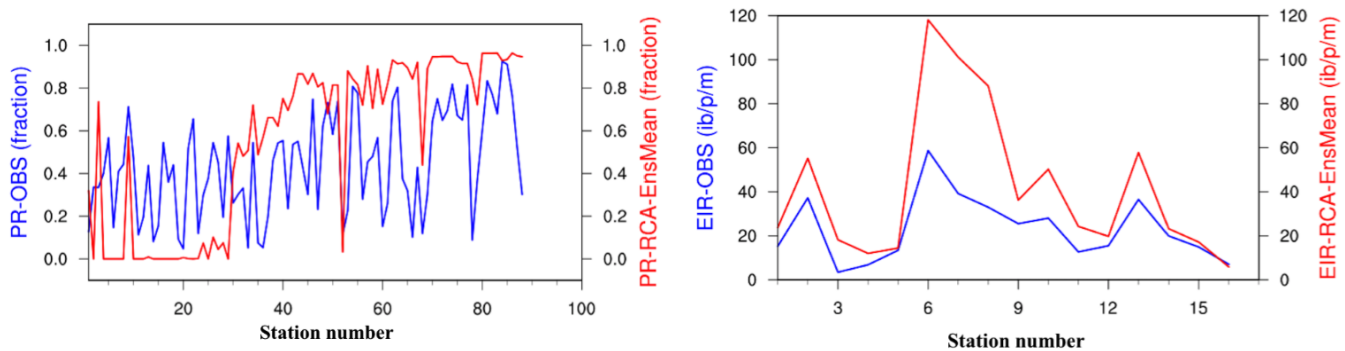
Figure 3.14: Results of combinations of VECTRI-observation (in blue) and VECTRI-RCA-EnsMean (in red) for PR (left panel) and EIR (right panel), function of rainfall (mm/day) and temperature (°C) over Cameroon. The x-axis values represent the station number. The two panels show how VECTRI forced with observed station measurements compares against VECTRI forced with RCA-EnsMean.

The results show that, although there are differences between the two experiments, the shapes of the curves are similar, meaning that the combination VECTRI-RCA-EnsMean succeeds to detect the signal of individual stations. The differences can be attributed to differences in rainfall amount and temperature. VECTRI outperforms in simulating EIR (right panel) than PR (left panel). It is important to recall the challenge of assessing model performance over equatorial Africa given observational uncertainty. Some differences may be associated with inhomogeneities in station measurements. The fact that the combination VECTRI-RCA-EnsMean satisfactorily reproduces the signal of variation of PR and EIR in most stations makes its usage reliable for projection. To get an insight into how the coupling

VECTRI-RCA-EnsMean simulates the spreading of malaria over the country, we showed in figure 3.15 the spatial distribution of the PR as modeled by VECTRI-RCA-EnsMean compared against the monthly observed PR over the period 1985-2005.
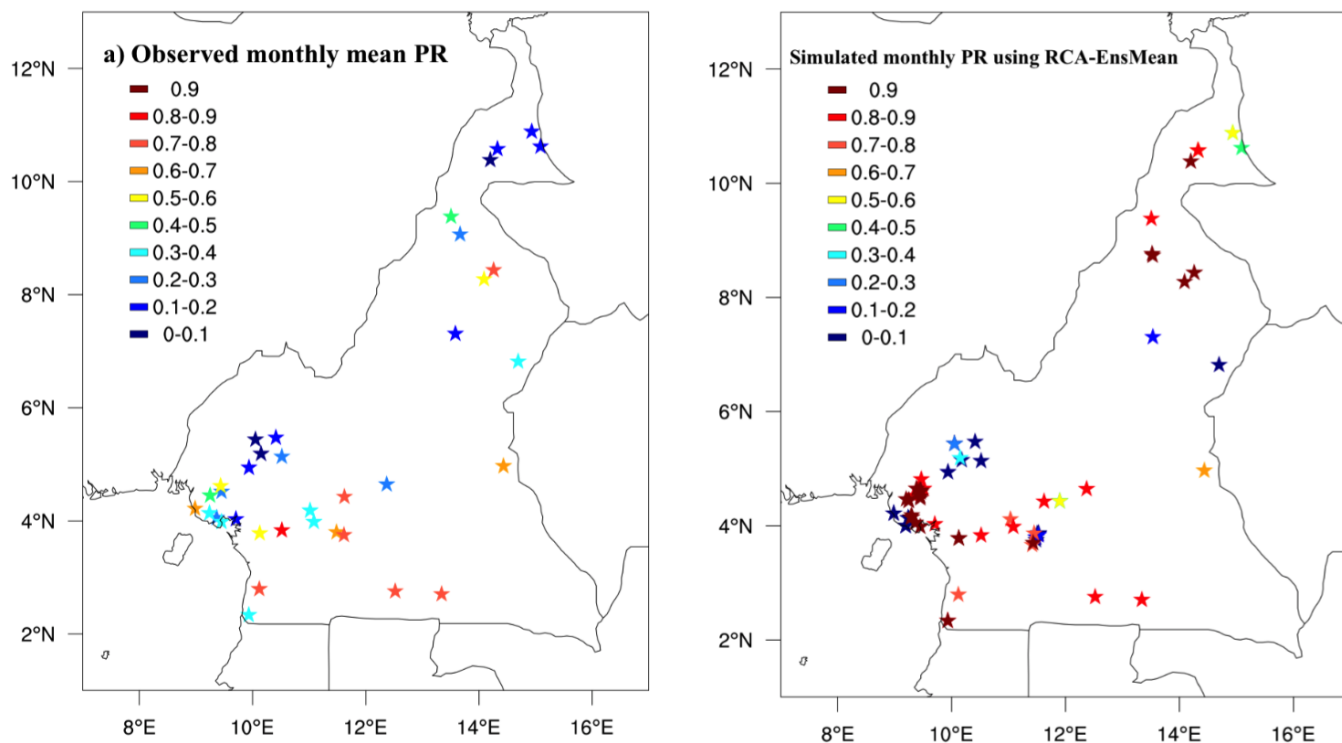
Figure 3.15: Observed (left) and simulated (right) monthly mean of PR for the available data sites in Cameroon over the period 1985-2005. The PR values represent the average of all the points located within the same geographical areas of study.

These spatial plots present a varied landscape of malaria PR over the country. There are some simulated biases in NCAM where PR values are above 0.5 (figure 3.15**b** which is mostly dry and warm whereas in the observation, (figure 3.15**a**) the mean PR is lower. Such a difference could be probably because, VECTRI model is much more sensitive to low rainfall. For ECAM, the differences in PR between observed and simulated values are more obvious compared to WCAM. The model somehow outperforms better in these two areas compared to the NCAM.

2. **Projected changes in the malaria metrics**

In this section, we explore the impacts of global warming on the aforementioned malaria metrics under the optimistic (RCP2.6) and the pessimistic (RCP8.5) scenarios. Analyses are conducted under two-time frames: the near future (2035-2065) and the far future (2071-2100), using the combination VECTRI-RCA-EnsMean.

- Changes in the Parasite Ratio (PR)

Figures 3.16 exhibits the monthly mean changes in PR over the near future and the far future under the high mitigated RCP2.6 scenario.
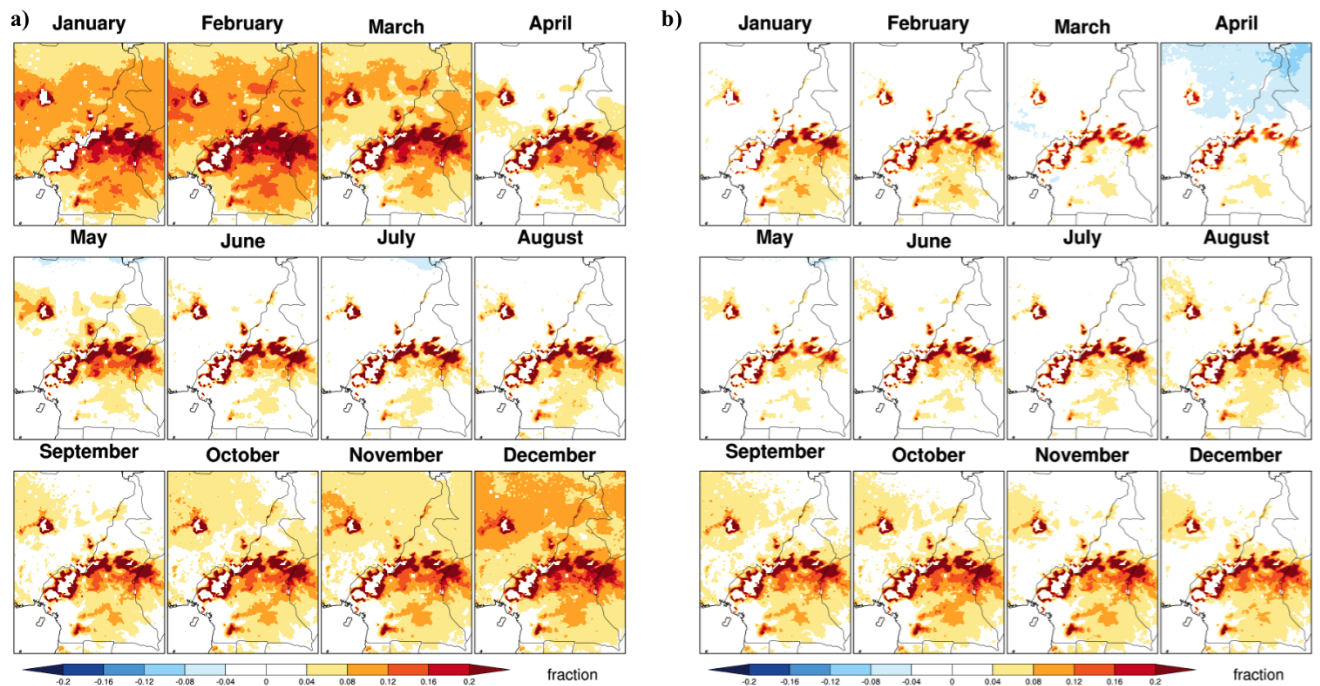
Figure 3.16: Monthly mean changes in PR under RCP 2.6 scenario. VECTRI model driven by RCA4-EnsMean for the period 2035-2065 **(a)** and 2071-2100 **(b)**.

Figure 3.16 presents the PR pattern obtained with RCA-EnsMean, under RCP 2.6 scenario. Results based on individual experiments are presented on the following figures as follows: figure 3.17 for RCA4-EC-EARTH-ES, figure 3.18 for RCA4-MPI-ESM-LR, figure 3.19 for RCA4-MIROC5, figure 3.20 for RCA4-HadGEM2 and figure 3.21 for RCA4-NorESM1-M. The PR tends to decrease when VECTRI is forced with RCA4-EC-EARTH-ES (figure 3.17) experiment with respect to

other VECTRI-RCA4 runs. Contrastingly, increases instead are expected in the PR when VECTRI is driven by RCA4-HadGEM2 (figure 3.21).
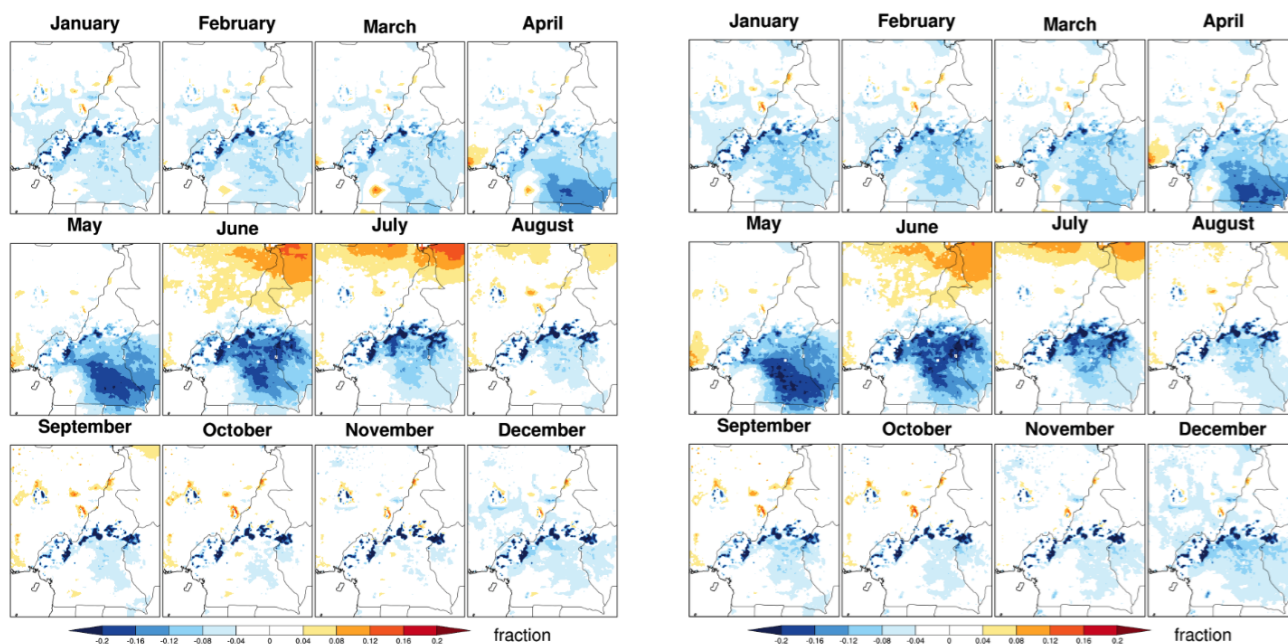
Figure 3.17: Monthly estimated PR projecting the fraction of the population being infected. VECTRI model driven by RCA4-EC-EARTH-ES for the period 2035-2065 **(a)** and 2071-2100 **(b)**.

Figure 3.17 exhibits the monthly mean changes in PR over the near future and the far future for RCA4-EC-EARTH-ES under RCP2.6 scenario.
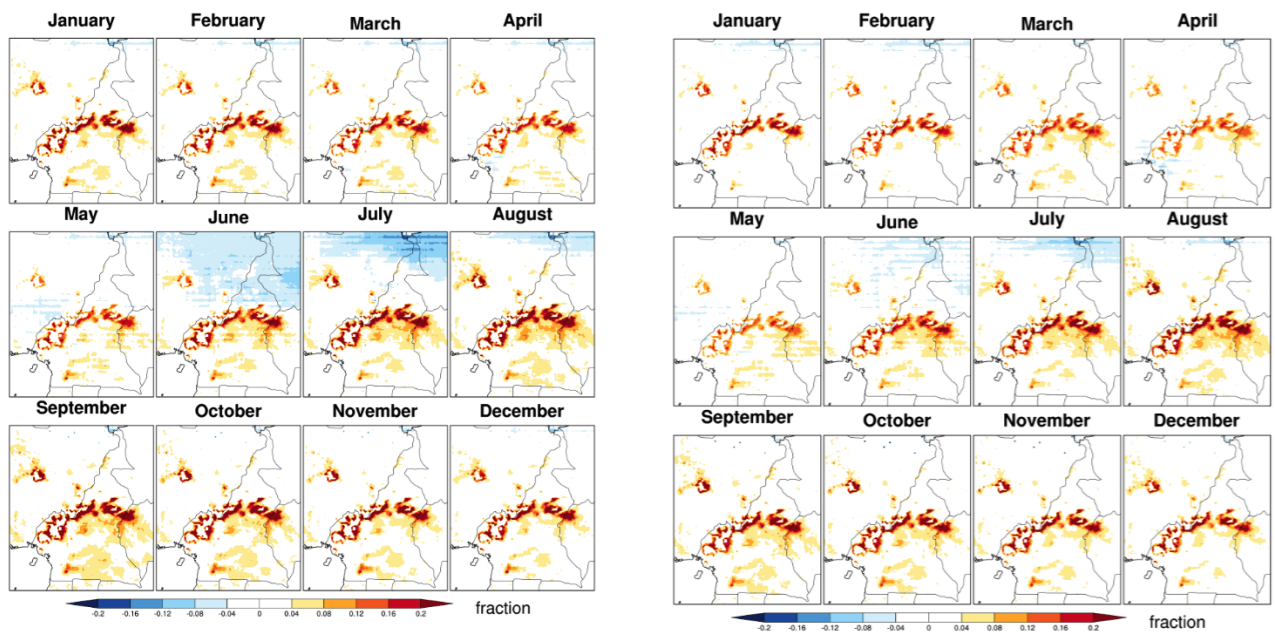
Figure 3.18: Monthly estimated PR projecting the fraction of the population being infected. VECTRI model driven by RCA4-MPI-ESM-LR for the period 2035-2065 **(a)** and 2071-2100 **(b)**.

Figure 3.18 exhibits the monthly mean changes in PR over the near future and the far future for RCA4-MPI-ESM-LR under RCP2.6 scenario.
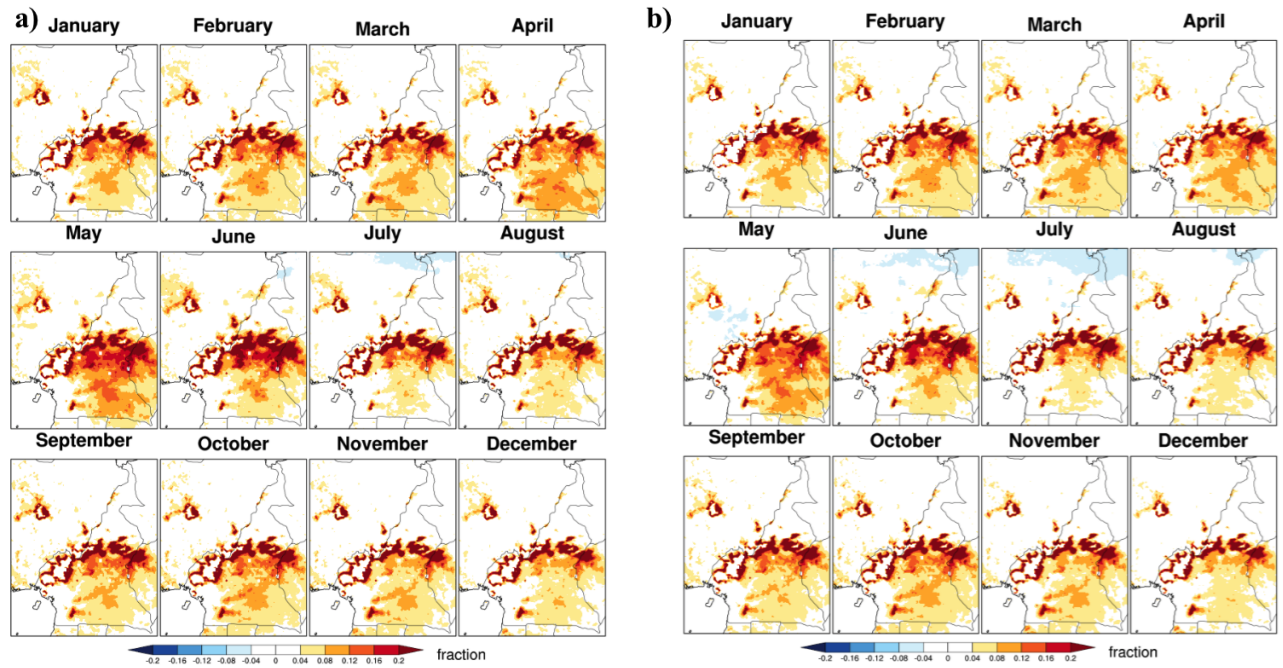
Figure 3.19: Monthly estimated PR projecting the fraction of the population being infected. VECTRI model driven by RCA4-MIROC5 for the period 2035-2065 **(a)** and 2071-2100 **(b)**.

Figure 3.19 exhibits the monthly mean changes in PR over the near future and the far future for RCA4-MIROC5 under RCP2.6 scenario.
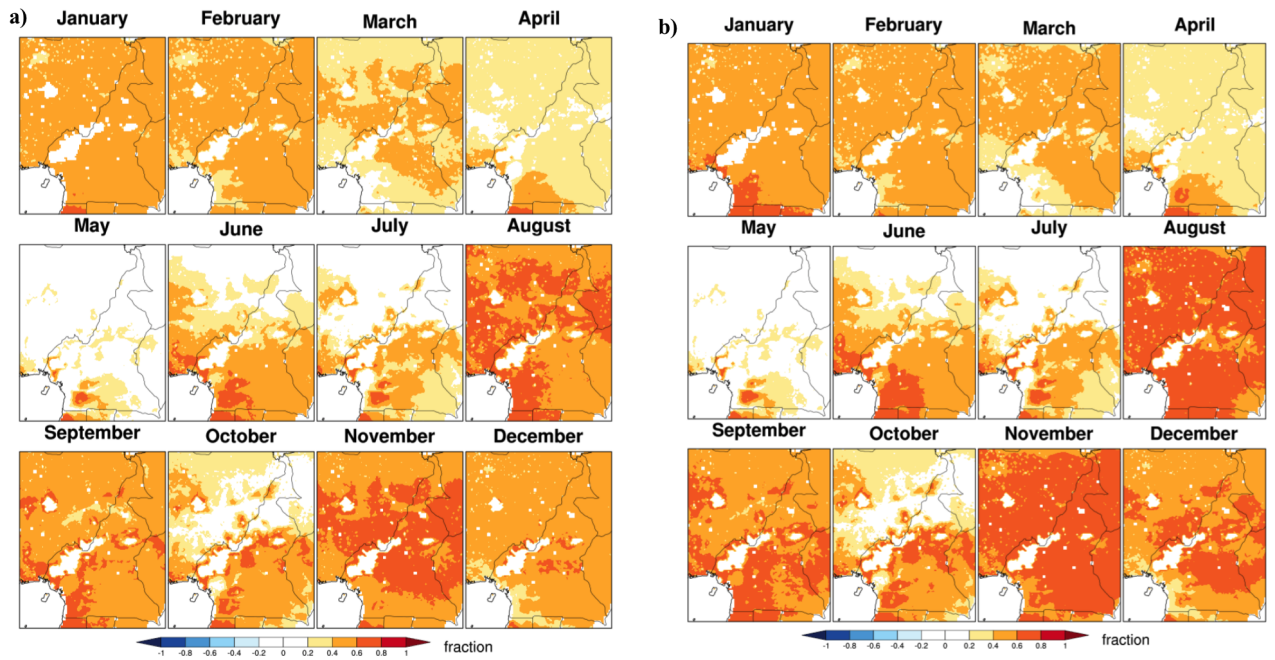
Figure 3.20: Monthly estimated PR projecting the fraction of the population being infected. VECTRI model driven by RCA4-HadGEM2 for the period 2035-2065 **(a)** and 2071-2100 **(b)**.

Figure 3.20 exhibits the monthly mean changes in PR over the near future and the far future for RCA4-HadGEM2 under RCP2.6 scenario.
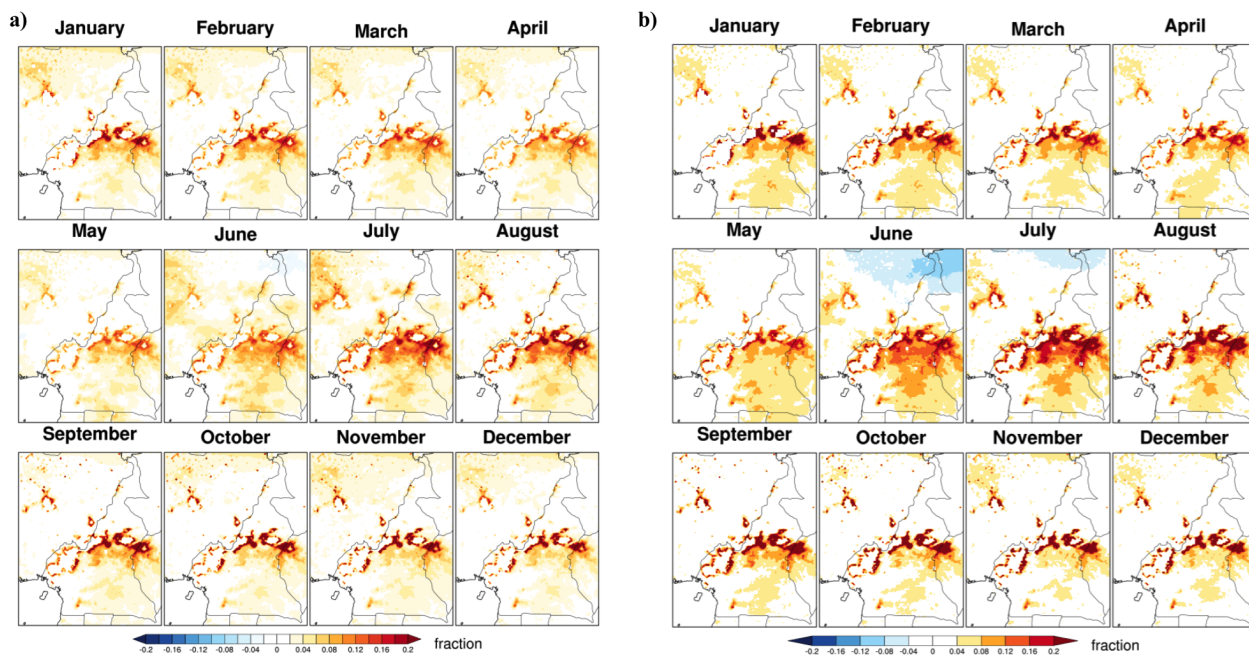
Figure 3.21: Monthly estimated PR projecting the fraction of the population being infected. VECTRI model driven by RCA4-NorESM1-M for the period 2035-2065 **(a)** and 2071-2100 **(b)**.

Figure 3.21 exhibits the monthly mean changes in PR over the near future and the far future for RCA4-NorESM1-M under RCP2.6 scenario.

Figures 3.22 that follow, shows the monthly mean changes in PR over the near future and the far future, under the low mitigated RCP8.5 scenario.
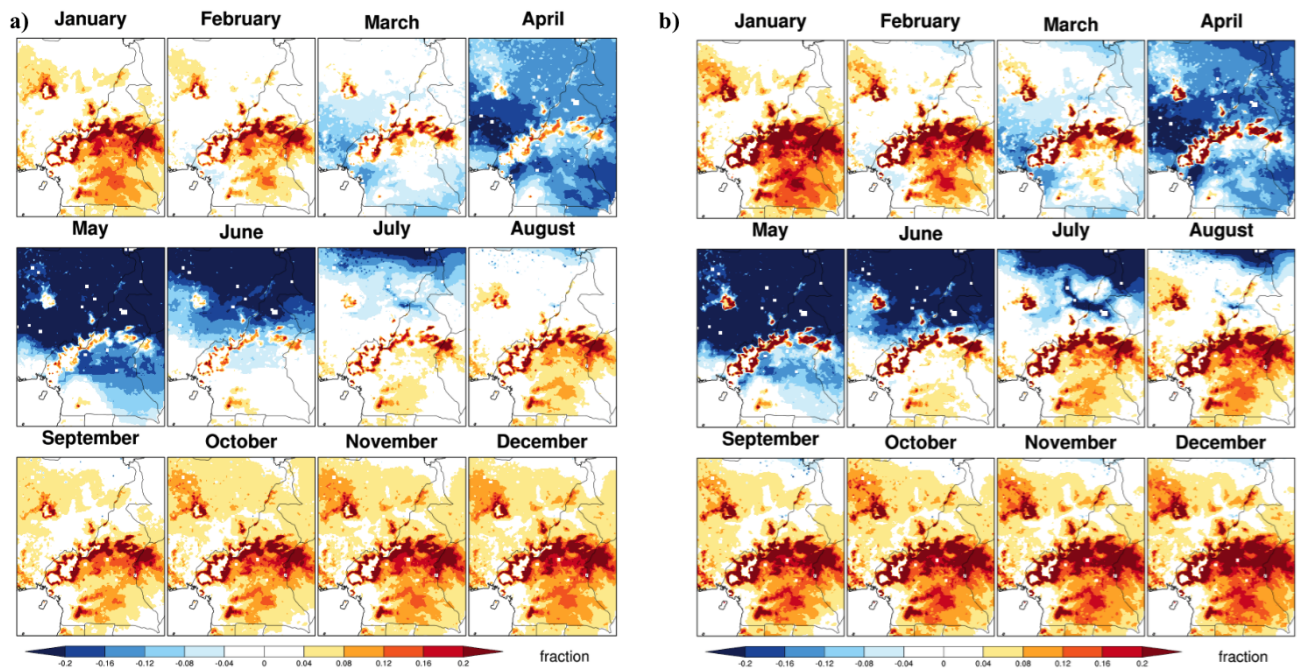
Figure 3.22: Monthly mean changes in PR under RCP 8.5 scenario. VECTRI model driven by RCA4-EnsMean for 2035-2065 **(a)** and 2071-2100 **(b)**.

Figure 3.22 presents the PR pattern with RCA-EnsMean as forcing under RCP 8.5 scenario. Results based on individual forcings of VECTRI by RCA4 experiments are highlighted on the following figures: figure 3.23 for RCA4-EC-EARTH-ES, figure 3.24 for RCA4-MPI-ESM-LR, figure 3.25 for RCA4-MIROC5, figure 3.26 for RCA4-HadGEM2 and figure 3.27 for RCA4-NorESM1-M. The increase in the PR is strongest when VECTRI is coupled with RCA4-HadGEM2 (figure 3.26).
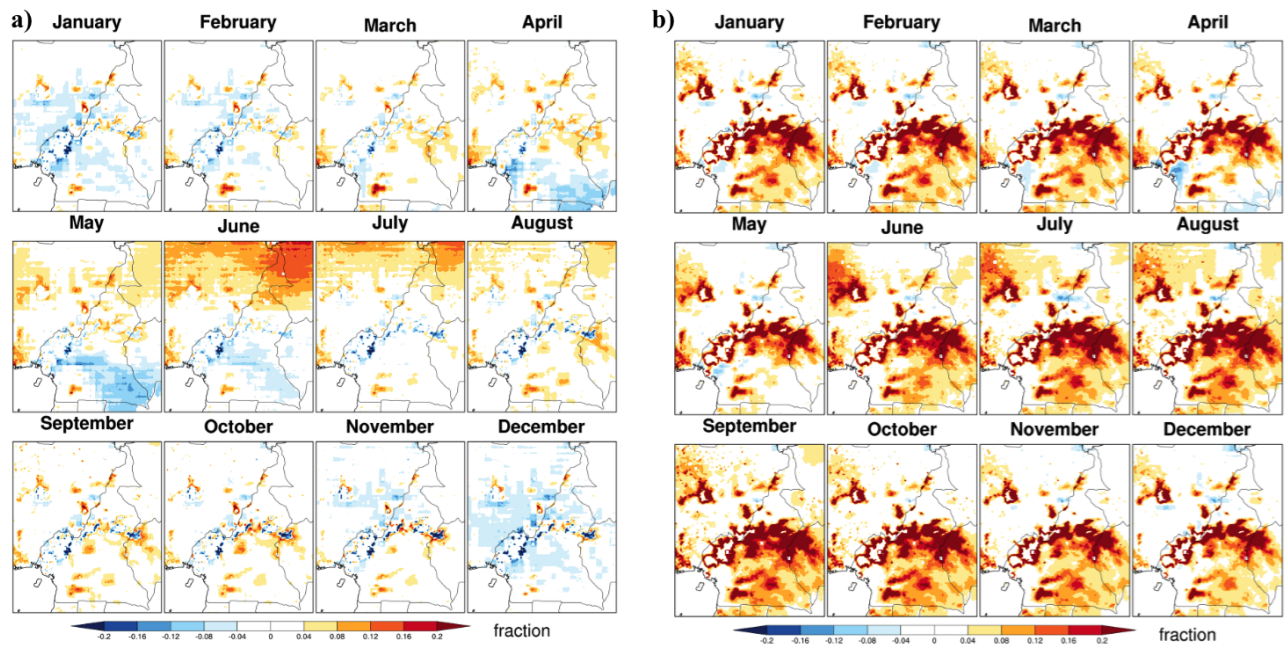
Figure 3.23: Monthly estimated PR projecting the fraction of the population being infected. VECTRI model driven by RCA4-EC-EARTH-ES for the period 2035-2065 **(a)** and 2071-2100 **(b)**.

Figure 3.23 presents the monthly mean changes in PR over the near future and the far future for RCA4-EC-EARTH-ES, under RCP8.5 scenario.
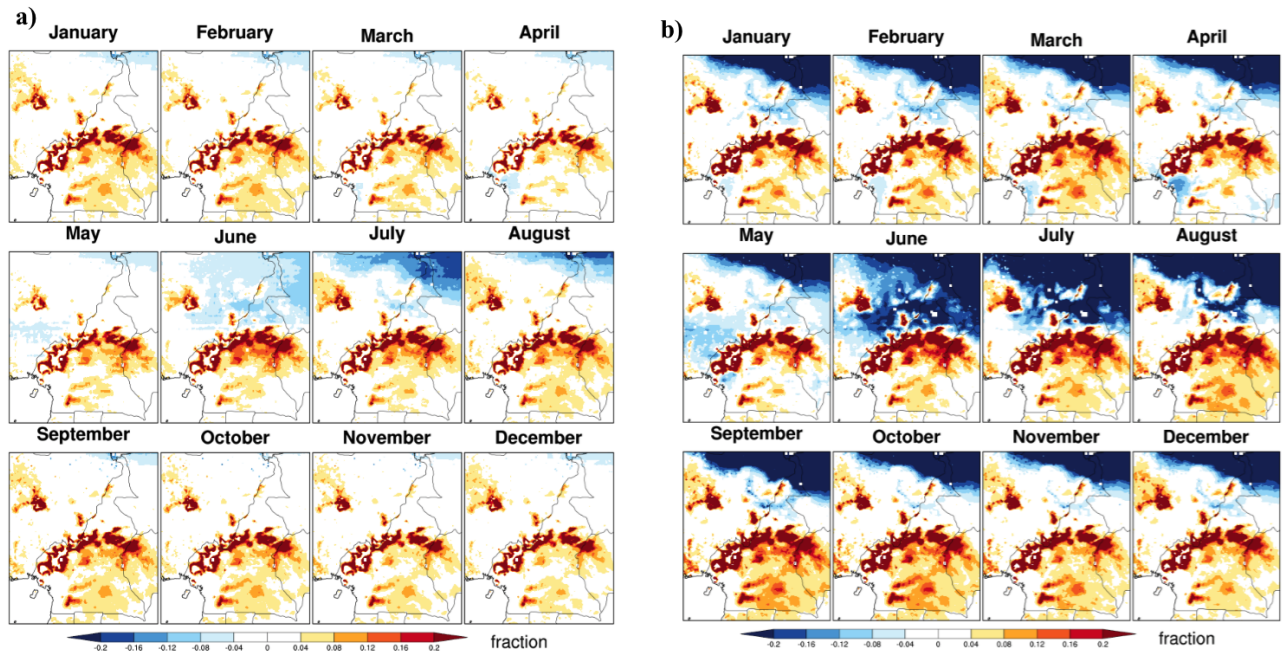
Figure 3.24: Monthly estimated PR projecting the fraction of the population being infected. VECTRI model driven by RCA4-MPI-ESM-LR, period 2035-2065 **(a)** and 2071-2100 **(b)**.

Figure 3.24 presents the monthly mean changes in PR over the near future and the far future for RCA4-MPI-ESM-LR, under RCP8.5 scenario.
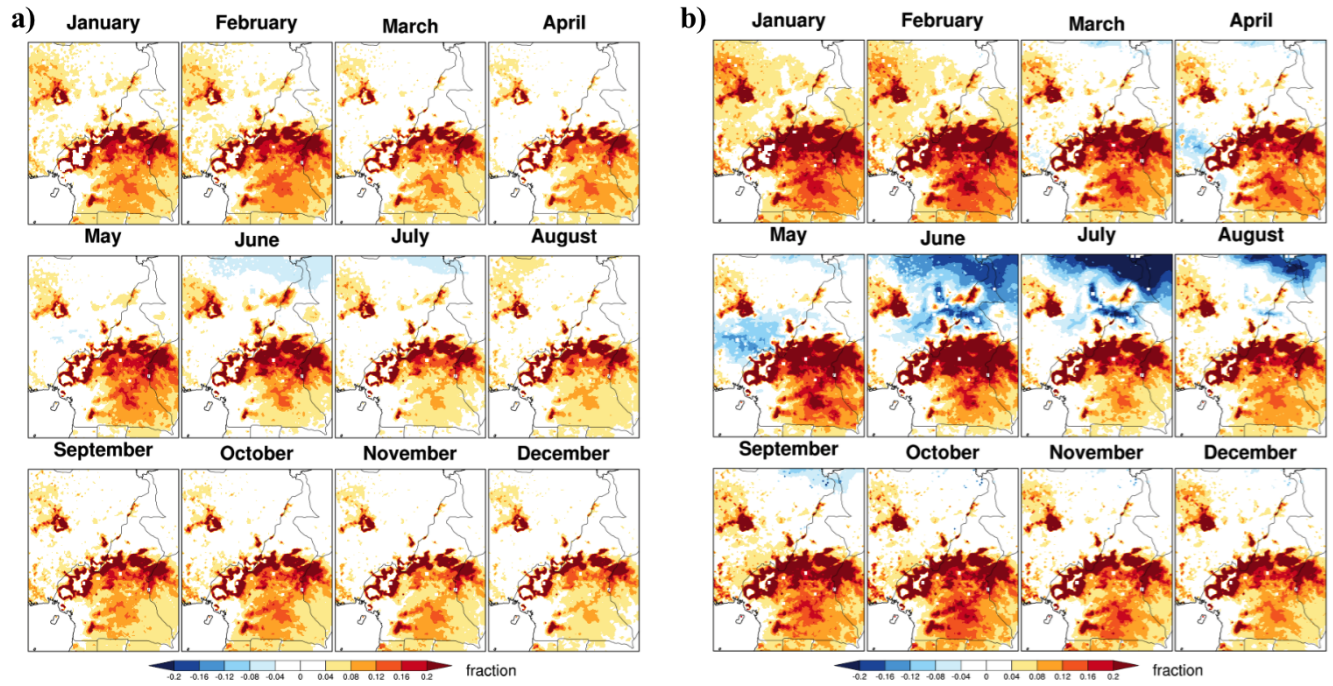
Figure 3.25: Monthly estimated PR projecting the fraction of the population being infected. VECTRI model driven by RCA4-MIROC5, period 2035-2065 **(a)** and 2071-2100 **(b)**.

Figure 3.25 presents the monthly mean changes in PR over the near future and the far future for RCA4-MIROC5, under RCP8.5 scenario.
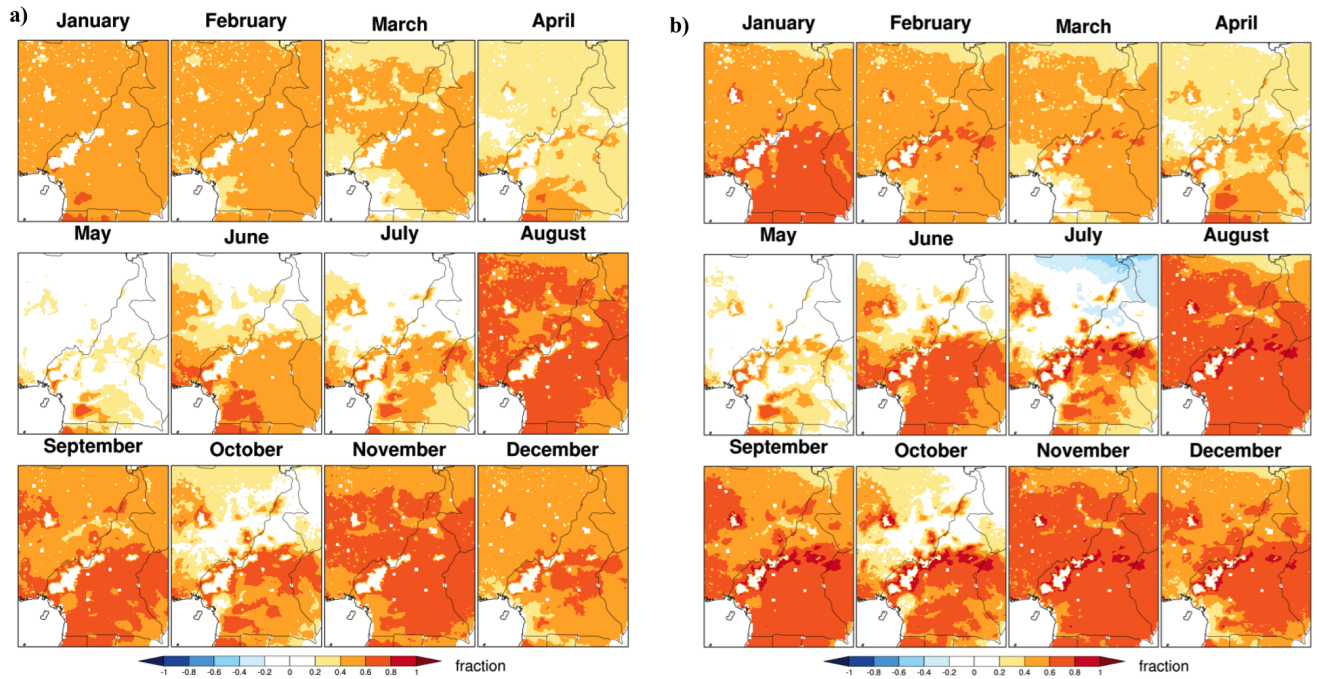
Figure 3.26: Monthly estimated PR projecting the fraction of the population being infected. VECTRI model driven by RCA4-HadGEM2 for the period 2035-2065 **(a)** and 2071-2100 **(b)**.

Figure 3.26 presents the monthly mean changes in PR over the near future and the far future for RCA4-HadGEM2, under RCP8.5 scenario.
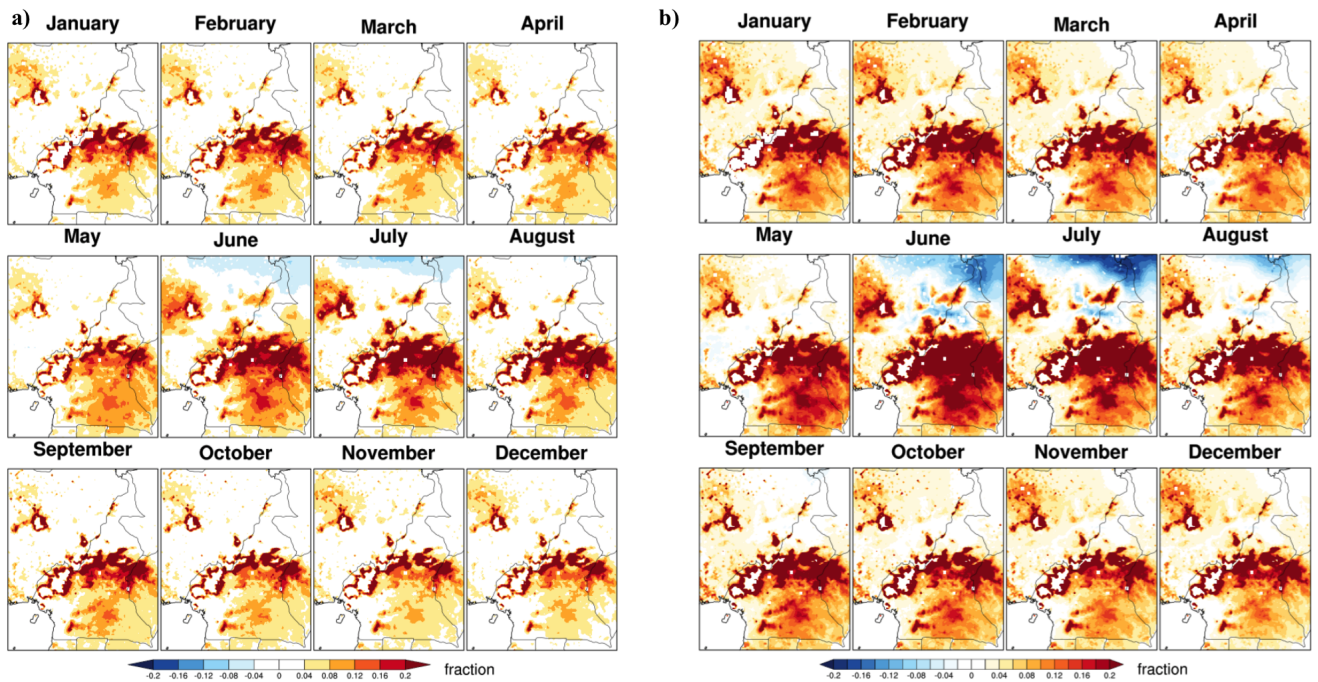
Figure 3.27: Monthly estimated PR projecting the fraction of the population being infected. VECTRI model driven by RCA4-NorESM1-M for the period 2035-2065 **(a)** and 2071-2100 **(b)**.

Figure 3.27 presents the monthly mean changes in PR over the near future and the far future for RCA4-NorESM1-M, under RCP8.5 scenario.

Under the high emission scenario RCP8.5 (figure 3.22), obvious differences between the near (figure 3.22**a**) and the far (Fig. 3.22**b**) future appears in the amplitude of changes in the PR. The PR generally tends to decrease from March to July, especially over NCAM and increase during the rest of the year, especially over WCAM and ECAM.

- Changes in the Entomological Inoculation Rate (EIR)

Figure 3.28 displays maps of monthly mean changes in the EIR pattern when VECTRI is forced by RCA4-EnsMean under RCP2.6.
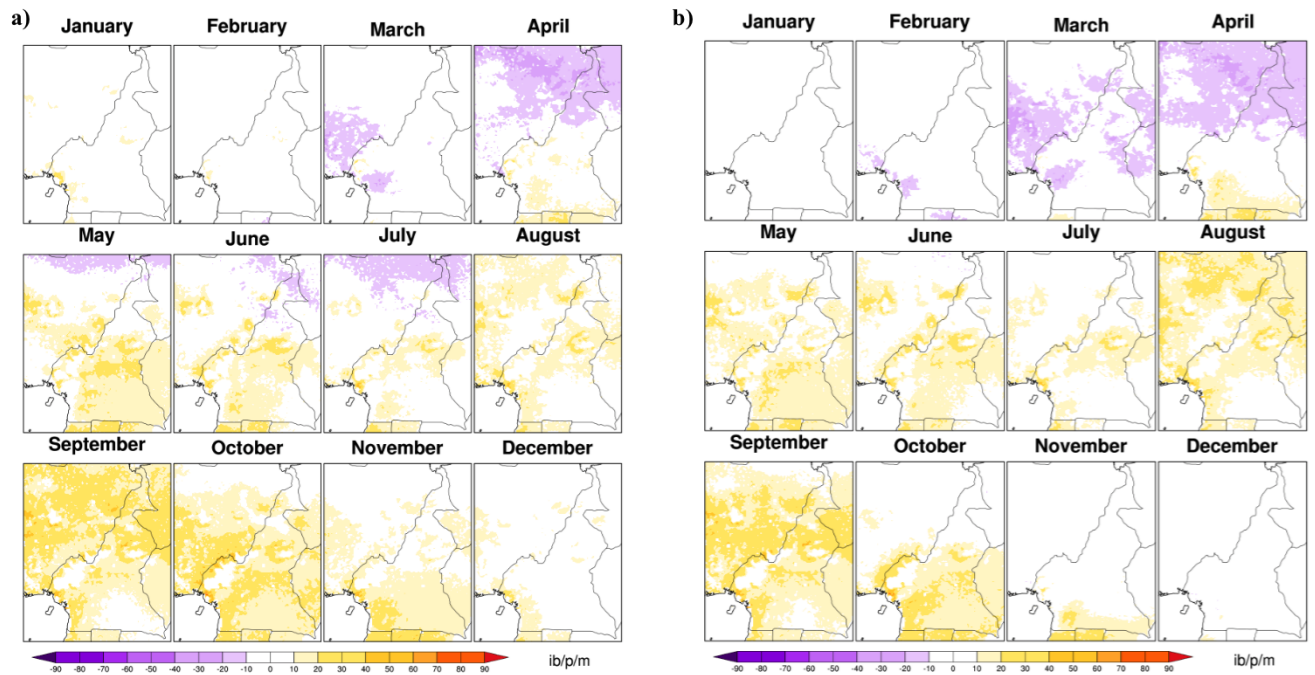
Figure 3.28: Monthly estimated changes in EIR indicating the number of infected bites per person per month (ib/p/m). This is obtained for the RCP 2.6 scenario from the coupling VECTRI-RCA4-EnsMean over the periods 2035-2065 **(a)** and 2071-2100 **(b)**.

Broadly under RCP2.6, EIR is projected to decrease from April to July in NCAM and during March in WCAM (Figure 3.28**a**). In the distant future, the EIR is expected to reduce from March to April, especially over NCAM (Figure 3.28**b**). Over WCAM and ECAM subregions, an intensification of EIR is projected from April to November whereas insignificant changes will occur for December and January.

For individual RCA4 model simulations, results are shown in the following figures (Figures 3.29, 3.30, 3.31, 3.32 and 3.33). EIR tends to gradually increase when VECTRI is forced with RCA4-HadGEM2 (figure 3.32), from June (WCAM and ECAM) to November with a peak in August-September (NCAM). There is a decrease in projections using rainfall and temperature from RCA4-EC-EARTH-ES (figure 3.29) whereas fewer changes are expected in EIR with RCA4-NorESM1-M (figure 3.33).
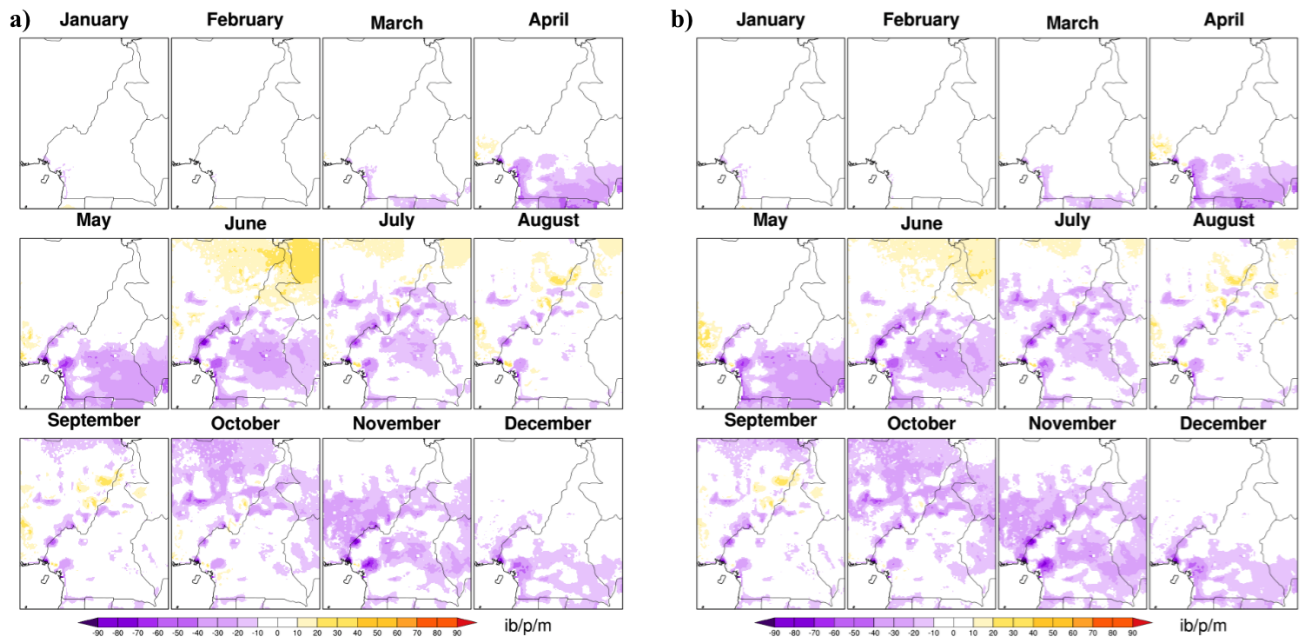
Figure 3.29: Monthly estimated EIR that indicates the number of infected bites per person. VECTRI model driven by RCA4-EC-EARTH-ES, period 2035-2065 **(a)** and 2071-2100 **(b)**.

Figure 3.29 highlights the monthly mean changes in EIR over the near future and the far future for RCA4-EC-EARTH-ES, under RCP2.6 scenario.
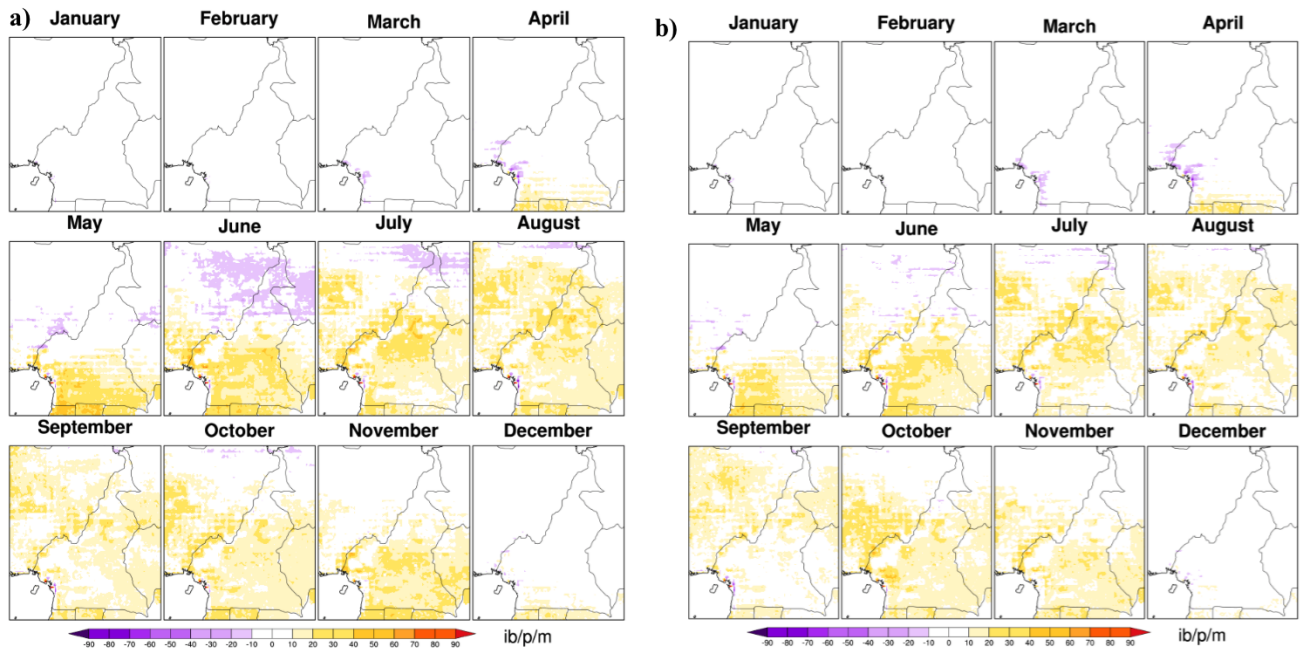
Figure 3.30: Monthly estimated EIR that indicates the number of infected bites per person. VECTRI model driven by RCA4-MPI-ESM-LR, period 2035-2065 **(a)** and 2071-2100 **(b)**.

Figure 3.30 highlights the monthly mean changes in EIR over the near future and the far future for RCA4-MPI-ESM-LR, under RCP2.6 scenario.
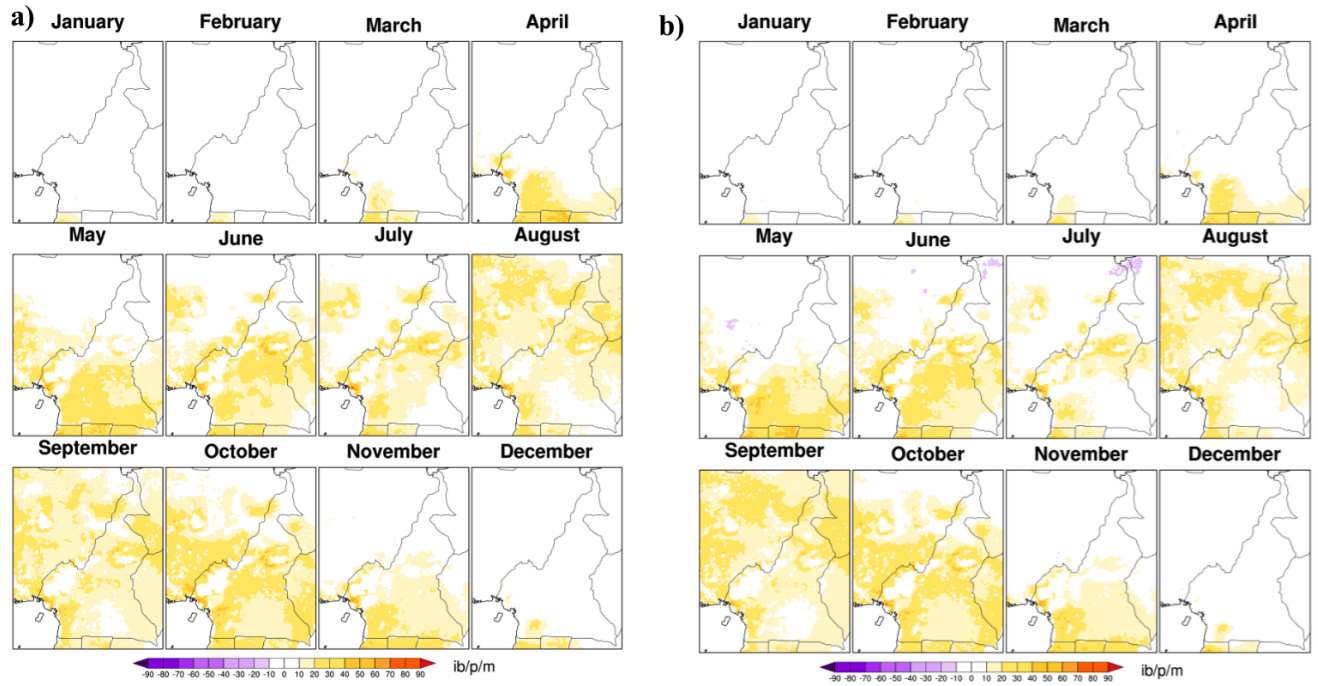
Figure 3.31: Monthly estimated EIR that indicates the number of infected bites per person. VECTRI model driven by RCA4-MIROC5, period 2035-2065 **(a)** and 2071-2100 **(b)**.

Figure 3.31 highlights the monthly mean changes in EIR over the near future and the far future for RCA4-MIROC5, under RCP2.6 scenario.
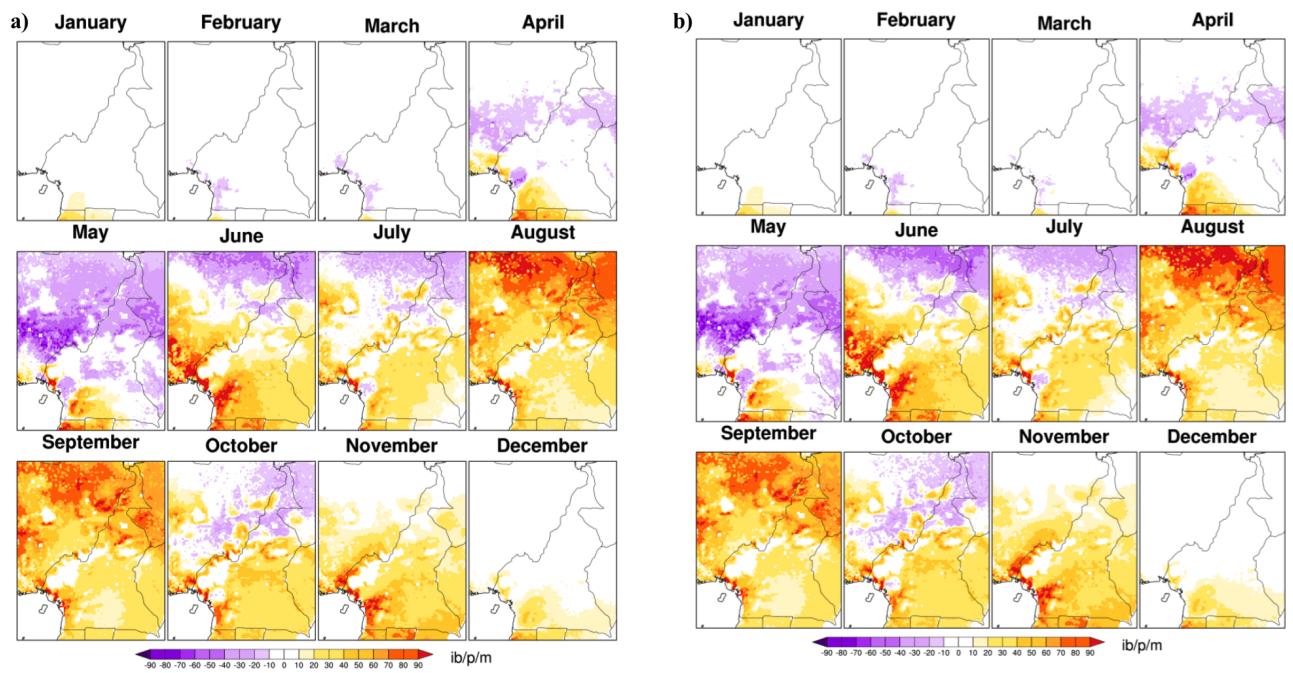
Figure 3.32: Monthly estimated EIR that indicates the number of infected bites per person. VECTRI model driven by RCA4-HadGEM2, period 2035-2065 **(a)** and 2071-2100 **(b)**.

Figure 3.32 highlights the monthly mean changes in EIR over the near future and the far future for RCA4-HadGEM2, under RCP2.6 scenario.
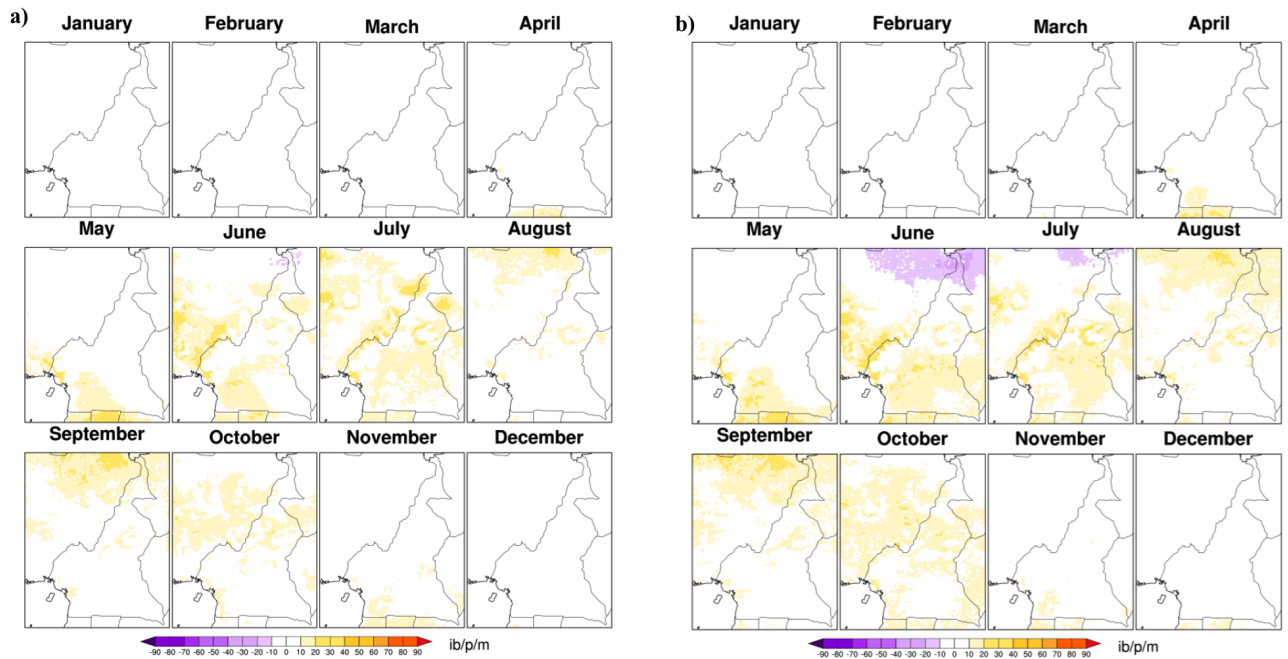
Figure 3.33: Monthly estimated EIR that indicates the number of infected bites per person. VECTRI model driven by RCA4-NorESM1-M, period 2035-2065 **(a)** and 2071-2100 **(b)**.

Figure 3.33 highlights the monthly mean changes in EIR over the near future and the far future for RCA4-NorESM1-M, under RCP2.6 scenario.

The following figure 3.34 presents maps of monthly mean changes in the EIR pattern when VECTRI is forced by RCA4-EnsMean under RCP8.5 .
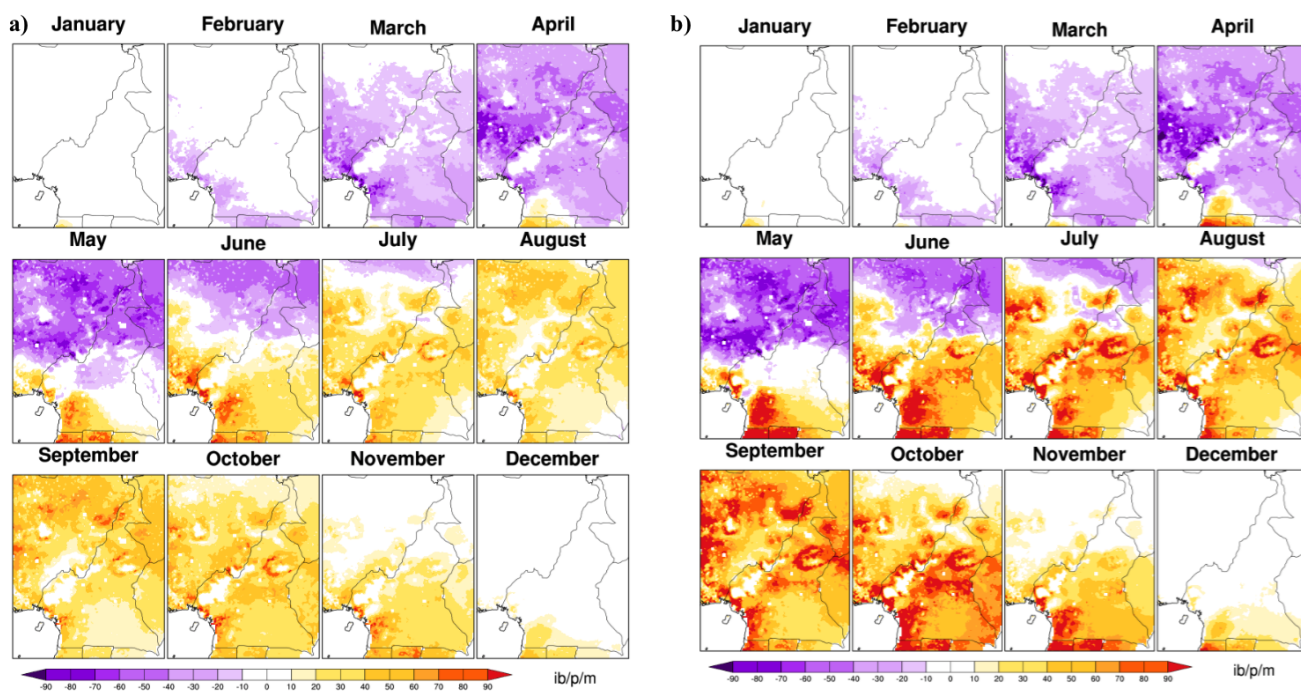
Figure 3.34: Monthly estimated changes in EIR, indicating the number of infected bites per person per month (ib/p/m). Results obtained from the coupling VECTRI-RCA-EnsMean under the RCP8.5 scenario and over 2035-2065 **(a)** and 2071-2100 **(b)** periods.

Under RCP8.5, EIR is expected to decrease significantly over almost the entire study area during March and April months and especially over NCAM from May to June (figures 3.34**a** and 3.34**b**). Conversely, EIR is projected to increase over WCAM and ECAM from May to November, and over NCAM from July to November. No particular changes are foreseen over almost the whole country from December to February, except for a small part of southern Cameroon where a strengthening of the EIR is noted in December and a weakening in February over the two projection periods.

Results with the coupling VECTRI-RCA4-EC-EARTH-ES, VECTRI-RCA4-MPI-ESM-LR, VECTRI-RCA4-MIROC5, VECTRI-RCA4-HadGEM2 and VECTRI-RCA4-NorESM1-M are presented in Figures 3.35, 3.36, 3.37, 3.38 and 3.39 respectively.
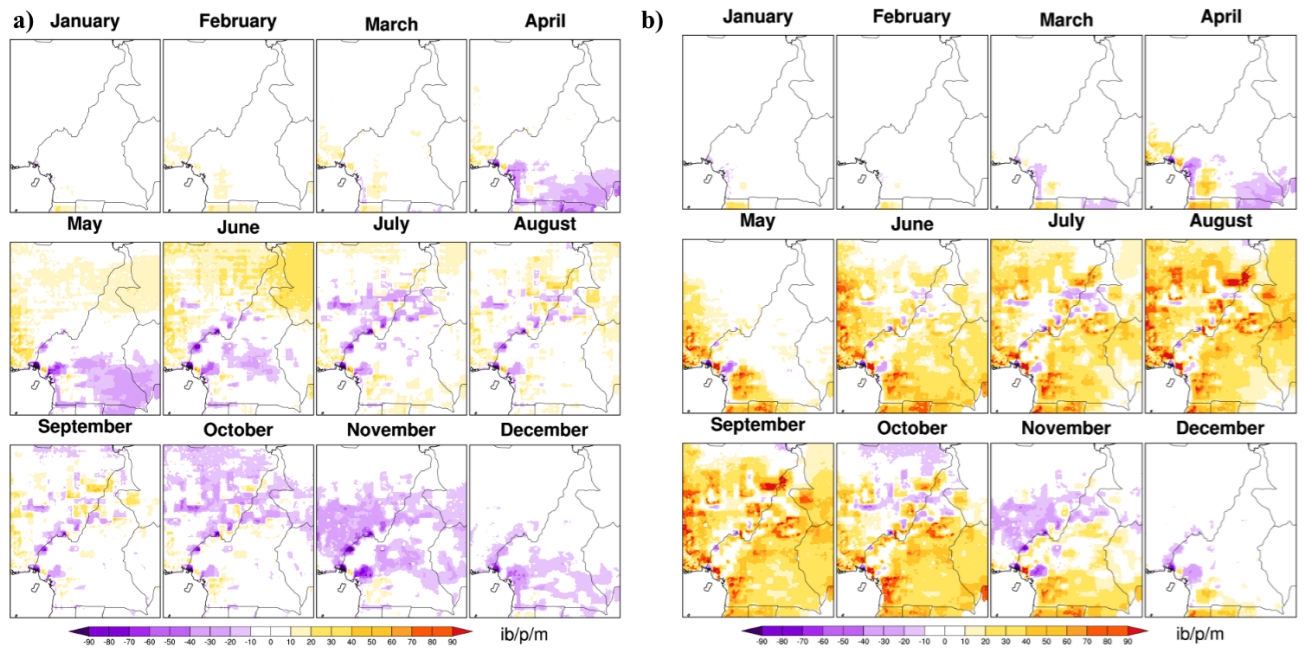
Figure 3.35: Monthly estimated EIR that indicates the number of infected bites per person. VECTRI model driven by RCA4-EC-EARTH-ES, period 2035-2065 **(a)** and 2071-2100 **(b)**.

Figure 3.35 shows the monthly mean changes in EIR over the near future and the far future for RCA4-EC-EARTH-ES, under RCP8.5 scenario.
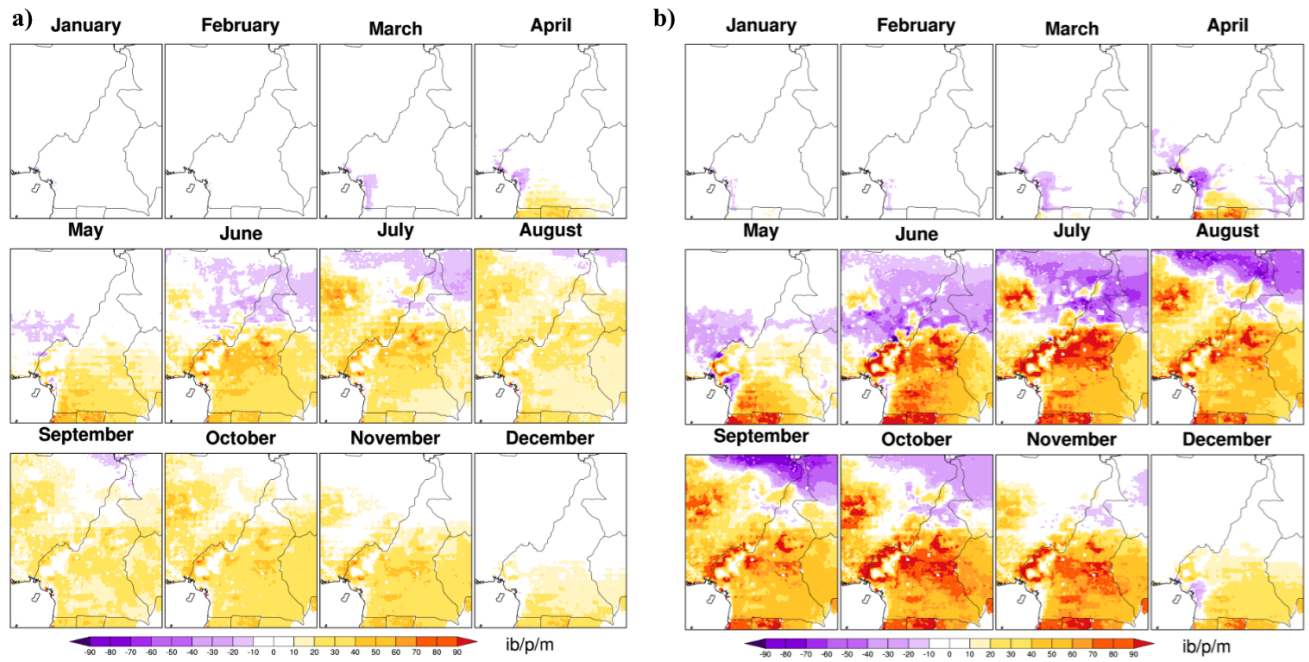
Figure 3.36: Monthly estimated EIR that indicates the number of infected bites per person. VECTRI model driven by RCA4-MPI-ESM-LR, period 2035-2065 **(a)** and 2071-2100 **(b)**.

Figure 3.36 shows the monthly mean changes in EIR over the near future and the far future for RCA4-MPI-ESM-LR, under RCP8.5 scenario.
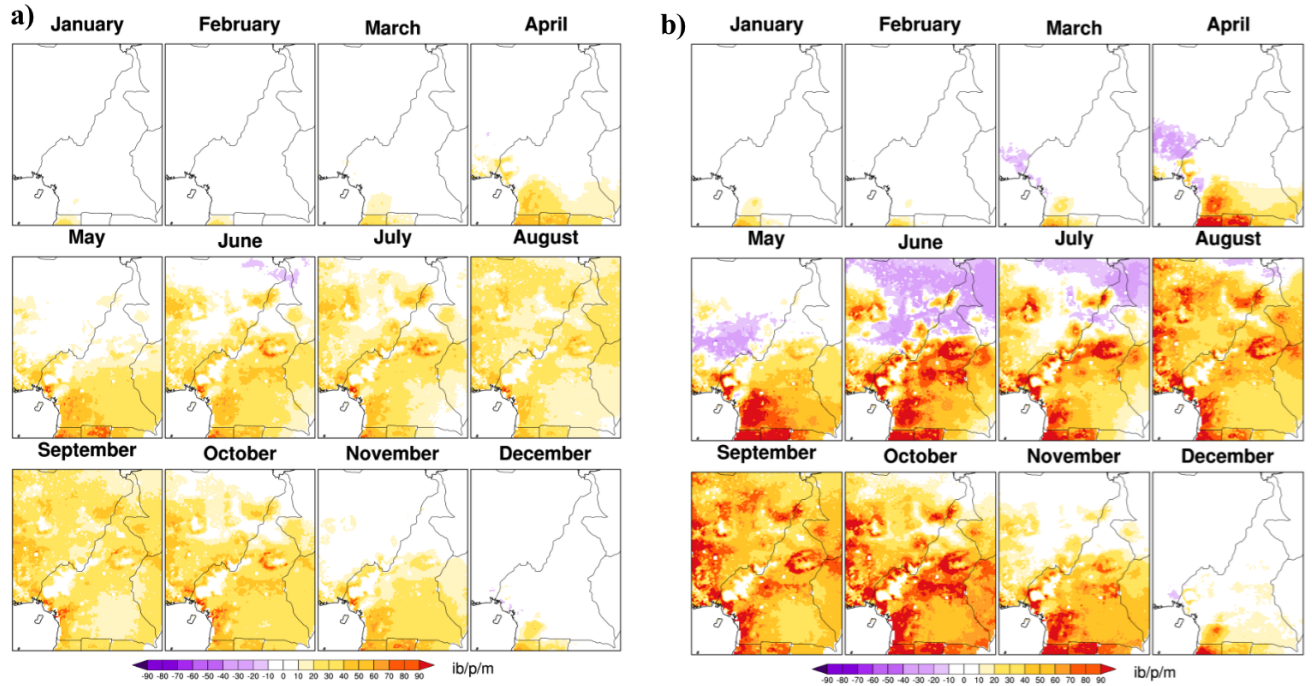
Figure 3.37: Monthly estimated EIR that indicates the number of infected bites per person. VECTRI model driven by RCA4-MIROC5, period 2035-2065 **(a)** and 2071-2100 **(b)**.

Figure 3.37 shows the monthly mean changes in EIR over the near future and the far future for RCA4-MIROC5, under RCP8.5 scenario.
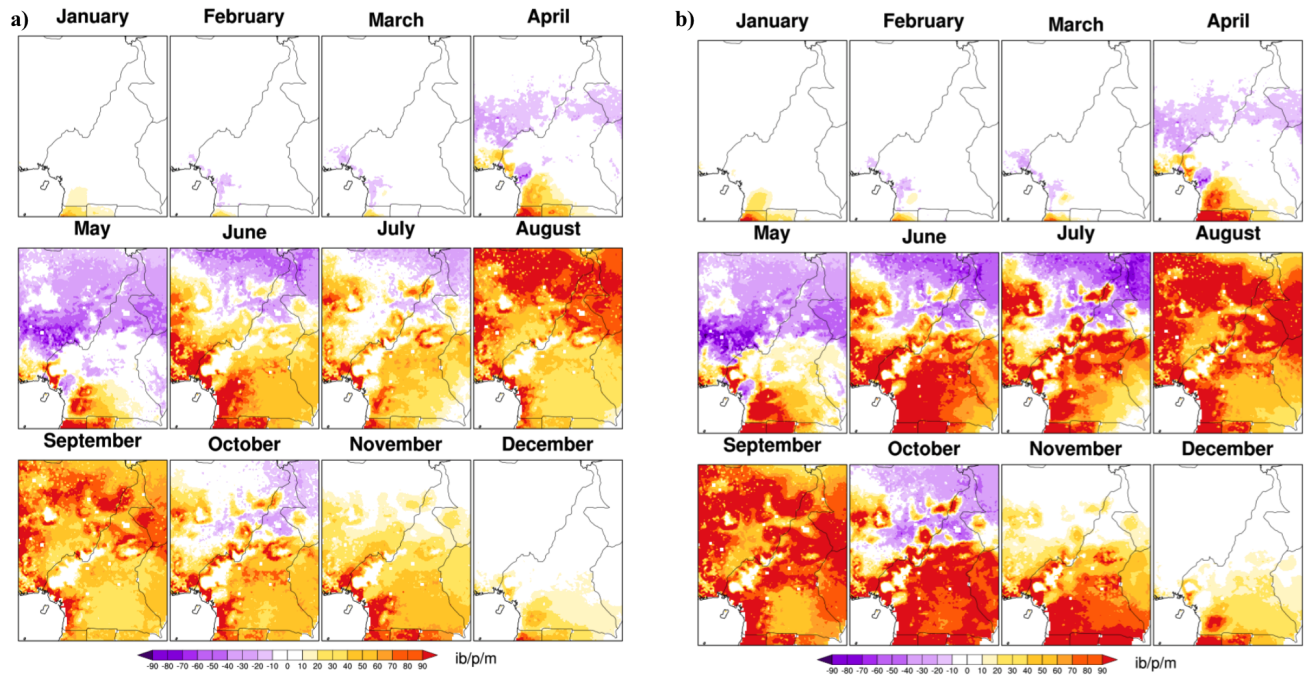
Figure 3.38: Monthly estimated EIR that indicates the number of infected bites per person. VECTRI model driven by RCA4-HadGEM2, period 2035-2065 **(a)** and 2071-2100 **(b)**.

Figure 3.38 shows the monthly mean changes in EIR over the near future and the far future for RCA4-HadGEM2, under RCP8.5 scenario.
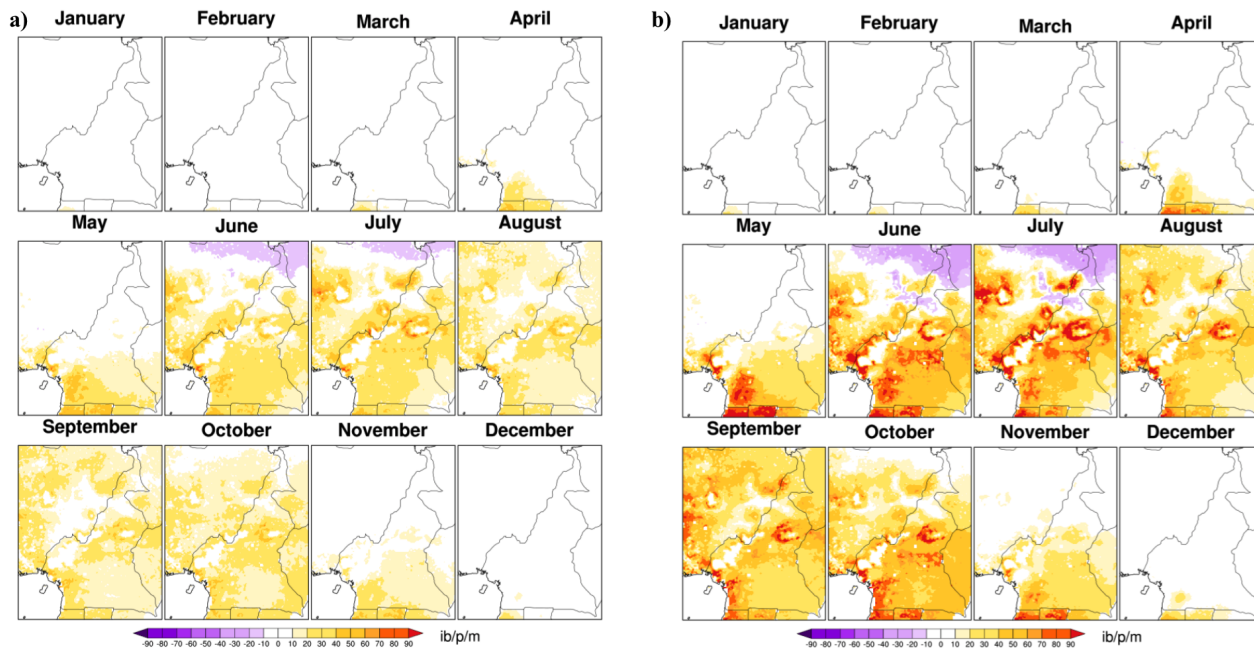
Figure 3.39: Monthly estimated EIR that indicates the number of infected bites per person. VECTRI model driven by RCA4-NorESM1-M, period 2035-2065 **(a)** and 2071-2100 **(b)**.

Figure 3.39 shows the monthly mean changes in EIR over the near future and the far future for RCA4-NorESM1-M, under RCP8.5 scenario.

3.2   Discussions

3.2.1   Parasite Ratio

The temperature and rainfall sensitivity to the parasite ratio (PR) data is broadly in line with earlier work. Favourable temperature ranges that support *Plasmodium falciparum* parasite transmission via *Anopheles* species, is generally between 18°C and 33°C [33]. Simple models of the temperature impact on the proportion of female adult vectors surviving long enough for the parasite to complete the sporogonic cycle and permit transmission suggest that, transmission should peak at temperatures of approximately 28 to 32°C [38]. Although these calculations are sensitive to the form of the adult mortality curve used and the temperature relationship with malaria remains poorly constrained. More recently, suggestions have been made that, accounting for the temperature sensitivity of the vector larvae stages, results in a cooler peak temperature of around 25°C [230]. Analysis of malaria indicators in

Uganda and Rwanda reveals the peaks of malaria transmission occurring at 28°C and 26°C respectively [231], while in Malawi, cases monotonically increa sed with temperature to the maximum temperature of 28°C [111]. In Cameroon, we found that the observed (surveyed) PR is maximum in the 22 to 26°C range, although there is a gap in the survey sampling in the 27 to 31°C range, and a warmer peak temperature can not be precluded. The model similarly produces peak PR at 26°C, in agreement with the survey data and previous work.

The precipitation relationship is more complex, with PR maximised in survey data at 7 mm day^{-1}. Usually moderate rainfall events are suitable for immature mosquitoes to complete the aquatic development stage, and emerge as adults [45]. Intense rains may cause flooding and flush out larvae from the habitats leading to a decrease in mosquito density [45, 232]. The survey data appears to be in good agreement with previous studies. In Botswana, cases peaked at a rainfall rate of approximately 4 mm day^{-1}, in Malawi the peak occurred at a high value of just over 6 mm day^{-1} [111] while in Uganda and Rwanda, highest cases numbers are associated with rainfall between 4 to 6 mm day^{-1} and 4 to 8 mm day^{-1}, respectively [231].

Available models will find it difficult to reproduce such prevalence survey data perfectly, due to many simplified assumptions used in malaria models. Even considering the climate-sensitive life-cycle processes that are accounted for, the model parameters are spatially and temporally homogeneous. For example, VECTRI hydrological scheme that determine the pond creation and subsequent loss through evaporation and infiltration are spatially constant, the temperature offset of breeding sites relative to the air temperature also. Moreover, many processes and factors that affect prevalence are not accounted for at all in the model, population movements are neglected, same as those of the vectors, no information on interventions usage, and the model for transmission in the host is extremely simple, neglecting superinfection and incorporating a very simple treatment of immunity. It could be argued that the data is not available to improve many of these aspects. That said, it is encouraging that the model at least manages to reproduce the underlying climate sensitivities revealed in the survey data.

Concerning the population density relation, PR in the survey data reduces as population density increases. This agrees with previous work [66], for instance, in Burkina Faso epidemiological profiles and clinical malaria transmission patterns tend to be high in rural compared to urban environments [44]. A review of entomological studies conducted across sub-Saharan

Africa countries demonstrated that the higher number of annual *Plasmodium falciparum* EIR were reported in rural populations, where population density < 100 inhabitants per km^2. However, low EIR were measured in urban areas where population density > 1000 inhabitants per km^2 [62]. This effect is also apparent in the model, but the model appears to exaggerate the effect, tending to be higher relative to observations for rural settings, while under predicting PR in urban centres. For example, one survey conducted in central Yaounde by Quakyi et al [129], with a prevalence of 0.5 to 0.6 revealed in the sampled population of 231 people. The population density in this location exceeds 9000 people km^{-2} and at such high densities the model fails to sustain transmission. One key process in such central urban locations is likely to be population movements, neglected in the model at present, with many of the cases likely to be imported. Other factors also impacts differences between rural and urban areas which are challenging to include in the model, for example, urban zones are associated with low transmission due to factors such as limited available breeding sites, improved environmental conditions, easy access to control interventions, housing types and among others [233]. For instance, Cameroon national malaria control programme reported that bed nets are more used in urban than rural zones [234]. Most of these social and environmental factors would act to increase disparities between rural and urban transmission, thus the crucial importance of mobility can not be overlooked. In addition, the fact that the model neglects superinfection will also act to exaggerate the population density impact. In the model's simple SEIR approach, once an infective bite results in successful transmission event, the host moves to an infective state. The impact of large inoculations of multiple strains when many infectious bites are recorded is not included, thus that individuals enhanced capacity to further transmit the disease is neglected. This would lead to the model overestimating the population dilution effect.

3.2.2 Entomological Inoculation Rate

In the survey data for the 16 EIR-sites, the EIR closely follows the seasonality of rainfall with a lag of approximately one month. The EIR maximises in April, May and June while the second peak is observed in October, November and December. The observed seasonal variability of EIR agrees with variability in reported malaria cases, with high case numbers observed during and after rainy seasons [234]. In Nkoteng for example, Cohuet et al [11] revealed that malaria transmission intensity reaches its peak in April during the rainy season. In a related study in Niete (South Cameroon), Bigoga et al [125] found a lower EIR during

dry season (1.09 ibp^{-1}n^{-1}) compared to rainy season (2.3 ibp^{-1}n^{-1}). Similarly, comparing Simbock and Etoa districts, Quakyi et al [129] found similar difference between rainy and dry seasons but a high disparity was observed for Etoa. They measured 1.9 ibp^{-1}n^{-1} and 1.2 ibp^{-1}n^{-1} for wet and dry seasons, respectively for Simbock and 2.4 ibp^{-1}n^{-1} and 0.4 ibp^{-1}n^{-1} for Etoa during the wet and dry season respectively.

The survey data for EIR in Sanaga villages, Mbebe, and Simbock contrasts strongly, and produces a seasonality of EIR which appears to be completely out of phase with the rainfall, with EIR at a maximum during the dry season, precisely January to March (for Sanaga villages and Mbebe) and January (for Simbock), behaviour that VECTRI was unable to capture. One possible explanation for this disparity could be linked to their geographical situation and local hydrology. Simbock is located at about 100m from the Mefou river creating a permanent swamp [198], while Sanaga villages and Mbebe are situated in the vicinity of the Sanaga river as presented on figure 3.40.
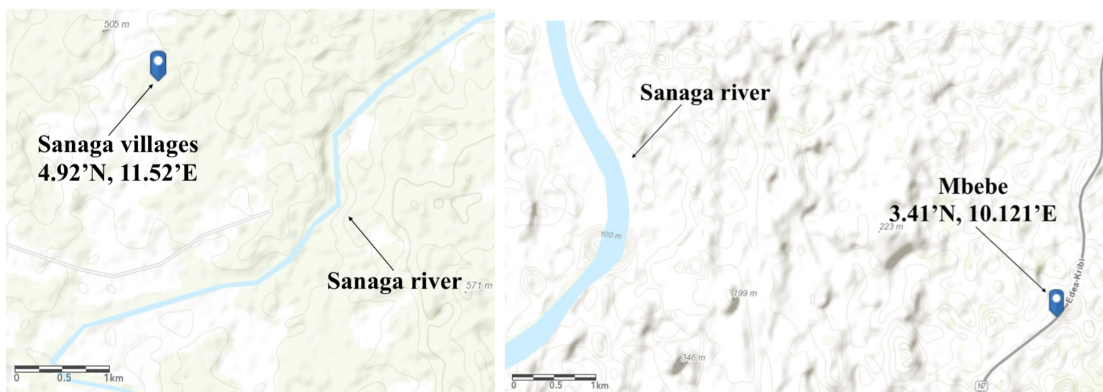
Figure 3.40: Sanaga villages and Mbebe locations, situated at the vicinity of the Sanaga river.

Rivers can support mosquito breeding by providing permanent source of water for aquatic stage development; which is the case for *Anopheles funestus*, *Anopheles nili* and *Anopheles gambiae* [194]. *Anopheles nili* usually breeds among the grass on the edges of the river and can be a key driver of malaria transmission in such environments [193]. However, the influence of rivers as potentiel breeding sites is enhanced during the dry season when flow is in the ability of standing pools leading to the proliferation of ideal breeding sites for *Anopheles* vectors [235, 136, 236]. The Mefou river was also found during the dry season, to provide breeding opportunities for *Anopheles funestus* within the emergent vegetation in swamps

along its edges [237]. The Sanaga river particularly undergoes a strong seasonal cycle in discharge, with flow at a minimum in February to April, with just a small fraction of the peak discharge during these months as presented on the following figure 3.41
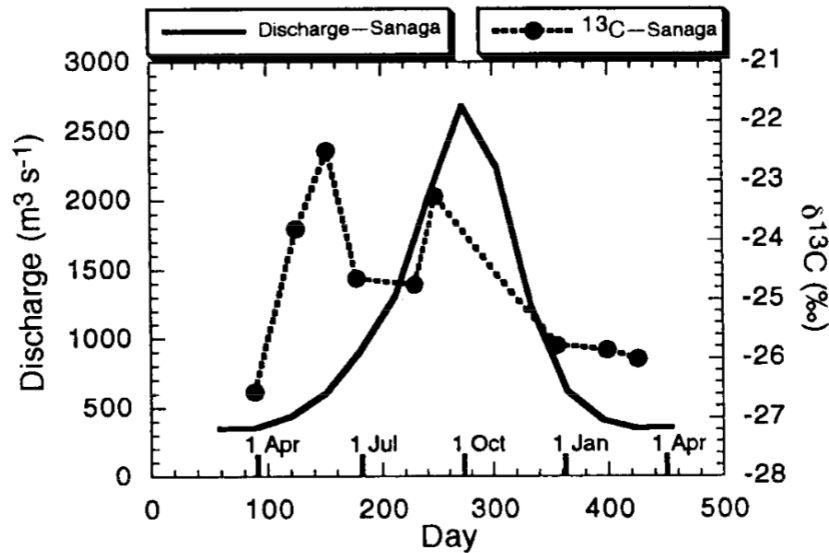
Figure 3.41: Sanaga discharge during dry period [238].

Thus it seems in Sanaga villages and Mbebe, peak in malaria is associated with the minimum in the Sanaga river flow, and an enhancement in ponding. As this version of VECTRI does not account for permanent breeding site associated with river systems, with enhanced ponding in low flow periods, it is not able to reproduce the seasonal cycle in EIR here.

3.2.3   PR and EIR projections from VECTRI

From figure 3.16**a** PR is projected to increase throughout the year with emphasis from October to March over the near future. A similar pattern is observed over the far future (figure 3.16**b**), where the PR tends to mostly increase over WCAM and decreases during the April month in NCAM. The PR is projected to significantly decrease in the distant future than in the near future.

The above results indicate that global warming would not much change the life cycles of the Anopheles mosquito and the malaria parasite *plasmodium falciparum*. Actually, rainfall creates suitable conditions (availability of ponds) for the mosquitoes breeding process. But extreme rainfall could negatively impact the productivity of mosquito breeding habitat by

flushing effect which leads to high mosquito losses ([53]). This is observed in Figures 3.16 and 3.22 from April to September referring to rainfall patterns presents on the following figures 3.42 and 3.43.
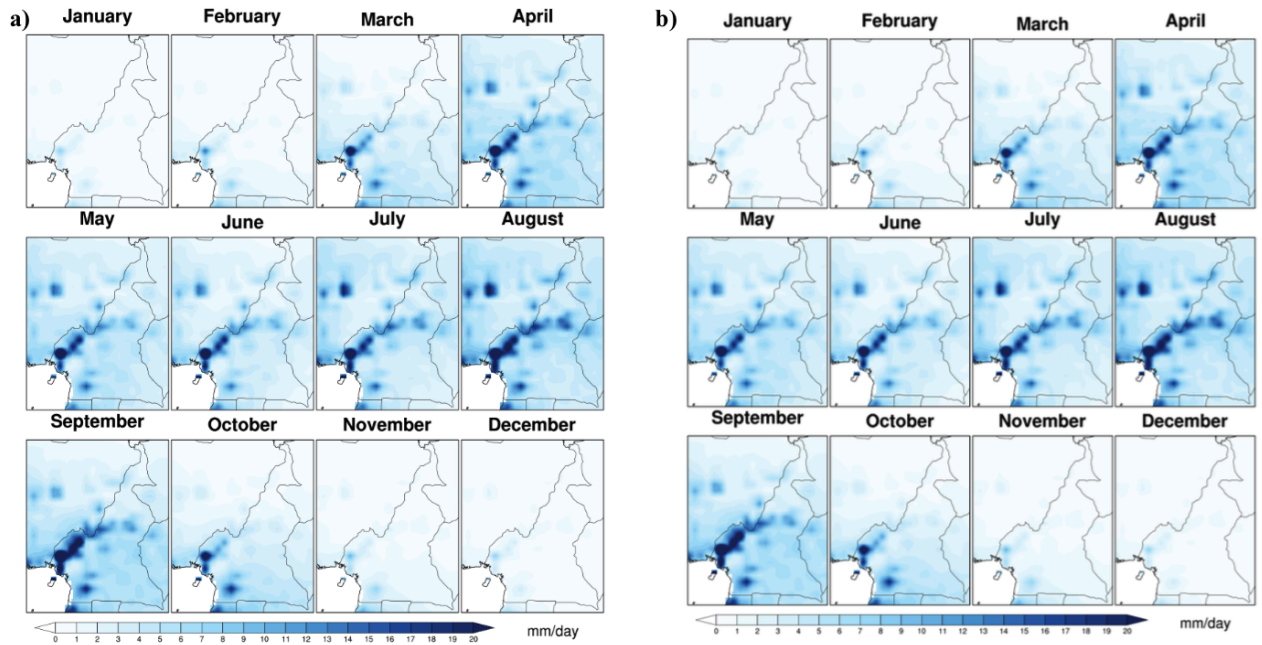
Figure 3.42: Monthly mean rainfall from 2035-2065 **(a)** and 2071-2100 **(b)** with RCP 2.6 RCA4-EnsMean.
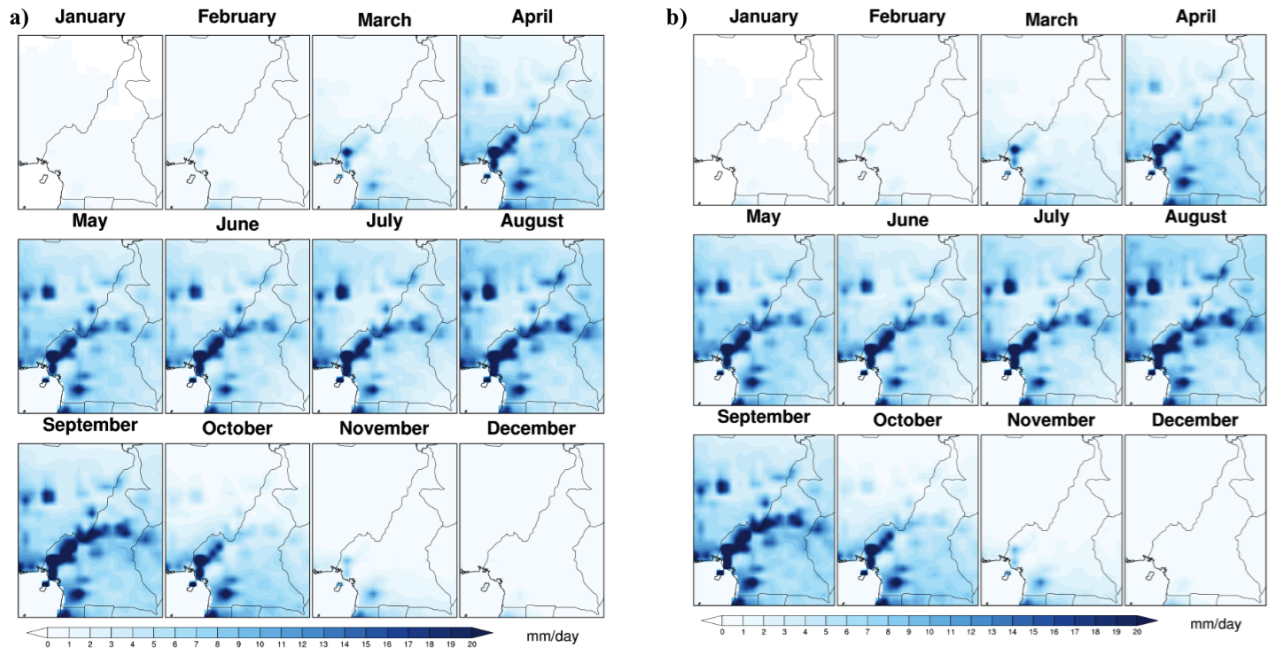
Figure 3.43: Monthly mean rainfall from 2035-2065 **(a)** and 2071-2100 **(b)** with RCP 8.5 RCA4-EnsMean.

Moreover, PR tends to intensify with temperature values less than 32°C as presented on the following figures 3.44 and 3.45.
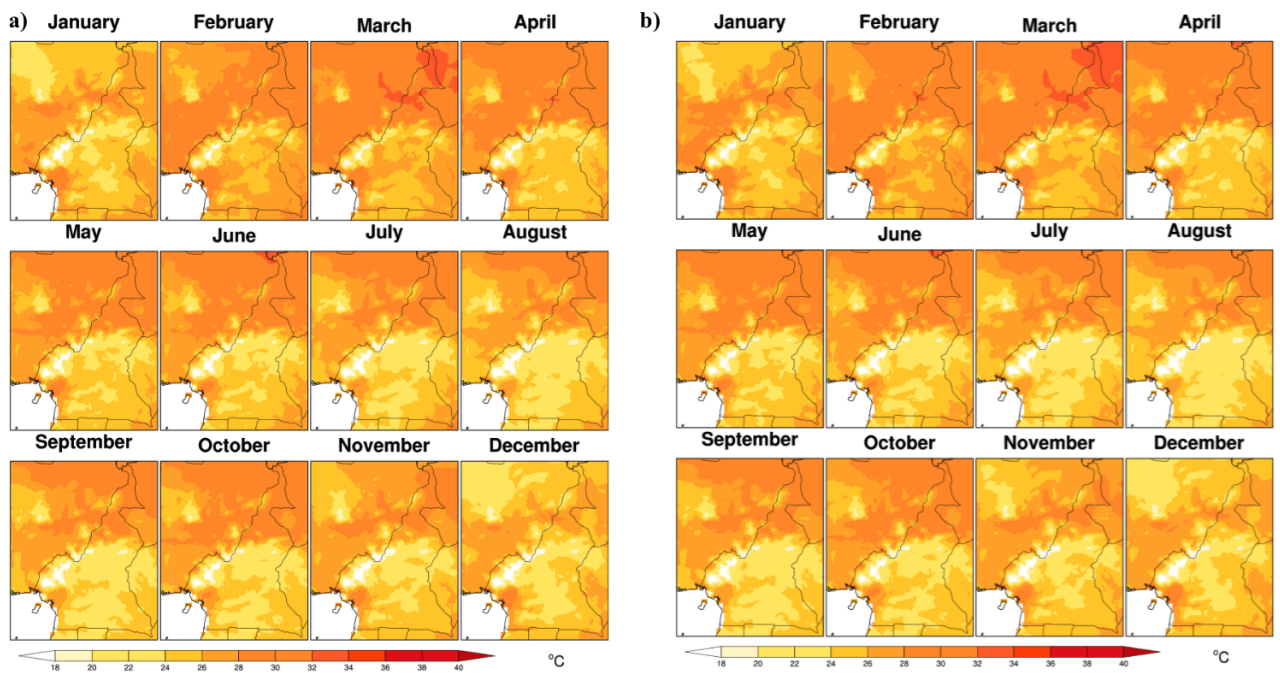
Figure 3.44: Monthly mean 2m-temperature from 2035-2065 **(a)** and 2071-2100 **(b)** with RCP 2.6 RCA4-EnsMean.
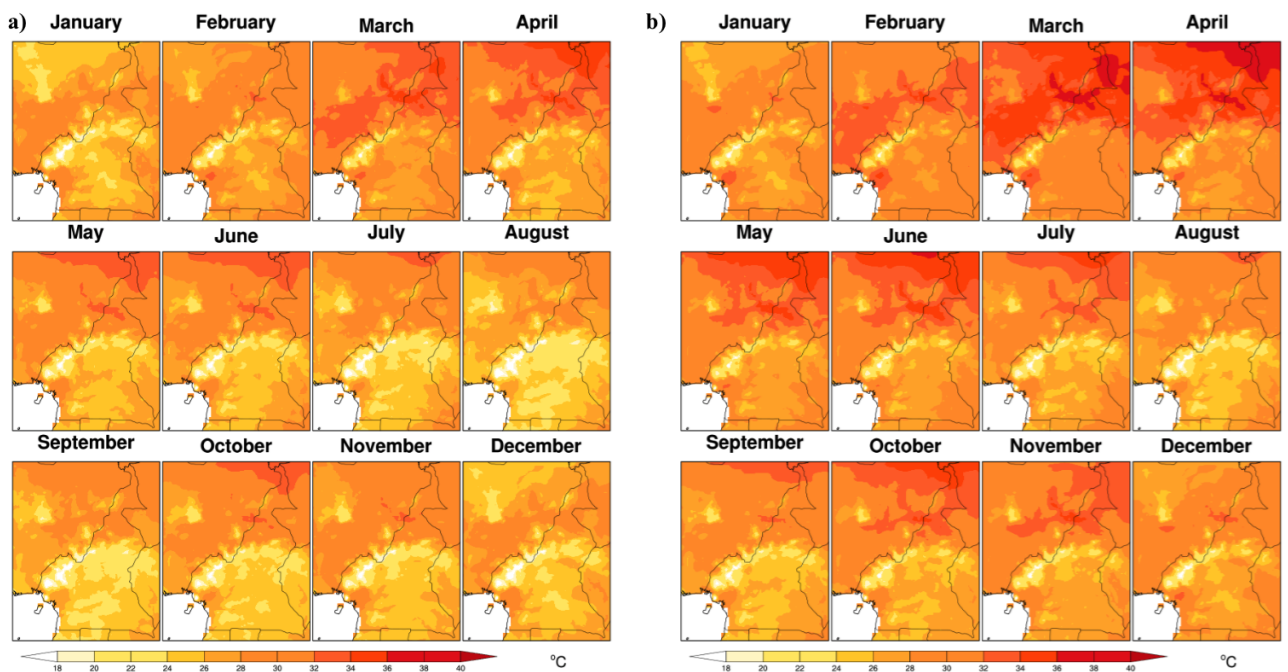
Figure 3.45: Monthly mean 2m-temperature from 2035-2065 **(a)** and 2071-2100 **(b)** with RCP 8.5 RCA4-EnsMean.

This is associated with the fact that there is a range of temperatures that allows malaria transmission. In fact, the temperature is able to create good conditions for malaria vectors to thrive. Generally, the increase in temperature accelerates vector life cycles and also decreases the incubation period of the parasite ([239]). This result is in line with previous studies conducted over Cameroon. They showed that the temperature suitability range for *Anopheles gambiae* and *Anopheles funestus* is between 20°C to 29°C ([240]). Similar results were reported over the Limpopo Province in South Africa ([241]). However, at a very high temperature, mortality is high thus reducing transmission ([242]), which corresponds to the situation expected in NCAM (figure 3.22 from April to July), and previously reported by [243], and [244].

Changes in EIR presented in figures 3.28 and 3.34 can be explained by the suitable range of temperature of 18-33°C ([33]) of the study area as highlighted in figures 3.44 and 3.45. But it should be recalled that temperatures above 30°C are prejudicial for anopheles development, and therefore leading to a decrease in EIR as demonstrated in [245].

EIR pattern is stronger in the far future than in the near future and vice-versa (figures 3.28 and 3.34). In general, the signal of change is stronger under RCP 8.5 than RCP 2.6, meaning an increased risk with the increased level of the radiative forcing. A similar study conducted by [246] over India showed that under global warming, malaria transmission is expected to strengthen together with the duration of the transmission season. The EIR results also highlight the important role of changes in rainfall and temperature on malaria incidence and show the seasonality of the disease. Similar work also demonstrated that a decline in precipitation is beneficial for the growth of the mosquito population, which causes higher EIR ([247]). Our study also attests to general expectations with regard to the impact of global warming on the spread of malaria. It is generally accepted that climate change will affect the spread of malaria as mentioned by [248], but it is also noted that malaria distribution is impacted by many factors in addition to climate change, including population mobility, changes in land use, changes in air and water temperatures, and the systematic increase in preventive interventions which, VECTRI has not yet incorporated and which should prompt future work.

General Conclusion

This work is an initial exploration of the relationship between Climate and Malaria indicators in Cameroon. The relation between climate and two common malaria indicators of parasite ratio (PR) and Entomological Inoculation rate (EIR) were examined, using a comprehensive of survey data for PR and others surveys for EIR that enabled the seasonality of transmission intensity to be examined. While many factors can impact malaria transmission, the established boards relationships of malaria climate drivers were apparent in the survey data, with PR increasing with temperature until a peak within 22-26°C and thereafter reducing, with peak prevalence occurring at rainfall rates at 7 mm day^{-1}. The analysis also confirmed previous research regarding the impact of population density, with PR higher in rural areas relative to urban areas.

The seasonal cycle of the EIR revealed very contrasting behaviour between peri-urban sites, and rural sites situated closely by the Sanaga or the Mefou river. In the peri-urban sites, the EIR seasonality closely follows that of the rainfall, with maxima lagging rainfall peaks by one to two months. Instead, in rural areas the EIR seasonality is out of phase with rainfall and peaks in March-April when the Sanaga discharge is at its annual minimum, indicating a strong role for the pooling in the river-bed in providing seasonal breeding sites for vectors.

The malaria model is able to reproduce some of these broad traits of the malaria transmission indicators, with a similar relationship between PR and the mean temperatures, while the prevalence peaks at a lower value of rainfall. The model also reproduces the reduction in PR with increasing population. In general the model produces a too high contrast between areas of high and low transmission relative to the surveys, indicating that a mixing effect, most likely in the form of human migration patterns is lacking in the model in addition to the lack of superinfection. The model is able to reproduce the seasonality of the EIR only in the locations where transmission intensity closely follows temporary breeding sites resulting

directly from rainfall, and it could not produce the dry season peak in the locations near the Sanaga river where breeding sites occur due to low stream flow and Mefou river as well.

For each of the models used under the two RCP scenarios, the impact of temperature on the evolution of malaria indicators is established and the seasonality is highlighted for the PR and EIR metrics. The integration of VECTRI with future climate scenarios reveals a modulator effect of changes in temperature and rainfall on changes in malaria transmission. Although factors like population mobility, effective intervention strategies against malaria are likely to improve VECTRI if they are implemented.

The limitations of this study relates to the fact that temperatures in the study area are limited to 2m air temperature. There is also a need to reduce uncertainties and errors in the climate forecasting and the malaria modelling system itself. Thus while there are numerous simplifications and neglected processes in the model, it would appear that the coupling of the malaria transmission scheme with a model to represent human population movements [249], and the improved representation of breeding sites due to permanent and semi-permanent water sources features such as rivers, lakes and dams should be a priority. The next step in line of this work is to ascertain how best to incorporate such as model effectively into a national or regional decision-making process concerning health planning and interventions. If the model is to be used to aid operational decisions in Cameroon, the use of machine learning techniques to calibrate the model parameters more effectively will be required, such as that recently introduced in Tompkins et al [202].

Bibliography

[1] Vipin M Vashishtha. World malaria report 2008: a billion-dollar moment for a centuries old disease. *Indian Pediatr*, 45:985–6, 2008.

[2] Gbenga J Abiodun, P Witbooi, and Kazeem O Okosun. Modelling the impact of climatic variables on malaria transmission. *Hacettepe J. Math. Stat*, 47:219–235, 2018.

[3] Arne Bomblies and Elfatih AB Eltahir. Assessment of the impact of climate shifts on malaria transmission in the sahel. *EcoHealth*, 6(3):426–437, 2009.

[4] Lawrence Fombe and Amenchwi G Amahnui. Impacts of climate variability on malaria incidence in the buea municipality of cameroon; implications for malaria control and prevention. *Current Journal of Applied Science and Technology*, pages 1–6, 2017.

[5] Stéven Chouto and Anselme Wakponou. Disparités spatio-temporelles et prévalence du paludisme à partir des données formelles: cas de kousséri (extrême-nord cameroun). *Ouvrage honoré du soutien financier de la Faculté des Lettres et Sciences Humaines de l?Université de Maroua*, 225, 2016.

[6] Who. World malaria report 2020: 20 years of global progress and challenges, 2020.

[7] Centers for Disease Control, Prevention, et al. *CDC Health Information for International Travel 2014: The Yellow Book*. Oxford University Press, 2013.

[8] Ernest O Asare and Leonard K Amekudzi. Assessing climate driven malaria variability in ghana using a regional scale dynamical model. *Climate*, 5(1):20, 2017.

[9] Sumana Bhattacharya, C Sharma, RC Dhiman, and AP Mitra. Climate change and malaria in india. *Current Science-Bangalore*, 90(3):369, 2006.

[10] Adrian M Tompkins and Volker Ermert. A regional-scale, high resolution dynamical malaria model that accounts for population density, climate and surface hydrology. *Malaria journal*, 12(1):65, 2013.

[11] Anna Cohuet, Frederic Simard, Charles S Wondji, Christophe Antonio-Nkondjio, Parfait Awono-Ambene, and Didier Fontenille. High malaria transmission intensity due to anopheles funestus (diptera: Culicidae) in a village of savannah–forest transition area in cameroon. *Journal of medical entomology*, 41(5):901–905, 2004.

[12] S Bonnet, RE l Paul, C Gouagna, I Safeukui, J-Y Meunier, R Gounoue, and Christian Boudin. Level and dynamics of malaria transmission and morbidity in an equatorial area of south cameroon. *Tropical Medicine & International Health*, 7(3):249–256, 2002.

[13] Jude D Bigoga, Lucien Manga, Vincent PK Titanji, Maureen Coetzee, and Rose GF Leke. Malaria vectors and transmission dynamics in coastal south-western cameroon. *Malaria Journal*, 6(1):5, 2007.

[14] Moshe B Hoshen and Andrew P Morse. A weather-driven model of malaria transmission. *Malaria Journal*, 3(1):32, 2004.

[15] Volker Ermert, Andreas H Fink, Anne E Jones, and Andrew P Morse. Development of a new version of the liverpool malaria model. i. refining the parameter settings and mathematical formulation of basic processes based on a literature review. *Malaria journal*, 10(1):35, 2011.

[16] Arne Bomblies, Jean-Bernard Duchemin, and Elfatih AB Eltahir. Hydrology of malaria: Model development and application to a sahelian village. *Water Resources Research*, 44(12), 2008.

[17] Louis-Clément Gouagna, Rodrigue S Poueme, Kounbobr Roch Dabiré, Jean-Bosco Ouédraogo, Didier Fontenille, and Frédéric Simard. Patterns of sugar feeding and host plant preferences in adult males of an. gambiae (diptera: Culicidae). *Journal of Vector Ecology*, 35(2):267–276, 2010.

[18] David A Warrell and Herbert M Gilles. *Essential malariology.* CRC Press, 2017.

[19] Marianne E Sinka, Bangs Michael J, Sylvie Manguin, Rubio-Palis Yasmin, Theeraphap Chareonviriyaphap, Maureen Coetzee, Charles M Mbogo, Janet

Hemingway, Anand P Patil, William H Temperley, et al. A global map of dominant malaria vectors. *Parasites & Vectors*, 5:1–11, 2012.

[20] Sweety Shrimali and Sukhmahendra Singh. Development team. *PLoS Comput Biol*, 2(6):e71, 2006.

[21] Andrej Trampuz, Matjaz Jereb, Igor Muzlovic, and Rajesh M Prabhu. Clinical review: Severe malaria. *Critical care*, 7(4):315, 2003.

[22] William E Collins and Geoffrey M Jeffery. Plasmodium ovale: parasite and disease. *Clinical microbiology reviews*, 18(3):570–581, 2005.

[23] William E Collins and Geoffrey M Jeffery. Plasmodium malariae: parasite and disease. *Clinical microbiology reviews*, 20(4):579–592, 2007.

[24] Janet Cox-Singh, Timothy ME Davis, Kim-Sung Lee, Sunita SG Shamsul, Asmad Matusop, Shanmuga Ratnam, Hasan A Rahman, David J Conway, and Balbir Singh. Plasmodium knowlesi malaria in humans is widely distributed and potentially life threatening. *Clinical infectious diseases*, 46(2):165–171, 2008.

[25] Hisashi Fujioka and Masamichi Aikawa. Structure and life cycle. In *Malaria immunology*, volume 80, pages 1–26. Karger Publishers, 2002.

[26] World Health Organization et al. *Malaria entomology and vector control*. World Health Organization, 2013.

[27] Spinello Antinori, Laura Galimberti, Laura Milazzo, and Mario Corbellino. Biology of human malaria plasmodia including plasmodium knowlesi. *Mediterranean journal of hematology and infectious diseases*, 4(1), 2012.

[28] Billy Ephraim Ngasala. *Improved malaria case management in under-fives in the era of Artemisinin-based combination therapy in Tanzania*. Institutionen för medicin/Department of Medicine, 2010.

[29] Miles B Markus. The hypnozoite concept, with particular reference to malaria. *Parasitology research*, 108(1):247–252, 2011.

[30] Francis EG Cox. History of the discovery of the malaria parasites and their vectors. *Parasites & vectors*, 3(1):1–9, 2010.

[31] TS Awolola, AO Oduola, JB Obansa, NJ Chukwurar, and JP Unyimadu. Anopheles gambiae ss breeding in polluted water bodies in urban lagos, southwestern nigeria. *Journal of vector borne diseases*, 44(4):241, 2007.

[32] N Minakawa, G Sonye, M Mogi, and G Yan. Habitat characteristics of anopheles gambiae ss larvae in a kenyan highland. *Medical and veterinary entomology*, 18(3):301–305, 2004.

[33] MN Bayoh and SW Lindsay. Effect of temperature on the development of the aquatic stages of anopheles gambiae sensu stricto (diptera: Culicidae). *Bulletin of entomological research*, 93(5):375–381, 2003.

[34] MT Gillies. The duration of the gonotrophic cycle in anopheles gambiae and anopheles funestus, with a note on the efficiency of hand catching. *East African medical journal*, 30(4), 1953.

[35] WJ Martens, Louis W Niessen, Jan Rotmans, Theo H Jetten, and Anthony J McMichael. Potential impact of global climate change on malaria risk. *Environmental health perspectives*, 103(5):458, 1995.

[36] Ernest Ohene Asare. *Development and evaluation of temperature and surface hydrology schemes for dynamical vector-borne disease models*. PhD thesis, Kwame Nkrumah University of Science and Technology, 2015.

[37] Kenneth L Gage, Thomas R Burkot, Rebecca J Eisen, and Edward B Hayes. Climate and vectorborne diseases. *American journal of preventive medicine*, 35(5):436–450, 2008.

[38] Marlies H Craig, RW Snow, and David le Sueur. A climate-based distribution model of malaria transmission in sub-saharan africa. *Parasitology today*, 15(3):105–111, 1999.

[39] Teun Bousema, Jamie T Griffin, Robert W Sauerwein, David L Smith, Thomas S Churcher, Willem Takken, Azra Ghani, Chris Drakeley, and Roly Gosling. Hitting hotspots: spatial targeting of malaria for control and elimination. *PLoS medicine*, 9(1):e1001165, 2012.

[40] Dominic B Dery, Charles Brown, Kwaku Poku Asante, Mohammed Adams, David Dosoo, Seeba Amenga-Etego, Mike Wilson, Daniel Chandramohan, Brian

Greenwood, and Seth Owusu-Agyei. Patterns and seasonality of malaria transmission in the forest-savannah transitional zones of ghana. *Malaria journal*, 9(1):314, 2010.

[41] Ulrike Fillinger, George Sonye, Gerry F Killeen, Bart GJ Knols, and Norbert Becker. The practical importance of permanent and semipermanent habitats for controlling aquatic stages of anopheles gambiae sensu lato mosquitoes: operational observations from a rural town in western kenya. *Tropical Medicine & International Health*, 9(12):1274–1289, 2004.

[42] Kim A Lindblade, Edward D Walker, Ambrose W Onapa, Justus Katungu, and Mark L Wilson. Highland malaria in uganda: prospective analysis of an epidemic associated with el niño. *Transactions of the Royal Society of Tropical Medicine and Hygiene*, 93(5):480–487, 1999.

[43] Russell E Fontaine, Abdallah E Najjar, and Julius S Prince. The 1958 malaria epidemic in ethiopia. *The American journal of tropical medicine and hygiene*, 10(6):795–803, 1961.

[44] Edmund Ilimoan Yamba. *Improvement and validation of dynamical malaria models in Africa*. PhD thesis, Universität zu Köln, 2016.

[45] Krijn P Paaijmans, Moses O Wandago, Andrew K Githeko, and Willem Takken. Unexpected high losses of anopheles gambiae larvae due to rainfall. *PLoS One*, 2(11):e1146, 2007.

[46] RA Brust. Weight and development time of different stadia of mosquitoes reared at various constant temperatures. *The Canadian Entomologist*, 99(9):986–993, 1967.

[47] C Garrett-Jones. Prognosis for interruption of malaria transmission through assessment of the mosquito's vectorial capacity. *Nature*, 204(4964):1173–1175, 1964.

[48] M Nabie Bayoh and Steve W Lindsay. Temperature-related duration of aquatic stages of the afrotropical malaria vector mosquito anopheles gambiae in the laboratory. *Medical and veterinary entomology*, 18(2):174–179, 2004.

[49] EO Lyimo, W Takken, and JC Koella. Effect of rearing temperature and larval density on larval survival, age at pupation and adult size of anopheles gambiae. *Entomologia experimentalis et applicata*, 63(3):265–271, 1992.

[50] MJ Kirby and SW Lindsay. Effect of temperature and inter-specific competition on the development and survival of anopheles gambiae sensu stricto and an. arabiensis larvae. *Acta tropica*, 109(2):118, 2009.

[51] Paul Reiter. Climate change and mosquito-borne disease. *Environmental health perspectives*, 109(Suppl 1):141, 2001.

[52] JA Patz and SH Olson. Climate change and health: global to local influences on disease risk. *Annals of tropical medicine and parasitology*, 100(5-6):535, 2006.

[53] Krijn P Paaijmans, Simon Blanford, Andrew S Bell, Justine I Blanford, Andrew F Read, and Matthew B Thomas. Influence of climate on malaria transmission depends on daily temperature variation. *Proceedings of the National Academy of Sciences*, 107(34):15135–15139, 2010.

[54] Ren Bødker, William Kisinza, Robert Malima, Hamisi Msangeni, and Steve Lindsay. Resurgence of malaria in the usambara mountains, tanzania, an epidemic of drug-resistant parasites. *Global Change and Human Health*, 1(2):134–153, 2000.

[55] Musawenkoi LH Mabaso, Penelope Vounatsou, Stanely Midzi, Joaquim Da Silva, and Thomas Smith. Spatio-temporal analysis of the role of climate in inter-annual variation of malaria incidence in zimbabwe. *International Journal of Health Geographics*, 5(1):20, 2006.

[56] Teresa K Yamana and Elfatih AB Eltahir. Incorporating the effects of humidity in a mechanistic model of anopheles gambiae mosquito population dynamics in the sahel region of africa. *Parasites & Vectors*, 6(1), 2013.

[57] MW Smith, MG Macklin, and CJ Thomas. Hydrological and geomorphological controls of malaria transmission. *Earth-science reviews*, 116:109–127, 2013.

[58] Ibrahima Diouf, Belen Rodriguez-Fonseca, Abdoulaye Deme, Cyril Caminade, Andrew P Morse, Moustapha Cisse, Ibrahima Sy, Ibrahima Dia, Volker Ermert, Jacques-André Ndione, et al. Comparison of malaria simulations driven by meteorological observations and reanalysis products in senegal. *International journal of environmental research and public health*, 14(10):1119, 2017.

[59] Musa Jawara, Margaret Pinder, Chris J Drakeley, Davis C Nwakanma, Ebrima Jallow, Claus Bogh, Steve W Lindsay, and David J Conway. Dry season ecology of

anopheles gambiae complex mosquitoes in the gambia. *Malaria Journal*, 7(1):156, 2008.

[60] E Onori and B Grab. Indicators for the forecasting of malaria epidemics. *Bulletin of the World Health Organization*, 58(1):91, 1980.

[61] Susan S Imbahale, Krijn P Paaijmans, Wolfgang R Mukabana, Ron van Lammeren, Andrew K Githeko, and Willem Takken. A longitudinal study on anopheles mosquito larval abundance in distinct geographical and environmental settings in western kenya. *Malaria journal*, 10(1):81, 2011.

[62] Louise A Kelly-Hope and F Ellis McKenzie. The multiplicity of malaria transmission: a review of entomological inoculation rate measurements and methods across sub-saharan africa. *Malaria Journal*, 8:19, 2009.

[63] V Robert, K Macintyre, J Keating, JF Trape, JB Duchemin, M Warren, and JC Beier. Malaria transmission in urban sub-saharan africa., 2003.

[64] Andrew J Tatem, Carlos A Guerra, Caroline W Kabaria, Abdisalan M Noor, and Simon I Hay. Human population, urban settlement patterns and their impact on plasmodium falciparum malaria endemicity. *Malaria Journal*, 7(1):1–17, 2008.

[65] Jennifer Keiser, Jürg Utzinger, Marcia Caldas De Castro, Thomas A Smith, Marcel Tanner, and Singer Burton H. Urbanization in sub-saharan africa and implication for malaria control. *Am. J. Trop. Med. Hyg*, 71(2):118–127, 2004.

[66] C Gardiner, RJ Biggar, WE Collins, and FK Nkrumah. Malaria in urban and rural areas of southern ghana: a survey of parasitaemia, antibodies, and antimalarial practices. *Bulletin of the World Health Organization*, 62(4):607, 1984.

[67] Caroline W Kabaria, Fabrizio Molteni, Renata Mandike, Frank Chacky, Abdisalan M Noor, Robert W Snow, and Catherine Linard. Mapping intra-urban malaria risk using high resolution satellite imagery: a case study of dar es salaam. *International journal of health geographics*, 15(1):26, 2016.

[68] Shr-Jie Wang, Christian Lengeler, Thomas A Smith, Penelope Vounatsou, Diallo A Diadie, Xavier Pritroipa, Natalie Convelbo, Mathieu Kientga, and Marcel Tanner. Rapid urban malaria appraisal (ruma) i: Epidemiology of urban malaria in ouagadougou. *Malaria Journal*, 4(1):43, 2005.

[69] Joao L Ferrao, Sergio Niquisse, Jorge M Mendes, and Marco Painho. Mapping and modelling malaria risk areas using climate, socio-demographic and clinical variables in chimoio, mozambique. *International journal of environmental research and public health*, 15(4):795, 2018.

[70] Prathiba M De Silva and John M Marshall. Factors contributing to urban malaria transmission in sub-saharan africa: a systematic review. *Journal of tropical medicine*, 2012, 2012.

[71] Jean-Romain Mourou, Thierry Coffinet, Fanny Jarjaval, Christelle Cotteaux, Eve Pradines, Lydie Godefroy, Maryvonne Kombila, et al. Malaria transmission in libreville: results of a one year survey. *Malaria Journal*, 11(1):1–14, 2012.

[72] Shr-Jie Wang, Christian Lengeler, Thomas A Smith, Penelope Vounatsou, Martin Akogbeto, and Marcel Tanner. Rapid urban malaria appraisal (ruma) iv: Epidemiology of urban malaria in cotonou (benin). *Malaria Journal*, 5:45, 2006.

[73] David Chikodzi. Spatial modelling of malaria risk zones using environmental, anthropogenic variables and geographical information systems techniques. *Journal of Geosciences and Geomatics*, 1(1):8–14, 2013.

[74] MJ Balls, R Bødker, CJ Thomas, W Kisinza, HA Msangeni, and SW Lindsay. Effect of topography on the risk of malaria infection in the usambara mountains, tanzania. *Transactions of the Royal Society of Tropical Medicine and Hygiene*, 98(7):400–408, 2004.

[75] Chris Drakeley, Colin Sutherland, J Teun Bousema, Robert W Sauerwein, and Geoffrey AT Targett. The epidemiology of plasmodium falciparum gametocytes: weapons of mass dispersion. *Trends in parasitology*, 22(9):424–430, 2006.

[76] Kacey C Ernst, Samson O Adoka, Dickens O Kowuor, Mark L Wilson, and Chandy C John. Malaria hotspot areas in a highland kenya site are consistent in epidemic and non-epidemic years and are associated with ecological factors. *Malaria journal*, 5(1):78, 2006.

[77] Jeffrey D Stanaway and Jonathan D Mayer. Climate variability and change and its effects on malaria. *Edited by Shlomit Paz*, 31:6–23, 2011.

[78] R Bødker, J Akida, D Shayo, W Kisinza, HA Msangeni, EM Pedersen, and SW Lindsay. Relationship between altitude and intensity of malaria transmission in the usambara mountains, tanzania. *Journal of medical entomology*, 40(5):706, 2003.

[79] Caroline A Maxwell, William Chambo, Mathew Mwaimu, Frank Magogo, Ilona A Carneiro, and Christopher F Curtis. Variation of malaria transmission and morbidity with altitude in tanzania and with introduction of alphacypermethrin treated nets. *Malaria Journal*, 2:28, 2003.

[80] WS Akhwale, JK Lum, A Kaneko, H Eto, C Obonyo, A Björkman, and T Kobayakawa. Anemia and malaria at different altitudes in the western highlands of kenya. *Acta tropica*, 91(2):167–175, 2004.

[81] Tedros A Ghebreyesus, Mitiku Haile, Karen H Witten, Asefaw Getachew, Ambachew M Yohannes, Mekonnen Yohannes, Hailay D Teklehaimanot, Steven W Lindsay, and Peter Byass. Incidence of malaria among children living near dams in northern ethiopia: community based incidence survey. *Bmj*, 319(7211):663–666, 1999.

[82] Lewis M Cowardin, Virginia Carter, Francis C Golet, and Edward T LaRoe. Classification of wetlands and deepwater habitats of the united states. Technical report, US Department of the Interior, US Fish and Wildlife Service, 1979.

[83] Ulrike Fillinger, Heleen Sombroek, Silas Majambere, Emiel van Loon, Willem Takken, and Steven W Lindsay. Identifying the most productive breeding sites for malaria mosquitoes in the gambia. *Malaria Journal*, 8:62, 2009.

[84] Jonathan Lautze, Matthew Mccartney, Paul Kirshen, Dereje Olana, Gayathree Jayasinghe, and Andrew Spielman. Effect of a large dam on malaria risk: the koka reservoir in ethiopia. *TM & IH. Tropical medicine & international health*, 12(8):982–989, 2007.

[85] Denis Ribeiro do Valle. *The effect of land use and climate on malaria risk in the Amazon region*. PhD thesis, Duke University, 2013.

[86] Wim Van Der Hoek, Flemming Konradsen, Priyanie H Amerasinghe, Devika Perera, MK Piyaratne, and Felix P Amerasinghe. Towards a risk map of malaria for sri lanka: the importance of house location relative to vector breeding sites. *International Journal of Epidemiology*, 32(2):280–285, 2003.

[87] Justin M Cohen, Kacey C Ernst, Kim A Lindblade, John M Vulule, Chandy C John, and Mark L Wilson. Topography-derived wetness indices are associated with household-level malaria risk in two communities in the western kenyan highlands. *Malaria journal*, 7(1):40, 2008.

[88] G Zhou, S Munga, N Minakawa, AK Githeko, and G Yan. Spatial relationship between adult malaria vector abundance and environmental factors in western kenya highlands. *The American journal of tropical medicine and hygiene*, 77(1):29–35, 2007.

[89] DM Gunawardena, AR Wickremasinghe, Lv Muthuwatta, S Weerasingha, J Rajakaruna, T Senanayaka, PK Kotta, N Attanayake, R Carter, and KN Mendis. Malaria risk factors in an endemic region of sri lanka, and the impact and cost implications of risk factor-based interventions. *The American journal of tropical medicine and hygiene*, 58(5):533–542, 1998.

[90] Thomas E Dahl. *Status and trends of wetlands in the conterminous United States 2004 to 2009*. US Department of the Interior, US Fish and Wildlife Service, Fisheries and Habitat Conservation, 2011.

[91] PER Dale and JM Knight. Wetlands and mosquitoes: a review. *Wetlands Ecology and Management*, 16(4):255–276, 2008.

[92] Jennifer Keiser, Marcia Caldas de Castro, Michael F Maltese, Robert Bos, Marcel Tanner, Burton H Singer, and Jürg Utzinger. Effect of irrigation and large dams on the burden of malaria on a global and regional scale. *The American journal of tropical medicine and hygiene*, 72(4):392–406, 2005.

[93] VP Sharma. Re-emergence of malaria in india. *Indian Journal of Medical Research*, 103:26–45, 1996.

[94] Junko Yasuoka and Richard Levins. Impact of deforestation and agricultural development on anopheline ecology and malaria epidemiology. *The American journal of tropical medicine and hygiene*, 76(3):450–460, 2007.

[95] Kim A Lindblade, Edward D Walker, Ambrose W Onapa, Justus Katungu, and Mark L Wilson. Land use change alters malaria transmission parameters by modifying temperature in a highland area of uganda. *Tropical Medicine & International Health*, 5(4):263–274, 2000.

[96] Anne Caroline Krefis, Norbert Georg Schwarz, Bernard Nkrumah, Samuel Acquah, Wibke Loag, Nimako Sarpong, Yaw Adu-Sarkodie, Ulrich Ranft, and Jürgen May. Principal component analysis of socioeconomic factors and their association with malaria in children from the ashanti region, ghana. *Malaria Journal*, 9(1):201, 2010.

[97] Jane Carter Ingram, Fabrice DeClerck, and Cristina Rumbaitis del Rio. *Integrating Ecology and Poverty Reduction: Ecological Dimensions*, volume 1. Springer Science & Business Media, 2012.

[98] Amy Yomiko Vittor, Robert H Gilman, James Tielsch, Gregory Glass, TIM Shields, Wagner Sanchez Lozano, Viviana Pinedo-Cancino, and Jonathan A Patz. The effect of deforestation on the human-biting rate of anopheles darlingi, the primary vector of falciparum malaria in the peruvian amazon. *The American journal of tropical medicine and hygiene*, 74(1):3–11, 2006.

[99] World Health Organization et al. Cooperation strategy between who and the republic of cameroon: 2017-2020. 2017.

[100] Fondib Modestus Ngwa Bandolo. Heavily indebted poor countries (hipc) initiative in cameroon and the fight to reduce malaria related under-five mortality. Master's thesis, Høgskolen i Oslo og Akershus. Fakultet for samfunnsfag, 2012.

[101] Gado Nana Désiré, Peyou Ndi Marlyse, and Pr Henri Gwet. Modelisation de l'impact de la prevention et de la prise en charge des cas sur la progression du paludisme chez la femme enceinte et les enfants de moins de cinq ans. *Résumé*, 10:1, 2010.

[102] Jane M Chuma, Michael Thiede, and Catherine S Molyneux. Rethinking the economic costs of malaria at the household level: evidence from applying a new analytical framework in rural kenya. *Malaria Journal*, 5(1):76, 2006.

[103] John Luke Gallup and Jeffrey D Sachs. The economic burden of malaria. *Center for International Development at Harvard*, 1998.

[104] RI Chima, CA Goodman, and A Mills. The economic impact of malaria in africa: a critical review of the evidence. *Health policy (Amsterdam, Netherlands)*, 63(1):17–36, 2003.

[105] JP Hervy, G Le Goff, JP Geoffroy, L Hervé, L Manga, and J Brunhes. Les anopheles de la région afro-tropicale. logiciel d'identification et d'enseignement. *ORSTOM édition. série Didactiques. Paris, France (in French, English, Portuguese)*, 1998.

[106] Didier Fontenille, S Wanji, R Djouaka, and HP Awono-Ambene. Anopheles hancocki, vector secondaire du paludisme au cameroun. *Bulletin de Liaison et de Documentation-OCEAC*, 33(2):23–26, 2000.

[107] Charles Wondji, Frédéric Simard, Vincenzo Petrarca, Josiane Etang, Federica Santolamazza, Alessandra Della Torre, and Didier Fontenille. Species and populations of the anopheles gambiae complex in cameroon with special emphasis on chromosomal and molecular forms of anopheles gambiae ss. *Journal of Medical Entomology*, 42(6):998–1005, 2005.

[108] Hamadou NM Ndjemaï, Salomon Patchoké, Jean Atangana, Josiane Etang, Fréderic Simard, Charles F Bilong Bilong, Lisa Reimer, Anthony Cornel, Gregory C Lanzaro, and Etienne Fondjo. The distribution of insecticide resistance in anopheles gambiae sl populations from cameroon: an update. *Transactions of the Royal Society of Tropical Medicine and Hygiene*, 103(11):1127–1138, 2009.

[109] JW Ngum, P Ongolo-Zogo, E Tallah, R Leke, and W Mbacham. Policy brief on scaling up malaria control interventions in cameroon. *Executive summary*, 2010.

[110] Claus Bøgh, Steven W Lindsay, Sian E Clarke, Andy Dean, Musa Jawara, Margaret Pinder, and Christopher J Thomas. High spatial resolution mapping of malaria transmission risk in the gambia, west africa, using landsat tm satellite imagery. *The American journal of tropical medicine and hygiene*, 76(5):875–881, 2007.

[111] Rachel Lowe, James Chirombo, and Adrian M Tompkins. Relative importance of climatic, geographic and socio-economic determinants of malaria in malawi. *Malaria journal*, 12(1):416, 2013.

[112] Nyaguara Amek, Nabie Bayoh, Mary Hamel, Kim A Lindblade, John E Gimnig, Frank Odhiambo, Kayla F Laserson, Laurence Slutsker, Thomas Smith, and Penelope Vounatsou. Spatial and temporal dynamics of malaria transmission in rural western kenya. *Parasites & vectors*, 5(1):86, 2012.

[113] Diego Ayala, Carlo Costantini, Kenji Ose, Guy C Kamdem, Christophe Antonio-Nkondjio, Jean-Pierre Agbor, Parfait Awono-Ambene, Didier Fontenille, and Frédéric Simard. Habitat suitability and ecological niche profile of major malaria vectors in cameroon. *Malaria Journal*, 8(1):307, 2009.

[114] Christophe Antonio-Nkondjio, Clément Hinzoumbe Kerah, Frédéric Simard, Parfait Awono-Ambene, Mohamadou Chouaibou, Timoléon Tchuinkam, and Didier Fontenille. Complexity of the malaria vectorial system in cameroon: contribution of secondary vectors to malaria transmission. *Journal of medical entomology*, 43(6):1215–1221, 2006.

[115] Jerome Fru-Cho, Violet V Bumah, Innocent Safeukui, Theresa Nkuo-Akenji, Vincent PK Titanji, and Kasturi Haldar. Molecular typing reveals substantial plasmodium vivax infection in asymptomatic adults in a rural area of cameroon. *Malaria journal*, 13(1):170, 2014.

[116] E Songue, C Tagne, P Mbouyap, P Essomba, and R Moyou-Somo. Epidemiology of malaria in three geo-ecological zones along the chad-cameroon pipeline. *Am J Epidemiol Infect Dis*, 1(4):27–33, 2013.

[117] Huguette Gaelle Ngassa Mbenda, Gauri Awasthi, Poonam K Singh, Inocent Gouado, and Aparup Das. Does malaria epidemiology project cameroon as africa in miniature? *Journal of biosciences*, 39(4):727–738, 2014.

[118] E Fondjo, Vincent Robert, Gilbert Le Goff, JC Toto, and Pierre Carnevale. Le paludisme urbain à yaoundé (cameroun): 2. etude entomologique dans deux quartiers peu urbanisés. *Bulletin de la Société de pathologie exotique*, 85(1):57–63, 1992.

[119] Timoléon Tchuinkam, Frédéric Simard, Espérance Lélé-Defo, Billy Téné-Fossog, Aimé Tateng-Ngouateu, Christophe Antonio-Nkondjio, Mbida Mpoame, Jean-Claude Toto, Thomas Njiné, Didier Fontenille, et al. Bionomics of anopheline species and malaria transmission dynamics along an altitudinal transect in western cameroon. *BMC infectious diseases*, 10(1):119, 2010.

[120] Jean-Yves Meunier, I Safeukui, Didier Fontenille, and Christian Boudin. Etude de la transmission du paludisme dans une future zone d?essai vaccinal en forêt équatoriale du sud cameroun. *Bull Soc Pathol Exot*, 92:309–312, 1999.

[121] Christophe Antonio-Nkondjio, Blaise Defo-Talom, Romuald Tagne-Fotso, Billy Tene-Fossog, Cyrille Ndo, Leopold Gustave Lehman, Timoléon Tchuinkam, Pierre Kengne, and Parfait Awono-Ambene. High mosquito burden and malaria transmission in a district of the city of douala, cameroon. *BMC infectious diseases*, 12(1):275, 2012.

[122] Jonathan A Patz, Michael A McGeehin, Susan M Bernard, Kristie L Ebi, Paul R Epstein, Anne Grambsch, Duane J Gubler, P Reither, Isabelle Romieu, Joan B Rose, et al. The potential health impacts of climate variability and change for the united states: executive summary of the report of the health sector of the us national assessment. *Environmental health perspectives*, 108(4):367, 2000.

[123] Roland Ngom. *Spatial and Statistical Prediction of Urban Malaria in Yaoundé: A Social and Environmental Modelling Approach for Health Promotion*. PhD thesis, Dissertation, Heidelberg University, http://opus. bszbw. de/phhd/volltexte/2010/7521/pdf/Roland_Ngom_Doctoral_thesis_Onli ne. pdf, 2010.

[124] Vincent Robert, A Van den Broek, P Stevens, R Slootweg, V Petrarca, M Coluzzi, G Le Goff, MA Di Deco, and Pierre Carnevale. Mosquitoes and malaria transmission in irrigated rice-fields in the benoue valley of northern cameroon. *Acta tropica*, 52(2-3):201–204, 1992.

[125] Jude D Bigoga, Ferdinand M Nanfack, Parfait H Awono-Ambene, Salomon Patchoké, Jean Atangana, Vitalis S Otia, Etienne Fondjo, Roger S Moyou, and Rose GF Leke. Seasonal prevalence of malaria vectors and entomological inoculation rates in the rubber cultivated area of niete, south region of cameroon. *Parasites & vectors*, 5(1):197, 2012.

[126] Jean Mouchet. Influence des fleuves sur la biologie d'anopheles gambiae pendant la saison sèche dans le sud-cameroun. *Bulletin de la Société de Pathologie exotique*, 55(6):1163–1171, 1962.

[127] G Le Goff, P Carneval, and Vincent Robert. Low dispersion of anopheline malaria vectors in the african equatorial forest. *Parasite*, 4(2):187–189, 1997.

[128] Christophe Antonio-Nkondjio, Frédéric Simard, Parfait Awono-Ambene, Pierre Ngassam, Jean-Claude Toto, Timoléon Tchuinkam, and Didier Fontenille. Malaria

vectors and urbanization in the equatorial forest region of south cameroon. *Transactions of the Royal Society of Tropical Medicine and Hygiene*, 99(5):347–354, 2005.

[129] Isabella A Quakyi, RG Leke, Rosa Befidi-Mengue, Martin Tsafack, Dennis Bomba-Nkolo, Lucien Manga, Viviane Tchinda, Emmanuel Njeungue, Samuel Kouontchou, Josephine Fogako, et al. The epidemiology of plasmodium falciparum malaria in two cameroonian villages: Simbok and etoa. *The American journal of tropical medicine and hygiene*, 63(5):222–230, 2000.

[130] HK Kimbi, Y Nana, IN Sumbele, JK Anchang-Kimbi, E Lum, C Tonga, M Nweboh, and LG Lehman. Environmental factors and preventive methods against malaria parasite prevalence in rural bomaka and urban molyko, southwest cameroon. *J Bacteriol Parasitol*, 4(162):4172, 2013.

[131] Bernadette Mbarga. 3eme rgph. rapport de présentation des résultats définitifs. *BUCREP (Bureau Central des Recensements et des Etudes de la Population), Yaoundé*, 2010.

[132] Tobias O Apinjoh, Judith K Anchang-Kimbi, Regina N Mugri, Delphine A Tangoh, Robert V Nyingchu, Hanesh F Chi, Rolland B Tata, Charles Njumkeng, Clarisse Njua-Yafi, and Eric A Achidi. The effect of insecticide treated nets (itns) on plasmodium falciparum infection in rural and semi-urban communities in the south west region of cameroon. *PLoS One*, 10(2):e0116300, 2015.

[133] HK Kimbi, D Nformi, AM Patchong, and KJ Ndamukong. Influence of urbanisation on asymptomatic malaria in school children in molyko, south western cameroon. *East African medical journal*, 83(11):602–610, 2006.

[134] Cyrille Ndo, Benjamin Menze-Djantio, and Christophe Antonio-Nkondjio. Awareness, attitudes and prevention of malaria in the cities of douala and yaoundé (cameroon). *Parasites & vectors*, 4(1):181, 2011.

[135] Christophe Antonio-Nkondjio, Maurice Demanou, Josiane Etang, and Bernard Bouchite. Impact of cyfluthrin (solfac ew050) impregnated bed nets on malaria transmission in the city of mbandjock: lessons for the nationwide distribution of long-lasting insecticidal nets (llins) in cameroon. *Parasites & vectors*, 6(1):10, 2013.

[136] G le Goff, Vincent Robert, E Fondjo, and Pierre Carnevale. Efficacy of insecticide impregnated bed-nets to control malaria in a rural forested area in southern cameron. *Memorias do Instituto Oswaldo Cruz*, 87:355–359, 1992.

[137] Albert Kilian, Marc Boulay, Hannah Koenker, and Matthew Lynch. How many mosquito nets are needed to achieve universal coverage? recommendations for the quantification and allocation of long-lasting insecticidal nets for mass campaigns. *Malaria journal*, 9(1):330, 2010.

[138] Laurence Slutsker and Robert D Newman. Malaria scale-up progress: is the glass half-empty or half-full? *The Lancet*, 373(9657):11–13, 2009.

[139] Ronald Ross. *The prevention of malaria*. John Murray; London, 1911.

[140] G MacDonald. The epidemiology and control of malaria. london: Oxford univ. pr, 1957.

[141] K Dietz, L Molineaux, and A Thomas. A malaria model tested in the african savannah. *Bulletin of the World Health Organization*, 50(3-4):347, 1974.

[142] CJ Struchiner, ME Halloran, and A Spielman. Modeling malaria vaccines. i: New uses for old ideas. *Mathematical biosciences*, 94(1):87–113, 1989.

[143] J Nedelman. Some new thoughts about some old malaria models-introductory review. *Mathematical biosciences*, 73(2):159–182, 1985.

[144] Joan L Aron. Mathematical modelling of immunity to malaria. *Mathematical Biosciences*, 90(1-2):385–396, 1988.

[145] Nakul Chitnis, Jim M Cushing, and JM Hyman. Bifurcation analysis of a mathematical model for malaria transmission. *SIAM Journal on Applied Mathematics*, 67(1):24–45, 2006.

[146] Gideon A Ngwa and William S Shu. A mathematical model for endemic malaria with variable human and mosquito populations. *Mathematical and Computer Modelling*, 32(7-8):747–763, 2000.

[147] Paul Edward Parham and Edwin Michael. Modeling the effects of weather and climate change on malaria transmission. *Environmental health perspectives*, 118(5):620, 2010.

[148] Frank C Tanser, Brian Sharp, and David Le Sueur. Potential effect of climate change on malaria transmission in africa. *The Lancet*, 362(9398):1792–1798, 2003.

[149] Paul E Parham and Edwin Michael. Modelling climate change and malaria transmission. In *Modelling Parasite Transmission and Control*, pages 184–199. Springer, 2010.

[150] JA Patz, AK Githeko, JP McCarty, S Hussein, U Confalonieri, N De Wet, et al. Climate change and infectious diseases. *Climate change and human health: risks and responses*, 6:103–37, 2003.

[151] Francois M Moukam Kakmeni, Ritter YA Guimapi, Frank T Ndjomatchoua, Sansoa A Pedro, James Mutunga, and Henri EZ Tonnang. Spatial panorama of malaria prevalence in africa under climate change and interventions scenarios. *International journal of health geographics*, 17(1):2, 2018.

[152] ET Pamo. Country pasture/forage resource profiles cameroon. *Eds: Suttle, JM & Reynolds, SG, FAO, Rome, Italy*, 2008.

[153] Ernest L Molua. The economic impact of climate change on agriculture in cameroon. *World Bank Policy Research Working Paper*, (4364), 2007.

[154] Ernest L Molua. Climatic trends in cameroon: implications for agricultural management. *Climate Research*, 30(3):255–262, 2006.

[155] Edouard K Penlap, Christoph Matulla, Hans von Storch, and F Mkankam Kamga. Downscaling of gcm scenarios to assess precipitation changes in the little rainy season (march–june) in cameroon. *Climate Research*, 26(2):85–96, 2004.

[156] Jean-Claude Olivry. Fleuves et rivières du cameroun. *Monographies hydrologiques ORSTOM*, (9), 1986.

[157] T Love. The climate prediction center rainfall algorithm version 2. *NOAA Climate Prediction Center Tech. Rep.[Available online at http://www. cpc. ncep. noaa. gov/products/fews/RFE2. 0_ tech. pdf.]*, 2002.

[158] DP Dee, SM Uppala, AJ Simmons, Paul Berrisford, P Poli, S Kobayashi, U Andrae, MA Balmaseda, G Balsamo, P Bauer, et al. The era-interim reanalysis:

Configuration and performance of the data assimilation system. *Quarterly Journal of the royal meteorological society*, 137(656):553–597, 2011.

[159] Peter W Gething, Anand P Patil, David L Smith, Carlos A Guerra, Iqbal RF Elyazar, Geoffrey L Johnston, Andrew J Tatem, and Simon I Hay. A new world malaria map: Plasmodium falciparum endemicity in 2010. *Malaria journal*, 10(1):378, 2011.

[160] L Manga, O Traore, M Cot, E Mooh, and P Carnevale. Malaria in the village of yaounde (cameroon). 3. parasitological study in 2 central districts. *Bulletin de la Societe de pathologie exotique (1990)*, 86(1):56–61, 1993.

[161] Samir Bhatt, DJ Weiss, E Cameron, D Bisanzio, B Mappin, U Dalrymple, KE Battle, CL Moyes, A Henry, PA Eckhoff, et al. The effect of malaria control on plasmodium falciparum in africa between 2000 and 2015. *Nature*, 526(7572):207, 2015.

[162] Josiane Etang, Mouhamadou Chouaibou, Jean-Claude Toto, Ousmane Faye, Lucien Manga, Albert Samè-Ekobo, Parfait Awono-Ambene, and Frédéric Simard. A preliminary test of the protective efficacy of permethrin-treated bed nets in an area of anopheles gambiae metabolic resistance to pyrethroids in north cameroon. *Transactions of the Royal Society of Tropical Medicine and Hygiene*, 101(9):881–884, 2007.

[163] P Gazin, JP Louis, L Mulder, F Eberle, R Jambou, C Hengy, et al. Evaluation of plasmodium falciparum susceptibility to chloroquine and amodiaquine using a simplified, in vivo, 7-day test in southern cameroon. *Medecine tropicale: revue du Corps de sante colonial*, 50(1):27–31, 1990.

[164] M Audibert, R Josseran, R Josse, and A Adjidji. Irrigation, schistosomiasis, and malaria in the logone valley, cameroon. *The American journal of tropical medicine and hygiene*, 42(6):550–560, 1990.

[165] GA Matthews, HM Dobson, PB Nkot, TL Wiles, and M Birchmore. Preliminary examination of integrated vector management in a tropical rainforest area of cameroon. *Transactions of the Royal Society of Tropical Medicine and Hygiene*, 103(11):1098–1104, 2009.

[166] EA Achidi, TO Apinjoh, E Mbunwe, R Besingi, C Yafi, N Wenjighe Awah, A Ajua, and JK Anchang. Febrile status, malarial parasitaemia and gastro-intestinal

helminthiases in schoolchildren resident at different altitudes, in south–western cameroon. *Annals of Tropical Medicine & Parasitology*, 102(2):103–118, 2008.

[167] A Ngalame, J Bigoga, J Fogako, P Nyonglema, G Sama, R Neba, J Bopda, D Taylor, and R Leke. Malaria in ntouessong primary and nursery school children: An epidemiological survey [mim-an-278939]. In *ACTA TROPICA*, volume 95, pages S463–S464. ELSEVIER SCIENCE BV PO BOX 211, 1000 AE AMSTERDAM, NETHERLANDS, 2005.

[168] R Chambon, P Lemardeley, C Boudin, P Ringwald, and J Chandenier. Surveillance of the in vivo sensitivity of plasmodium falciparum to antimalarial agents: the results of initial tests of the oceac malaria network. *Medecine tropicale: revue du Corps de sante colonial*, 57(4):357–360, 1997.

[169] R Josse, A Trebucq, G Jaureguiberry, A Ghogomou, O Ndzinga, V Foumane, I Combourieu, J Tribouley, and C Ripert. Evaluation of malarial indices in the forest region of djoum (southern cameroon). *Medecine tropicale: revue du Corps de sante colonial*, 50(1):47–51, 1990.

[170] R Josse, M Merlin, A Combe, R Josseran, JY Hesran Le, F Avennec, B Ngnintedem, AM Nkongtso, M Kamwa, and JT Eboumbou. Comparative study of the malaria indices in nanga-eboko, yaoundé and edea (cameroon). *Medecine tropicale: revue du Corps de sante colonial*, 48(3):201–208, 1988.

[171] M Merlin, JY Hesran Le, R Josse, R Josseran, JM Sicard, G Mao Le, D Eteki, A Combe, J Tribouley, and C Ripert. Evaluation of the clinical, parasitological and immunological indices of malaria in the bonny's bay area of central africa. *Bulletin de la Societe de pathologie exotique et de ses filiales*, 79(5 Pt 2):707–720, 1986.

[172] Kenneth JN Ndamukong, John S Dinga, Mary A Ayuk, Theresa N Akenji, Victor A Ndiforchu, and Vincent PK Titanji. Microscopy is more reliable than questionnaire-based methods in the diagnosis of malaria in school children. *African journal of health sciences*, 9(2):147–152, 2002.

[173] J Atangana, A Fomena, J Lebel Tamesse, and E Fondjo. Agricultural activities and epidemiology of malaria in soudano-sahelian zone in cameroon. *Bulletin de la Societe de pathologie exotique (1990)*, 105(1):23–29, 2012.

[174] Francis Zeukeng, Viviane Hélène Matong Tchinda, Jude Daiga Bigoga, Clovis Hugues Tiogang Seumen, Edward Shafe Ndzi, Géraldine Abonweh, Valérie Makoge, Amédée Motsebo, and Roger Somo Moyou. Co-infections of malaria and geohelminthiasis in two rural communities of nkassomo and vian in the mfou health district, cameroon. *PLoS neglected tropical diseases*, 8(10):e3236, 2014.

[175] J Gardon, F Eberle, JP Louis, H Cheringou, A Trebucq, and C Hengy. Evaluation de la chloroquino-sensibilité de plasmodium falciparum au cameroun. *Médecine d'Afrique Noire*, 38(4), 1991.

[176] Mike van der Kolk, Anne Etti Tebo, Hermann Nimpaye, Delphine Ngo Ndombol, Robert W Sauerwein, and Wijnand MC Eling. Transmission of plasmodium falciparum in urban yaounde, cameroon, is seasonal and age-dependent. *Transactions of the Royal Society of tropical Medicine and Hygiene*, 97(4):375–379, 2003.

[177] Florence Gardella, Serge Assi, Fabrice Simon, Hervé Bogreau, Teunis Eggelte, Fatou Ba, Vincent Foumane, Marie-Claire Henry, Pélagie Traore Kientega, Léonardo Basco, et al. Antimalarial drug use in general populations of tropical africa. *Malaria journal*, 7(1):124, 2008.

[178] E Fondjo. Etude du comportement du complexe anopheles gambiae et de la transmission du paludisme dans deux faciès éco-climatique au mali et au cameroun. *Université de Bamako: Thèse de 3ème Cycle*, 1996.

[179] T Nkuo Akenji, NN Ntonifor, HK Kimbi, EL Abongwa, JK Ching, MB Ndukum, DN Anong, A Nkwescheu, M Songmbe, MG Boyo, et al. The epidemiology of malaria in bolifamba, a rural community on the eastern slopes of mount cameroon: seasonal variation in the parasitological indices of transmission. *Annals of Tropical Medicine & Parasitology*, 99(3):221–227, 2005.

[180] R Moyou-Somo, LG Lehman, S Awahmukalah, and P Enyong Ayuk. Deltamethrin impregnated bednets for the control of urban malaria in kumba town, south-west province of cameroon. *The Journal of tropical medicine and hygiene*, 98(5):319–324, 1995.

[181] R Josse, R Josseran, M Audibert, M Merlin, A Combe, MF Sauneron, S Adjidji, Bernard Mondet, JY Le Hesran, D Kouka-Bemba, et al. Paludométrie et variations

saisonnières du paludisme dans la région du projet rizicole de maga (nord-cameroun) et dans la région limitrophe. *Cahiérs Ostorm; Série Entomologie Médicale et Parasitologie*, 25:63–71, 1987.

[182] Francis Louis, Gilbert Le Goff, Bert Mulder, and Marc Desfontaine. *Enquête paludologique à Bilalang (Edea, Cameroun): rapport de mission 26-29 novembre 1990.* PhD thesis, Organisation de Coordination pour la lutte contre les Endémies en Afrique ?, 1990.

[183] N Awah, H Kimbi, K Ndamukong, and J Mbuh. The epidemiology and consequences of malaria infection in primary school children in the muea area and its environs [mim-na-363565]. In *ACTA TROPICA*, volume 95, pages S149–S149. ELSEVIER SCIENCE BV PO BOX 211, 1000 AE AMSTERDAM, NETHERLANDS, 2005.

[184] E Mbunwe, J Anchang, T Apinjoh, R Besingi, C Njua, V Awah, and E Achidi. Malaria parasitaemia and helminthic infections in assymptomatic school-pupils from fako division, south western cameroon [mim-em-244080]. In *ACTA TROPICA*, volume 95, pages S390–S391. ELSEVIER SCIENCE BV PO BOX 211, 1000 AE AMSTERDAM, NETHERLANDS, 2005.

[185] Philippe Rey. *Aspects épidémiologiques du paludisme dans la ville de Kumba, Cameroun-Province du sud-ouest.* PhD thesis, Bordeaux 2, 1989.

[186] CP Raccurt, C Bourianne, MT Lambert, J Tribouley, O Mandji, A Amadou, J Bouloumie, and C Ripert. Malaria indices, larval ecology and trophic activity of anopheles mosquitoes in djohong (adamaoua, cameroon) in the rainy season. *Medecine tropicale: revue du Corps de sante colonial*, 53(3):355–362, 1993.

[187] Pierre Gazin, C Farges, R Jambou, F Eberlé, JP Louis, and C Hengy. Evaluation in vivo de la chimiosensibilité de plasmodium falciparum à la chloroquine dans la région de yaoundé. 1-ecole de pouma. *Doc. tech. OCEAC No677/SEM*, 1989.

[188] R Josse, C Hengy, C Bailly, T Calvez, P Ambassa, R Wandji, H Gabon, D Kouka-Bemba, and M Merlin. Etude épidémiologique du paludisme dans la ville de nkongsamba.(province du littoral, république du cameroun). *Médecine d'Afrique noire*, 35(1):17–24, 1988.

[189] Ayoade MJ Oduola, Roger S Moyou-Somo, Dennis E Kyle, Samuel K Martin, Lucia Gerena, and Wilbur K Milhous. Chloroquine resistant plasmodium falciparum in indigenous residents of cameroon. *Transactions of the Royal Society of Tropical Medicine and Hygiene*, 83(3):308–310, 1989.

[190] MH Birley and JD Charlewood. Sporozoite rate and malaria prevalence. *Parasitology Today*, 3(8):231–232, 1987.

[191] Edmund I Yamba, Adrian M Tompkins, Andreas H Fink, Volker Ermert, Mbouna D Amelie, Leonard K Amekudzi, and Olivier JT Briët. Monthly entomological inoculation rate data for studying the seasoanality of malaria transmission in africa. *Data*, 5(2):31, 2020.

[192] Sonia Altizer, Andrew Dobson, Parviez Hosseini, Peter Hudson, Mercedes Pascual, and Pejman Rohani. Seasonality and the dynamics of infectious diseases. *Ecology letters*, 9(4):467–484, 2006.

[193] Pierre Carnevale, G LE Goff, J-C Toto, and Vincent Robert. Anopheles nili as the main vector of human malaria in villages of southern cameroon. *Medical and Veterinary Entomology*, 6(2):135–138, 1992.

[194] Gilbert Le Goff, Pierre Carnevale, E Fondjo, and Vincent Robert. Comparison of three sampling methods of man-biting anophelines in order to estimate the malaria transmission in a village of south cameroon. *Parasite*, 4(1):75–80, 1997.

[195] Mbi Chrysantus Tanga and WI Ngundu. Ecological transition from natural forest to tea plantations: effect on the dynamics of malaria vectors in the highlands of cameroon. *Transactions of the Royal Society of Tropical Medicine and Hygiene*, 104(10):659–668, 2010.

[196] MC Tanga, WI Ngundu, and PD Tchouassi. Daily survival and human blood index of major malaria vectors associated with oil palm cultivation in cameroon and their role in malaria transmission. *Tropical Medicine & International Health*, 16(4):447–457, 2011.

[197] A Njan Nloga, Vincent Robert, JC Toto, and Pierre Carnevale. Anopheles moucheti, vecteur principal du paludisme au sud-cameroun. *Bulletin de Liaison et de Documentation-OCEAC*, 26(2):63–67, 1993.

[198] Christophe Antonio-Nkondjio, Parfait Awono-Ambene, Jean-Claude Toto, Jean-Yves Meunier, Sylvie Zebaze-Kemleu, Rose Nyambam, Charles S Wondji, Timoléon Tchuinkam, and Didier Fontenille. High malaria transmission intensity in a village close to yaounde, the capital city of cameroon. *Journal of medical entomology*, 39(2):350–355, 2002.

[199] JY Meunier, I Safeukui, D Fontenille, and C Boudin. Malaria transmission in an area of future vaccination in equatorial forest of south cameroon. *Bulletin de la Societe de pathologie exotique (1990)*, 92(5):309–312, 1999.

[200] Eric Moise Bakwo Fils, Patrick Akono Ntonga, Philippe Belong, and Jean Messi. Contribution of mosquito vectors in malaria transmission in an urban district of southern cameroon. *Journal of Entomology and Nematology*, 2(2):13–17, 2010.

[201] L Manga, JC Toto, and Pierre Carnevale. Malaria vectors and transmission in an area deforested for a new international airport in southern cameroon. In *ANNALES-SOCIETE BELGE DE MEDECINE TROPICALE*, volume 75, pages 43–43. INSTITUTE OF TROPICAL MEDICINE, 1995.

[202] Adrian M Tompkins and Madeleine C Thomson. Uncertainty in malaria simulations in the highlands of kenya: Relative contributions of model parameter setting, driving climate and initial condition errors. *PloS one*, 13(9):e0200638, 2018.

[203] WF Jepson, A Moutia, and C Courtois. The malaria problem in mauritius: the bionomics of mauritian anophelines. *Bulletin of entomological research*, 38(1):177–208, 1947.

[204] Jean-Marc O Depinay, Charles M Mbogo, Gerry Killeen, Bart Knols, John Beier, John Carlson, Jonathan Dushoff, Peter Billingsley, Henry Mwambi, John Githure, et al. A simulation model of african anopheles ecology and population dynamics for the analysis of malaria transmission. *Malaria Journal*, 3:29, 2004.

[205] Madeleine C Thomson, Simon J Mason, Thandie Phindela, and Stephen J Connor. Use of rainfall and sea surface temperature monitoring for malaria early warning in botswana. *The American journal of tropical medicine and hygiene*, 73(1):214–221, 2005.

[206] Arnaud Le Menach, Shannon Takala, F Ellis McKenzie, Andre Perisse, Anthony Harris, Antoine Flahault, and David L Smith. An elaborated feeding cycle model for reductions in vectorial capacity of night-biting mosquitoes by insecticide-treated nets. *Malaria journal*, 6(1):10, 2007.

[207] Tatiana Sergeevna Detinova, Douglas S Bertram, World Health Organization, et al. *Age-grouping methods in Diptera of medical importance, with special reference to some vectors of malaria.* World Health Organization, 1962.

[208] DL Smith, J Dushoff, RW Snow, and SI Hay. The entomological inoculation rate and plasmodium falciparum infection in african children. *Nature*, 438(7067):492, 2005.

[209] David L Smith, F Ellis McKenzie, Robert W Snow, and Simon I Hay. Revisiting the basic reproductive number for malaria and its implications for malaria control. *PLoS biology*, 5(3):e42, 2007.

[210] JA Armstrong and WR Bransby-Williams. The maintenance of a colony of anopheles gambiae, with observations on the effects of changes in temperature. *Bulletin of the World Health Organization*, 24(4-5):427, 1961.

[211] WJM Martens, TH Jetten, J Rotmans, and LW Niessen. Climate change and vector-borne diseases: a global modelling perspective. *Global environmental change*, 5(3):195–209, 1995.

[212] Willem JM Martens, Theo H Jetten, and Dana A Focks. Sensitivity of malaria, schistosomiasis and dengue to global warming. *Climatic change*, 35(2):145–156, 1997.

[213] Mohamed Nabie Bayoh. *Studies on the development and survival of Anopheles gambiae sensu stricto at various temperatures and relative humidities.* PhD thesis, Durham University, 2001.

[214] Max J Miller. Observations on the natural history of malaria in the semi-resistant west african. *Transactions of the Royal Society of Tropical Medicine and Hygiene*, 52(2):152–168, 1958.

[215] KP Day, RE Hayward, and M Dyer. The biology of plasmodium falciparum transmission stages. *Parasitology*, 116(S1):S95–S109, 1998.

[216] Jean-Christophe Desconnets, Jean-Denis Taupin, Thierry Lebel, and Christian Leduc. Hydrology of the hapex-sahel central super-site: surface water drainage and aquifer recharge through the pool systems. *Journal of Hydrology*, 188:155–178, 1997.

[217] Alfonso Garmendia and Joan Pedrola Monfort. Simulation model comparing the hydroperiod of temporary ponds with different shapes. *Limnetica*, 29(1):0145–152, 2010.

[218] Adrian M. Tompkins, Rachel Lowe, Hannah Nissan, Nadége Martiny, Pascal Roucou, Madeleine C. Thomson, and Tetsuo Nakazawa. Predicting climate impacts on health at sub -seasonal to seasonal timescales. In A. W. Robertson and F. Vitart, editors, *The gap between weather and climate forecasting: sub-seasonal to seasonal prediction*, page in press. Elsevier, 2018.

[219] Ernest O Asare, Adrian M Tompkins, Leonard K Amekudzi, and Volker Ermert. A breeding site model for regional, dynamical malaria simulations evaluated using in situ temporary ponds observations. *Geospatial health*, 11(1s), 2016.

[220] Ernest O Asare, Adrian M Tompkins, Leonard K Amekudzi, Volker Ermert, and Robert Redl. Mosquito breeding site water temperature observations and simulations towards improved vector-borne disease models for africa. *Geospatial health*, pages 67–77, 2016.

[221] E Asare, AM Tompkins, and A Bomblies. Evaluation of a simple puddle breeding site model for malaria vectors using high resolution explicit surface hydrology simulations. *PLoS One*, 2016.

[222] Catherine Linard, Marius Gilbert, Robert W Snow, Abdisalan M Noor, and Andrew J Tatem. Population distribution, settlement patterns and accessibility across africa in 2010. *PloS one*, 7(2):e31743, 2012.

[223] Wilco Hazeleger, Camiel Severijns, Tido Semmler, Simona Ştefănescu, Shuting Yang, Xueli Wang, Klaus Wyser, Emanuel Dutra, José M Baldasano, Richard Bintanja, et al. Ec-earth: a seamless earth-system prediction approach in action. *Bulletin of the American Meteorological Society*, 91(10):1357–1364, 2010.

[224] Dagmar Popke, Bjoern Stevens, and Aiko Voigt. Climate and climate change in a radiative-convective equilibrium version of echam6. *Journal of Advances in Modeling Earth Systems*, 5(1):1–14, 2013.

[225] Shingo Watanabe, T Hajima, K Sudo, T Nagashima, T Takemura, H Okajima, Toru Nozawa, H Kawase, M Abe, TJGMD Yokohata, et al. Miroc-esm 2010: Model description and basic results of cmip5-20c3m experiments. *Geoscientific Model Development*, 4(4):845–872, 2011.

[226] Mats Bentsen, Ingo Bethke, Jens B Debernard, Trond Iversen, A Kirkevåg, Ø Seland, Helge Drange, Caroline Roelandt, Ivar A Seierstad, Corinna Hoose, et al. The norwegian earth system model, noresm1-m–part 1: description and basic evaluation of the physical climate. *Geoscientific Model Development*, 6(3):687–720, 2013.

[227] WJ Collins, Nicolas Bellouin, M Doutriaux-Boucher, N Gedney, P Halloran, T Hinton, J Hughes, CD Jones, M Joshi, S Liddicoat, et al. Development and evaluation of an earth-system model–hadgem2. *Geoscientific Model Development*, 4(4):1051–1075, 2011.

[228] Detlef P Van Vuuren, James A Edmonds, Mikiko Kainuma, Keywan Riahi, and John Weyant. A special issue on the rcps. *Climatic Change*, 109(1):1–4, 2011.

[229] Simon I Hay, Carlos A Guerra, Andrew J Tatem, Peter M Atkinson, and Robert W Snow. Urbanization, malaria transmission and disease burden in africa. *Nature reviews. Microbiology*, 3(1):81, 2005.

[230] Torleif Markussen Lunde, Mohamed Nabie Bayoh, and Bernt Lindtjørn. How malaria models relate temperature to malaria transmission. *Parasites & vectors*, 6(1):20, 2013.

[231] Felipe J Colón-González, Adrian M Tompkins, Riccardo Biondi, Jean Pierre Bizimana, and Didacus Bambaiha Namanya. Assessing the effects of air temperature and rainfall on malaria incidence: an epidemiological study across rwanda and uganda. *Geospatial health*, 11(1s), 2016.

[232] Yousif E Himeidan, Guofa Zhou, Laith Yakob, Yaw Afrane, Stephen Munga, Harrysone Atieli, El-Amin El-Rayah, Andrew K Githeko, and Guiyun Yan. Habitat

stability and occurrences of malaria vector larvae in western kenya highlands. *Malaria journal*, 8(1):234, 2009.

[233] Andrew J Tatem and Simon I Hay. Measuring urbanization pattern and extent for malaria research: a review of remote sensing approaches. *Journal of Urban Health*, 81(3):363–376, 2004.

[234] PM de la Santé. Plan national de développement sanitaire 2011-2015. *Ministère de la Santé Publique*, 2010.

[235] Jan Arie Rozendaal. Relations between anopheles darlingi breeding habitats, rainfall, river level and malaria transmission rates in the rain forest of suriname. *Medical and veterinary entomology*, 6(1):16–22, 1992.

[236] PHD Kusumawathie, AR Wickremasinghe, ND Karunaweera, MJS Wijeyaratne, and AMGM Yapabandara. Anopheline breeding in river bed pools below major dams in sri lanka. *Acta tropica*, 99(1):30–33, 2006.

[237] Landre Djamouko-Djonkam, Diane Leslie Nkahe, Edmond Kopya, Abdou Talipouo, Carmene Sandra Ngadjeu, Patricia Doumbe-Belisse, Roland Bamou, Parfait Awono-Ambene, Timoléon Tchuinkam, Charles Sinclair Wondji, et al. Implication of anopheles funestus in malaria transmission in the city of yaoundé, cameroon. *Parasite*, 27, 2020.

[238] Michael I Bird, Pierre Giresse, and Simon Ngos. A seasonal cycle in the carbon-isotope composition of organic carbon in the sanaga river, cameroon. *Limnology and Oceanography*, 43(1):143–146, 1998.

[239] Michael Van Lieshout, RS Kovats, MTJ Livermore, and Pim Martens. Climate change and malaria: analysis of the sres climate and socio-economic scenarios. *Global environmental change*, 14(1):87–99, 2004.

[240] Mbi Chrysantus Tanga, WI Ngundu, N Judith, J Mbuh, N Tendongfor, Frédéric Simard, and Samuel Wanji. Climate change and altitudinal structuring of malaria vectors in south-western cameroon: their relation to malaria transmission. *Transactions of the Royal Society of Tropical Medicine and Hygiene*, 104(7):453–460, 2010.

[241] Kibii Komen, Jane Olwoch, Hannes Rautenbach, Joel Botai, and Adetunji Adebayo. Long-run relative importance of temperature as the main driver to malaria transmission in limpopo province, south africa: A simple econometric approach. *EcoHealth*, 12(1):131–143, 2015.

[242] Kristie L Ebi, Jessica Hartman, Nathan Chan, John Mcconnell, Michael Schlesinger, and John Weyant. Climate suitability for stable malaria transmission in zimbabwe under different climate change scenarios. *Climatic Change*, 73(3):375, 2005.

[243] Alizée Chemison, Gilles Ramstein, Adrian M Tompkins, Dimitri Defrance, Guigone Camus, Margaux Charra, and Cyril Caminade. Impact of an accelerated melting of greenland on malaria distribution over africa. *Nature Communications*, 12(1):1–12, 2021.

[244] Cyril Caminade, Sari Kovats, Joacim Rocklov, Adrian M Tompkins, Andrew P Morse, Felipe J Colón-González, Hans Stenlund, Pim Martens, and Simon J Lloyd. Impact of climate change on global malaria distribution. *Proceedings of the National Academy of Sciences*, 111(9):3286–3291, 2014.

[245] Andreas Béguin, Simon Hales, Joacim Rocklöv, Christofer Åström, Valérie R Louis, and Rainer Sauerborn. The opposing effects of climate change and socio-economic development on the global distribution of malaria. *Global Environmental Change*, 21(4):1209–1214, 2011.

[246] Shweta Chaturvedi and Suneet Dwivedi. Understanding the effect of climate change in the distribution and intensity of malaria transmission over india using a dynamical malaria model. *International Journal of Biometeorology*, 65(7):1161–1175, 2021.

[247] Volker Ermert, Andreas H Fink, Andrew P Morse, and Heiko Paeth. The impact of regional climate change on malaria risk due to greenhouse forcing and land-use changes in tropical africa. *Environmental Health Perspectives*, 120(1):77–84, 2012.

[248] Obed Matundura Ogega and Moses Alobo. Impact of 1.5 oc and 2 oc global warming scenarios on malaria transmission in east africa. *AAS Open Research*, 3, 2020.

[249] Adrian M Tompkins and Nicky McCreesh. Migration statistics relevant for malaria transmission in senegal derived from mobile phone data and used in an agent-based migration model. *Geospatial health*, 11(1 Suppl):408, 2016.

List of publications

A Publications in scientific reviews

1. **Mbouna, Amelie D.**, Adrian M. Tompkins, Andre Lenouo, Ernest O. Asare, Edmund I. Yamba, and Clement Tchawoua: **Modelled and observed mean and seasonal relationships between climate, population density and malaria indicators in Cameroon**. *Malaria Journal 18, no.1(2019): 359. DOI: 10.1186/ s12936-019-2991-8 (Impact factor 3.570)*;

2. **Mbouna, Amelie D.**, Alain T. Tamoffo, Ernest O. Asare, Andre Lenouo and Clement Tchawoua: **Malaria metrics distribution under global warming: assessment of the VECTRI malaria model over Cameroon**. *International Journal of biometeorology. https://doi.org/10.1007/s00484-022-02388-x (Impact Factor 3.738)*.

B Poster session

3. **Mbouna, Amelie D.**, Adrian M. Tompkins, Andre Lenouo, Ernest O. Asare, Edmund I. Yamba, and Clement Tchawoua: **Assessing rainfall, temperature and population impacts on malaria incidence in Cameroon and use to validate the VECTRI malaria model.** Poster presented at the ***African Climate Risks Conference ACRC 2019*** organised by **Future Climate For Africa** in Addis Ababa, Ethiopia, from 7-9 October 2019.

C Oral presentation

4. **Mbouna, Amelie D.**, Adrian M. Tompkins, Andre Lenouo, Ernest O. Asare, Edmund I. Yamba, and Clement Tchawoua: **Assessing rainfall, temperature and population impacts on malaria incidence in Cameroon and use to validate**

the VECTRI malaria model. Oral presentation at the *70th workshop on Mathematical and Computational Epidemiology of Infectious Diseases - Mathematically Shaping Global and Local Public Health Policies*, from the 28th August to the 5th September 2018 at the Ettore Majorana Foundation and Centre for Scientific Culture (EMFCSC), Erice, Sicily, Italy.

Workshops and conferences

A Workshops

1. Participation at the ***Workshop on Mathematical Models of Climate Variability, Environmental Change and Infectious Diseases*** from 8th to 16th May 2017 at ICTP, Trieste, Italy.

2. Participation at the ***70th workshop on Mathematical and Computational Epidemiology of Infectious Diseases - Mathematically Shaping Global and Local Public Health Policies***, from the 28th August to the 5th September 2018 at the Ettore Majorana Foundation and Centre for Scientific Culture (EMFCSC), Erice, Sicily, Italy.

B Conferences

3. Attendance at the ***Conference on Future of Earth-Space Science and education (Future ESSE)*** from 2nd to 6th November 2015 at ICTP, Trieste, Italy.

4. Attendance at ***The 2nd Conference on Impact of Environmental Changes on Infectious Diseases*** from 17th to 19th May 2017 at ICTP, Trieste, Italy.

5. Attendance at the ***African Climate Risks Conference ACRC 2019*** from 7th to 9th October 2019 in Addis Ababa, Ethiopia.

RESEARCH

Open Access

Modelled and observed mean and seasonal relationships between climate, population density and malaria indicators in Cameroon

Amelie D. Mbouna[1,2]* , Adrian M. Tompkins[2], Andre Lenouo[3], Ernest O. Asare[4], Edmund I. Yamba[5] and Clement Tchawoua[1]

Abstract

Background: A major health burden in Cameroon is malaria, a disease that is sensitive to climate, environment and socio-economic conditions, but whose precise relationship with these drivers is still uncertain. An improved understanding of the relationship between the disease and its drivers, and the ability to represent these relationships in dynamic disease models, would allow such models to contribute to health mitigation and adaptation planning. This work collects surveys of malaria parasite ratio and entomological inoculation rate and examines their relationship with temperature, rainfall, population density in Cameroon and uses this analysis to evaluate a climate sensitive mathematical model of malaria transmission.

Methods: Co-located, climate and population data is compared to the results of 103 surveys of parasite ratio (PR) covering 18,011 people in Cameroon. A limited set of campaigns which collected year-long field-surveys of the entomological inoculation rate (EIR) are examined to determine the seasonality of disease transmission, three of the study locations are close to the Sanaga and Mefou rivers while others are not close to any permanent water feature. Climate-driven simulations of the VECTRI malaria model are evaluated with this analysis.

Results: The analysis of the model results shows the PR peaking at temperatures of approximately 22 °C to 26 °C, in line with recent work that has suggested a cooler peak temperature relative to the established literature, and at precipitation rates at 7 mm day^{-1}, somewhat higher than earlier estimates. The malaria model is able to reproduce this broad behaviour, although the peak occurs at slightly higher temperatures than observed, while the PR peaks at a much lower rainfall rate of 2 mm day^{-1}. Transmission tends to be high in rural and peri-urban relative to urban centres in both model and observations, although the model is oversensitive to population which could be due to the neglect of population movements, and differences in hydrological conditions, housing quality and access to healthcare. The EIR follows the seasonal rainfall with a lag of 1 to 2 months, and is well reproduced by the model, while in three locations near permanent rivers the annual cycle of malaria transmission is out of phase with rainfall and the model fails.

Conclusion: Malaria prevalence is maximum at temperatures of 24 to 26 °C in Cameroon and rainfall rates of approximately 4 to 6 mm day^{-1}. The broad relationships are reproduced in a malaria model although prevalence is highest at a lower rainfall maximum of 2 mm day^{-1}. In locations far from water bodies malaria transmission seasonality closely follows that of rainfall with a lag of 1 to 2 months, also reproduced by the model, but in locations close to a seasonal

---

*Correspondence: ameldany18@gmail.com
[1] Laboratory for Environmental Modelling and Atmospheric Physics
(LEMAP), Department of Physics, Faculty of Science, University of Yaoundé
I, Yaoundé, Cameroon
Full list of author information is available at the end of the article

river the seasonality of malaria transmission is reversed due to pooling in the transmission to the dry season, which the model fails to capture.

Keywords: Malaria, Climate, Cameroon, Parasite ratio, Entomological inoculation rate

Background

Malaria is a life-threatening disease caused by parasites that are transmitted through the bites of infected mosquitoes [1]. Globally the disease is present and endemic in tropical regions where the climate and hydrological conditions are suitable for the vector survival and development of the parasite. In Cameroon, malaria has always been and still remains a major health problem [2]. It is a major endemic illness and the leading cause of morbidity and mortality in the country. Children aged 0 to 5 and pregnant women are the most vulnerable category with a total of 22% of morbidity and mortality risk [3, 4]. Moreover the 2000–2010 national health report precise that the disease was responsible for medical consultation (40–45%), morbidity (50%), deaths in children under five (40%), deaths in health institutions (30 to 40%), days spent in hospital (57%) and sick leave (26%) in the country [2, 5].

Intervention strategies have recently been increased by the national programme to fight malaria, in the form of free distribution of insecticide-treated mosquito nets (ITNs) and free consultation and treatment of uncomplicated malaria in children under 5 years [2]. The high incidence of malaria in Cameroon is not surprising due to the presence of the three key vectors: namely *Anopheles gambiae*, *Anopheles funestus* and *Anopheles arabiensis* across the country [6, 7]. In terms of species distribution, Hamadou et al. [8] found that *An. gambiae* alone accounts for 90%, with the remaining 10% made up of *An. funestus* and *An. arabiensis*.

As in other sub-Saharan African countries [9–13], there is a spatio-temporal variation in malaria transmission across ecological zones in Cameroon (namely, the Soudano-Sahelian zone, the Adamaoua plateau, the Savannah-forest, the south equatorial forest, the western plateau and the costal zone [14]). The peak transmission period is related to the key periods of rainfall with a delay of 1 or 2 months for the vector/parasite cycles to amplify, as temperatures are usually within the range that support both mosquito survival and parasite development [15, 16]. During the monsoon season, temporary transient ponds and puddles become abundant, and can serves as potential breeding habitats for malaria vectors [11]. Temperatures are important for regulating the intensity of transmission however, as they impact the life cycles and mortalities rate of the vector as well as the sporogonic cycle of the parasite [17].

While the broad relationships between climate and malaria transmission are broadly under-stood, the exact nature of is still uncertain. Regarding the temperature relationship, earlier work [17] suggested that falciparum transmission increased above a threshold of approximately 18 °C to peak at a temperature of around 28 to 32 °C, decreasing thereafter due to the higher mortality of the adult vector. Ermert et al. [18] highlighted the large uncertainty of vector mortality at warm temperatures, while more recently, incorporation of new data and knowledge of the temperature sensitivity larvae stages of the vector has led to the suggestion that the transmission peak in fact occurs at considerably cooler temperatures [19–21].

In view of this uncertainty, the first aim of this work is to relate the malaria prevalence as measured by the parasite ratio (PR) gathered from a large number of field surveys to the mean climate in each locations in the months preceding the field survey, using data mostly gathered in the period before the large scale up of interventions. While such an analysis can reveal broad time-averaged relationships between malaria and climate, it cannot inform on the seasonality of the disease. Firstly, the prevalence is a time-integrated metric of the disease due to slow natural clearance times, with immune individuals often having low background parasite counts continuously in endemic areas [22, 23], and additionally field PR surveys are isolated in time. A better metric for seasonality is the transmission rate, as measured by the entomological inoculation rate (EIR), the number of infective bites per person per unit time. A newly released database of EIR is thus utilized [24], which contains year-long records of monthly EIR measurements in order to be able to examine the seasonality of disease transmission in Cameroon.

Many previous studies have shown how vicinity to breeding sites could be a key determinant of hazard of exposure to the disease [25–28], but few have studied how water proximity may alter the seasonality of disease transmission. Away from permanent water bodies, one expects the disease transmission to track the occurrence of seasonal rains closely, as these provide the temporary breeding sites preferred by the vector *An. gambiae* [29, 30], but with a temperature-determined delay of 1 to 2 months due to the "spin-up" amplification of the vector and parasite life cycles [27, 31]. Vicinity to breeding sites that may form near the

edges of permanent water bodies, such as lakes, may reduce the seasonal variation of transmission, or may even reverse the relationship altogether in the case of river systems that are either intermittent or perennial but subject to large seasonal flow variations, and that may form large-scale pooling during their transition to the dry season [32].

In addition to climate, differences in population density contribute to the observed variability in malaria transmission intensity between rural, peri-urban and urban settings [33], due to land use patterns, density of households, access to social and health services and the dilution effect [34]. Thus, analysis are also made on how population density may influence the malaria diagnostics. If the climate and population link to malaria can be represented in dynamical models [35–37], these models can act as useful tools to understand how climate trends, extreme seasonal anomalies or variability associated with, for example, the El Nino southern oscillation, may potentially affect transmission and such models could possibly be used for mitigation or adaptation decision support. The second aim of this paper is to use the malaria-climate-population analysis to evaluate gridded simulations of malaria transmission made with dynamical malaria model that accounts for both population density and climate.

Methods

Study area and climate data

The study is conducted in Cameroon situated in central Africa within 1.5–13° N and 8–17° E with others neighbouring countries (Fig. 1). The country climate is influenced by the Harmattan and the Atlantic Monsoon winds. Cameroon is characterized by two climatic domains: the tropical climatic domain that stretches to the north, extending into the Sahel zone (~ 8° to 13° N) [38, 39] and the humid equatorial domain that covers the rest of the country (~ 1.5° to 8° N).

The equatorial domain is characterized by heavy rainfall events, with increasing temperatures and a degrading vegetation as one moves far from the Equator [40]. It presents two rainy seasons with abundant rainfall that can reach 2200 mm year^{-1} and two dry seasons with average temperature of 25° C [41]. The tropical area, which is usually recognized with high temperatures (up to 33 °C) and low rainfall (maximum of 1500 mm year^{-1}), presents one rainy and one dry season [38, 41]. The mean rainfall and temperature of Cameroon and neighbours countries from 1985 to 2006 shows higher rainfall intensity in the western and coastal part of the country and increasing mean temperature moving north towards the Soudano-Sahelian zone (Fig. 1).

Fig. 1 Map of Cameroon and neighbouring countries showing mean rainfall and temperature from 1985 to 2006. **a** Rainfall (mm/day); **b** temperature (℃)

Mbouna *et al. Malar J*   (2019) 18:359

Page 4 of 14
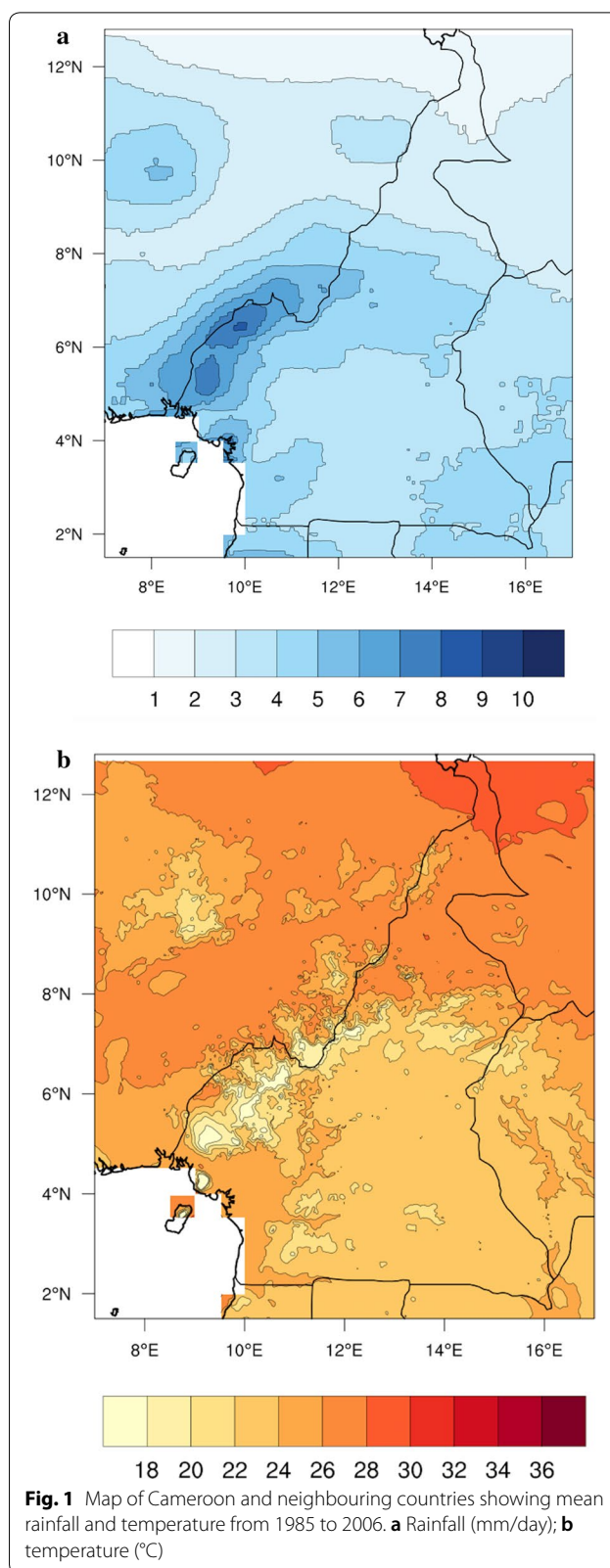
Malaria data

Two malaria indicators are used in this study. The parasite ratio (PR) expresses the pro-portion of individuals infected at a given point in time [42]. A publicly available database of parasite ratio is obtained from the Malaria Atlas Project (MAP) programme [43]. The public PR database consists of data collected by individuals researchers or organizations and published in literature, which were collected within the MAP programme. Since there is no continuous measurement of PR, the available PR data with georeferenced coordinates are used. The location of the PR surveys is given in Fig. 2, which shows that the majority of surveys are located in the west or the far north, ant east of the country. In total, 103 surveys are used, with a total of 18,011 people tested in these surveys, with the survey dates ranging from 1985 to 2006.

All database entries have been quality controlled in terms of data collection methodology and geographical location to ensure continuity across the 20-year collection period. In addition to climate, population density and vicinity to water, many other factors may influence malaria transmission such as socioeconomic conditions, conflict, breakdown in health services, population movements and interventions, which are challenging to account for, not least due to lack of availability of data. As long as these factors are not correlated with spatial or temporal variability of climate, they will act as a form of noise in the analysis, increasing scatter in the climate-malaria relationships, but not obscuring them completely
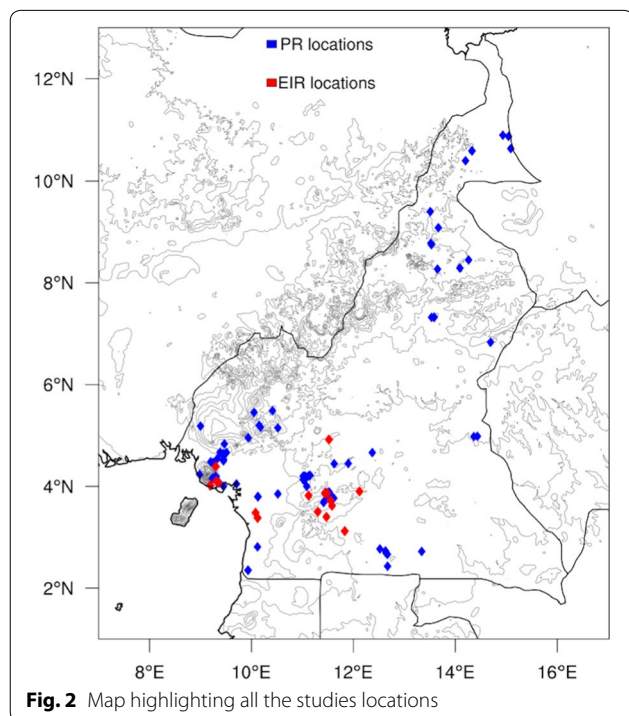

Fig. 2 Map highlighting all the studies locations

if climate is a significant driver of malaria variability. This is also the case for data inaccuracies and uncertainties in both the climate due to instrument error and sampling uncertainty [44] and health records. One complication might be if these facts lead to slow trends over the period, but this would most likely be associated with ramping up of interventions (climate trends are captured in the analysis) and this period predates the large-scale up of interventions that occurred in Cameroon that could confound the climate-malaria relationship. In addition, there have been entomological studies but none found changes is vector distribution during this period, and we assume that such changes would thus not have affected the mean climate-malaria relationships.

The second malaria indicator is the entomological inoculation rate (EIR), which measures the number of infected bites received per person for a given period of time [43], and as such is an indicator of the malaria transmission intensity. It is often calculated as the product of the human biting rate (HBR) and the sporozoite rate. HBR represents the number of bites per person per day, while the sporozoite rate is the fraction of vector mosquitoes that are infectious [45]. A new database of monthly EIR values has been constructed from various sources for all Africa by Yamba et al. [24], with the emphasis on long term field studies lasting at least a year in order to be able to study the seasonality of malaria transmission. For Cameroon, the database has recorded 16 sites with validated data presented in the following Table 1.

The rarity of long-term, continuous monthly EIR records that allow the analysis of seasonality, necessitates the use of data from 30 years ago, but we reiterate that this has the advantage that recent upscaling of (sometimes seasonal) interventions does not obfuscate the analysis. The availability of data for only 2 years in time precludes any analysis of longer terms changes in seasonality that may be associated with climate warming which could potentially be significant [57]. The EIR data sites are highlighted on Fig. 2 below.

VECTRI malaria model

The VECToR borne disease model of ICTP (VECTRI) is an open source gridded distributed dynamical model, that couples a biological model for the vector and parasite life cycles, to a simple compartmental Suceptible-Exposed-Infectious-Recovered (SEIR) representation of the disease progression in the human host. The model runs using daily time step temperature and rainfall data, but also accounts for the population density which is important for the calculation of daily biting rates [37]. The model incorporates several parameterizations schemes for larvae, adult vector and parasite development rates, which are both temperature sensitive, as are

Mbouna *et al. Malar J*   (2019) 18:359

Page 5 of 14

Table 1 Sites of EIR data points used in Cameroon

Site	Location	Longitude	Latitude	Period	References
1	Sanaga village	11.52	4.92	April 1989–March 1990	[46]
2	Mbebe	10.12	3.38	April 1989–March 1990	[47]
3	Nkol-bikok	11.52	3.87	March 1989–February 1990	[15]
4	Nkol-bisson	11.44	3.86	April 1989–March 1990	[15]
5	Limbe	9.19	4.02	August 2001–June 2002	[48]
6	Tiko	9.35	4.07	August 2001–June 2002	[48]
7	Likoko	9.3	4.39	October 2002–September 2003	[49]
8	Essuke-camp	9.31	4.1	October 2004–September 2005	[50]
9	Ebogo	11.47	3.4	April 1991–March 1992	[51]
10	Simbock	11.3	3.5	January 1999–December 1999	[52]
11	Koundou	12.12	3.9	June 1997–May 1998	[53]
12	Ekombite	11.83	3.12	January 2007–December 2007	[54]
13	Nsimalen-Ekoko	12.12	3.82	April 1991–March 1992	[55]
14	Nsimalen-Nkol-mefou	11.58	3.62	April 1991–March 1992	[55]
15	Nsimalen-3	11.55	3.72	April 1991–March 1992	[55]
16	Ndogpassi	10.08	3.48	January 2011–December 2011	[56]

the larvae and adult vector daily survival. Larvae survival, especially in the early development stages, is also impacted negatively by intense precipitation through the inclusion of a flushing effect [58]. The model also allows for over-dispersive biting rates and incorporates a simple treatment of host immunity [59]. Another feature of the model is that it also includes a simple treatment of rain-driven pond formation and loss through evaporation and infiltration [29, 60, 61]. The model allows the user to specify a permanent water breeding fraction but this is not used in the experiments reported here. VECTRI simulates several parameters that help in assessing malaria incidence. Among them are the parasite ratio and entomological inoculation rate.

In this study, the model is integrated for 22 years (1985–2006) with a 3-year spin-up period at $0.03° \times 0.03°$ resolution. Mean daily precipitation data are obtained from Famine Early Warning Systems Network ARC vesion 2 (FEWS-ARC2) [62], available at a spatial resolution of $0.1° \times 0.1°$. The daily gridded 2 m temperature data is taken from the ECMWF ERA-Interim reanalysis data at $0.75° \times 0.75°$ spatial resolution [63], which are then statistically downscaled to the model resolution assuming a lapse rate of 6.5 K km^{-1} to adjust to the high resolution topography. For each grid cell point, population density is obtained from AFRIPOP [64], again interpolated to the model resolution using conservative remapping. AFRIPOP database links informations on contemporary census data across Africa using geographical longitude and latitude position points. After the integration is complete, the nearest grid cell to each field survey location is extracted for comparison. When the comparison

to climate variables is made, for each field survey of PR, the average rainfall and temperature from the preceding 2 months are used, in order to account for the observed lag of 1 to 2 months between malaria and rainfall and the fact that PR is a time-integrated and thus smoothed quantity that reflects climatic conditions over the preceding period [27]. For the time series analysis of EIR, comparisons are made directly to the time series of climate variables for the observed period. As the precise days of surveys were not usually available, only the month, then there is an uncertainty in the lag of 2 weeks.

Results
Parasite ratio evaluation
The spatial maps of PR (Fig. 3) reveals a very heterogeneous landscape of malaria prevalence, particularly in the observed surveys, but also in the model. It should be recalled that the surveys are taken during different years and periods of the year, thus some of the variations are simply due to changes in the meteorology between survey times. Other factors such as interventions and population movements will also impact prevalence, but will not be reflected in the model simulations. Concerning the model, some regional biases stand out clearly. For example, the model produces PR values around 0.5 in the drier and warmer north east of the country, indicating conditions that are borderline between meso and hyperendemic, while the prevalence in the observations is far lower, indicating that the model is too sensitive to low rain rates.

To examine the mean relationship between PR and climate in more details, the survey and model results are

Mbouna *et al. Malar J*   (2019) 18:359

Page 6 of 14

Fig. 3 Observed (**a**) and simulated (**b**) monthly mean parasite ratio values for 36 sites in Cameroon. The PR values represent the average of all the points located within the same coordinates
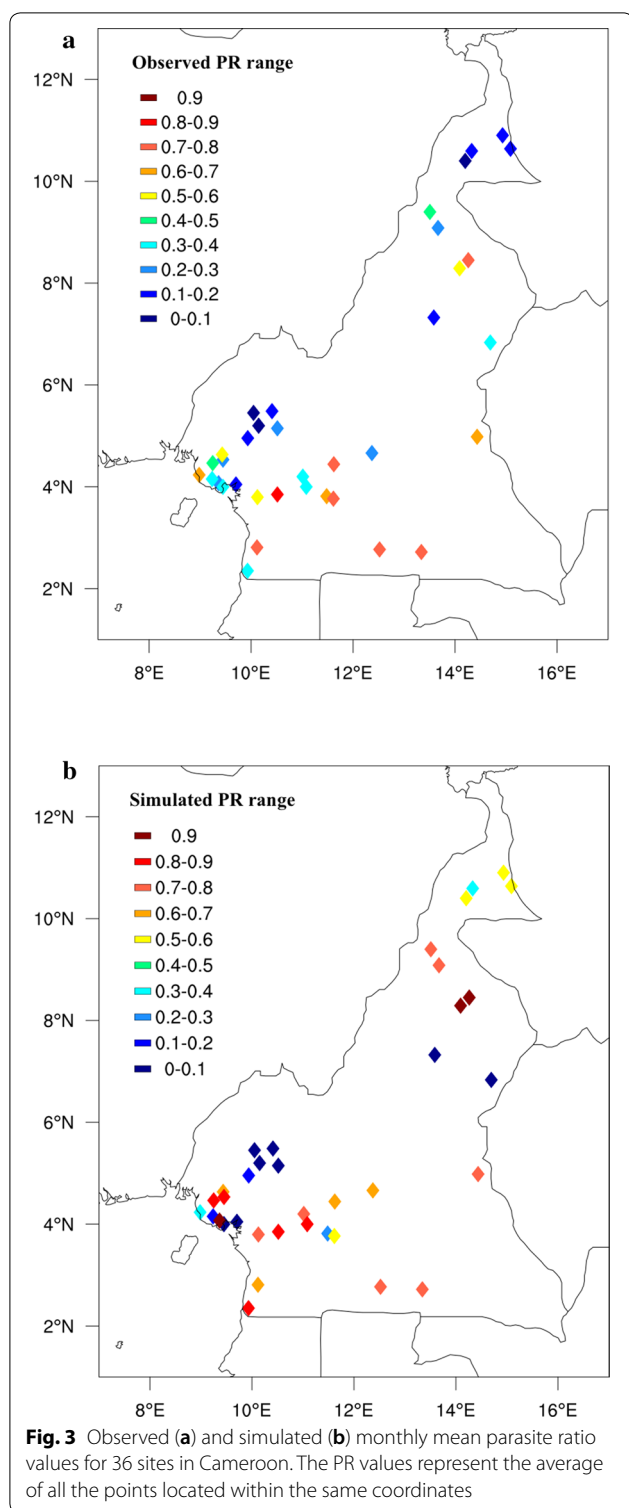
divided into bins according to the two key climatic drivers of mean rainfall and temperature (Fig. 4). The field studies show the prevalence as measured by PR increases to a broad maximum from 22 to 26 °C. Prevalence then

falls off but in still non-zero in the locations with mean temperatures above 30oC. The relationship with temperature is not smooth, as expected due to the fact that climate is only one of many external factors that impact the prevalence from location to location. The model produces a much sharper response to temperature, with low prevalence in the 18–21 °C range, and the peak transmission occurring around 26 °C with prevalence far higher than reported in the survey exceeding 80%. The response in PR to precipitation is more distinct in the model than observations. The observations reveal an increase in PR with increasing rainfall to a local maximum at 7 mm day^{-1}. After the peak, PR decreases with increasing rainfall with the exception of the two bins of 11–13 mm day^{-1}. The model instead peaks at a lower rainfall rate of 2 mm day^{-1}, reducing thereafter, again with the exception of the second last, high rainfall bin.

The PR ratio is compared to population density assigned to three classes of rural (0 to 250 inhabitants per km^2); peri-urban (250 to 1000 inhabitants per km^2); and urban (>1000 inhabitants per km^2) according to Hay et al. [65]. The results are shown on Fig. 5. PR reduces with increasing population density, but with the relationship much stronger in the model relative to observations, a trait that was also observed by Tompkins et al. [37] when comparing EIR as a function of population to the survey data compiled by Kelly-Hope et al. [33]. Thus, the model appears to overestimate malaria prevalence in rural locations and underestimate it in urban centres.

Seasonal EIR evaluation

The seasonal changes in monthly EIR for both model and observations during the study period for the sixteen locations as well as rainfall are presented in Fig. 6. The EIR in the model follows the patterns in rainfall in the studies locations with EIR lagging rainfall peaks by 1 to 2 months in each case. It is also the case for the survey data except in Ekombitie where the value are higher all year long. In certain locations like Sanaga village, Mbebe or Simbock, EIR seasonality is reversed, with peaks EIR values occurring during the relatively dry periods.

Discussion

The temperature and rainfall sensitivity of the prevalence data is broadly in line with earlier works [66–68]. Favourable temperature ranges that support *Plasmodium falciparum* transmission via *Anopheles* species, is generally between 18 and 33 °C [69]. Simple models of the temperature impact on the proportion of female adult vectors surviving long enough for the parasite to complete the sporogonic cycle and permit transmission suggest that, transmission should peak at temperatures of approximately 28 to 32 °C [70]. Although these calculations are
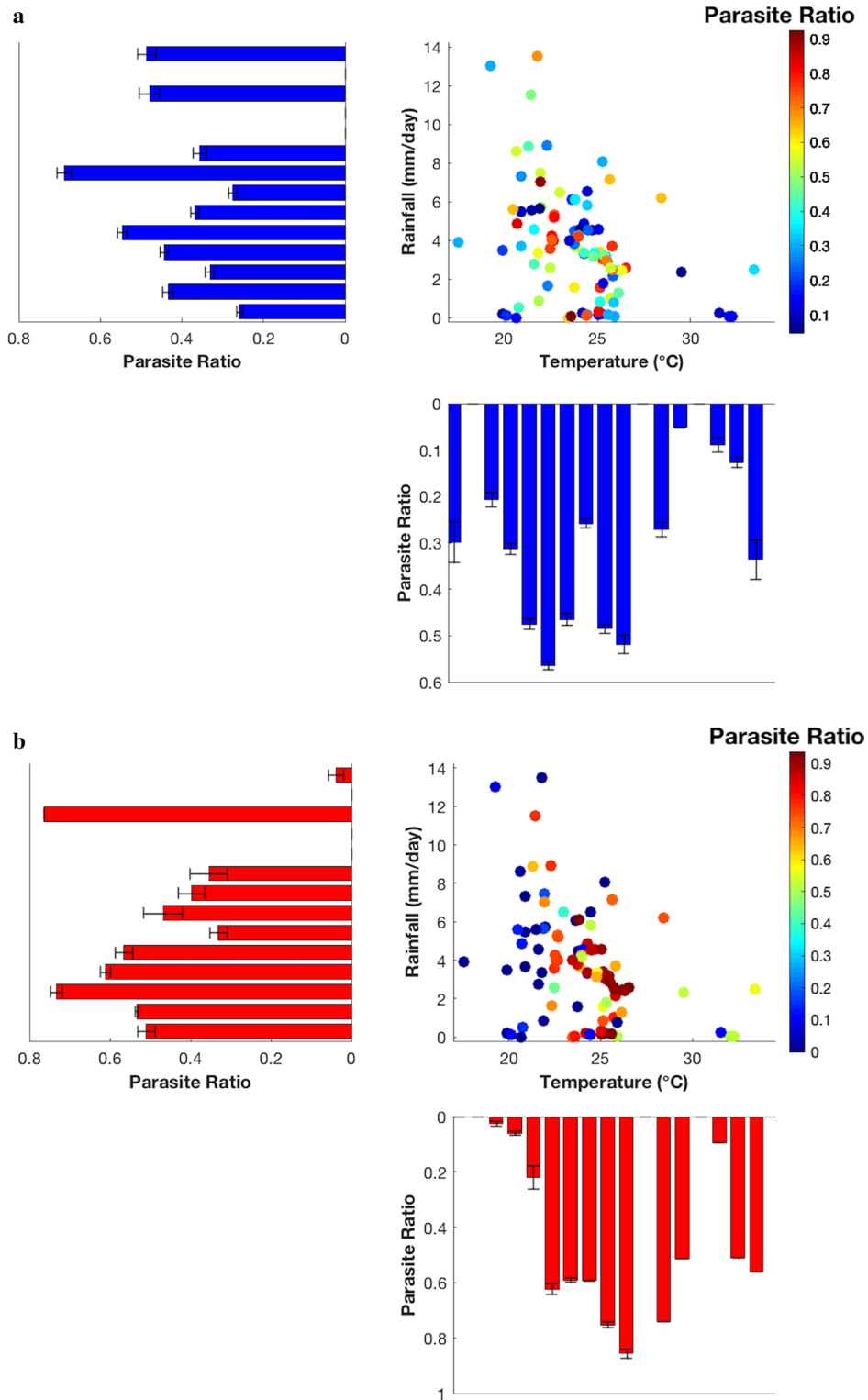
Fig. 4 Observed and simulated parasite ratio, function of rainfall (mm/day) and temperature (°C) over Cameroon. Panels plots present how parasite ratio fluctuates with ranges of rainfall and temperature for observations and simulations. The bars indicate uncertainty, which for the observations is based on a statistical test on the proportion given the total number of people surveys in each bin. For the model the uncertainty measure is the standard deviation of the survey locations in each bin. **a** Observed data, **b** VECTRI model
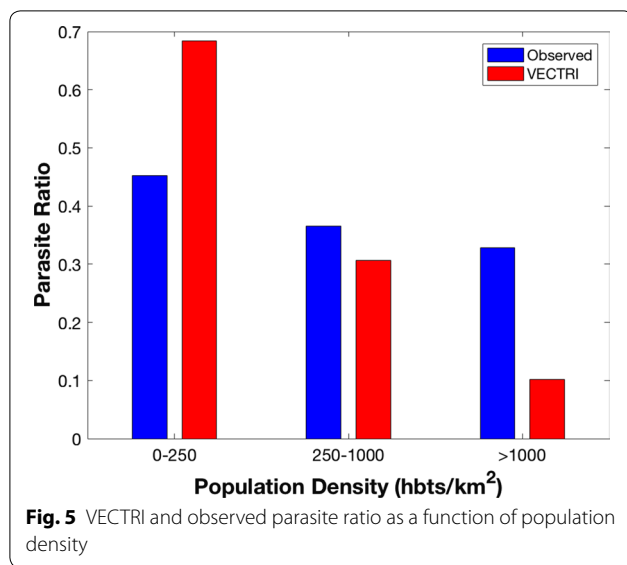
Mbouna *et al. Malar J* (2019) 18:359

Page 8 of 14

Fig. 5 VECTRI and observed parasite ratio as a function of population density

sensitive to the form of the adult mortality curve used and the temperature relationship with malaria remains poorly constrained. More recently suggestions have been made that, accounting for the temperature sensitivity of the vector larvae stages, results in a cooler peak temperature of around 25 °C [19]. Analysis of malaria indicators in Uganda and Rwanda reveals the peaks of malaria transmission occurring at 28 °C and 26 °C, respectively [71]. In the Zomba district in Malawi, a study found that malaria spread is at peak when temperature is at 24 °C [72]; while in the whole country cases monotonically increased with temperature to the maximum temperature sampled of 28 °C [12]. In Cameroon, the analysis reveals that the prevalence measured in surveys is maximum in the 22 to 26 °C range, although there is a gap in the survey sampling in the 27 to 31 °C range, and a warmer peak temperature cannot be precluded. The model similarly produces peak PR at 26 °C, in approximate agreement with the survey data and previous work.

The precipitation relationship is more complex, with PR maximized in survey data at 7 mm day^{-1}. Usually moderate rainfall events are suitable for immature mosquitoes to complete the aquatic development stage, and emerge as adults [58]. Intense rains may cause flooding and flush out larvae from the habitats leading to a decrease in mosquito density [58, 73]. The survey data appears to be in good agreement with previous studies. In Botswana, cases peaked a rainfall rate of approximately 4 mm day^{-1}, in Malawi the peak occurred at a high value of just over 6 mm day^{-1} [12] while in Uganda and Rwanda, highest cases numbers are associated with rainfall between 4 to 6 mm day^{-1} and 4 to 8 mm day^{-1}, respectively [71].

No model will be able to reproduce such prevalence survey data perfectly, a model is necessarily a gross-simplification of reality. Even considering the climate-sensitive life-cycle processes that are accounted for, the model parameters are spatially and temporally homogeneous. For example, the hydrological parameters that determine the pond creation and subsequent loss through evaporation and infiltration are spatially constant, the temperature offset of breeding sites relative to the air temperature also. Moreover, many processes and factors that affect prevalence are not accounted for at all in the model, population movements are neglected, as are those of the vectors, no information on interventions is used, and the model for transmission in the host is extremely simple, neglecting superinfection and incorporating a very simple treatment of immunity. It could be argued that the data is not available to improve many of these aspects. That said, it is encouraging that the model at least manages to reproduce the underlying climate sensitivities revealed in the survey data.

Concerning the population sensitivity, PR in the survey data reduces as population density increases. This agrees with previous work [74], for instance, in Burkina Faso epidemiological profiles and clinical malaria transmission patterns tend to be high in rural compared to urban environments [24]. A review of entomological studies conducted across sub-Saharan Africa countries demonstrated that the higher number of annual *Plasmodium falciparum* EIR were reported in rural populations, where population density < 100 inhabitants per km^2. However,

low EIR were measured in urban areas where population density > 1000 inhabitants per km^2 [33]. This sensitivity is also apparent in the model, but the model appears to exaggerate the effect, tending to be higher relative to observations for rural settings, while under predicting PR in urban centres. For example, one survey was conducted in central Yaoundé by Quakyi et al. [75], with a prevalence of 0.5 to 0.6 revealed in the sampled population of 231 people. The population density in this location exceeds 9000 people km^{-2} and at such high densities the model fails to sustain transmission. One key process in such central urban locations is likely to be population movements, neglected in the model at present, with many of the cases likely to be imported. Other factors also impacts differences between rural and urban areas which are challenging to include in the model, for example, urban zones are associated with low transmission due to factors such as limited availability of breeding sites, improved environmental conditions, easy access to control interventions, housing types and among others [76]. For instance, Cameroon National Malaria Control Programme reported that bed nets are more used in
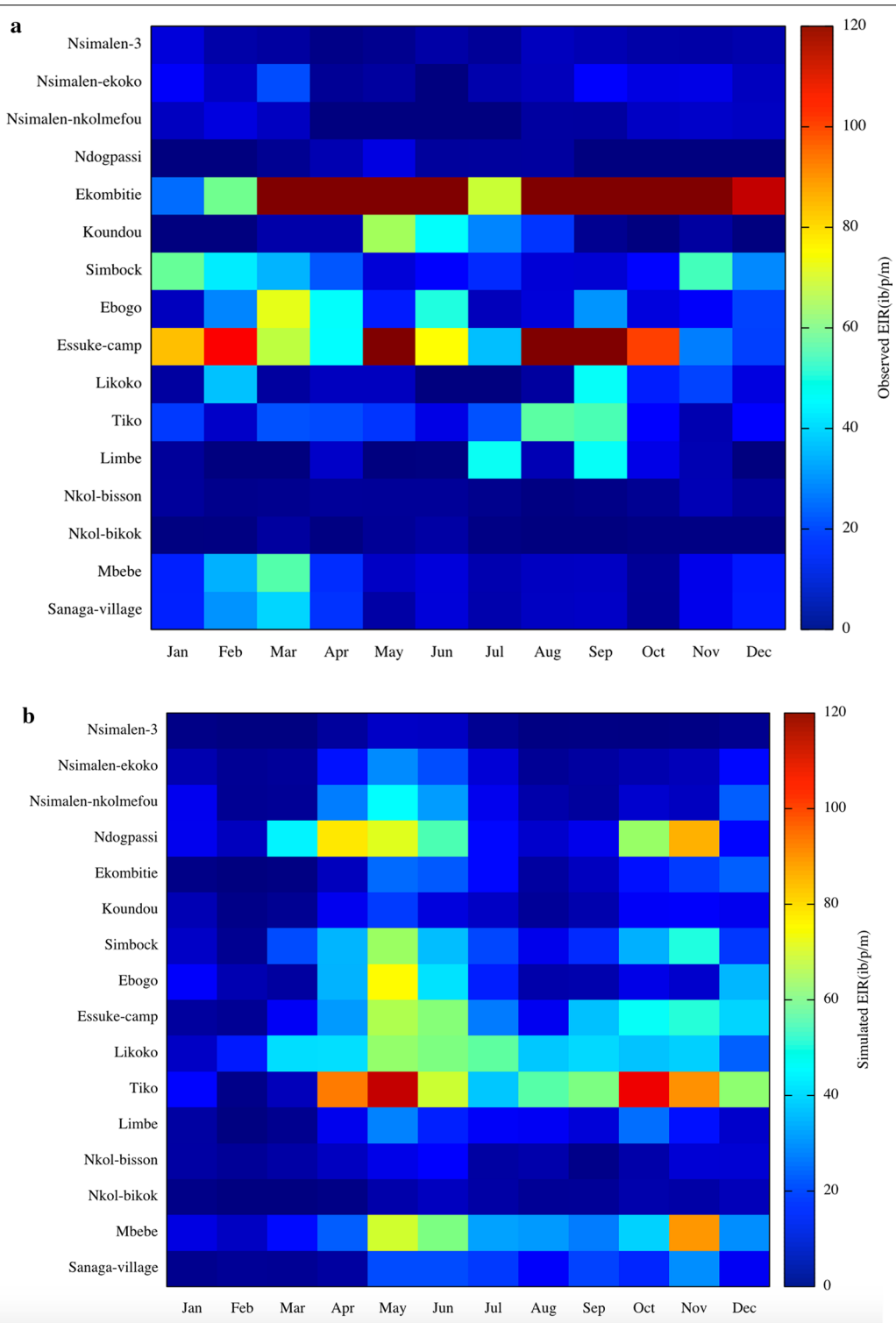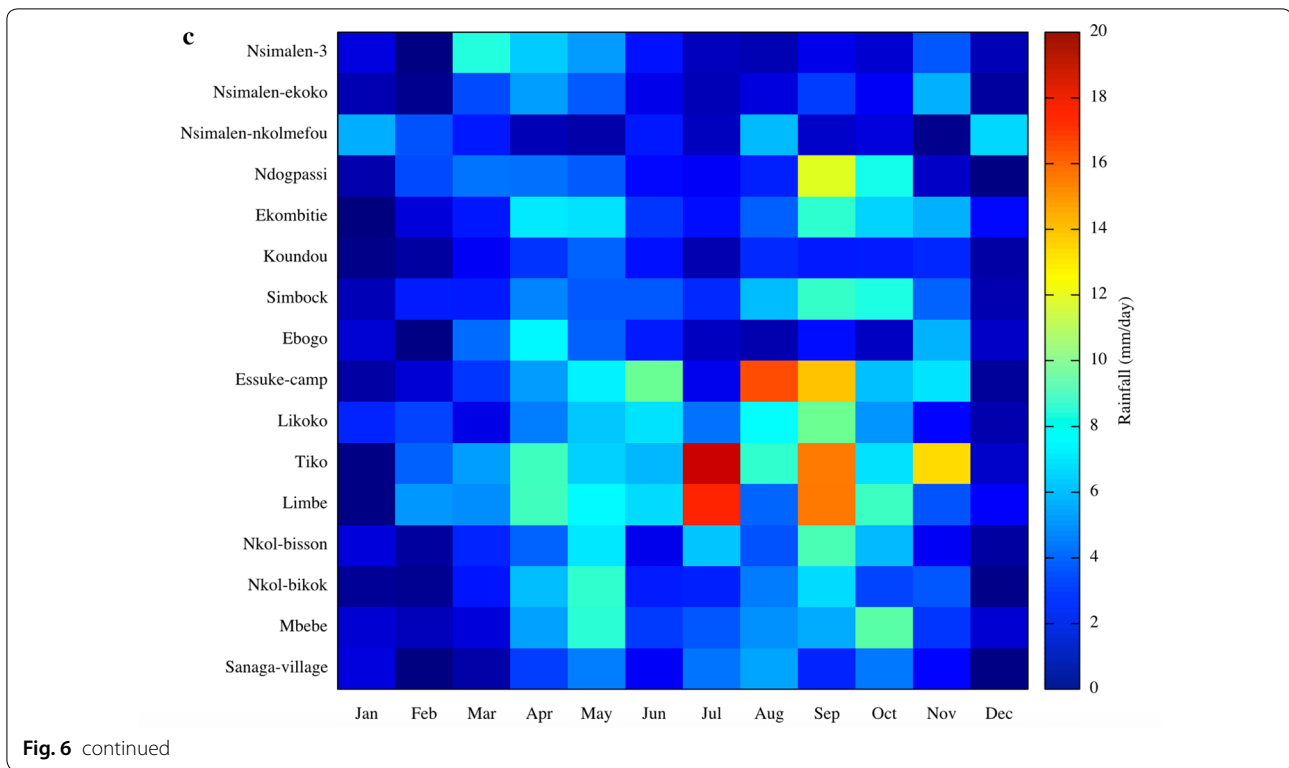
Mbouna *et al. Malar J*   (2019) 18:359

Page 9 of 14

Fig. 6 Observed (**a**), simulated (**b**) monthly mean entomological inoculation rate and **c** rainfall maps for the 16 EIR sites in Cameroon

Mbouna *et al. Malar J*   (2019) 18:359

Page 10 of 14


Fig. 6 continued

urban than rural zones [77]. Most of these latter social and environmental impacts would act to increase disparities between rural and urban transmission, thus the crucial importance of mobility cannot be overlooked. In addition, the fact that the model neglects superinfection will also act to exaggerate the population density impact. In the model's simple SEIR approach, once an infective bite results in successful transmission event, the host moves to an exposed state. The impact of large inoculations of multiple strains when many infectious bites are recorded is not included, thus that individuals enhanced capacity to further transmit the disease is neglected. This would lead to the model overestimating the population dilution effect.

In the survey data for the 16 EIR-sites, the EIR closely follows the seasonality of rainfall with a lag of approximately 1 month. The EIR maximizes in April, May and June while the second peak is observed in October, November and December. The observed seasonal variability of EIR agrees with variability in reported malaria cases, with high case numbers observed during and after rainy seasons [77]. In Nkoteng for example, Cohuet et al. [78] showed that malaria transmission intensity reaches its peak in April during the rainy season. In a related study in Niete (South Cameroon), Bigoga et al. [79] found a lower EIR during dry season (1.09 ibp^{-1}n^{-1}) compared to rainy season (2.3 ibp^{-1}n^{-1}). Similarly,

comparing Simbock and Etoa districts, Quakyi et al. [75] found similar difference between rainy and dry seasons but a high disparity was observed for Etoa. They measured 1.9 ibp^{-1}n^{-1} and 1.2 ibp^{-1}n^{-1} for wet and dry seasons, respectively for Simbock and 2.4 ibp^{-1}n^{-1} and 0.4 ibp^{-1}n^{-1} for Etoa during the wet and dry season, respectively.

The survey data for EIR in Sanaga villages, Mbebe, and Simbock contrasts strongly, and produces a seasonality of EIR which appears to be completely out of phase with the rainfall, with EIR at a maximum during the dry season, precisely January to March (for Sanaga villages and Mbebe) and (for Simbock), behaviour that VECTRI was unable to capture. One possible explanation for this disparity could be linked to their geographical situation and local hydrology. Simbock is located at about 100 m from the Mefou river creating a permanent swamp [52], while Sanaga villages and Mbebe are situated in the vicinity of the Sanaga river as presented on Fig. 7.

Rivers can and do support vectors at ponds formed at their edges, in particular *An. funestus*, and indeed the forested locations typical of these sites have identified *Anopheles nili*, *An. gambiae* and *An. funestus* as key malaria vectors [47]. *Anopheles nili* usually breeds among the grass on the edges of the river and can be a key driver of malaria transmission in such environments [46]. However, when such river systems are not managed, their

Mbouna *et al. Malar J* (2019) 18:359

Page 11 of 14

Fig. 7 Sanaga villages and Mbebe locations, situated at the vicinity of the Sanaga river
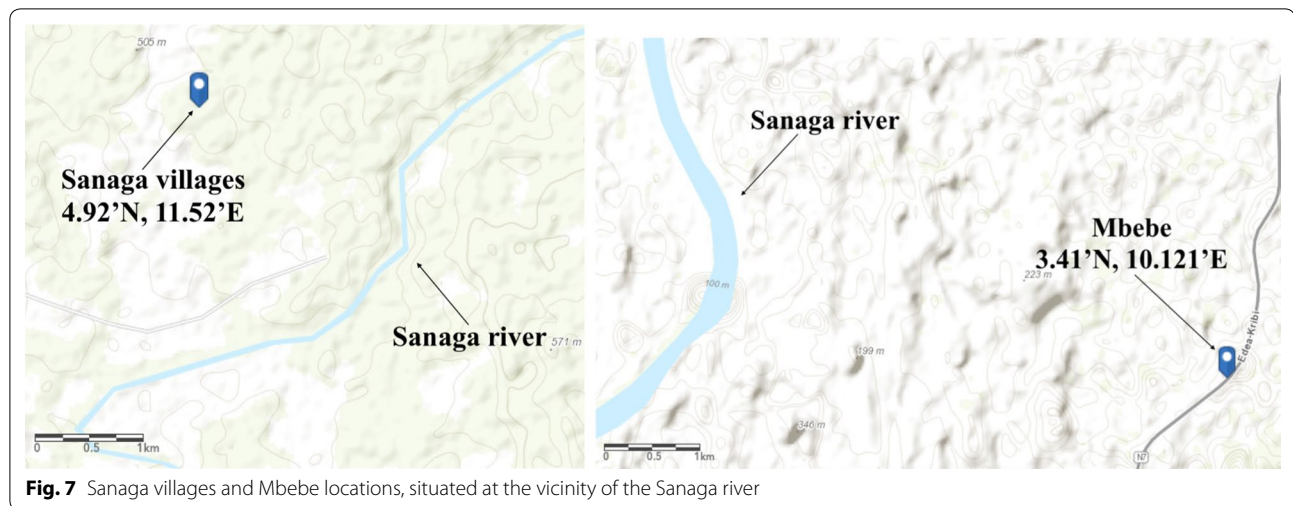
impact on breeding sites can sometimes be enhanced during the dry season when flow is restricted and a large increase in the availability of standing pools can occur, constituting a proliferation of ideal breeding sites for *Anopheles* vectors [32, 80, 81]. The Sanaga river particularly undergoes a strong seasonal cycle in discharge, with flow at a minimum in February to April, with just a small fraction of the peak discharge during these months [82]. Thus, it seems in Sanaga villages and Mbebe, peak in malaria is associated with the minimum in the Sanaga river flow, and an enhancement in ponding. As this version of VECTRI does not account for permanent breeding site associated with river systems, with enhanced ponding in low flow periods, it is not able to reproduce the seasonal cycle in EIR here.

Conclusion

The relation between climate and two common malaria indicators of parasite ratio (PR) and entomological inoculation rate (EIR) were examined in Cameroon, using a comprehensive of survey data for PR and others surveys for EIR that enabled the seasonality of transmission intensity to be examined. While many factors can impact malaria transmission, the established boards relationships of malaria climate drivers were apparent in the.

survey data, with PR increasing with temperature until a peak within 22–26 °C and thereafter reducing, with peak prevalence occurring at rainfall rates at 7 mm day^{-1}. The analysis also confirmed previous research regarding the impact of population density, with PR higher in rural areas relative to urban areas.

The seasonal cycle of the EIR revealed very contrasting behaviour between peri-urban sites, and rural sites situated closely by the Sanaga or the Mefou river. In the peri-urban sites, the EIR seasonality closes follows that of the rainfall, with maxima lagging rainfall peaks by 1 to 2 months. Instead, in rural ones the EIR seasonality is out of phase with rainfall and peaks in March–April when the Sanaga discharge is at its annual minimum, indicating a strong role for the pooling in the river-bed in providing seasonal breeding sites for vectors.

The malaria model is able to reproduce some of these broad traits of the malaria transmission indicators, with a similar relationship between PR and the mean temperatures, while the prevalence peaks at a lower value of rainfall. The model also reproduces the reduction in PR with increasing population. In general, the model produces a too high contrast between areas of high and low transmission relative to the surveys, indicating that a mixing effect, most likely in the form of human migration patterns is lacking in the model in addition to the lack of superinfection. The model is able to reproduce the seasonality of the EIR only in the locations where transmission intensity closely follows temporary breeding sites resulting directly from rainfall, and it cannot produce the dry season peak in the locations near the Sanaga river where breeding sites occur due to low rain flow and Mefou river as well. Thus, while there are numerous simplifications and neglected processes in the model, it would appear that the coupling of the malaria transmission scheme with a model to represent human population movements [83], and the improved representation of breeding sites due to semi-permanent features such as rivers, lakes and dams should be a priority. In general, the model produces infectious biting rates that exceed those observed, and it is likely that, if the model is to be used to aid operational decisions in Cameroon, the use of machine learning techniques to calibrate the model parameters more effectively will be required, such as that recently introduced in Tompkins et al. [44].

Mbouna *et al. Malar J*   (2019) 18:359

Page 12 of 14

Abbreviations

Author details

[1] Laboratory for Environmental Modelling and Atmospheric Physics (LEMAP), Department of Physics, Faculty of Science, University of Yaoundé I, Yaoundé, Cameroon. [2] Earth System Physics, Abdus Salam International Centre for Theoretical Physics (ICTP), Strada Costiera 11, Trieste, Italy. [3] Department of Physics, Faculty of Science, University of Douala, Douala, Cameroon. [4] Department of Epidemiology of Microbial Diseases, Yale School of Public Health, Yale University, New Haven, USA. [5] Department of Physics, Kwame Nkrumah University of Science and Technology, Kumasi, Ghana.

References

1. WHO. World malaria report 2014. Geneva: World Health Organization; 2014. http://www.who.int/malaria/publications/world_malaria_report_2014/en/. Accessed 24 2015.
2. Bandolo FMN. Heavily indebted poor countries (HIPC) initiative in cameroon and the fight to reduce malaria related under-five mortality. Master's thesis, Høgskolen i Oslo og Akershus. Fakultet for Samfunnsfag; 2012.
3. WHO. Cooperation strategy between WHO and the Republic of Cameroon: 2017–2020. Geneva: World Health Organization; 2017.
4. Chouto S, Wakponou A. Disparités spatio-temporelles et prévalence du paludisme à partir des données formelles: cas de Kousséri (Extrême-Nord Cameroun). Ouvrage honoré du soutien financier de la Faculté des Lettres et Sciences Humaines de l'Université de Maroua, 225.
5. Desiré GN, Marlyse PN, Gwet PH. Modelisation de l'impact de la prevention et de la prise en charge des cas sur la progression du paludisme chez la femme enceinte et les enfants de moins de cinq ans. 2010.
6. Fontenille D, Wanji S, Djouaka R, Awono-Ambene H. *Anopheles hancocki*, vecteur secondaire du paludisme au Cameroun. Bull Liaison OCEAC. 2000;33:23–6.
7. Wondji C, Simard F, Petrarca V, Etang J, Santolamazza F, Della Torre A, et al. Species and populations of the *Anopheles gambiae* complex in Cameroon with special emphasis on chromosomal and molecular forms of *Anopheles gambiae s.s.*. J Med Entomol. 2005;42:998–1005.
8. Ndjemaï HN, Patchoké S, Atangana J, Etang J, Simard F, Bilong CFB, et al. The distribution of insecticide resistance in *Anopheles gambiae s.l.* populations from Cameroon: an update. Trans R Soc Trop Med Hyg. 2009;103:1127–38.
9. Asare EO, Amekudzi LK. Assessing climate driven malaria variability in Ghana using a regional scale dynamical model. Climate. 2017;5:20.
10. Bøgh C, Lindsay SW, Clarke SE, Dean A, Jawara M, Pinder M, et al. High spatial resolution mapping of malaria transmission risk in the Gambia, west Africa, using LANDSAT TM satellite imagery. Am J Trop Med Hyg. 2007;76:875–81.
11. Diouf I, Rodriguez-Fonseca B, Deme A, Caminade C, Morse AP, Cisse M, et al. Comparison of malaria simulations driven by meteorological observations and reanalysis products in Senegal. Int J Environ Res Public Health. 2017;14:1119.
12. Lowe R, Chirombo J, Tompkins AM. Relative importance of climatic, geographic and socio-economic determinants of malaria in Malawi. Malar J. 2013;12:416.
13. Amek N, Bayoh N, Hamel M, Lindblade KA, Gimnig JE, Odhiambo F, et al. Spatial and temporal dynamics of malaria transmission in rural Western Kenya. Parasit Vectors. 2012;5:86.
14. Antonio-Nkondjio C, Kerah CH, Simard F, Awono-Ambene P, Chouaibou M, Tchuinkam T, et al. Complexity of the malaria vectorial system in Cameroon: contribution of secondary vectors to malaria transmission. J Med Entomol. 2006;43:1215–21.
15. Fondjo E, Robert V, Le Goff G, Toto J, Carnevale P. Le paludisme urbain à Yaoundé (Cameroun): 2. Etude entomologique dans deux quartiers peu urbanisés. Bull Soc Pathol Exot. 1992;85:57–63.
16. Tchuinkam T, Simard F, Lélé-Defo E, Téné-Fossog B, Tateng-Ngouateu A, Antonio-Nkondjio C, et al. Bionomics of Anopheline species and malaria transmission dynamics along an altitudinal transect in Western Cameroon. BMC Infect Dis. 2010;10:119.
17. Craig MH, Snow RW, le Sueur D. A climate-based distribution model of malaria transmission in sub-Saharan Africa. 1999;15:105–11.
18. Ermert V. Risk assessment with regard to the occurrence of malaria in Africa under the influence of observed and projected climate change. PhD thesis, Universität zu Köln; 2010.
19. Lunde TM, Bayoh MN, Lindtjørn B. How malaria models relate temperature to malaria transmission. Parasit Vectors. 2013;6:20.
20. Mordecai EA, Paaijmans KP, Johnson LR, Balzer C, Ben-Horin T, de Moor E, et al. Optimal temperature for malaria transmission is dramatically lower than previously predicted. Ecol Lett. 2013;16:22–30.
21. Beck-Johnson LM, Nelson WA, Paaijmans KP, Read AF, Thomas MB, Bjørnstad ON. The effect of temperature on Anopheles mosquito population dynamics and the potential for malaria transmission. PLoS ONE. 2013;8:79276.
22. Struchiner C, Halloran M, Spielman A. Modeling malaria vaccines. i: new uses for old ideas. Math Biosci. 1989;94:87–113.
23. Langhorne J, Ndungu FM, Sponaas A-M, Marsh K. Immunity to malaria: more questions than answers. Nat Immunol. 2008;9:725.
24. Yamba EI. Improvement and validation of dynamical malaria models in Africa. PhD thesis, Universität zu Köln. 2016.
25. Carter R, Mendis KN, Roberts D. Spatial targeting of interventions against malaria. Bull World Health Organ. 2000;78:1401–11.
26. Lunde TM, Korecha D, Loha E, Sorteberg A, Lindtjørn B. A dynamic model of some malaria-transmitting anopheline mosquitoes of the Afrotropical region. I. Model description and sensitivity analysis. Malar J. 2013;12:28.
27. Bomblies A, Duchemin JB, Eltahir EA. Hydrology of malaria: model development and application to a sahelian village. Water Resour Res. 2008. https://doi.org/10.1029/2008WR006917.

Mbouna *et al. Malar J*   (2019) 18:359

Page 13 of 14

28. Hajison PL, Feresu SA, Mwakikunga BW. Malaria in children under-five: a comparison of risk factors in lakeshore and highland areas, Zomba district, Malawi. PLoS ONE. 2018;13:0207207.
29. Asare EO, Tompkins AM, Amekudzi LK, Ermert V. A breeding site model for regional, dynamical malaria simulations evaluated using in situ temporary ponds observations. Geospat Health. 2016;11(Suppl 1):390.
30. Mutuku FM, Alaii JA, Bayoh MN, Gimnig JE, Vulule JM, Walker ED, et al. Distribution, description, and local knowledge of larval habitats of *Anopheles gambiae s.l.* in a village in western kenya. Am J Trop Med Hyg. 2006;4:44–53.
31. Bomblies A. Modeling the role of rainfall patterns in seasonal malaria transmission. Clim Change. 2012;112:673–85.
32. Kusumawathie P, Wickremasinghe A, Karunaweera N, Wijeyaratne M, Yapabandara A. Anopheline breeding in river bed pools below major dams in Sri Lanka. Acta Trop. 2006;99:30–3.
33. Kelly-Hope LA, McKenzie FE. The multiplicity of malaria transmission: a review of entomological inoculation rate measurements and methods across sub-Saharan Africa. Malar J. 2009;8:19.
34. Robert V, Macintyre K, Keating J, Trape JF, Duchemin JB, Warren M, et al. Malaria transmission in urban sub-Saharan Africa. Am J Trop Med Hyg. 2003;68:169–76.
35. Hoshen MB, Morse AP. A weather-driven model of malaria transmission. Malar J. 2004;3:32.
36. Eckhoff PA. A malaria transmission-directed model of mosquito life cycle and ecology. Malar J. 2011;10:303.
37. Tompkins AM, Ermert V. A regional-scale, high resolution dynamical malaria model that accounts for population density, climate and surface hydrology. Malar J. 2013;12:65.
38. Pamo E. Country pasture/forage resource profiles: Cameroon. Food and Agriculture Organization of the United Nations (FAO). 2008;52.
39. Molua E, Molua EL. The economic impact of climate change on agriculture in Cameroon. Policy Research Working papers, World Bank, 2007.
40. Molua EL. Climatic trends in Cameroon: implications for agricultural management. Clim Res. 2006;30:255–62.
41. Olivry JC. Fleuves et rivières du Cameroun. Monographies hydrologiques IRD; pp 745, 1986.
42. Gething PW, Patil AP, Smith DL, Guerra CA, Elyazar IR, Johnston GL, et al. A new world malaria map: *plasmodium falciparum* endemicity in 2010. Malar J. 2011;10:378.
43. Macdonald G. The epidemiology and control of malaria. World Health Organization, WHO/Mal/132, 1957.
44. Tompkins AM, Thomson MC. Uncertainty in malaria simulations in the highlands of Kenya: relative contributions of model parameter setting, driving climate and initial condition errors. PLoS ONE. 2018;13:0200638.
45. Birley M, Charlewood J. Sporozoite rate and malaria prevalence. Parasitol Today. 1987;3:231–2.
46. Carnevale P, Goff G, Toto JC, Robert V. *Anopheles nili* as the main vector of human malaria in villages of southern Cameroon. J Med Entomol. 1992;6:135–8.
47. Le Goff G, Carnevale P, Fondjo E, Robert V. Comparison of three sampling methods of man-biting Anophelines in order to estimate the malaria transmission in a village of south Cameroon. Parasite. 1997;4:75–80.
48. Bigoga JD, Manga L, Titanji VP, Coetzee M, Leke RG. Malaria vectors and transmission dynamics in coastal south-western Cameroon. Malar J. 2007;6:5.
49. Tanga MC, Ngundu W. Ecological transition from natural forest to tea plantations: effect on the dynamics of malaria vectors in the highlands of Cameroon. Trans R Soc Trop Med Hyg. 2010;104:659–68.
50. Tanga M, Ngundu W, Tchouassi P. Daily survival and human blood index of major malaria vectors associated with oil palm cultivation in Cameroon and their role in malaria transmission. Trop Med Int Health. 2011;16:447–57.
51. Njan Nloga A, Robert V, Toto J, Carnevale P. *Anopheles moucheti*, vecteur principal du paludisme au sud-Cameroun. Bull Liaison OCEAC. 1993;26:63–7.
52. Antonio-Nkondjio C, Awono-Ambene P, Toto JC, Meunier JY, Zebaze-Kemleu S, Nyambam R, et al. High malaria transmission intensity in a village close to Yaounde, the capital city of Cameroon. J Med Entomol. 2002;39:350–5.
53. Meunier J, Safeukui I, Fontenille D, Boudin C. [Malaria transmission in an area of future vaccination in Equatorial forest of south Cameroon](in French). Bull Soc Pathol Exot. 1999;92:309–12.
54. Fils EMB, Ntonga PA, Belong P, Messi J. Contribution of mosquito vectors in malaria transmission in an urban district of southern Cameroon. JEN. 2010;2:13–7.
55. Manga L, Toto J, Carnevale P. Malaria vectors and transmission in an area deforested for a new international airport in southern Cameroon. Ann Soc belge Med Trop. 1995;75:43–9.
56. Antonio-Nkondjio C, Defo-Talom B, Tagne-Fotso R, Tene-Fossog B, Ndo C, Lehman LG, et al. High mosquito burden and malaria transmission in a district of the city of Douala, Cameroon. BMC Infect Dis. 2012;12:275.
57. Altizer S, Dobson A, Hosseini P, Hudson P, Pascual M, Rohani P. Seasonality and the dynamics of infectious diseases. Ecol Lett. 2006;9:467–84.
58. Paaijmans KP, Wandago MO, Githeko AK, Takken W. Unexpected high losses of *Anopheles gambiae* larvae due to rainfall. PLoS ONE. 2007;2:1146.
59. Tompkins AM, Lowe R, Nissan H, Martiny N, Roucou P, Thomson MC, et al. Predicting climate impacts on health at sub-seasonal to seasonal timescales. In: Robertson AW, Vitart F, editors. The gap between weather and climate forecasting: sub-seasonal to seasonal prediction. Amsterdam: Elsevier; 2018.
60. Asare EO, Tompkins AM, Amekudzi LK, Ermert V, Redl R. Mosquito breeding site water temperature observations and simulations towards improved vector-borne disease models for Africa. Geospat Health. 2016;11(Suppl 1):391.
61. Asare E, Tompkins A, Bomblies A. A regional model for malaria vector developmental habitats evaluated using explicit, pond-resolving surface hydrology simulations. PLoS ONE. 2016;11:e0150626.
62. Love T. The climate prediction center rainfall algorithm version 2. NOAA Climate Prediction Center Tech. 2002. http://www.cpc.ncep.noaa.gov/products/fews/RFE2.0_tech.pdf. Accessed 2017.
63. Dee D, Uppala S, Simmons A, Berrisford P, Poli P, Kobayashi S, et al. The era-interim reanalysis: configuration and performance of the data assimilation system. Quart J R Met Soc. 2011;137:553–97.
64. Linard C, Gilbert M, Snow RW, Noor AM, Tatem AJ. Population distribution, settlement patterns and accessibility across Africa in 2010. PLoS ONE. 2012;7:31743.
65. Hay SI, Guerra CA, Tatem AJ, Atkinson PM, Snow RW. Urbanization, malaria transmission and disease burden in Africa. Nat Rev Microbiol. 2005;3:81.
66. Mourou J-R, Coffinet T, Jarjaval F, Cotteaux C, Pradines E, Godefroy L, et al. Malaria transmission in Libreville: results of a one year survey. Malar J. 2012;11:40.
67. Mabaso ML, Vounatsou P, Midzi S, Da Silva J, Smith T. Spatio-temporal analysis of the role of climate in inter-annual variation of malaria incidence in Zimbabwe. Int J Health Geogr. 2006;5:20.
68. Ngom R. Spatial and statistical prediction of urban malaria in yaoundé: a Social and Environmental Modelling Approach for Health Promotion. PhD thesis, Heidelberg University, 2010. http://opus.bszbw.de/phhd/volltexte/2010/7521/pdf/Roland_Ngom_Doctoral_thesis_Online.pdf. Accessed 2019.
69. Bayoh M, Lindsay S. Effect of temperature on the development of the aquatic stages of *Anopheles gambiae* sensu stricto (Diptera: Culicidae). Bull Entomol Res. 2003;93:375–81.
70. Craig MH, Snow R, le Sueur D. A climate-based distribution model of malaria transmission in sub-Saharan Africa. Parasitol Today. 1999;15:105–11.
71. Colón-González FJ, Tompkins AM, Biondi R, Bizimana JP, Namanya DB. Assessing the effects of air temperature and rainfall on malaria incidence: an epidemiological study across Rwanda and Uganda. Geospat Health. 2016;11(Suppl 1):379.
72. Hajison PL, Mwakikunga BW, Mathanga DP, Feresu SA. Seasonal variation of malaria cases in children aged less than 5 years old following weather change in Zomba district, Malawi. Malar J. 2017;6:264.
73. Himeidan YE, Zhou G, Yakob L, Afrane Y, Munga S, Atieli H, et al. Habitat stability and occurrences of malaria vector larvae in western Kenya highlands. Malar J. 2009;8:234.
74. Gardiner C, Biggar R, Collins W, Nkrumah F. Malaria in urban and rural areas of southern Ghana: a survey of parasitaemia, antibodies, and anti-malarial practices. Bull World Health Organ. 1984;62:607.

Mbouna *et al. Malar J* (2019) 18:359

Page 14 of 14

75. Quakyi IA, Leke R, Befidi-Mengue R, Tsafack M, Bomba-Nkolo D, Manga L, et al. The epidemiology of *Plasmodium falciparum* malaria in two Cameroonian villages: Simbok and Etoa. Am J Trop Med Hyg. 2000;63:222–30.

76. Tatem AJ, Hay SI. Measuring urbanization pattern and extent for malaria research: a review of remote sensing approaches. J Urban Health. 2004;81:363–76.

77. Plan national de développement sanitaire 2011–2015. Ministère de la Santé Publique. 2010.

78. Cohuet A, Simard F, Wondji CS, Antonio-Nkondjio C, Awono-Ambene P, Fontenille D. High malaria transmission intensity due to *Anopheles funestus* (Diptera: Culicidae) in a village of savannah–forest transition area in Cameroon. J Med Entomol. 2004;41:901–5.

79. Bigoga JD, Nanfack FM, Awono-Ambene PH, Patchoké S, Atangana J, Otia VS, et al. Seasonal prevalence of malaria vectors and entomological inoculation rates in the rubber cultivated area of Niete, South Region of Cameroon. Parasit Vectors. 2012;5:197.

80. Rozendaal JA. Relations between *Anopheles darlingi* breeding habitats, rainfall, river level and malaria transmission rates in the rain forest of Suriname. J Med Entomol. 1992;6:16–22.

81. Goff G, Robert V, Fondjo E, Carnevale P. Efficacy of insecticide impregnated bed-nets to control malaria in a rural forested area in Southern Cameroon. Mem Instituto Oswaldo Cruz. 1992;87:355–9.

82. Bird MI, Giresse P, Ngos S. A seasonal cycle in the carbon-isotope composition of organic carbon in the Sanaga River, Cameroon. Limnol Oceanogr. 1998;43:143–6.

83. Tompkins AM, McCreesh N. Migration statistics relevant for malaria transmission in Senegal derived from mobile phone data and used in an agent-based migration model. Geospat Health. 2016;11(Suppl 1):408.

Publisher's Note

Springer Nature remains neutral with regard to jurisdictional claims in published maps and institutional affiliations.

ORIGINAL PAPER

Malaria metrics distribution under global warming: assessment of the VECTRI malaria model over Cameroon

Amelie D. Mbouna[1] · Alain T. Tamoffo[1,2] · Ernest O. Asare[3] · Andre Lenouo[4] · Clement Tchawoua[1]

Abstract

Malaria is a critical health issue across the world and especially in Africa. Studies based on dynamical models helped to understand inter-linkages between this illness and climate. In this study, we evaluated the ability of the VECTRI community vector malaria model to simulate the spread of malaria in Cameroon using rainfall and temperature data from FEWS-ARC2 and ERA-interim, respectively. In addition, we simulated the model using five results of the dynamical downscaling of the regional climate model RCA4 within two time frames named near future (2035–2065) and far future (2071–2100), aiming to explore the potential effects of global warming on the malaria propagation over Cameroon. The evaluated metrics include the risk maps of the entomological inoculation rate (EIR) and the parasite ratio (PR). During the historical period (1985–2005), the model satisfactorily reproduces the observed PR and EIR. Results of projections reveal that under global warming, heterogeneous changes feature the study area, with localized increases or decreases in PR and EIR. As the level of radiative forcing increases (from 2.6 to 8.5 W.m^{-2}), the magnitude of change in PR and EIR also gradually intensifies. The occurrence of transmission peaks is projected in the temperature range of 26–28 °C. Moreover, PR and EIR vary depending on the three agro-climatic regions of the study area. VECTRI still needs to integrate other aspects of disease transmission, such as population mobility and intervention strategies, in order to be more relevant to support actions of decision-makers and policy makers.

Introduction

The World Health Organization (WHO report 2015) reports that malaria remains one of the most important killer diseases in the world. Eighty-two percent of the cases and 94% of deaths are recorded in Africa. Malaria, therefore, is the primary cause of mortality and morbidity in Africa (WHO report 2008). This disease is endemic in tropical and subtropical areas, and sub-Saharan African countries continue to be the most affected. Specifically in Cameroon, the illness is the leading cause of mortality and morbidity with children under five and pregnant women being the most affected (Bandolo 2012). In 2006, there were approximately 5 million cases of malaria in the country (WHO report 2008), making the disease the country's priority health issue.

Malaria is caused by a parasite which is a protozoan from the genus plasmodium and transmitted to people through the bites of infected female mosquitoes. A single bite by a malaria-carrying mosquito can lead to extreme sickness or death. Malaria starts with extreme cold, followed by a high fever and severe sweating. These can be accompanied by joint pain, abdominal pain, headaches, vomiting and extreme tiredness.

Malaria disease is very sensitive to climatic conditions, and in tropical areas, the disease is prevalent (Bomblies and Eltahir 2009), because of the abundance of mosquitoes' breeding sites and favourable weather conditions. The

✉ Amelie D. Mbouna
  ameldany18@gmail.com

1 Laboratory for Environmental Modelling and Atmospheric Physics (LEMAP), Department of Physics, Faculty of Science, University of Yaoundé I, P.O. Box 812, Yaounde, Cameroon

2 Physics Department, Kwame Nkrumah University of Science and Technology, Kumasi, Ghana

3 Department of Epidemiology of Microbial Diseases, Yale School of Public Health, Yale University, New Haven, USA

4 Department of Physics, Faculty of Science, University of Douala, Douala, Cameroon

⦿ Springer

link between climate and malaria is well documented. In fact, rainfall and temperature influence the life cycles of the anopheles' mosquito vector as well as the malarial parasite *plasmodium falciparum* (Lindsay et al. 2000; Abiodun et al. 2018). Temperature determines the length of the mosquito cycle and the sporogonic cycle of the malarial parasite within the mosquito (Hajison et al., 2017; Egbendewe-Mondzozo et al. 2011). Rainfall provides suitable temporary water bodies (breeding sites) for mosquitoes to grow and develop (Komen et al 2015; Garske et al. 2013). But extreme rainfall appears to be harmful to mosquito development, as it flushes out mosquitoes from their aquatic habitat and kills them (Paaijmans et al., 2007).

The disease sensitivity to climate can also be demonstrated using models. In fact, considerable efforts are made by scientists by constructing some mathematical models to forecast malaria distribution. For instance, Ayanlade et al. (2020) demonstrated the modulator effect of rainfall and temperature indices on malaria propagation with a high Spearman correlation coefficient for rainfall as well as temperature. Ermert et al. (2012) using the Liverpool malaria model (LMM) demonstrated the strong influence of changes in rainfall and temperature on the malaria distribution in various ecological African zones. Diouf et al. (2017) also established with the LMM that the risk of malaria transmission is mainly associated with variability in rainfall and temperature.

Among studies related to climate change and malaria, Ye et al. (2007) found that rainfall and temperature significantly influence the malaria's incidence with emphasis on temperature. In some West African countries, Diouf et al. (2020) demonstrated that the malaria's high transmission periods are directly linked to heavy rainfall events. Malaria endemicity would be little affected by climate change (Beguin et al. 2011). This suggests that warm temperatures (due to global warming) are likely to increase or/and decrease malaria in endemic areas. In fact, high temperatures could significantly impact growing conditions of the mosquito. However, the temperature might not be the only factor as the WHO's report in 1975 highlighted the migration's effect of population from endemic zones to free malaria areas on the dynamics of the malaria disease. This aspect is supported by previous work by Ngarakana-Gwasira et al. (2016). In addition, the impact of global warming on the health is not expected to be homogenous across regions as Costello et al. (2009) argued.

Numerous studies across Africa (e.g. Peterson 2009, Yamana et al. 2016) project a gradual southward shift of malaria from the Sahelian zones of the West African, including northern Cameroon. This may suggest unfavourable conditions for malaria proliferation by the 2080s (Caminade et al. 2014). Other studies demonstrated inconsistencies between projected changes in malaria spread and global warming, especially over the Sahel (Beguin et al. 2011; Escobar et al. 2016).

A study conducted by Asare and Amekudzi (2017) using the Abdus Salam International Centre for Theoretical physics (ICTP) vector borne disease model (VECTRI) also simulated malaria transmission dynamics at both national and local scales in Ghana and specified the predominant role of rainfall. Mbouna et al. (2019) modelled the malaria distribution over Cameroon using the VECTRI malaria model. They showed that malaria prevalence is maximum at temperatures of 24 to 26 °C and rainfall rates of approximately 4 to 6 mm/day. This rainfall amount features a smaller rate in locations far from water bodies and where the transmission seasonality is close to that of rainfall with a lag of 1 to 2 months (also found by Diouf et al. 2020), satisfactorily simulated by the VECTRI model. The particularity of the VECTRI model is that apart from temperature and rainfall, it pays particular attention to the human population density's modulator effect on the malaria transmission and distribution (Caminade et al. 2014).

Although several studies demonstrated the performances of VECTRI coupled with temperature and rainfall to simulate malaria metrics, studies conducted under global warming are still needed. Yet, such analyses might contribute to a long-term plan for disease prevention, adaptation and mitigation of the transmission. Therefore in the present study, we use the VECTRI model with the atmospheric regional climate model RCA4 (VECTRI-RCA4) to address the issue. The goal of the study is twofold: first, assess the ability of the combination VECTRI-RCA4 to model malaria metrics over Cameroon and, second, explore the impact of global warming under the Representative Concentration Pathway (RCP) 2.6 and 8.5 on malaria distribution. Through examination of projections, we hope to portray preliminary aspects of malaria propagation in a warmer world over Cameroon, as well as alerting decision-makers to the challenges and opportunities for mitigation. The paper is organized as follows: the "Data and methods" section describes the data and methods used. The "Results and discussion" section presents the obtained results and discusses the key findings. A summary concludes this work in the "Conclusion" section.

Data and methods

Study area

Our study domain is Cameroon, located over Central Africa within latitudes 1.5°N–13°N and longitudes 8°E–17°E, an area covering other neighbouring countries as presented in Fig. 1.

Cameroon's climate varies from humid in the south to arid and hot in the north. Cameroon's climate is particularly
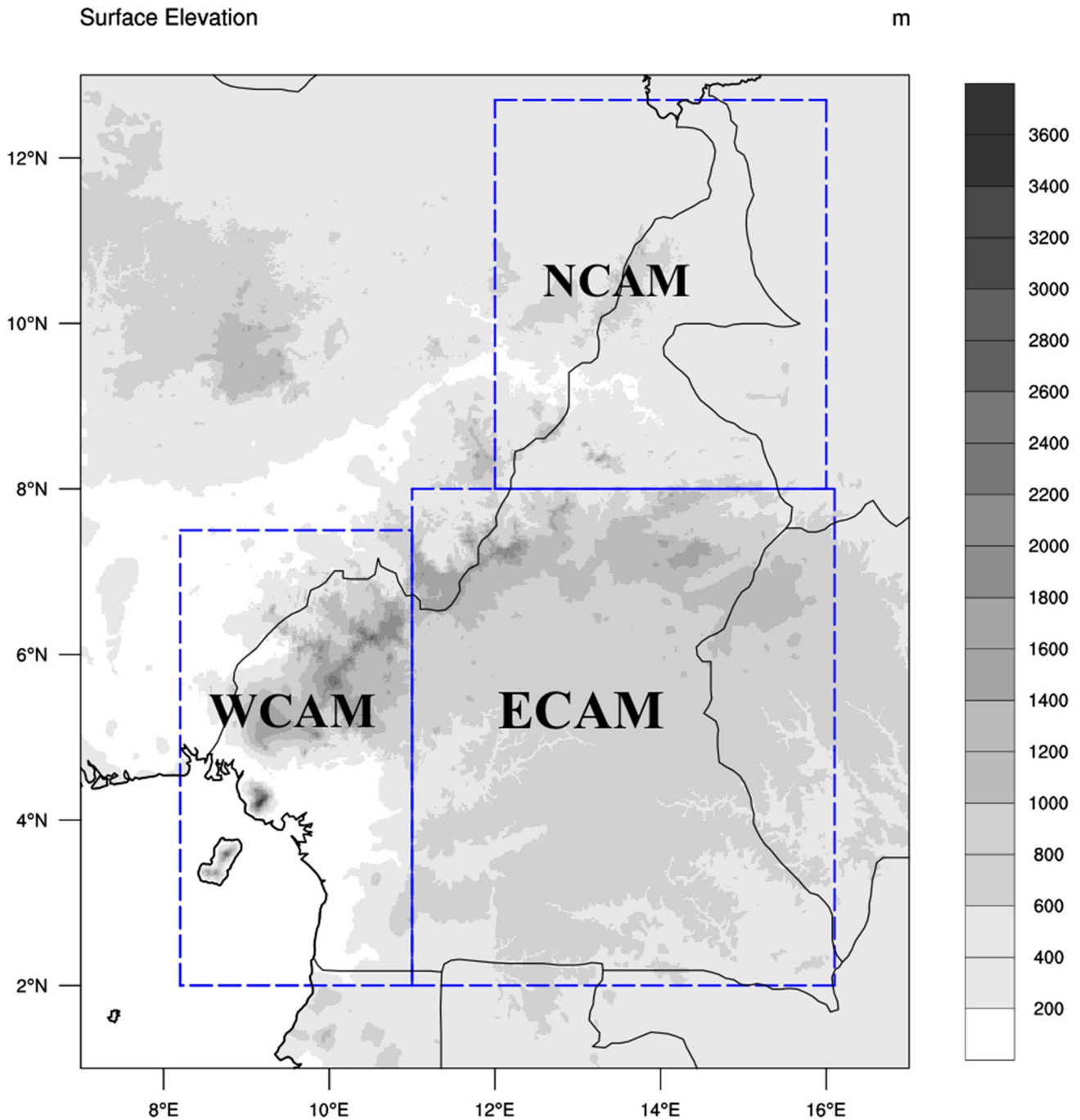
Fig. 1 Map of Cameroon and neighbouring countries. Highlighted in blue are the three agro-climatic sub-regions: North Cameroon (NCAM), West Cameroon (WCAM) and East Cameroon (ECAM)

influenced by the Harmattan and the Atlantic Monsoon winds and is then characterized by two climatic domains, namely the tropical and the equatorial domain (Zaroug and Reynolds 2006; Molua and Lambi 2007). The area has also been subdivided into three agro-climatic sub-regions, namely the North Cameroon (NCAM), West Cameroon (WCAM) and East Cameroon (ECAM).

VECTRI malaria model

The model used in this work is an open-source, the Abdus Salam International Centre for Theoretical Physics (ICTP) vector borne disease model (VECTRI). VECTRI is a grid distributed dynamical model that couples a biological model for the vector and parasite life cycles, to a simple

compartmental Susceptible-Exposed-Infectious-Recovered (SEIR) representation of the disease progression in the human host. VECTRI has the particularity to incorporate interactions between the human host (H) and vectors using the human biting rate (hbr) expressed as presented in Eq. 1 as follows (Tompkins and Ermert 2013).

$$hbr = \left(1 - e^{\frac{-H}{\tau zoo}}\right)\frac{\sum_{j=1}^{N_{sporo}} V(1,j)}{H} \tag{1}$$

The factor $1-\exp(-H/\tau_{z00})$ represents the level of vector zoophily. The exponential factor reflects this, with the e-folding population density for the effect set to $\tau zoo = 50\ km^{-2}$. The vector status is also bin resolved, consisting of two properties: the gonotrophic and sporogonic cycles. It is thus represented as a two dimensional array $V(Ngono, Nsporo)$. All vectors in the first gonotrophic bin $\sum_{j=1}^{Nsporo} V(1,j)$ are in the meal-searching step of the model.

The probability of transmission of an infectious vector to the host after a single bite is noted as P_{vh}. If its value is assumed constant, then the probability of transmission for an individual receiving n infection bites is given by $1 - (1 - P_{vh})^n$. The daily overall transmission probability per person is then expressed as in Eq. 2 (Tompkins and Ermert 2013):

$$P_{v \to h} = \sum_{n=1}^{\infty} G_{\overline{EIR_d}}(n)\left(1 - \left(1 - P_{vh}\right)^n\right) \tag{2}$$

G_{EIR} is the Poisson distribution for mean entomological inoculation rate (EIR). EIR, which is the daily number of infectious bites by infectious vectors, is calculated as the product of human biting rate (hbr) and circumsporozoite protein rate (CSPR). Equation 2 is subject to modification if factors such as the use of mosquito nets, which cause fluctuations in the biting rate, are to be taken into account. Generally, a population host has about 20 days after infection to assume the infective status (Day et al. 1998). The calculation of parasite ratio (PR) and EIR relies on both Eqs. 1 and 2 of the VECTRI model. Further information on the physical and mathematical formulation is available in the supplementary material.

Data used

Climate inputs for VECTRI, specifically rainfall and temperature data at 0.44° grid spacing, are taken from the results of dynamical downscaling of the fourth version of the Rossby Centre Atmospheric (RCA) model (RCA4), participating in the Coordinated Regional Climate Downscaling Experiment (CORDEX) project. RCA4 was forced with five global climate models (GCMs) involved in the Coupled Model Intercomparison Project phase 5 (CMIP5; Taylor et al. 2012). Details of downscaled GCMs are provided in Table 1.

Observed malaria PR data are obtained from the Malaria Atlas Project programme (MAP) that collects results of individuals researchers or organizers already published in the literature while EIR is obtained from a recent database for Africa (Yamba et al. 2020).

VECTRI was first integrated from January 1985 through December 2005 using historical data from the downscaled GCMs which is compared against simulations when VECTRI is forced by the observation FEWS-ARC2, Famine Early Warning Systems Network ARC version 2 (Love 2002) for rainfall and the reanalysis ECMWF ERA-Interim (Dee et al. 2011) for temperature. Secondly, the model is integrated under global warming using two Representative Concentration Pathway scenarios: the high-mitigated, low-emission RCP2.6 and the low-mitigated, high-emission RCP8.5 scenarios (Vuuren et al. 2011). Using these two contrasted scenarios enables us to get an insight into the way each warming level might impact the malaria metrics' distribution over Cameroon. Therefore, this offers the possibility to stimulate discussion about the opportunity or not to mitigate the changing climate.

Population density is taken from AFRIPOP (Linard et al. 2012) for each grid cell point in order to account for the growth of the population in the malaria simulations. We set the population growth parameter in VECTRI to be equal to the annual population growth rate in Cameroon, which is 2.6 according to the results of the third National Population Census (Mbarga 2010) taking advantage of the fact that the model is dynamic. VECTRI's simulations are performed with a 0.1° × 0.1° horizontal resolution. Driving data are statistically downscaled to the land model

Table 1 Details of GCMs used to force RCA4 in this study

Model name	Institution	Native resolution	References
EC-EARTH-ES	European community Earth-System Model Consortium	1.125° × 1.125°	Hazeleger et al. (2010)
MPI-ESM-LR	Max Planck Institute for Meteorology	1.9° × 1.9°	Popke et al. (2013)
MIROC-5	Atmosphere and Ocean Research Institute (University of Tokyo)	1.40° × 1.40°	Watanabe et al. (2011)
NorESM1-M	Norwegian Climate Centre	2.5° × 1.9°	Bentsen et al. (2013)
HadGEM2-ES	Met Office Hadley Centre	1.875° × 1.25°	Collins et al. (2011)

resolution assuming a lapse rate of 6.5 K km^{-1} to adjust to the high-resolution topography.

Results and discussion

Models' evaluation

This section aims at evaluating the ability of the RCA4 model to reproduce the climatology of the study area as well as the VECTRI model to simulate malaria (malaria metrics) observed data.

RCA4 model evaluation

We started by investigating whether the atmospheric regional climate model RCA4 satisfactorily reproduces the mean climatology of Cameroon rainfall and temperature. To this, we investigated the three agro-climatic sub-regions termed North Cameroon (NCAM), West Cameroon (WCAM) and East Cameroon (ECAM) (see Fig. 1). Only the results based on the ensemble mean of RCM experiments (RCA-EnsMean thereafter) are presented in the main document, whereas outcomes from individual RCM simulations are shown in the supplementary material.

Figure 2 shows the seasonality of rainfall (left panels) and temperature (right panels) over the three agro-climatic regions. The grey shade band is the standard deviation
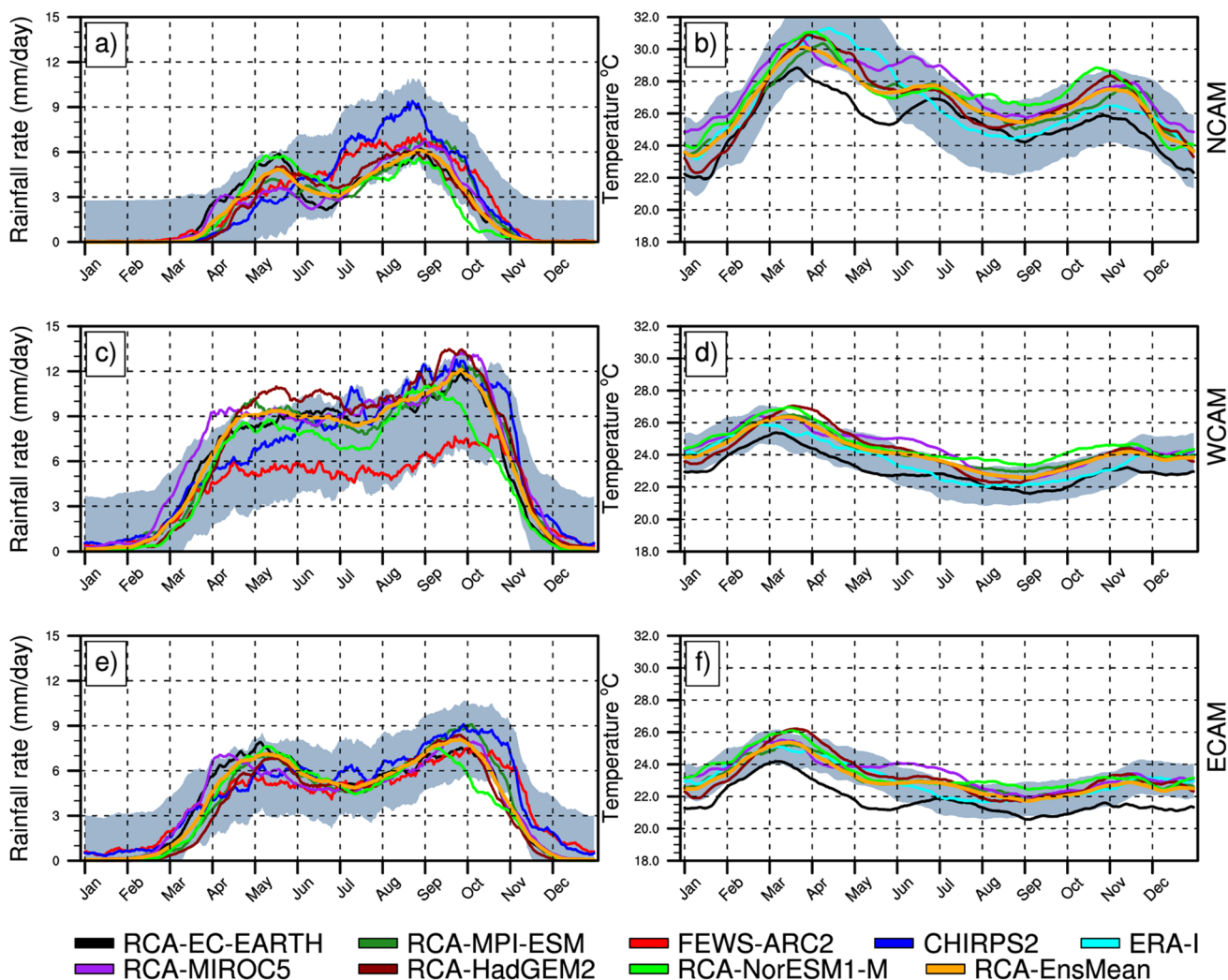

Fig. 2 Seasonality of mean (1985–2005) rainfall (in mm/day, left panels) and temperature (in °C, right panels). The study area is subdivided into three agro-climatic regions: **a**, **b** North Cameroon (NCAM, row 1), **c**, *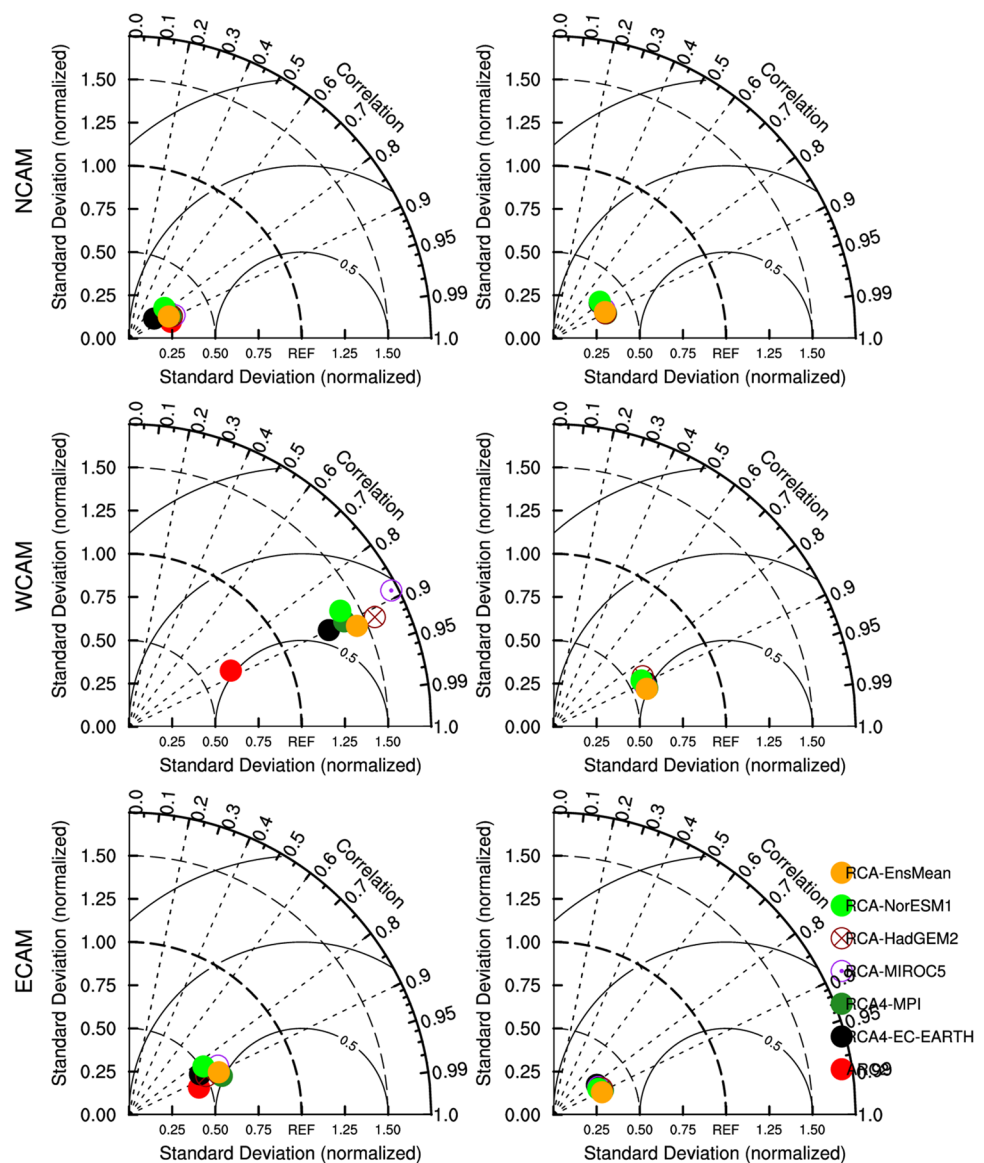*d** West Cameroon (WCAM, row 2) and **e**, **f** East Cameroon (ECAM, row 3). Data used are from RCA4 simulations and the ensemble mean of RCM runs (RCA-EnsMean) and from observed rainfall FEWS-ARC2 (red), CHIRPS2 (blue). The temperature reference is extracted from the ERA-Interim (cyan) reanalysis dataset

obtained from the FEWS-ARC2 for precipitation and from the reanalysis ERA-Interim for the temperature. For a given month, a mean rainfall value greater than the corresponding standard deviation is considered as a clear failing of the considered experiment. Two peaks are observed for rainfall in WCAM (Fig. 2a) and ECAM (Fig. 2e) in May and October (highest peak at ~12 mm/day and ~9 mm/day respectively), while NCAM experiences a unimodal rainfall regime, with the peak (~9 mm/day) occurring during August to September months (Fig. 2c). Although some divergences in terms of rainfall magnitude are noticed between datasets (more pronounced in NCAM), they all nevertheless vary within the range of the observed standard deviation. The seasonality of temperature is also well captured with the highest values in March and the ones in December for WCAM (Fig. 2b) and ECAM (Fig. 2f). Two obvious peaks are observed within

April to May (up to 30 °C) and within November to December (up to 28 °C) for NCAM (Fig. 2d). RCA-EC-EARTH failed to simulate the temperature for NCAM from April to June (Fig. 2d); from April to June and from November to December over ECAM (Fig. 2f). Overall, the climatological annual cycle of both rainfall and temperature are realistically captured over all subregions. The RCA-EnsMean is quite similar to individual RCM runs and is well contained in the natural variability of observations. This suggests that the ensemble mean of experiments is representative of individual simulations and can be used without changing the conclusion.

Statistical performance measures are summarized in Fig. 3, through the Taylor diagram. Three statistical metrics are used, including the root-mean-square difference (RMSD), the pattern correlation (r) and the standard

Fig. 3 Taylor diagrams displaying the statistics of daily precipitation and comparing RCA4's experiments and the ensemble mean (RCA-EnsMean) with observations FEWS-ARC2 (reference field for precipitation). For temperature, the reanalysis ERA-Interim is used as a point of reference. The first row shows statistical parameters over NCAM, the second over WCAM and the third over ECAM. The first column displays statistical parameters for precipitation while the second does so for temperature

deviation (STD), computed between downscaled results and FEWS-ARC2 for precipitation, and ERA-Interim for temperature used as a point of reference.

Regarding precipitation statistics, for NCAM and ECAM, RCA4's experiments and FEWS-ARC2 clustered but not so close to the reference field with average performances (RMSD < 1; $r \sim 0.90$ and STD < 0.75). There are fewer performances of RCA4's model for WCAM compared to the reference field with 1 < RMSD < 1.5, $r \sim 0.90$ and 1 < STD < 1.5. For temperature, RCA4's runs clustered and outperformed (compared to what was observed with precipitation) over the three agro-climatic regions, with $r \sim 0.90$, 0.5 < RMSD < 1 and STD < 0.75.

VECTRI model evaluation

Figure 4 presents how observed PR and EIR (blue lines) fit with simulated values (red lines) over the different measurement stations. Here, simulated values are results of the combination VECTRI-RCA-EnsMean, i.e. VECTRI driven by RCA-EnsMean. The PR and EIR observed and simulated values in Fig. 4 can be found in Table S1 and Table S2 in the supplementary material.

The results show that, although there are differences between the two experiments, the shapes of the curves are similar, meaning that the combination VECTRI-RCA-EnsMean succeeds to detect the signal of individual stations. The differences can be attributed to differences in rainfall amount and temperature. VECTRI outperforms in simulating EIR (right panel) than PR (left panel). It is important to recall the challenge of assessing model performance over equatorial Africa given observational uncertainty. Some differences may be associated with inhomogeneities in station measurements. The fact that the combination VECTRI-RCA-EnsMean satisfactorily reproduces the signal of variation of PR and EIR in most stations makes its usage reliable for projection.
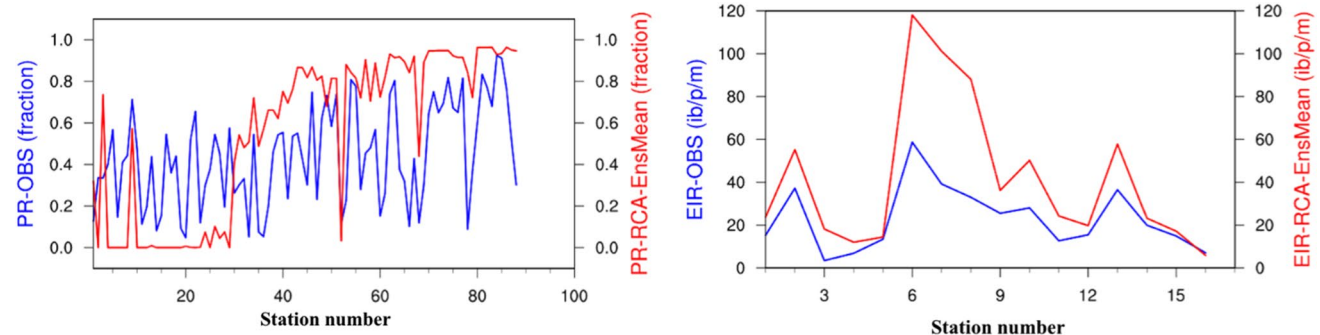
To get an insight into how the coupling VECTRI-RCA-EnsMean simulates the spreading of malaria over the country, we showed in Fig. 5 the spatial distribution of the PR as modelled by VECTRI-RCA-EnsMean compared against the monthly observed PR over the period 1985–2005.

These spatial plots present a varied landscape of malaria PR over the country. There are some simulated biases in NCAM where PR values are above 0.5 (Fig. 5b) which is mostly dry and warm, whereas in the observation (Fig. 5a), the mean PR is lower. Such a difference could be probably related to the sensitivity of VECTRI to low rainfall. For ECAM, the differences in PR between observed and simulated values are more obvious compared to WCAM. The model somehow outperforms better in these two areas compared to the NCAM.

Projected changes in the malaria metrics

In this section, we explore the impacts of global warming on the aforementioned malaria metrics under the optimistic (RCP2.6) and the pessimistic (RCP8.5) scenarios. Analyses are conducted under two-time frames: the near future (2035–2065) and the far future (2071–2100), using the combination VECTRI-RCA-EnsMean.

Changes in the parasite ratio (PR)

Figures 6 and 7 exhibit the monthly mean changes in PR over the near future and the far future under the high mitigated RCP2.6 (Fig. 6) and the low mitigated RCP8.5 (Fig. 7) scenarios.

Figure 6 presents the PR pattern obtained with RCA-EnsMean, under RCP2.6 scenario. Results based on individual experiments are presented in the supplementary material as follows: Fig. S1 for RCA4-EC-EARTH-ES, Fig. S3 for RCA4-MPI-ESM-LR, Fig. S5 for RCA4-MIROC5, Fig. S7 for RCA4-HadGEM2 and Fig. S9 for RCA4-NorESM1-M.

Fig. 4 Results of combinations of VECTRI-observation (in blue) and VECTRI-RCA-EnsMean (in red) for PR (left panel) and EIR (right panel), function of rainfall (mm/day) and temperature (°C) over Cam-

eroon. The *x*-axis values represent the station number. The two panels show how VECTRI forced with observed station measurements compares against VECTRI forced with RCA-EnsMean
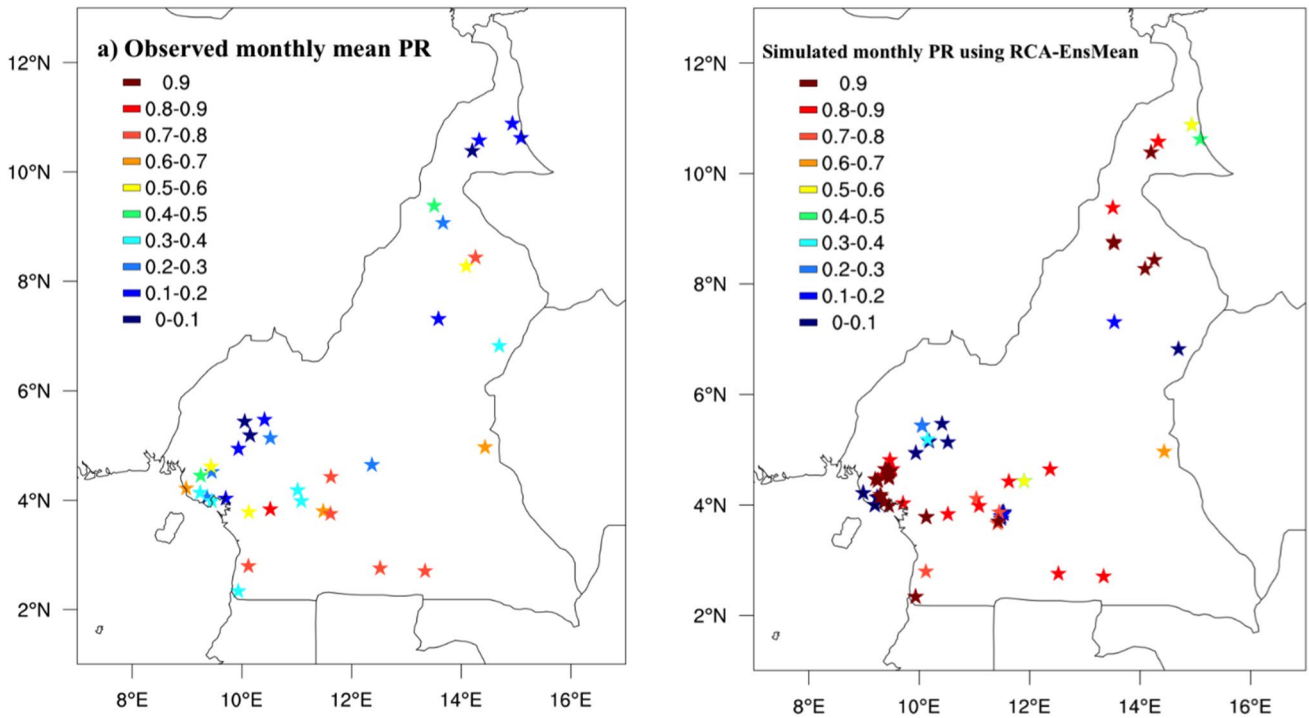
Fig. 5 Observed (left) and simulated (right) monthly mean of PR for the available data sites in Cameroon over the period 1985–2005. The PR values represent the average of all the points located within the same geographical areas of study
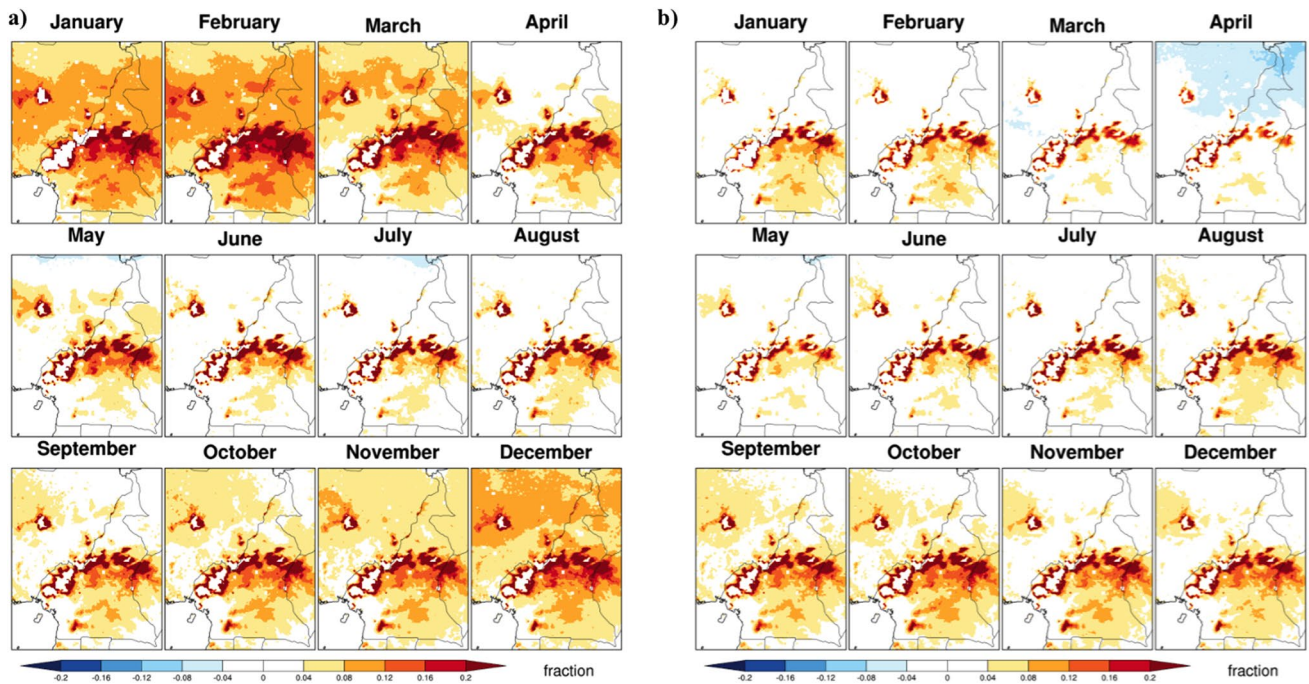

Fig. 6 Monthly mean changes in PR under RCP2.6 scenario. VECTRI model driven by RCA4-EnsMean for the period 2035–2065 (**a**) and 2071–2100 (**b**)
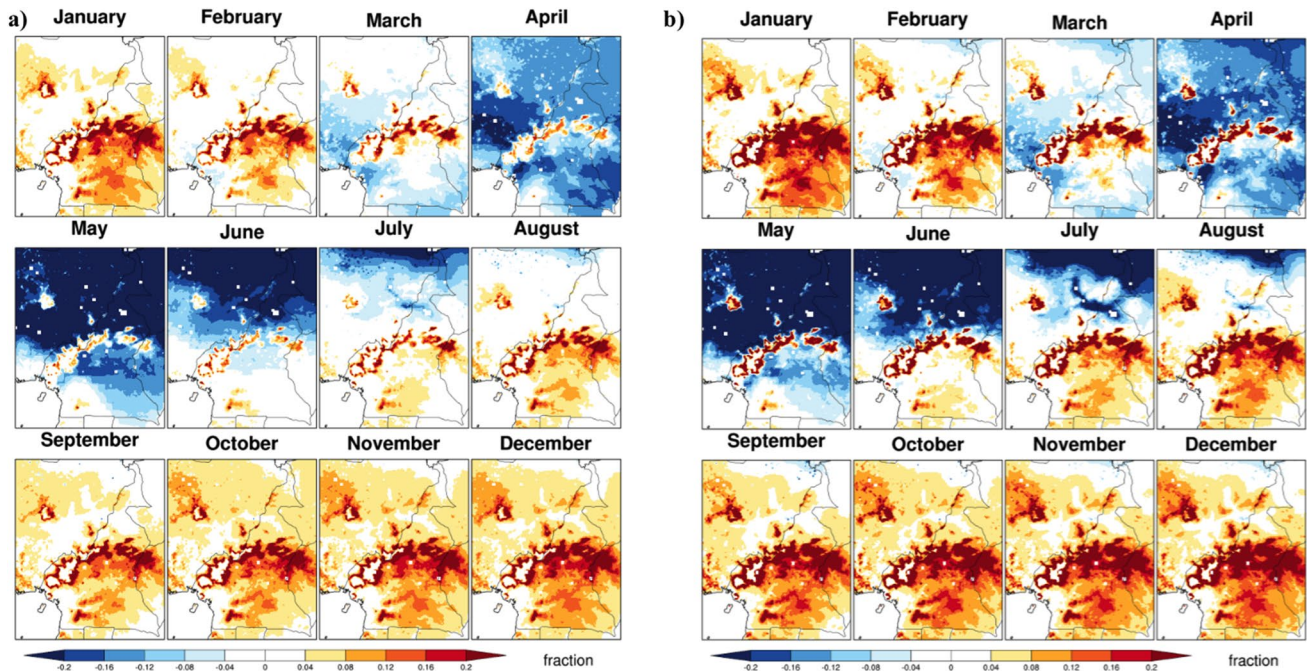
Fig. 7 Monthly mean changes in PR under RCP8.5 scenario. VECTRI model driven by RCA4-EnsMean for 2035–2065 (**a**) and 2071–2100 (**b**)

The PR tends to decrease when VECTRI is forced with RCA4-EC-EARTH-ES (Fig. S1) experiment with respect to other VECTRI-RCA4 runs. Contrastingly, increases instead are expected in the PR when VECTRI is driven by RCA4-HadGEM2 (Fig. S7).

PR is then projected to increase throughout the year with emphasis from October to March over the near future (Fig. 6a). A similar pattern is observed over the far future (Fig. 6b), where the PR tends to mostly increase over WCAM and decreases during the April month in NCAM. The PR is projected to significantly decrease in the distant future than in the near future.

Figure 7 presents the PR pattern with RCA-EnsMean as forcing under RCP8.5 scenario. Results based on individual forcings of VECTRI by RCA4 experiments are highlighted in the supplementary material: Fig. S2 for RCA4-EC-EARTH-ES, Fig. S4 for RCA4-MPI-ESM-LR, Fig. S6 for RCA4-MIROC5, Fig. S8 for RCA4-HadGEM2 and Fig. S10 for RCA4-NorESM1-M. The increase in the PR is strongest when VECTRI is coupled with RCA4-HadGEM2 (Fig. S8).

Under the high emission scenario RCP8.5 (Fig. 7), obvious differences between the near (Fig. 7a) and the far (Fig. 7b) future appear in the amplitude of changes in the PR. The PR generally tends to decrease from March to July, especially over NCAM, and increase during the rest of the year, especially over WCAM and ECAM.

The above results indicate that global warming would not much change the life cycles of the Anopheles mosquito and the malaria parasite *plasmodium falciparum*. Actually, rainfall creates suitable conditions (availability of ponds) for the mosquitoes' breeding process. But extreme rainfall could negatively impact the productivity of mosquito breeding habitat by flushing effect which leads to high mosquito losses (Paaijmans et al. 2010). This is observed in Figs. 6 and 7 from April to September referring to rainfall patterns in Figs. S21 and S23 of the Supplementary material.

Moreover, PR tends to intensify with temperature values less than 32 °C (see Figs. S22 and S24 in the supplementary material). This is associated with the fact that there is a range of temperatures that allows malaria transmission. In fact, the temperature is able to create good conditions for malaria vectors to thrive. Generally, the increase in temperature accelerates vector life cycles and also decreases the incubation period of the parasite (Van-Lieshout et al. 2004). This result is in line with previous studies conducted over Cameroon. They showed that the temperature suitability range for *Anopheles gambiae* and *Anopheles funestus* is between 20 and 29 °C (Tanga et al. 2010). Similar results were reported over the Limpopo Province in South Africa (Komen et al. 2015). However, at a very high temperature, mortality is high thus reducing transmission (Ebi et al. 2005), which corresponds to the situation expected in NCAM (Fig. 7 from April to July) and previously reported by Chemison et al. (2021) and Caminade et al. (2014).
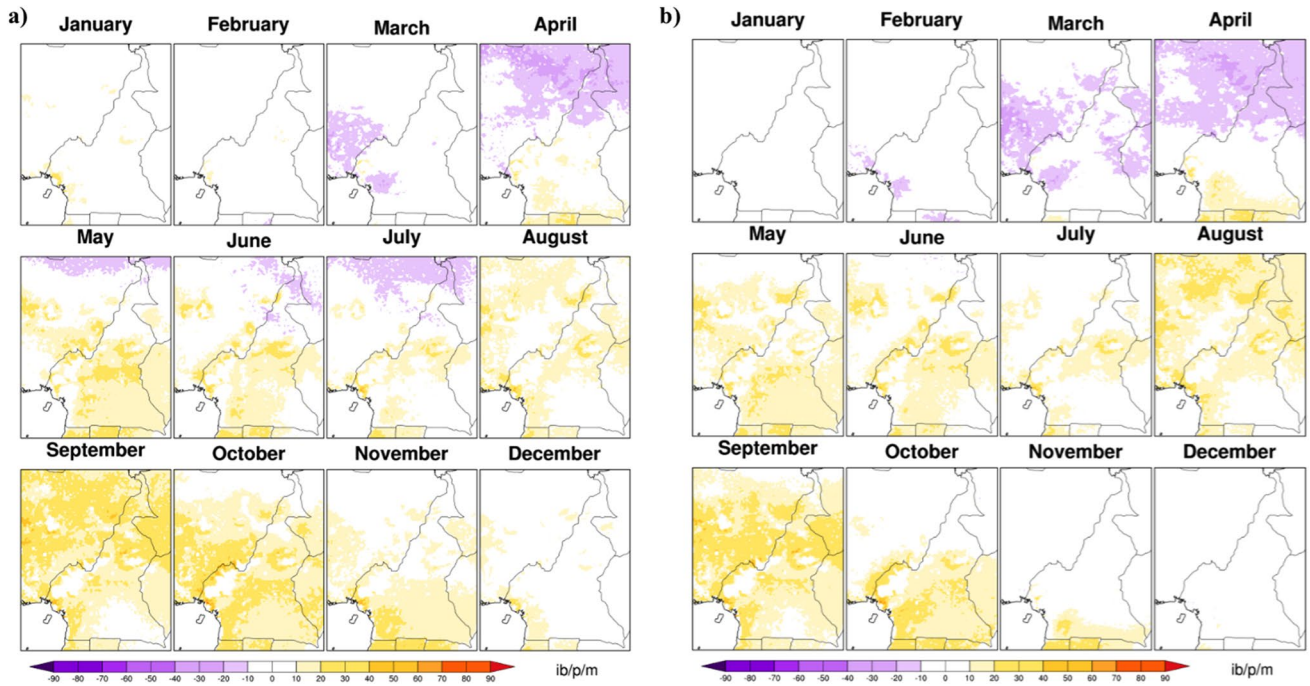
Fig. 8 Monthly estimated changes in EIR indicating the number of infected bites per person per month (ib/p/m). This is obtained for the RCP2.6 scenario from the coupling VECTRI-RCA4-EnsMean over the periods 2035–2065 (**a**) and 2071–2100 (**b**)
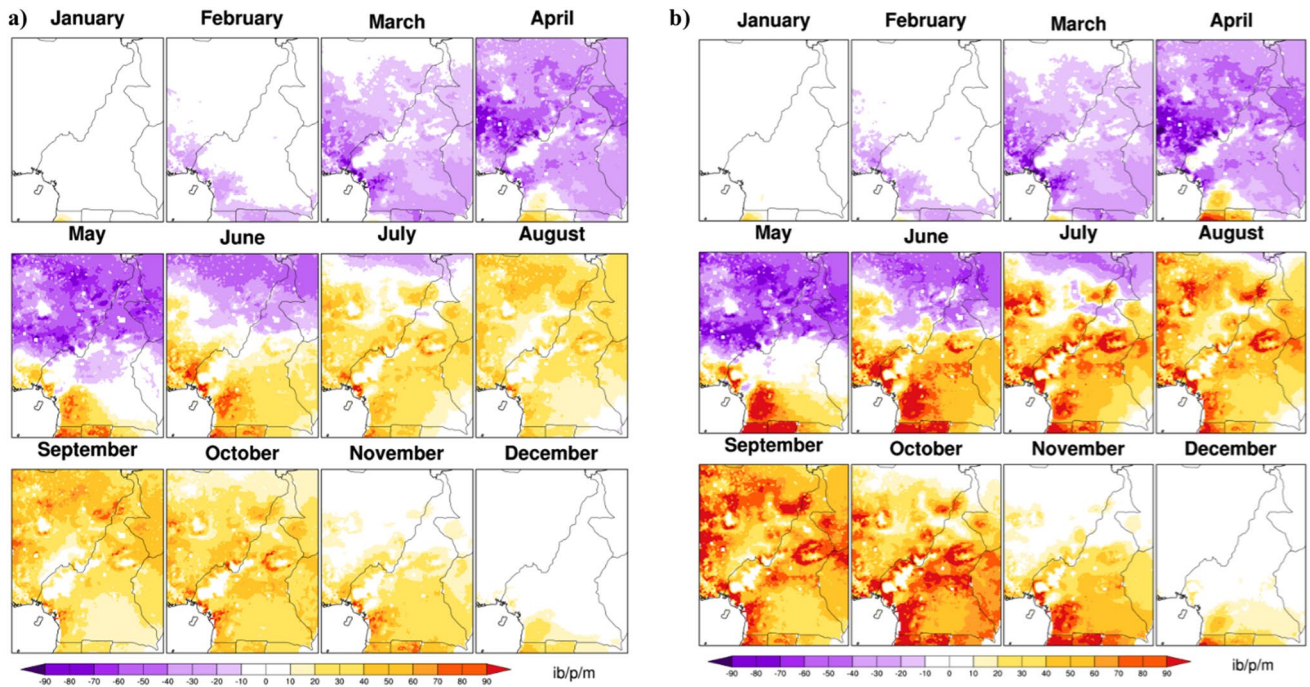

Fig. 9 Monthly estimated changes in EIR, indicating the number of infected bites per person per month (ib/p/m). Results obtained from the coupling VECTRI–RCA-EnsMean under the RCP8.5 scenario and over 2035–2065 (**a**) and 2071–2100 (**b**) periods

Changes in the entomological inoculation rate (EIR)

Figures 8 and 9 display maps of monthly mean changes in the EIR pattern when VECTRI is forced by RCA4-EnsMean under RCP2.6 and RCP8.5 respectively.

Broadly under RCP2.6, EIR is projected to decrease from April to July in NCAM and during March in WCAM (Fig. 8a). In the distant future, the EIR is expected to reduce from March to April, especially over NCAM (Fig. 8b). Over WCAM and ECAM subregions, an intensification of EIR is projected from April to November, whereas insignificant changes will occur for December and January.

For individual RCA4 model simulations, results are shown in the supplementary materials (Figs. S11, S13, S15, S17 and S19). EIR tends to gradually increase when VEC-TRI is forced with RCA4-HadGEM2 (Fig. S17), from June (WCAM and ECAM) to November with a peak in August to September (NCAM). There is a decrease in projections using rainfall and temperature from RCA4-EC-EARTH-ES (Fig. S11), whereas fewer changes are expected in EIR with RCA4-NorESM1-M (Fig. S19).

Under RCP8.5, EIR is expected to decrease significantly over almost the entire study area during March and April months and especially over NCAM from May to June (Fig. 9a and b). Conversely, EIR is projected to increase over WCAM and ECAM from May to November and over NCAM from July to November. No particular changes are foreseen over almost the whole country from December to February, except for a small part of southern Cameroon where a strengthening of the EIR is noted in December and a weakening in February over the two projection periods.

Results with the coupling VECTRI-RCA4-EC-EARTH-ES, VECTRI-RCA4-MPI-ESM-LR, VECTRI-RCA4-MIROC5, VECTRI-RCA4-HadGEM2 and VECTRI-RCA4-NorESM1-M are presented in Figs. S12, S14, S16, S18 and S19, respectively.

Changes in EIR presented in Figs. 8 and 9 can be explained by the suitable range of temperature of 18–33 °C (Bayoh and Lindsay 2003) of the study area as highlighted in Figs. S22 and S24 in the supplementary material. But it should be recalled that temperatures above 30 °C are prejudicial for anopheles' development, therefore leading to a decrease in EIR as demonstrated in Béguin et al. (2011).

Changes in EIR are stronger in the far future than in the near future and vice-versa (Figs. 8 and 9). In general, the signal of change is stronger under RCP8.5 than RCP2.6, meaning an increased risk with the increased level of the radiative forcing. A similar study conducted by Chaturvedi and Dwivedi (2021) over India showed that under global warming, malaria transmission is expected to strengthen together with the duration of the transmission season. The EIR results also highlight the important role of changes in rainfall and temperature on malaria incidence and show the

seasonality of the disease. Similar work also demonstrated that a decline in precipitation is beneficial for the growth of the mosquito population, which causes higher EIR (Ermert et al. 2012). Our study also attests to general expectations with regard to the impact of global warming on the spread of malaria. It is generally accepted that climate change will affect the spread of malaria as mentioned by Ogega and Alobo (2020), but it is also noted that malaria distribution is impacted by many factors in addition to climate change, including population mobility, changes in land use, changes in air and water temperatures and the systematic increase in preventive interventions, which VECTRI has not yet incorporated and which should prompt future work.

Conclusion

This work is an initial exploration of the relationship between climate and malaria in Cameroon using dynamical models under future climate scenarios of the CORDEX project for Africa. The link between these parameters and two common malaria indicators, parasite ratio (PR) and entomological inoculation rate (EIR), was established. The results demonstrated that there is a close relationship between rainfall, temperature and malaria transmission in Cameroon under future climate change. For each of the models used under the two RCP scenarios, the impact of temperature on the evolution of malaria indicators is established, and the seasonality is highlighted for the PR and EIR metrics. The integration of VECTRI with future climate scenarios reveals a modulating effect of changes in temperature and rainfall on changes in malaria transmission, although factors such as population mobility and effective intervention strategies against malaria are likely to improve VECTRI results if implemented. The next step in line of this work is to ascertain how best to incorporate such a model effectively into a national or regional decision-making process concerning health planning and interventions. If such a model should be used to aid operational decisions in Cameroon, using machine learning techniques for an effectiveness model's calibration of parameters is required as recently introduced in Tompkins and Thomson (2018).

in this study. We are grateful to anonymous reviewers and the editor for the thorough reviews and critical comments.

Declarations

Competing interests The authors declare no competing interests.

References

Abiodun GJ, Witbooi P, Okosun KO (2018) Modelling the impact of climatic variables on malaria transmission. Hacettepe J. Math Stat 47:219–235. https://doi.org/10.15672/HJMS.2017.452

Asare EO, Amekudzi LK (2017) Assessing climate driven malaria variability in Ghana using a regional scale dynamical model. Climate 5(1):20. https://doi.org/10.3390/cli5010020

Ayanlade A, Sergi C, Ayanlade OS (2020) (2020) Malaria and meningitis under climate change: initial assessment of climate information service in Nigeria. Meteorol Appl 27:e1953. https://doi.org/10.1002/met.1953

Bandolo FMN (2012) Heavily indebted poor countries (HIPC) initiative in cameroon and the fight to reduce malaria related under-five mortality (Master's thesis, Høgskolen i Oslo og Akershus. Fakultet for samfunnsfag). https://hdl.handle.net/10642/1803

Bayoh MN, Lindsay SW (2003) Effect of temperature on the development of the aquatic stages of Anopheles gambiae sensu stricto (Diptera: Culicidae). Bull Entomol Res 93(5):375–381. https://doi.org/10.1079/BER2003259

Béguin A, Hales S, Rocklöv J, Åström C, Louis VR, Sauerborn R (2011) The opposing effects of climate change and socio-economic development on the global distribution of malaria. Glob Environ Chang 21(4):1209–1214. https://doi.org/10.1079/BER2003259

Bentsen M, Bethke I, Debernard J, Iversen T, Kirkevåg A, Seland Ø, Drange H, Roelandt C, Seierstad I, Hoose C et al (2013) The Norwegian earth system model, NORESM1-part 1: description and basic evaluation of the physical climate. Geosci Model Dev 6(3):687–720. https://doi.org/10.5194/gmd-6-687-2013

Bomblies A, Eltahir EA (2009) Assessment of the impact of climate shifts on malaria transmission in the Sahel. EcoHealth 6(3):426–437. https://doi.org/10.0007/s10393-010-0274-5

Caminade C, Kovats S, Rocklov J, Tompkins AM, Morse AP, Colón-González FJ, Lloyd SJ (2014) Impact of climate change on global malaria distribution. Proc Natl Acad Sci. https://doi.org/10.1073/pnas.130289111

Chaturvedi, Dwivedi S (2021) Understanding the effect of climate change in the distribution and intensity of malaria transmission over India using a dynamical malaria model. Int J Biometeorology 1-15.https://doi.org/10.1007/s00484-021-02097-x

Chemison A, Ramstein G, Tompkins AM, Defrance D, Camus G, Charra M, Caminade C (2021) Impact of an accelerated melting of Greenland on malaria distribution over Africa. Nat Commun 12(1):1–12. https://doi.org/10.1038/s41467-021-24134-4

Collins WJ, Bellouin N, Doutriaux-Boucher M, Gedney N, Halloran P, Hinton T, Hughes J, Jones CD, Joshi M, Liddicoat S, Martin G, O'Connor F, Rae J, Senior C, Sitch S, Totterdell

I, Wiltshire A, Woodward S (2011) Development and evaluation of an earth-system model HadGEM2. Geosci Model Dev 4(4):1051–1075.https://doi.org/10.5194/gmd-4-1051-2011 https://www.geosci-model-dev.net/4/1051/2011/

Costello A, Abbas M, Allen A, Ball S, Bell S, Bellamy R, Friel S, Groce N, Johnson A, Kett M, Lee M (2009) Managing the health effects of climate change: lancet and University College London Institute for Global Health Commission. The Lancet 373(9676):1693–1733

Day KP, Hayward RE, Dyer M (1998) The biology of Plasmodium falciparum transmission stages. Parasitology-Cambridge 116:S95–S110

Dee DP, Uppala SM, Simmons AJ, Berrisford P, Poli P, Kobayashi S, Andrae U, Balmaseda MA, Balsamo G, Bauer DP, Bechtold P (2011) The ERA-Interim reanalysis: Configuration and performance of the data assimilation system. Q J R Meteorol Soc 137(656):553–597. https://doi.org/10.1002/qj.828

Diouf I, Rodriguez-Fonseca B, Deme A, Caminade C, Morse AP, Cisse M, Gaye AT (2017) Comparison of malaria simulations driven by meteorological observations and reanalysis products in Senegal. Int J Environ Res Public Health 14(10):1119. https://doi.org/10.3390/ijerph14101119

Diouf I, Fonseca BR, Caminade C, Thiaw WM, Deme A, Morse AP, Ndione JA, Gaye AT, Diaw A, Ndiaye MKN (2020) Climate variability and malaria over West Africa. Am J Trop Med Hyg 102(5):1037. https://doi.org/10.4269/ajtmh.19-0062

Ebi KL, Hartman J, Chan N, Mcconnell J, Schlesinger M, Weyant J (2005) Climate suitability for stable malaria transmission in Zimbabwe under different climate change scenarios. Clim Change 73(3):375–393. https://doi.org/10.1007/s10584-005-6875-2

Egbendewe-Mondzozo A, Musumba M, McCarl BA, Wu X (2011) Climate change and vector-borne diseases: an economic impact analysis of malaria in Africa. Int J Environ Res Public Health 8(3):913–930. https://doi.org/10.3390/ijerph8030913

Ermert V, Fink AH, Morse AP, Paeth H (2012) The impact of regional climate change on malaria risk due to greenhouse forcing and land-use changes in tropical Africa. Environ Health Perspect 120(1):77–84. https://doi.org/10.1289/ehp.1103681

Escobar LE, Romero-Alvarez D, Leon R, Lepe-Lopez MA, Craft ME, Borbor-Cordova MJ, Svenning JC (2016) Declining prevalence of disease vectors under climate change. Sci Rep 6(1):1–8. https://doi.org/10.1038/srep39150

Garske Tini, Ferguson Neil M, Ghani Azra C (2013) Estimating air temperature and its influence on malaria transmission across Africa. PloS one 8(2):e56487. https://doi.org/10.1371/journal.pone.0056487

Hajison PL, Mwakikunga BW, Mathanga DP, Feresu SA (2017) Seasonal variation of malaria cases in children aged less than 5 years old following weather change in Zomba district, Malawi. Malaria J 16(1):1–12. https://doi.org/10.1186/s129336-017-1913-x

Hazeleger W, Severijns C, Semmler T, Ştefănescu S, Yang S, Wang X, ... Willén U (2010) EC-Earth: a seamless earth-system prediction approach in action. Bull Am Meteorol Soc 91(10):1357-1364.https://doi.org/10.1175/2010BAMS2877.1

Komen K, Olwoch J, Rautenbach H, Botai J, Adebayo A (2015) Long-run relative importance of temperature as the main driver to malaria transmission in Limpopo Province, South Africa: a simple econometric approach. EcoHealth 12(1):131–143. https://doi.org/10.1007/s10393-014-0992-1

Linard C, Gilbert M, Snow RW, Noor AM, Tatem AJ (2012) Population distribution, settlement patterns and accessibility across Africa in 2010. PLoS One 7(2):e31743. https://doi.org/10.1371/journal.pone.0031743

Lindsay SW, Bødker R, Malima R, Msangeni HA, Kisinza W (2000) Effect of 1997–98 EI Niño on highland malaria in Tanzania.

The Lancet 355(9208):989–990. https://doi.org/10.1016/S0140-6736(00)90022-9

Love T (2022) The climate prediction center rainfall algorithm version 2." NOAA Climate Prediction Center Tech. http://www.cpc.ncep.noaa.gov/products/fews/RFE2.0_tech.pdf. Accessed May 2022

Mbarga B (2010) 3eme rgph. rapport de présentation des résultats définitifs. BUCREP (Bureau Central des Recensements et des Etudes de la Population), Yaoundé. http://www.bucrep.cm/index.php/fr/component/phocadownload/category/20-prsentation-des-rsultats

Mbouna AD, Tompkins AM, Lenouo A, Asare EO, Yamba EI, Tchawoua C (2019) (2019) Modelled and observed mean and seasonal relationships between climate, population density and malaria indicators in Cameroon. Malar J 18(1):359. https://doi.org/10.1186/s112936-019-2991-8

Molua EL, Lambi CM (2007) The economic impact of climate change on agriculture in cameroon, Volume 1of 1. The World Bank.

Ngarakana-Gwasira ET, Bhunu CP, Masocha M, Mashonjowa E (2016) Assessing the role of climate change in malaria transmission in Africa. Malaria Res Treat 2016.https://doi.org/10.1155/2016/7104291

Ogega OM, Alobo M (2020) Impact of 1.5 o C and 2 o C global warming scenarios on malaria transmission in East Africa [version 2; peer review. https://doi.org/10.12688/aas0penres.13074.1

Paaijmans KP, Wandago MO, Githeko AK, Takken W, Carter D (2007) Unexpected high losses of anopheles gambiae larvae due to rainfall. PLoS ONE 2(11):e1146. https://doi.org/10.1371/journal.pone0001146

Paaijmans KP, Blanford S, Bell AS, Blanford JI, Read AF, Thomas MB (2010) Influence of climate on malaria transmission depends on daily temperature variation. Proc Natl Acad Sci 107(34):15135–15139. https://doi.org/10.1073/pnas.1006422107

Peterson AT (2009) Shifting suitability for malaria vectors across Africa with warming climates. BMC Infect Dis 9(1):1–6. https://doi.org/10.1186/147-2334-9-59

Popke Dagmar, Stevens Bjoern, Voigt Aiko (2013) Climate and climate change in a radiative-convective equilibrium version of ECHAM6. J Adv Model Earth Syt 5(1):1–14. https://doi.org/10.1029/2012MS000191

Tanga MC, Ngundu WI, Judith N, Mbuh J, Tendongfor N, Simard F, Wanji S (2010) Climate change and altitudinal structuring of malaria vectors in south-western Cameroon: their relation to malaria transmission. Trans R Soc Trop Med Hyg 104(7):453–460. https://doi.org/10.1016/j.trstmh.2010.02.006

Taylor KE, Stouffer RJ, Meehl GA (2012) An overview of CMIP5 and the experiment design. Bull Am Meteor Soc 93(4):485–498. https://doi.org/10.1175/bams-d-11-00094.1

Tompkins AM, Ermert V (2013) A regional-scale, high resolution dynamical malaria model that accounts for population density, climate and surface hydrology. Malar J 12(1):65. https://doi.org/10.1186/1475-2875-12-65

Tompkins AM, Thomson MC (2018) Uncertainty in malaria simulations in the highlands of Kenya: relative contributions of model parameter setting, driving climate and initial condition errors. PLoS ONE 13(9):e0200638. https://doi.org/10.1371/journal.pone.0200638

Van Lieshout M, Kovats RS, Livermore MTJ, Martens P (2004) Climate change and malaria: analysis of the SRES climate and socio-economic scenarios. Glob Environ Change 14(1):87–99. https://doi.org/10.1016/j.gloenvcha.2003.10.009

Watanabe S, Hajima T, Sudo K, Nagashima T, Takemura T, Okajima H, Nozawa T, Kawase H, Abe M, Yokohata T et al (2011) Miroc-esm 2010: model description and basic results of cmip5- 20c3m experiments. Geosci Model Dev Discuss 4:1063–1128. https://doi.org/10.5194/gmdd-4-1063-2011

World Health Organization, World malaria report (2008) Geneva: WHO library cataloguing-in-publication data. p 215. https://www.who.int/publications/i/item/9789241563697

World Health Organization and Mahler, Halfdan (1975) The work of WHO, 1974: annual report of the Director-General to the World Health Assembly and to the United Nations. World Health Organization. https://apps.who.int/iris/handle/10665/85882. Accessed May 2022

World Health Organization (2015) World malaria report 2015. World Health Organization. https://apps.who.int/iris/handle/10665/200018. Accessed May 2022

Yamana TK, Bomblies A, Eltahir EA (2016) Climate change unlikely to increase malaria burden in West Africa. Nat Clim Chang 6(11):1009–1013. https://doi.org/10.1038/nclimate3085

Yamba EI, Tompkins AM, Fink AH, Ermert V, Amelie MD, Amekudzi LK, Briët OJT (2020) Monthly Entomological Rate Data for Studying the Seasonality of Malaria Transmission in Africa. Data 5(2):31. https://doi.org/10.3390/data5020031

Yé Y, Louis VR, Simboro S, Sauerborn R (2007) Effect of meteorological factors on clinical malaria risk among children: an assessment using village-based meteorological stations and community-based parasitological survey. BMC public health 7(1):1–11. https://doi.org/10.1186/1471-2458-7-101

Zaroug MG, Reynolds S (2006) Country pasture/forage resource profiles. FAO, Rome